



Stability Modeling with SLOPE/W

An Engineering Methodology

John Krahn

First Edition, May 2004

Copyright © 2004 by GEO-SLOPE/W International, Ltd.

All rights reserved. No part of this work may be reproduced or transmitted in any form or by any means, electronic or mechanical, including photocopying, recording, or by any information storage or retrieval system, without the prior written permission of GEO-SLOPE/W International, Ltd.

Printed in Canada.

Acknowledgements

To say that this book is “by John Krahn” grossly overstates the case. This book is the result of a group effort by everybody at GEO-SLOPE. My name is listed as author primarily for referencing convenience.

At the top of the list of contributors are Leonard Lam and Lori Newman.

All of us who participated in creating the content are grateful to Carola Preusser, Patricia Stooke and Greg Newman for their valuable assistance with editing and formatting this book.

GEO-SLOPE/W International Ltd

1400, 633 – 6th Ave SW

Calgary, Alberta, Canada T2P 2Y5

E-mail: info@geo-slope.com

Web: <http://www.geo-slope.com>

Table of Contents

1	Introduction	1
2	Limit Equilibrium Fundamentals	7
2.1	Introduction	7
2.2	Background and history	7
2.3	Method basics	8
2.4	General limit equilibrium method	11
2.5	Interslice force functions	15
2.6	Slip surface shapes	16
	Circular slip surface	16
	Planar slip surface	17
	Composite slip surface	18
	Block slip surface	19
	Shoring wall	20
2.7	Stress distributions	21
2.8	Limit equilibrium forces and stresses	27
2.9	Janbu generalized method	28
2.10	Missing physics	29
2.11	Other limitations	30
2.12	Slip surface shapes	31
2.13	Seepage forces	32
2.14	Concluding remarks	34
3	Factor of Safety Methods	37
3.1	Introduction	37
3.2	General limit equilibrium method	37
3.3	Ordinary or Fellenius method	42

3.4	Bishop's simplified method	47
3.5	Janbu's simplified method	50
3.6	Spencer method	51
3.7	Morgenstern-Price method	54
3.8	Corps of Engineers method	58
	Interslice assumption one	58
	Interslice assumption two	60
3.9	Lowe-Karafiath method.....	63
3.10	Sarma method	65
3.11	Janbu's Generalized method	67
3.12	Finite element stress-based method	69
3.13	Commentary on finite element stress-based method	76
3.14	Selecting an appropriate method.....	79
4	Slip Surface Shapes	81
4.1	Introduction and background	81
4.2	Grid and radius for circular slips	82
	Single radius point.....	84
	Multiple radius points.....	85
	Lateral extent of radius lines	85
	Factor of Safety contours	86
4.3	Composite slip surfaces.....	89
4.4	Fully specified slip surfaces	92
4.5	Block specified slip surface.....	94
	General cross-over form	94
	Specific parallel form	97
4.6	Entry and exit specification	99
4.7	Optimization	101
4.8	Auto-search.....	104

4.9	Effect of soil strength	106
	Purely frictional case	106
	Undrained strength case	108
	Cause of unrealistic response	109
	Minimum depth	111
	Most realistic slip surface position.....	111
4.10	Tension cracks and exit projections	112
	Tension crack angle	112
	Automatic tension crack search	113
	Constant tension crack depth.....	113
	Tension crack fluid pressures	113
	Toe projection.....	114
4.11	Physical admissibility	114
4.12	Invalid slip surfaces and factors of safety.....	116
4.13	Concluding remarks	122
5	Geometry	125
5.1	Introduction	125
5.2	Regions.....	125
5.3	Slice discretization	128
5.4	Ground surface line	131
5.5	Surface surcharge pressures.....	132
5.6	Tension crack line	135
5.7	Concentrated line loads	136
6	Material Strength.....	139
6.1	Introduction	139
6.2	Mohr-Coulomb	139
6.3	Undrained strength	141

6.4	No strength	141
6.5	Impenetrable (Bedrock)	141
6.6	Bilinear	141
6.7	General data-point strength envelope	142
6.8	Anisotropic strength	144
6.9	Strength using an anisotropic function	144
6.10	Strength as a function of depth.....	146
	Relative to top of soil layer	146
	Relative to specified datum	146
6.11	Frictional-undrained combined models.....	147
6.12	SHANSEP or strength = f(overburden) model.....	148
6.13	Hoek and Brown model	149
6.14	Unsaturated shear strength	156
6.15	Soil unit weight.....	157
6.16	Other soil parameters	159
7	Pore-water	161
7.1	Introduction	161
7.2	Piezometric surfaces	161
	Single piezometric line	162
	Multiple piezometric lines	162
	Phreatic correction	163
7.3	R_u Coefficients	164
7.4	B-bar coefficients	166
7.5	Pore-water pressures at discrete points	167
7.6	Negative pore-water pressures.....	168
7.7	Finite element computed pressures	168
7.8	Recommended practice	171

8	Reinforcement and Structural Components.....	173
8.1	Introduction	173
8.2	Fundamentals related to concentrated lateral loads	174
	Mobilization of reinforcement forces	174
	Slice forces and stress distributions.....	176
	Convergence	181
	Safety factors of the various components.....	183
	Recommended analysis approach.....	183
	Summary	183
8.3	Anchors.....	184
	Bar capacity and reinforcement load.....	185
	Bond resistance.....	185
	Applied load.....	186
	Shear force	190
8.4	Nails	190
8.5	Geo-fabric reinforcement	193
	Bond resistance a specified constant.....	193
	Bond resistance a function of overburden stress	195
	Load orientation.....	196
8.6	Wall facing	196
8.7	Piles and dowels	197
8.8	Sheet pile walls	198
8.9	Deep-seated instability	200
8.10	Mitigation of numerical problems	200
8.11	Finite element stress-based approach	201
	Wall with nails.....	201
	Tie-back wall	206
	Soil-structure interaction safety factors	210

	Shear wall.....	211
	Key issues.....	214
9	Seismic and Dynamic Stability.....	217
9.1	Introduction	217
9.2	Rapid loading strength.....	217
9.3	Pseudostatic analysis	219
9.4	Dynamic analysis.....	224
9.5	Permanent deformation	226
9.6	Liquefaction stability	230
10	Probabilistic and Sensitivity Analyses.....	233
10.1	Introduction	233
10.2	Probability density functions	233
	Normal function	233
	Lognormal function.....	237
	Uniform function	239
10.3	Triangular probability function.....	241
10.4	General probability function	242
10.5	C – ϕ correlation.....	244
10.6	Probability of failure and reliability index	245
10.7	Spatial variability	247
10.8	Multiple statistical parameters	253
10.9	Sensitivity analyses	253
11	Illustrative Examples.....	257
11.1	Circular slip surface analysis	257
11.2	Composite slip surface analysis	261
11.3	Hand calculation comparison of SLOPE/W	266
	Lambe and Whitman's solutions	266

	SLOPE/W Solutions	269
11.4	Comparison with stability charts	272
	Bishop and Morgenstern's solution	272
	SLOPE/W solution stability chart	273
11.5	Comparison with closed form solutions for an infinite slope.....	274
	Closed form solution for an infinite slope	274
	SLOPE/W solution closed form.....	276
11.6	Comparison study	278
11.7	Fully specified slip surface analysis.....	282
11.8	Block specified slip surface analysis	286
11.9	Pore-water pressures defined by pressure data points	291
11.10	Example with slip surface projection under a footing	295
11.11	Use of anisotropic features	299
	Soil #1 – anisotropic strength model	303
	Soil #2 – anisotropic function	305
	Soil #3 – S = function (overburden)	306
11.12	SEEP/W pore-water pressures used in a stability analysis.....	308
11.13	Finite element slope stability method	313
11.14	Rapid drawdown analysis	317
	Before drawdown	318
	After drawdown	320
11.15	Slope reinforcement with anchor	323
11.16	Slope reinforcement with geo-fabric	328
11.17	Probabilistic analysis example.....	333
11.18	Auto locate slip surface example.....	339
11.19	Partially and fully submerged slope	344
11.20	Permanent deformation analysis	351

12	Theory.....	357
12.1	Introduction	357
12.2	Definition of variables	357
12.3	General limit equilibrium method	363
12.4	Moment equilibrium factor of safety.....	364
12.5	Force equilibrium factor of safety.....	364
12.6	Slice normal force at the base	365
12.7	M-alpha values.....	366
12.8	Interslice forces.....	368
12.9	Effect of negative pore-water pressures.....	370
12.10	Factor of safety for unsaturated soil	371
12.11	Use of unsaturated shear strength parameters.....	372
12.12	Solving for the factors of safety	373
	Stage 1 solution.....	373
	Stage 2 solution.....	373
	Stage 3 solution.....	373
	Stage 4 solution.....	374
12.13	Simulation of the various methods.....	375
12.14	Spline interpolation	376
12.15	Moment axis.....	378
12.16	Finite element stress method.....	379
	Stability factor	379
	Normal stress and mobilized shear stress	381
12.17	Probabilistic slope stability analysis.....	383
	Monte Carlo method.....	383
	Parameter variability.....	384
	Random number generation	385
	Correlation coefficient.....	385

Number of Monte Carlo trials	386
References	387
Index	391

1 Introduction

Analyzing the stability of earth structures is the oldest type of numerical analysis in geotechnical engineering. The idea of discretizing a potential sliding mass into slices was introduced early in the 20th Century. In 1916, Petterson (1955) presented the stability analysis of the Stigberg Quay in Gothenberg, Sweden where the slip surface was taken to be circular and the sliding mass was divided into slices. During the next few decades, Fellenius (1936) introduced the Ordinary or Swedish method of slices. In the mid-1950s Janbu (1954) and Bishop (1955) developed advances in the method. The advent of electronic computers in the 1960's made it possible to more readily handle the iterative procedures inherent in the method which led to mathematically more rigorous formulations such as those developed by Morgenstern and Price (1965) and by Spencer (1967). One of the reasons the limit equilibrium method was adopted so readily, is that solutions could be obtained by hand-calculations. Simplifying assumption had to be adopted to obtain solutions, but the concept of numerically dividing a larger body into smaller pieces for analysis purposes was rather novel at the time.

Even to this day, stability analyses are by far the most common type of numerical analysis in geotechnical engineering. This is in part because stability is obviously a key issue in any project – will the structure remain stable or collapse? This, however, is not the only reason. Concepts associated with the method of slices are not difficult to grasp and the techniques are rather easy to implement in computer software – the simpler methods can even be done on a spreadsheet. Consequently, slope stability software became available soon after the advent of computers. The introduction of powerful desktop personal computers in the early 1980s made it economically viable to develop commercial software products based on these techniques, and the ready availability today of such software products has led to the routine use of limit equilibrium stability analysis in geotechnical engineering practice.

Modern limit equilibrium software is making it possible to handle ever-increasing complexity within an analysis. It is now possible to deal with complex stratigraphy, highly irregular pore-water pressure conditions, various linear and nonlinear shear strength models, almost any kind of slip surface shape, concentrated loads, and structural reinforcement. Limit equilibrium formulations based on the method of slices are also being applied more and more to the stability analysis of structures such as tie-back walls, nail or fabric reinforced slopes, and

even the sliding stability of structures subjected to high horizontal loading arising, for example, from ice flows.

While modern software is making it possible to analyze ever-increasingly complex problems, the same tools are also making it possible to better understand the limit equilibrium method itself. Computer-assisted graphical viewing of data used in the calculations makes it possible to look beyond the factor of safety. For example, graphically viewing all the detailed forces on each slice in the potential sliding mass, or viewing the distribution of a variety of parameters along the slip surface, helps greatly to understand the details of the technique.

While the graphical viewing of computed details has led to a greater understanding of the method, particularly the differences between the various methods available, it has also led to the exposure of limitations in the limit equilibrium formulations. Exposure of the limitations has revealed that the method is perhaps being pushed too far beyond its initial intended purpose. The method of slices was initially conceived for the situation where the normal stress along the slip surface is primarily influenced by gravity (weight of the slice). Including reinforcement in the analysis goes far beyond the initial intention. Even though the limitations do not necessarily obviate using the method in practice, understanding the limitations is vital to understanding and relying on the results.

Despite the extensive and routine use of stability analyses in practice, it seems the fundamentals of the limit equilibrium method of slices are not well understood. The fact that the limit equilibrium method of slices is based on nothing more than statics often seems to be forgotten, and the significance of one factor of safety for all slices is not appreciated.

SLOPE/W, in one form, or another has been on the market since 1977. The initial code was developed by Professor D.G. Fredlund at the University of Saskatchewan. The first commercial version was installed on mainframe computers and users could access the software through software bureaus. Then in the 1980s when Personal Computers (PCs) became available, the code was completely re-written for the PC environment. Processing time was now available at the relatively low fixed cost of the computer, but computer memory was scarce and so the code had to be re-structured for this hardware environment. The product was renamed PC-SLOPE/W and released in 1983. Later in the 1980s it became evident that graphical interaction with PC software was going to be the wave of the future, and consequently a graphical CAD-like user interface was developed. The software was again renamed as SLOPE/W to reflect the Microsoft Windows

environment and that it now had a graphical user interface. SLOPE/W was the very first geotechnical software product available commercially for analyzing slope stability. Currently, SLOPE/W is being used by thousands of professionals both in education and in practice.

Over the years, as computer technology has advanced, SLOPE/W has continually been enhanced and upgraded. This book is based on Version 6 of the program.

When using software like SLOPE/W with its myriad of options, it is often necessary to look at more than just the factor of safety. Other issues to consider include, but are not limited to: Was the intended data correctly specified? Was the data used correctly by the software? Why are there differences between factors of safety from the various methods? To help answer these types of questions, SLOPE/W has many tools for inspecting the input data and evaluating the results – tools like allowing you to graph a list of different variables along the slip surface or to display the detail forces on each slice, for example. These types of tools are vitally important to judging and being confident in the results.

Earlier it was noted that despite the extensive use of limit equilibrium methods in routine practice, the fundamentals of the formulations and the implications of the inherent assumptions are not well understood. An entire chapter is consequently devoted to a review of the fundamentals of limit equilibrium as a method of analysis. The chapter looks at the consequences of a pure statics formulation, what are the differences between the various methods, why are interslice forces important, what effect does the shape of the slip surface have, and so forth. In addition, the chapter discusses the limitations of the limit equilibrium method and discusses ways of overcoming the limitations. Gaining a thorough understanding of these fundamentals is essential to effective use of SLOPE/W.

SLOPE/W is one component in a complete suite of geotechnical products called GeoStudio. One of the powerful features of this integrated approach is that it opens the door to types of analyses of a much wider and more complex spectrum of problems, including the use of finite element computed pore-water pressures and stresses in a stability analysis. Not only does an integrated approach widen the analysis possibilities, it can help overcome some limitations of the purely limit equilibrium formulations. Although, it is not necessary to use this advanced feature as SLOPE/W can be used as an individual product, there is certainly an increase in the capability of the program by using it as one component of a complete suite of geotechnical software programs.

The very large number of options in SLOPE/W can be somewhat confusing, especially when you are using the software for the first time. Some semblance of order can be made of these options by thinking of a problem in terms of five components. They are:

- Geometry – description of the stratigraphy and shapes of potential slip surfaces.
- Soil strength - parameters used to describe the soil (material) strength
- Pore-water pressure – means of defining the pore-water pressure conditions
- Reinforcement or soil-structure interaction – fabric, nails, anchors, piles, walls and so forth.
- Imposed loading – surcharges or dynamic earthquake loads

Separate chapters are devoted to each of these main components.

More and more engineers are interested in conducting probabilistic types of stability. An entire chapter is devoted to the special subject of probabilistic analysis and sensitivity studies.

Examples are included throughout the book to illustrate features and explain behavior. In addition there is a special section devoted to illustrative examples, which are intended to provide ideas on how to model various situations. The examples are not intended to be complete case histories, but instead are intended to be simple illustrations used to highlight possible situations including complete submergence, stability on a synthetic liner, and bearing pressure.

At the end of the book is a chapter on theory. This chapter is included primarily as a reference, as a connection to the past and as information for those who are curious about the fundamental details used in SLOPE/W. Generally, it should not be necessary to spend too much time in this chapter to use SLOPE/W effectively.

This book is aimed at highlighting engineering concepts and stability analysis modeling techniques. This book is not aimed at describing all the software interaction commands and the meaning of all the various parameters in the dialogs boxes. These details are provided in the online help.

SLOPE/W has been designed and developed to be a general software tool for the stability analysis of earth structures. SLOPE/W is not designed for certain specific

cases. SLOPE/W was not created specifically to design retaining walls, although SLOPE/W can certainly be used to assess the sliding stability of a gravity retaining wall, or to find the active earth forces on the wall. Likewise, SLOPE/W was not specifically designed for earth-reinforced retaining walls, but SLOPE/W can be used to analyze the stability of a wedge of soil that has been reinforced with a structural component such as a pre-stressed anchor, a soil nail, geo-fabric or some other material. Using a general tool such as SLOPE/W sometimes requires careful thought as to how to model a certain situation, but at the same time it greatly expands the range of possible situations you can model, which has been our main intention. The general nature allows for much greater creativity. Once you understand how the general features function, the types of problems that can be analyzed are primarily limited by your creativity. The main purpose of this book is to help you be creative, not to outline an endless list of rules you must follow.

2 Limit Equilibrium Fundamentals

2.1 Introduction

In 2003, at the Canadian Geotechnical Conference in Calgary, Alberta, Krahn (2003) presented the R.M. Hardy Lecture. The title of the lecture was, *The Limits of Limit Equilibrium Analyses*. This chapter is in large part a replication of this Lecture and as published in the Canadian Geotechnical Journal, Vol. 40, pages 643 to 660.

The main message of the lecture was that limit equilibrium methods for assessing the stability of earth structures are now used routinely in practice. In spite of this extensive use, the fundamentals of the methods are often not that well understood and expectations exceed what the methods can provide. The fact and implications that limit equilibrium formulations are based on nothing more than equations of statics with a single, constant factor of safety is often not recognized. A full appreciation of the implications reveals that the method has serious limitations.

To use limit equilibrium methods effectively, it is important to understand and comprehend the inherent limitations. This chapter discusses the fundamentals of limit equilibrium formulations, points out the limitations, explores what can be done to overcome the limitations, and ends with general guidelines on the continued use of the method in practice.

2.2 Background and history

Limit equilibrium types of analyses for assessing the stability of earth slopes have been in use in geotechnical engineering for many decades. The idea of discretizing a potential sliding mass into vertical slices was introduced early in the 20th century and is consequently the oldest numerical analysis technique in geotechnical engineering.

In 1916, Petterson (1955) presented the stability analysis of the Stigberg Quay in Gothenberg, Sweden where the slip surface was taken to be circular and the sliding mass was divided into slices. During the next few decades, Fellenius (1936) introduced the Ordinary or Swedish method of slices. In the mid-1950s Janbu (1954) and Bishop (1955) developed advances in the method. The advent of electronic computers in the 1960s made it possible to more readily handle the iterative procedures inherent in the method, which led to mathematically more

rigorous formulations such as those developed by Morgenstern and Price (1965) and by Spencer (1967). The introduction of powerful desktop personal computers in the early 1980s made it economically viable to develop commercial software products based on these techniques, and the ready availability today of such software products has led to the routine use of limit equilibrium stability analysis in geotechnical engineering practice.

Modern limit equilibrium software such as SLOPE/W is making it possible to handle ever-increasing complexity in the analysis. It is now possible to deal with complex stratigraphy, highly irregular pore-water pressure conditions, a variety of linear and nonlinear shear strength models, virtually any kind of slip surface shape, concentrated loads, and structural reinforcement. Limit equilibrium formulations based on the method of slices are also being applied more and more to the stability analysis of structures such as tie-back walls, nail or fabric reinforced slopes, and even the sliding stability of structures subjected to high horizontal loading arising, for example, from ice flows.

While modern software is making it possible to analyze ever-increasingly complex problems, the same tools are also making it possible to better understand the limit equilibrium method. Computer-assisted graphical viewing of data used in the calculations makes it possible to look beyond the factor of safety. For example, graphically viewing all the detailed forces on each slice in the potential sliding mass, or viewing the distribution of a variety of parameters along the slip surface, helps greatly to understand the details of the technique. From this detailed information, it is now becoming evident that the method has its limits and that it is perhaps being pushed beyond its initial intended purpose. Initially, the method of slices was conceived for the situation where the normal stress along the slip surface is primarily influenced by gravity (weight of the slice). Including reinforcement in the analysis goes far beyond the initial intention.

2.3 *Method basics*

Many different solution techniques for the method of slices have been developed over the years. Basically, all are very similar. The differences between the methods are what equations of statics are included and satisfied, which interslice forces are included and what is the assumed relationship between the interslice shear and normal forces. Figure 2-1 illustrates a typical sliding mass discretized into slices and the possible forces on the slice. Normal and shear forces act on the slice base and on the slice sides.

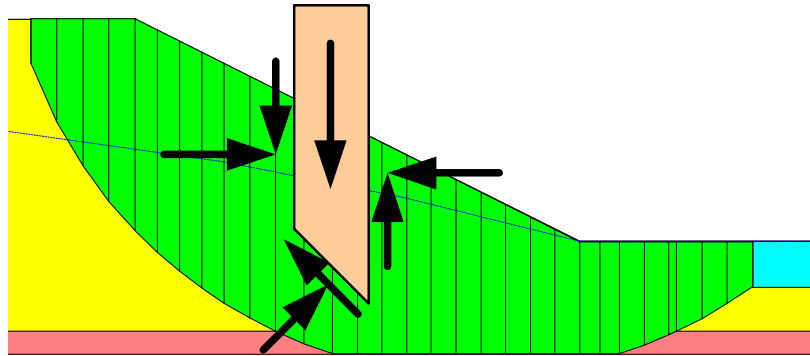


Figure 2-1 Slice discretization and slice forces in a sliding mass

The Ordinary, or Fellenius method was the first method developed. The method ignored all interslice forces and satisfied only moment equilibrium. Adopting these simplified assumptions made it possible to compute a factor of safety using hand calculations, which was important since there were no computers available.

Later Bishop (1955) devised a scheme that included interslice normal forces, but ignored the interslice shear forces. Again, Bishop's Simplified method satisfies only moment equilibrium. Of interest and significance with this method is the fact that by including the normal interslice forces, the factor of safety equation became nonlinear and an iterative procedure was required to calculate the factor of safety. The Janbu's Simplified method is similar to the Bishop's Simplified method in that it includes the normal interslice forces and ignores the interslice shear forces. The difference between the Bishop's Simplified and Janbu's Simplified methods is that the Janbu's Simplified method satisfies only horizontal force equilibrium, as opposed to moment equilibrium.

Later, computers made it possible to more readily handle the iterative procedures inherent in the limit equilibrium method, and this led to mathematically more rigorous formulations which include all interslice forces and satisfy all equations of statics. Two such methods are the Morgenstern-Price and Spencer methods.

Table 2-1 lists the methods available in SLOPE/W and indicates what equations of statics are satisfied for each of the methods. Table 2-2 gives a summary of the interslice forces included and the assumed relationships between the interslice shear and normal forces.

Further details about all the methods are presented elsewhere.

Table 2-1 Equations of Statics Satisfied

Method	Moment Equilibrium	Force Equilibrium
Ordinary or Fellenius	Yes	No
Bishop's Simplified	Yes	No
Janbu's Simplified	No	Yes
Spencer	Yes	Yes
Morgenstern-Price	Yes	Yes
Corps of Engineers – 1	No	Yes
Corps of Engineers – 2	No	Yes
Lowe-Karafiath	No	Yes
Janbu Generalized	Yes (by slice)	Yes
Sarma – vertical slices	Yes	Yes

Table 2-2 Interslice force characteristics and relationships

Method	Interslice Normal (E)	Interslice Shear (X)	Inclination of X/E Resultant, and X-E Relationship
Ordinary or Fellenius	No	No	No interslice forces
Bishop's Simplified	Yes	No	Horizontal
Janbu's Simplified	Yes	No	Horizontal
Spencer	Yes	Yes	Constant
Morgenstern-Price	Yes	Yes	Variable; user function
Corps of Engineers – 1	Yes	Yes	Inclination of a line from crest to
Corps of Engineers – 2	Yes	Yes	Inclination of ground surface at top of slice
Lowe-Karafiath	Yes	Yes	Average of ground surface and slice base inclination
Janbu Generalized	Yes	Yes	Applied line of thrust and moment equilibrium of slice
Sarma – vertical slices	Yes	Yes	$X = C + E \tan \phi$

2.4 General limit equilibrium method

A general limit equilibrium (GLE) formulation was developed by Fredlund at the University of Saskatchewan in the 1970s (Fredlund and Krahn 1977; Fredlund et al. 1981). This method encompasses the key elements of all the methods listed in Table 1. The GLE formulation is based on two factors of safety equations and allows for a range of interslice shear-normal force conditions. One equation gives the factor of safety with respect to moment equilibrium (F_m) while the other equation gives the factor of safety with respect to horizontal force equilibrium (F_f). The idea of using two factor of safety equations was actually first published by Spencer (1967).

The interslice shear forces in the GLE method are handled with an equation proposed by Morgenstern and Price (1965). The equation is:

$$X = E \lambda f(x)$$

where:

$f(x)$	=	a function,
λ	=	the percentage (in decimal form) of the function used,
E	=	the interslice normal force, and
X	=	the interslice shear force.

Figure 2-2 shows a typical half-sine function. The upper curve in this figure is the actual specified function. The lower curve is the function used. The ratio between the two curves represents λ . Lambda (λ) in Figure is 0.43. At Slice 10, $f(x) = 0.83$. If, for example, $E = 100$ kN, then $X = E f(x) \lambda = 100 \times 0.43 \times 0.83 = 35.7$ kN. $\tan^{-1}(35.7/100) = 19.6$ degrees. This means the interslice resultant force is inclined at 19.6 degrees from the horizontal at Slice 10. One of the key issues in the limit equilibrium formulation, as will be illustrated later, is knowing how to define this interslice function.

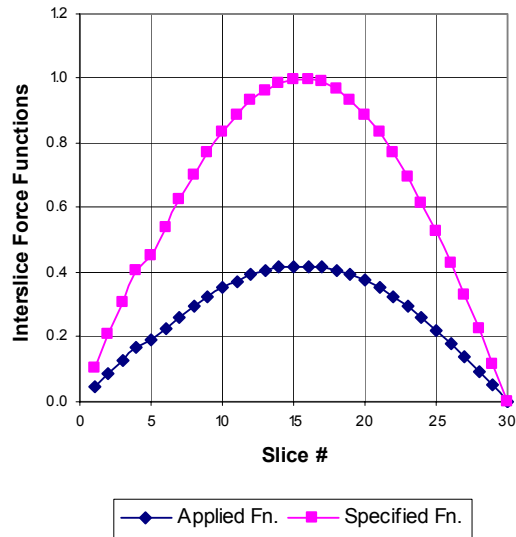


Figure 2-2 Half-sine interslice force function

The GLE factor of safety equation with respect to moment equilibrium is:

$$F_m = \frac{\sum (c' \beta R + (N - u \beta) R \tan \phi')}{\sum W_x - \sum N f \pm \sum D d}$$

The factor of safety equation with respect to horizontal force equilibrium is:

$$F_f = \frac{\sum (c' \beta \cos \alpha + (N - u \beta) \tan \phi' \cos \alpha)}{\sum N \sin \alpha - \sum D \cos \omega}$$

The terms in the equations are:

c'	=	effective cohesion
ϕ'	=	effective angle of friction
u	=	pore-water pressure
N	=	slice base normal force
W	=	slice weight
D	=	line load

$\beta, R, x, f, d, \omega$ = geometric parameters
 α = inclination of slice base

(There are additional terms in the factor of safety equations, but they are not required for the discussion on limit equilibrium fundamentals; the complete equations are presented in the theory chapter.)

One of the key variables in both equations is N , the normal at the base of each slice. This equation is obtained by the summation of vertical forces, thus vertical force equilibrium is consequently satisfied. In equation form, the base normal is defined as:

$$N = \frac{W + (X_R - X_L) - \frac{c' \beta \sin \alpha + u \beta \sin \alpha \tan \phi'}{F}}{\cos \alpha + \frac{\sin \alpha \tan \phi'}{F}}$$

F is F_m when N is substituted into the moment factor of safety equation and F is F_f when N is substituted into the force factor of safety equation. The literature on slope stability analysis often refers to the denominator of this equation as m_α .

A very important point to make here is that the slice base normal is dependent on the interslice shear forces X_R and X_L on either side of a slice. The slice base normal is consequently different for the various methods, depending on how each method deals with the interslice shear forces.

The GLE method computes F_m and F_f for a range of lambda (λ) values. With these computed values, a plot similar to Figure 2-3 can be drawn which shows how F_m and F_f vary with lambda (λ).

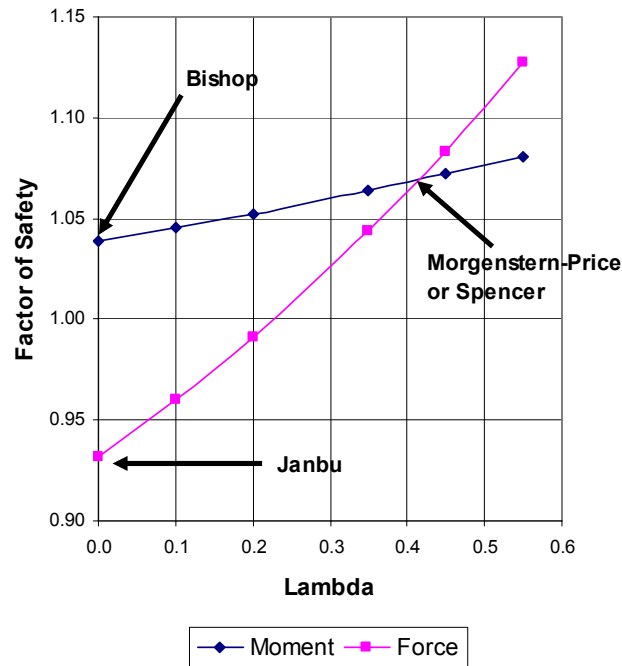


Figure 2-3 A factor of safety versus lambda (λ) plot

As listed in Table 2-1 and Table 2-2, Bishop's Simplified method ignores interslice shear forces and satisfies only moment equilibrium. In the GLE terminology, neglecting interslice shear forces means λ is zero. As a result, the Bishop's Simplified factor of safety falls on the moment curve in Figure 2-3 where lambda is zero. Janbu's Simplified method also ignores interslice shear forces and only satisfies force equilibrium. The Janbu's Simplified factor of safety consequently falls on the force curve in Figure 2-3 where λ is zero. The Spencer and Morgenstern-Price (M-P) factors of safety are determined at the point where the two curves cross in Figure 2-3. At this point, the factor of safety satisfies both moment and force equilibrium. Whether the crossover point is the Spencer or M-P factor of safety depends on the interslice force function. Spencer only considered a constant X/E ratio for all slices, which in the GLE formulation corresponds to a constant (horizontal) interslice force function. The M-P method can utilize any general appropriate function. The Corp of Engineers and Lowe-Karafiath factors of safety fall on the force curve in Figure 2-3. The position on the force curve depends on the procedure used to establish the inclinations of the interslice

resultant. The inclination of the interslice resultant is $\arctan(\lambda)$ when $f(x)$ is a constant 1.0 as in the Spencer method.

The GLE method is very useful for explaining the differences between the various methods and for determining how the interslice force functions influence the computed factor of safety, as discussed in more detail below.

There is one characteristic in the two factor of safety equations and the base normal equation that have a profound consequence. In the end there is only one factor of safety for the overall slope. F_m and F_f are the same when both moment and force equilibrium are satisfied. This same value appears in the equation for the normal at the slice base. This means the factor of safety is the same for each and every slice. As we will see later, this has a significant effect on the resulting computed stress distributions within the sliding mass and along the slip surface.

Another important point about the GLE method is that it is not restricted by the shape of the slip surface. The Bishop's Simplified method was initially developed for circular slip surfaces, but the assumptions inherent in the Bishop's Simplified method can be applied to any noncircular slip surface. In fact, with the GLE formulation, all methods listed in Table 2-1 can be applied to any kinematically admissible slip surface shape.

2.5 Interslice force functions

How the interslice shear forces are handled and computed is a fundamental point with most of the methods listed in Table 2-1. The Spencer method, for example, uses a constant function which infers that the ratio of shear to normal is a constant between all slices. You do not need to select the function; it is fixed to be a constant function in the software when the Spencer method is selected.

Only the Morgenstern-Price and GLE methods allow for user-specified interslice functions. Some of the functions available are the constant, half-sine, clipped-sine, trapezoidal and data-point specified. The most commonly used functions are the constant and half-sine functions. A Morgenstern-Price or GLE analysis with a constant function is the same as a Spencer analysis.

SLOPE/W by default uses the half-sine function for the M-P and GLE methods. The half-sine function tends to concentrate the interslice shear forces towards the middle of the sliding mass and diminishes the interslice shear in the crest and toe areas. Defaulting to the half-sine function for these methods is based primarily on

experience and intuition and not on any theoretical considerations. Other functions can be selected if deemed necessary.

The Sarma method deals with the interslice shear-normal relationship somewhat differently. Most methods use a specified function or a specified direction to establish the relationship between the interslice shear and normal. The Sarma method uses a shear strength equation as noted in Table 2-2. This approach does not offer any particular advantages over the other approaches, for reasons that will become clear later in this chapter. In the end, this is just another mechanism to compute interslice shear forces from the normal forces, and is included primarily for completeness and to accommodate user preferences.

The influence and importance of the interslice forces is discussed in the next section.

2.6 Slip surface shapes

The importance of the interslice force function depends to a large extent on the amount of contortion the potential sliding mass must undergo to move. The function is not important for some kinds of movement while the function may significantly influence the factor of safety for other kinds of movement. The following examples illustrate this sensitivity.

Circular slip surface

Figure 2-4 presents a simple circular slip surface together with the associated FS vs λ plot. In this case the moment equilibrium is completely independent of the interslice shear forces, as indicated by the horizontal moment equilibrium curve. The force equilibrium, however, is dependent on the interslice shear forces.

The moment equilibrium is not influenced by the shear forces because the sliding mass as a free body can rotate without any slippage between the slices. However, substantial interslice slippage is necessary for the sliding mass to move laterally. As a consequence the horizontal force equilibrium is sensitive to interslice shear.

Since the moment equilibrium is completely independent of interslice shear, any assumption regarding an interslice force function is irrelevant. The interslice shear can be assumed to be zero, as in the Bishop's Simplified method, and still obtain an acceptable factor of safety, provided the method satisfies moment equilibrium. This is, of course, not true for a method based on satisfying only horizontal force equilibrium such as the Janbu's Simplified method. Ignoring the interslice shear

when only horizontal force equilibrium is satisfied for a curved slip surface results in a factor of safety significantly different than when both force and moment equilibrium is satisfied.

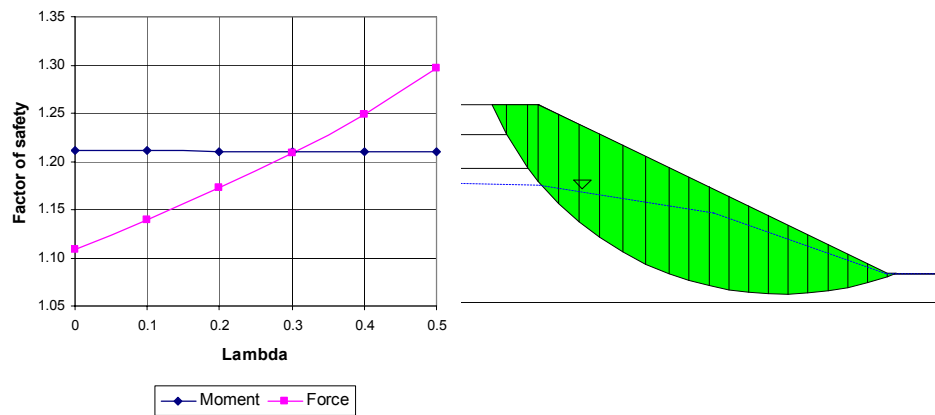


Figure 2-4 Conditions for a simple circular slip surface

The moment equilibrium curve is not always perfectly horizontal for circular slip surfaces. The moment curve in Figure 2-4 was obtained from a circular slip surface analysis and it is slightly inclined. Usually, however, the slope of the moment curve is nearly horizontal. This is why the Bishop and Morgenstern-Price factors of safety are often similar for circular slip surfaces.

Planar slip surface

Figure 2-5 illustrates a planar slip surface. The moment and force equilibrium curves now have reverse positions from those for a circular slip surface. Now force equilibrium is completely independent of interslice shear, while moment equilibrium is fairly sensitive to the interslice shear. The soil wedge on the planar slip surface can move without any slippage between the slices. Considerable slippage is, however, required for the wedge to rotate.

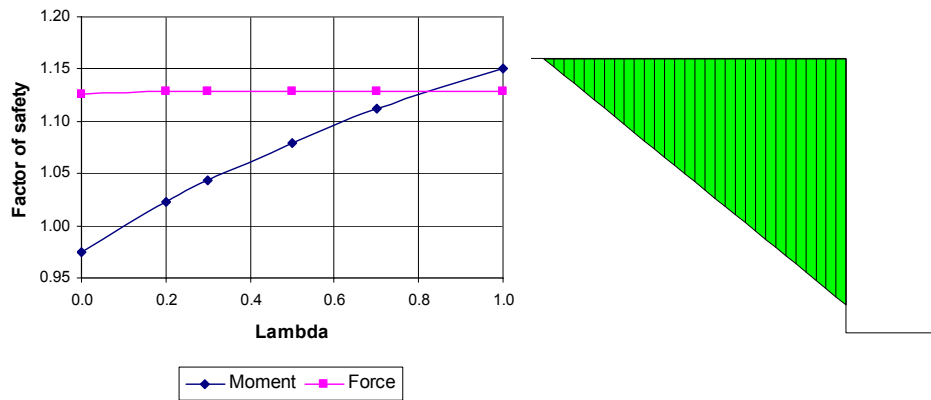


Figure 2-5 Situation for a planar slip surface

Composite slip surface

A composite slip surface is one where the slip surface is partly on the arc of a circle and partly on a planar surface, as illustrated in Figure 2-6. The planar portion in this example follows a weak layer, a common situation in many stratigraphic settings. In this case, both moment and force equilibrium are influenced by the interslice shear forces. Force equilibrium factors of safety increase, while moment equilibrium factors of safety decrease as the interslice shear forces increase (higher lambda values).

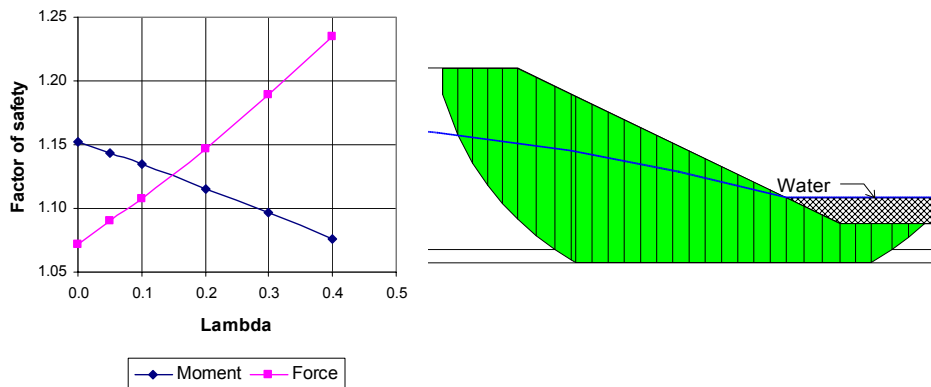


Figure 2-6 Situation for a typical composite slip surface

This illustrates that a Bishop's Simplified type of analysis does not always err on the safe side. A more rigorous formulation such as the Morgenstern-Price or Spencer method will give a lower factor of safety than a Bishop Simplified factor of safety. This is not necessarily true for all composite slip surfaces. For some composite slip surfaces, a mathematically more rigorous factor of safety may be higher than the Bishop's Simplified. It is not possible to generalize as to when a more simplified factor of safety will or will not err on the safe side.

Slippage between the slices needs to occur for both moment and force equilibrium for a slip surface of this shape and, consequently, the interslice shear is important for both types of equilibrium.

Block slip surface

Figure 2-7 shows a block-type slip surface. As with the previous composite slip surface, the moment and force equilibrium are both influenced by the interslice shear. The force equilibrium is more sensitive to the shear forces than the moment equilibrium, as indicated by the curve gradients in Figure 2-7. Once again it is easy to visualize that significant slippage is required between the slices for both horizontal translation and rotation, giving rise to the importance of the shear forces.

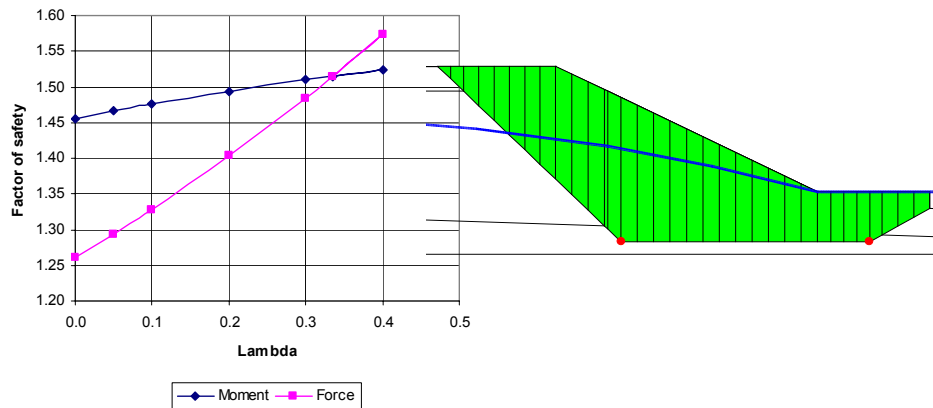


Figure 2-7 Typical situation for a block slip surface

Shoring wall

Figure 2-8 provides an example that examines the deep-seated stability of a shoring wall. The slip surface is beneath the lower tip of the sheet piling. This example comes from the analysis of a deep excavation in downtown Calgary. The FS vs λ plot shows that the moment and force equilibrium curves are similar in this case. They are both very sensitive to the interslice shear forces. Ignoring the interslice shear forces for this case results in a significant underestimation of the factor of safety. Without including the interslice shear forces, the factor of safety is less than 1.0 indicating an unstable situation. Including the shear forces increases the factor of safety to 1.22. The difference again is due to the contortion the potential failing mass would have to undergo to rotate or move laterally.

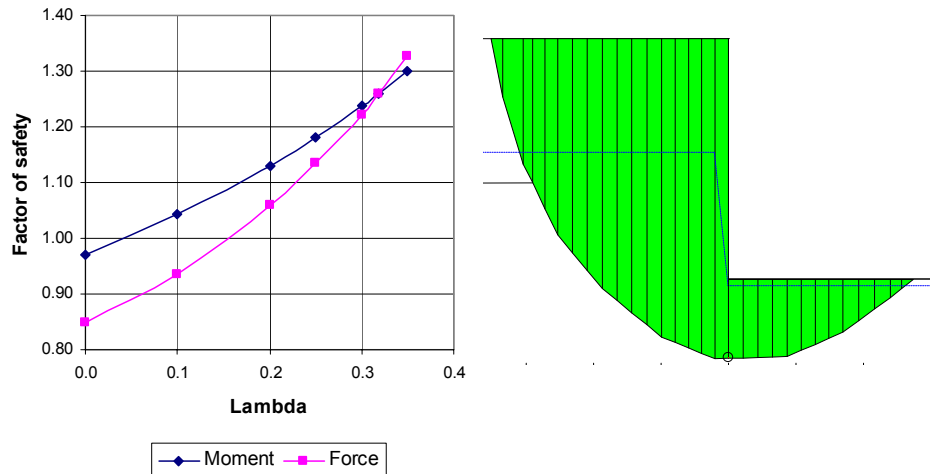


Figure 2-8 A deep stability analysis of a shoring wall

These examples show that the importance of the interslice force functions is strongly related to the shape of the potential slip surface, which in turn is related to the amount of contortion the sliding mass needs to undergo to rotate or move laterally.

When the adopted interslice force function becomes critical in a stability analysis, the limit equilibrium method of slices is approaching the limits of its applicability. Alternative approaches such as described later may then be required.

2.7 Stress distributions

The primary unknown in a limit equilibrium formulation is the normal at the base of the slice. Plotting the stresses along a slip surface gives an indication of the stress distribution in the slope. The computed stresses are, however, not always representative of the true stresses in the ground.

Consider the simple 45-degree slope in Figure 2-9 and Figure 2-10 with a slip surface through the toe and another deeper slip surface below the toe. The normal stress distribution along the slip surface from a limit equilibrium Morgenstern-Price analysis with a constant interslice force function is compared with the normal stress distribution from a linear-elastic finite element stress analysis. For the toe slip surface, the normal stresses are quite different, especially in the toe area. The normal stress distributions for the deeper slip surface are closer, but still different for a good portion of the slip surface.

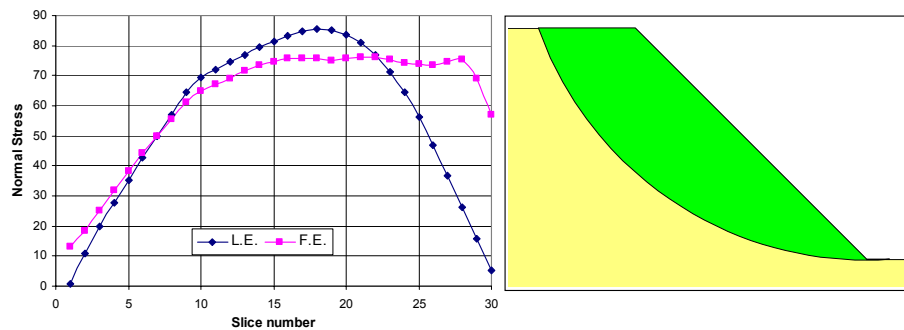


Figure 2-9 Normal stress distribution along a toe slip surface

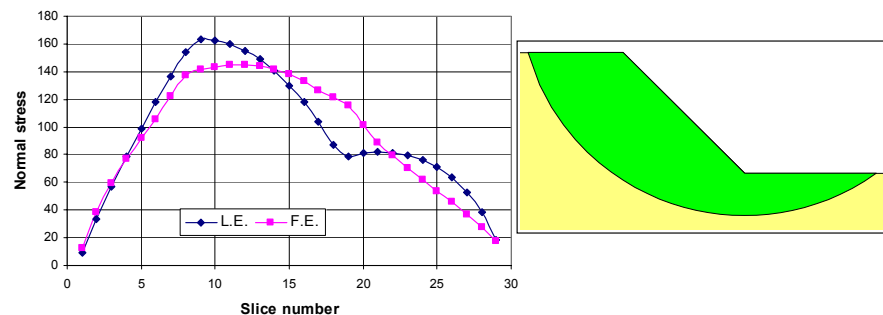


Figure 2-10 Normal stress distribution along a deep slip surface

Figure 2-11 presents a case with reinforcement. The reinforcement loads are applied at the point where the slip surface intersects the line of action. Again there are significant differences between the limit equilibrium normal stresses and the finite element stresses, particularly for the slices which include the line loads. The finite element stresses show some increase in normal stresses due to the nails, but not as dramatic as the limit equilibrium stresses.

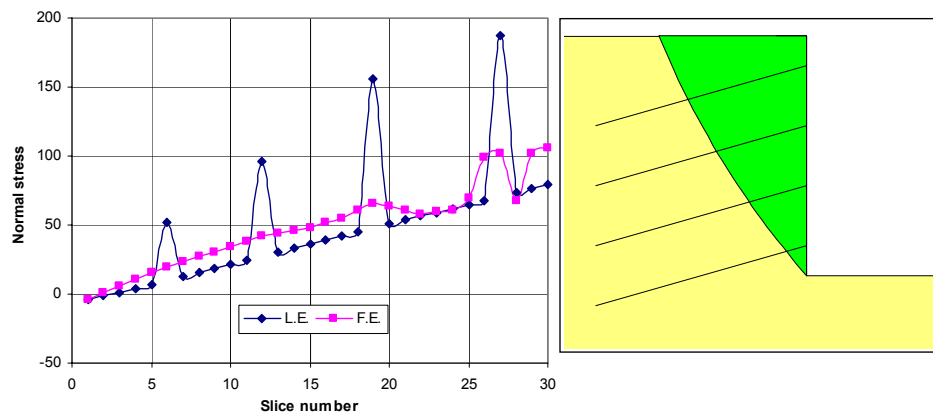


Figure 2-11 Normal stress distributions with reinforcement

These examples show that the stress conditions as computed from a limit equilibrium analysis may be vastly different from finite element computed stresses. The finite element stresses are more realistic and are much closer to the actual conditions in the ground. The implication is that the limit equilibrium computed stresses are not representative of actual field conditions.

The sliding mass internal stresses are also not necessarily representative of actual field conditions. Figure 2.12 presents the case of a tie-back wall with two rows of anchors. The anchor forces are applied where the slip surface intersects the anchor.

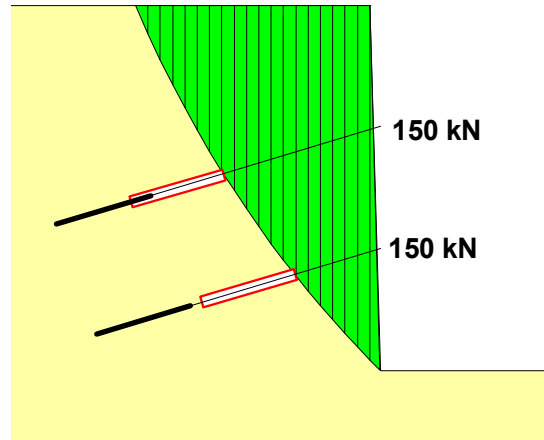


Figure 2-12 Tie-back wall example

The free body diagrams and force polygons for two different slices are presented in Figure 2-13 and Figure 2-14.

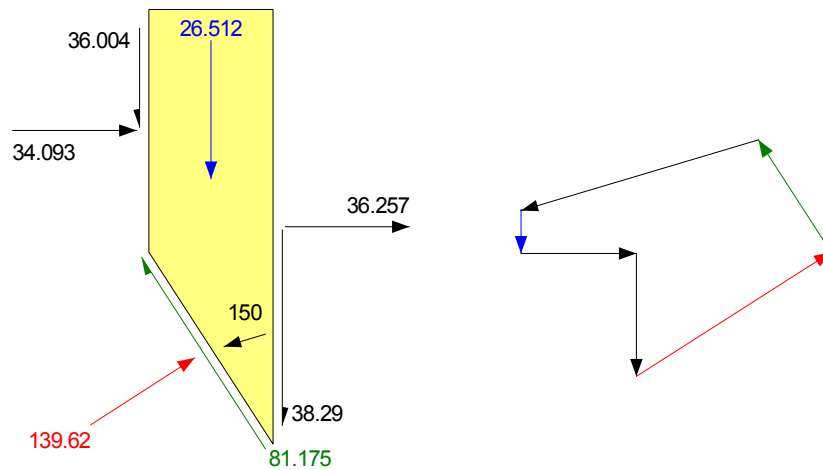


Figure 2-13 Free body and force polygon for upper anchor

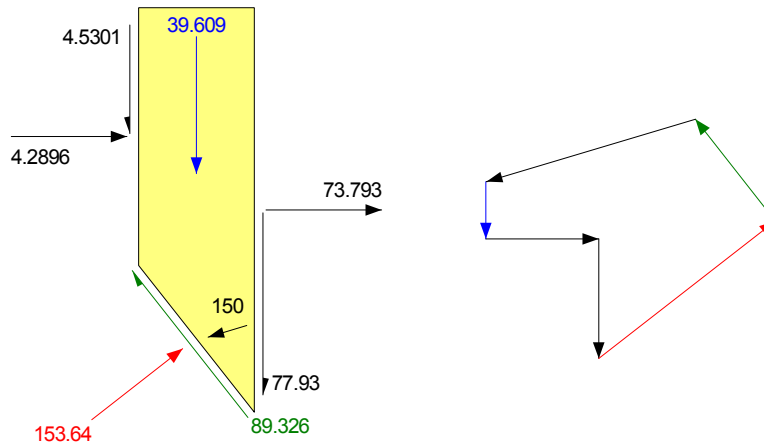


Figure 2-14 Free body and force polygon for lower anchor

Note that the interslice normals point away from the slice on the right side. This indicates tension between the slides, which is obviously not the case in the field. Plotting the interslice forces as in Figure 2-15 further highlights this difficulty. At each of the anchor locations, the interslice normals become negative and the interslice shear forces reverse direction. Of great significance, however, is the fact that the force polygons close signifying that the slices are in equilibrium. In this sense, the results fulfill in part the objectives of the limit equilibrium formulation.

When looking at the exact same situation, but with the anchor loads applied at the wall, the interslice forces are now completely different. Figure 2-16 again shows the interslice shear and normal forces. The normal force increases evenly and gradually except for the last two slices. Of interest is the interslice shear force. The direction is now the reverse of that which usually occurs when only the self weight of the slices is included (simple gravity loading). The shear stress reversal is a reflection of a negative lambda (λ).

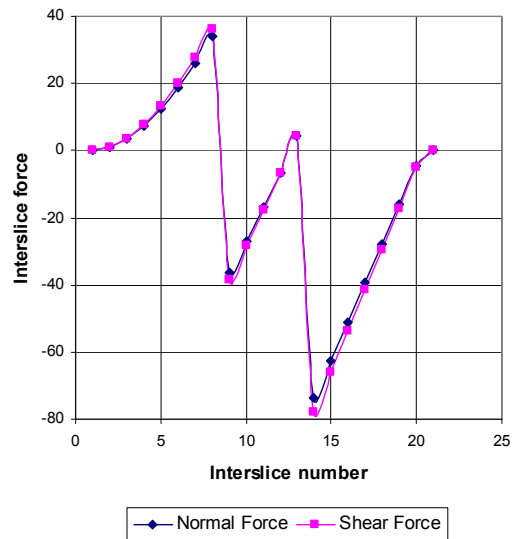


Figure 2-15 Interslice shear and normal forces with anchor loads applied at the slip surface

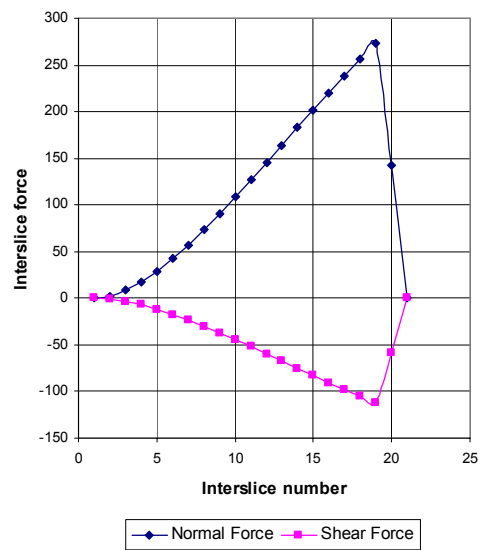


Figure 2-16 Interslice shear and normal forces with anchor loads applied at face of wall

The large differences in the interslice forces also lead to significantly different normal stress distributions along the slip surface, as shown in Figure 2-17. It was noted earlier that the equation for the normal at the base of the slices includes terms for the interslice shear forces. This example vividly illustrates this effect.

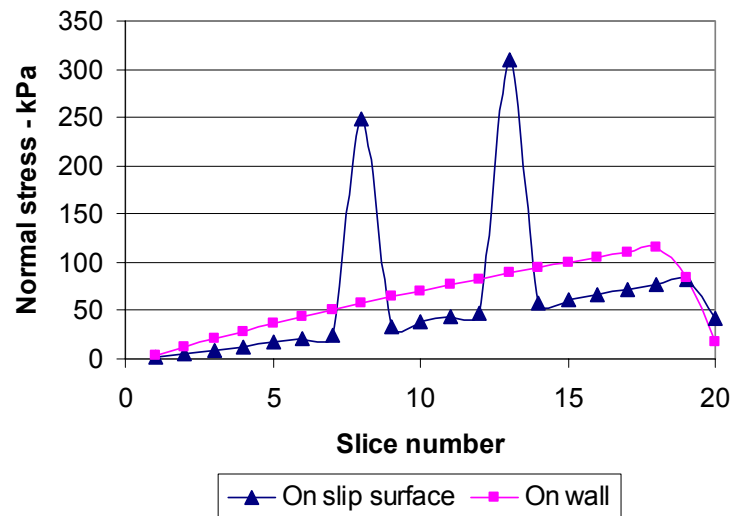


Figure 2-17 Comparison of normal stress distributions

Interestingly, in spite of the vastly different stresses between the slices and along the slip surface, the factors of safety are nearly identical for these two approaches of applying the concentrated line loads. With the anchors applied at the slip surface location, the factor of safety is 1.075 and when they are applied at the wall, the factor of safety is 1.076. The following table highlights this important and significant result.

Anchor Force Location	Factor of Safety
On slip surface	1.075
On wall	1.076

For all practical purposes they are the same. The reason for this is discussed later.

Another reason why the stresses do not represent field conditions is that in the limit equilibrium formulation the factor of safety is assumed to be the same for each slice. In reality this is not correct. In reality the local factor of safety varies significantly, as demonstrated in Figure 2-18.

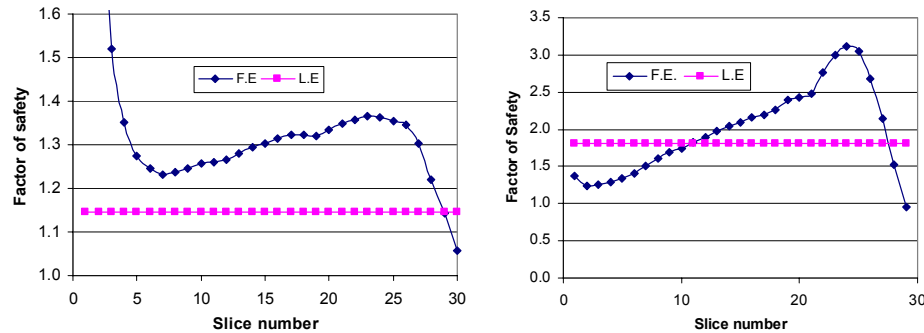


Figure 2-18 Local variation safety factors

Forcing the factor of safety to be the same for all slices over-constrains the problem, with the result that computed stresses are not always real.

2.8 Limit equilibrium forces and stresses

Why can such unrealistic stresses as discussed in the previous section give a seemingly reasonable factor of safety? The answer lies in the fundamental assumption that the factor of safety is the same for each slice. The limit equilibrium method of slices requires iterative techniques to solve the nonlinear factor of safety equations. In the Morgenstern-Price or Spencer methods, a second level of iterations is required to find the slice forces that result in the same F_m and F_f . Fundamentally, the iterations are required to meet two conditions, namely:

- To find the forces acting on each slice so the slice is in force equilibrium, and
- To find the forces on each slice that will make the factor of safety the same for each slice.

This means that interslice and slip surface forces are not necessarily representative of the actual insitu conditions, but they are the forces that satisfy the above two conditions for each slice.

If the slice forces are not representative of actual insitu ground conditions, then it is also not possible to determine a realistic line of thrust for the interslice shear-normal resultant. The forces on each slice that meet the above two conditions can result in a line of thrust outside the slice, a further indication that the slice forces are not always realistic.

Fortunately, even though the limit equilibrium statics formulation does not give realistic slice forces locally, the global factor of safety is nonetheless realistic. Once all the mobilized driving forces and base resisting shear forces are integrated, the local irregularities are smoothed out, making the overall factor of safety for the entire sliding mass quite acceptable.

As a footnote, it is interesting that the early developers of the method of slices recognized the limitations of computing realistic stresses on the slip surface. Lambe & Whitman (1969) in their text book *Soil Mechanics* point out that the normal stress at a point acting on the slip surface should be mainly influenced by the weight of the soil lying above that point. This, they state, forms the basis of the method of slices. Morgenstern and Sangrey (1978) state that one of the uses "... of the factor of safety is to provide a measure of the average shear stress mobilized in the slope." They go on to state that, "This should not be confused with the actual stresses." Unfortunately, these fundamental issues are sometimes forgotten as use of a method is gradually adopted in routine practice.

While the early developers of the method of slices intuitively recognized that the slice stress may not be real, they did not have finite element tools to demonstrate the way in which they differ from the actual ground stresses. Now, with the help of finite element analyses, it is possible to show that the difference is quite dramatic.

2.9 Janbu generalized method

In the context of stress distributions, it is of interest to examine the Janbu Generalized formulation (Janbu, 1954; Janbu, 1957). The Janbu Generalized method imposes a stress distribution on each slice. The interslice stress distribution is often assumed hydrostatic and the resultant is assumed to act on the lower third point along the side of the slice. A line which passes through the interslice force resultants on either side of the slice is known as the line of thrust. Assuming a line of thrust and taking moments about the base of each slice makes it possible to determine the magnitudes of the interslice force.

This approach works reasonably well provided the actual stress distribution in the ground is close to the imposed stress distribution, such as when the slip surface does not have sharp corners and the sliding mass is long relative to the slide depth. More generally, the approach works well when the potential sliding mass does not have significant stress concentrations. If stress concentrations exist which deviate significantly from the Janbu Generalized imposed stress distribution, the problem is over-constrained. This leads to convergence problems and lack of force equilibrium for some slices. This is particularly true when features like anchors or nails are included in the analysis. As Abramson et al. (2002) points out, the calculations for the Janbu Generalized method are very sensitive to the line of thrust location.

Earlier it was mentioned that the line of thrust could potentially fall outside the slice. With the GLE method, the slices are always in force equilibrium, but it is possible that the interslice forces would have to act outside the slice for the slice itself to be in moment equilibrium. The Janbu Generalized approach, on the other hand, forces the line of thrust to be at a particular point on the side of the slice, but this may lead to the slice not being in force equilibrium. So it is not always possible to achieve both conditions. Sometimes the line of thrust needs to be outside the slice to have slice force equilibrium, or the slice cannot be in force equilibrium if the line of thrust is fixed at a particular point on the slice.

The behavior of the Janbu Generalized method reinforces the earlier observation that limit equilibrium methods based purely on statics can, in some circumstances, over-constrain the problem, resulting in unrealistic stress conditions. In this sense the Janbu Generalized approach is no different than any other limit equilibrium method. The inherent interslice force assumptions are different, but in the end the limitations are similar.

2.10 Missing physics

The limit equilibrium method of slices is based purely on the principle of statics; that is, the summation of moments, vertical forces, and horizontal forces. The method says nothing about strains and displacements, and as a result it does not satisfy displacement compatibility. It is this key piece of missing physics that creates many of the difficulties with the limit equilibrium method.

The missing physics in a limit equilibrium formulation is the lack of a stress-strain constitutive relationship to ensure displacement compatibility.

Overcoming the gap left by the missing piece of physics means somehow incorporating a stress-strain constitutive relationship into the formulation. One way of doing this is to use finite element computed stresses instead of determining the stresses from equations of statics. This type of scheme has been implemented in GeoStudio. Stresses computed by SIGMA/W, for example, can be used in SLOPE/W to compute a factor of safety. The details are presented in the Factor of Safety Methods chapter of this book.

2.11 Other limitations

Besides unrealistic stress distributions, limit equilibrium formulations have other limitations. One of the most primary limitations is the difficulty with convergence under certain conditions. Most of the convergence problems arise with lateral loads representing anchors, nails, fabrics and so forth. Earth structures requiring reinforcement usually have a steep face and, consequently, the critical slip surface position is inclined at a steep angle. The lateral forces, together with a steep slip surface, make it difficult to obtain a converged solution. In addition, the minimum obtainable factor of safety is often directly adjacent to trial slip surfaces for which a converged solution cannot be computed. This casts doubt on the validity of the obtainable factors of safety. This problem is discussed further in the chapter on modeling reinforcement in SLOPE/W.

Soil-structure interaction also creates some difficulties in a limit equilibrium analysis. Consider the case of a sheet pile wall as illustrated in Figure 2-19.

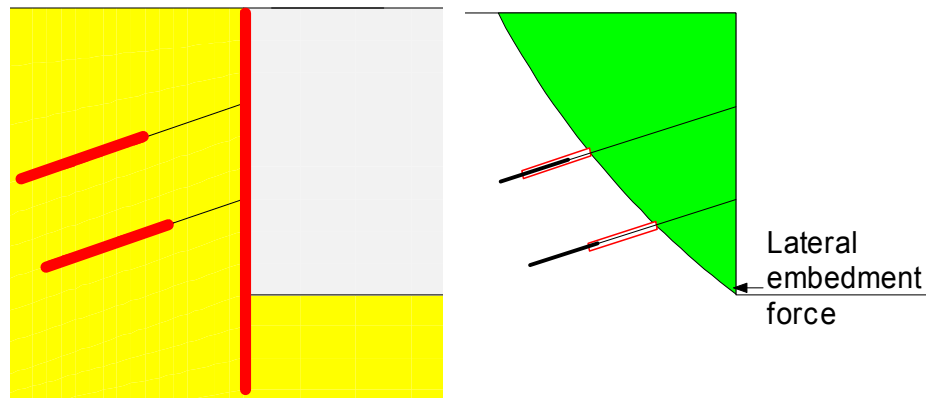


Figure 2-19 Inclusion of pile embedment in a limit equilibrium analysis

When structural components are included in a limit equilibrium analysis, the influence of the structure can extend outside the potential sliding mass. The issue is how to include the lateral resistance provided by the buried portion of the sheet piling when looking at a potential mode of failure, where the slip surface exits at the excavation base. The passive resistance in front of the pile is an integral part of the stability of the system, but it is outside the free body of the sliding mass.

One way of including the passive resistance in front of the wall is to do an independent analysis. This could be done with closed form solutions or even with a limit equilibrium analysis. The computed available force can then be included in the wall stability analysis as a line load just above the slip surface exit point as shown in the diagram on the right side of Figure 2-19.

The issue is further complicated by the fact that the passive resistance is sensitive to the friction between the wall and the soil. The passive earth pressure coefficient can vary greatly depending on the assumed friction between the soil and the steel. Also, large movement is sometimes required to develop the complete passive resistance. To account for this, only a portion of the passive resistance can be relied upon in the wall stability analysis. In other words, the passive resistance needs its own factor of safety which is likely much higher than the factor of safety for the wall stability.

2.12 Slip surface shapes

Inherent in limit equilibrium stability analyses is the requirement to analyze many trial slip surfaces and find the slip surface that gives the lowest factor of safety. Included in this trial approach is the form of the slip surface; that is, whether it is circular, piece-wise linear or some combination of curved and linear segments. SLOPE/W has a variety of options for specifying trial slip surfaces.

Often the slip surface shape is controlled, at least in part by stratigraphic boundaries or geologic features such as faults or pre-sheared surfaces. Defining these features becomes part of forming trial slip surfaces. The point is that even with such structural controls, there is still a need to examine many trial slip surfaces since the slip surface is not completely defined by the stratigraphic boundaries.

The position of the critical slip surface is affected by the soil strength properties. The position of the critical slip surface for a purely frictional soil ($c = 0$) is radically different than for a soil assigned an undrained strength ($\phi = 0$). This

complicates the situation, because it means that in order to find the position of the critical slip surface, it is necessary to accurately define the soil properties in terms of effective strength parameters.

Recent research has shown that assumed user-specified slip surface shapes do not necessarily give the lowest possible factor of safety. Algorithms that alter the slip surface shape in some systematic manner tend to give lower safety factors than for a predetermined slip surface shape. For example, say a minimum factor of safety has been found for a circular slip surface. Further refinement of the shape can lead to a non-circular slip surface with a lower factor of safety. In SLOPE/W this is called optimization, auto-search or auto location of the slip surface shape and position.

Finding the critical slip surface shape and position still remains one of the key issues in any limit equilibrium stability analysis, in spite of all the advanced techniques available. It is not as yet a black box solution. Guidance from the user still remains an essential ingredient, and to help you with providing this guidance, a complete chapter is devoted to this topic.

2.13 Seepage forces

Seepage forces in a stability analysis can create considerable confusion. The concept of seepage forces is easy to comprehend, but including seepage forces in a limit equilibrium stability analysis is fraught with misunderstanding.

Consider the slice in Figure 2-20 where the phreatic surface passes through the slice at a steep angle relative to the slice base. The water force on the left side of the slice is larger than on the right side. The difference in water forces from one side to other side of the slice is known as a seepage force. Energy is lost or dissipated as water flows across the slice and the seepage force is proportional to the energy loss.

Now if the seepage force is to be considered in a limit equilibrium formulation, it is necessary to deal with multiple interslice forces. Below the phreatic surface we need a water force and a soil force, where the soil force is determined from the submerged or buoyant unit weight. Above the phreatic surface, the soil force is determined from the total unit weight. This is illustrated in Figure 2-20.

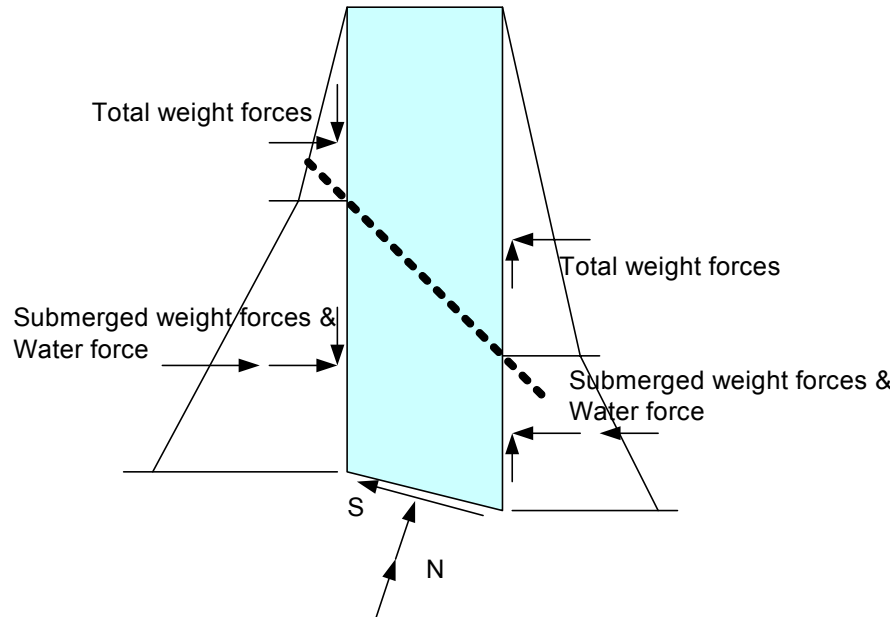


Figure 2-20 Interslice forces when seepage forces are considered

Breaking out the interslice force components unnecessarily complicates the formulation. One normal and one shear force on each side is adequate for satisfying the inherent equations of statics. As discussed above, the prime objective is to ensure force equilibrium of each slice. Also, attempting to apply interslice forces at specific locations on the sides of slices as in the Janbu Generalized method can over constrain the problem. As noted earlier, the Janbu Generalized approach may satisfy slice moment equilibrium, but by doing so the slice may not be in force equilibrium. Conversely, the GLE method ensures slice force equilibrium, but cannot at the same time ensure slice moment equilibrium. Furthermore, it was pointed out earlier that limit equilibrium formations based purely on satisfying equations of statics do not necessarily lead to computed stresses representative of actual field conditions. This being the case, there is no benefit to refining the interslice forces. Fortunately, unrealistic stress distributions do not invalidate the resulting factor of safety. The factor of safety is valid provided the overall potential sliding mass is in force and moment equilibrium – the forces internal to the sliding mass are of secondary importance. The internal forces need to be such that each slice is in force equilibrium and the factor of safety is the same for each slice. This can be accomplished without the

complication of subdividing the interslice forces into submerged soil forces, total soil forces and seepage forces.

Lambe and Whitman (1968, p. 261) argue the point from a different perspective, but reach the same conclusion. They point out that to analyze the forces acting on an element we can use either *boundary water* forces with *total* weights or *seepage* forces with *submerged* weights. Then they go on to state that, although the two methods give exactly the same answer, the use of boundary forces and total weights is nearly always the more convenient method. This is certainly true in the SLOPE/W formulation. The SLOPE/W formulation uses the concept of boundary forces and total weights - SLOPE/W does **not** use the alternative concept of seepage forces and submerged or buoyant unit weights.

It is important to be aware of the SLOPE/W formulation when viewing slice forces. The slice forces are all total forces. SLOPE/W does not break out any water forces when displaying the slice forces and the force polygons. Water pressures come into play in the base shear force calculation, but water forces *per se* do not come into play in the slice equilibrium calculations.

It is critical not to mix submerged weights and seepage forces with boundary water forces and total weights. SLOPE/W uses total weights throughout and no attempt should be made to manually add seepage forces via concentrated line loads.

2.14 Concluding remarks

Geotechnical limit equilibrium stability analysis techniques have limitations. The limitations arise principally because the method does not consider strain and displacement compatibility. This has two serious consequences. One is that local variations in safety factors cannot be considered, and the second is that the computed stress distributions are often unrealistic. To allow for variations in local safety factors along the slip surface and to deal with somewhat realistic stresses, the formulation and analysis technique needs to include a stress-strain constitutive relationship. It is the absence of a stress-strain relationship in conventional limit equilibrium analysis methods that is the fundamental piece of missing physics.

The limit equilibrium method for analyzing stability of earth structures remains a useful tool for use in practice, in spite of the limitations inherent in the method. Care is required, however, not to abuse the method and apply it to cases beyond its limits. To effectively use limit equilibrium types of analyses, it is vitally important

to understand the method, its capabilities and its limits, and not to expect results that the method is not able to provide. Since the method is based purely on the principles of statics and says nothing about displacement, it is not always possible to obtain realistic stress distributions. This is something the method cannot provide and consequently should not be expected to provide. Fortunately it does not mean the overall factor of safety is necessarily unacceptable just because some unrealistic stresses exist for some slices. The greatest caution and care is required when stress concentrations exist in the potential sliding mass due to the slip surface shape or due to soil-structure interaction.

A full understanding of the method and its limits leads to greater confidence in the use and in the interpretation of the results. In order to obtain this level of understanding, it is important to look at more than just the factor of safety. To use the limit equilibrium method effectively, it is also important to examine the detailed slice forces and the variation of parameters along the slip surface during the course of a project. Looking at a FS versus lambda plot can be of significant help in deciding how concerned one needs to be about defining an interslice force function.

Finally, limit equilibrium analyses applied in practice should as a minimum use a method that satisfies both force and moment equilibrium such as the Morgenstern-Price or Spencer methods. With software such as SLOPE/W, it is just as easy to use one of the mathematically more rigorous methods than to use the simpler methods that only satisfy some of the statics equations.

3 Factor of Safety Methods

3.1 Introduction

Over the years, many different methods have been developed for computing factors of safety. This chapter describes each of the methods available in SLOPE/W. All the methods are based on limit equilibrium formulations except for one method, the finite element method, which uses finite element computed stresses.

The final section of the chapter contains suggestions on how to select an appropriate method for use in practice.

3.2 General limit equilibrium method

A general limit equilibrium (GLE) formulation was developed by Fredlund at the University of Saskatchewan in the 1970s (Fredlund and Krahn 1977; Fredlund et al. 1981). This method encompasses the key elements of all the other methods available in SLOPE/W. The GLE method provides a framework for discussing, describing and understanding all the other methods.

The GLE formulation is based on two factor of safety equations and allows for a range of interslice shear-normal force assumptions. One equation gives the factor of safety with respect to moment equilibrium (F_m), while the other equation gives the factor of safety with respect to horizontal force equilibrium (F_f). The idea of using two factor of safety equations follows from the work of Spencer (1967).

The interslice shear forces in the GLE method are handled with an equation proposed by Morgenstern and Price (1965). The equation is:

$$X = E \lambda f(x)$$

where, $f(x)$ is a function, λ is the percentage (in decimal form) of the function used, E is the interslice normal force and X is the interslice shear force. Figure 3-1 shows a typical half-sine function. The upper curve in this figure is the actual specified function, while the lower curve is the function used in the solution. The ratio between the two curves is called lambda (λ). The lambda value (λ) in Figure 3-1 is 0.43, which becomes apparent by looking at the value of the applied function where the specified function is 1.0. At Slice 10, $f(x) = 0.83$. If, for example, the

interslice normal force, $E = 100$ kN, then the interslice shear force, $X = E f(x) \lambda = 100 \times 0.43 \times 0.83 = 35.7$ kN. $\text{Arc tan}(35.7/100) = 19.6$ degrees. This means the interslice resultant force is inclined at 19.6 degrees from the horizontal at Slice 10.

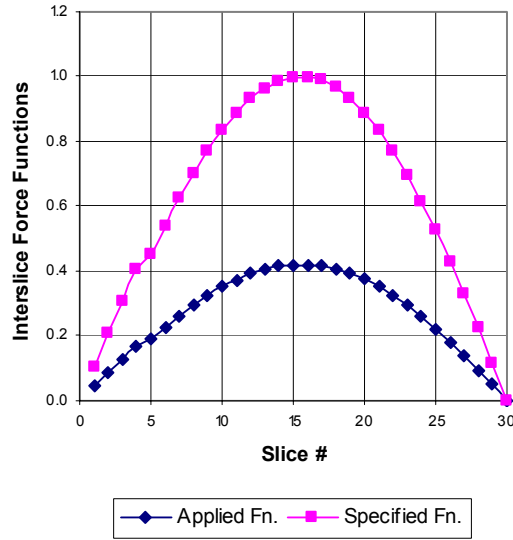


Figure 3-1 Interslice applied and specified functions

The GLE factor of safety equation with respect to moment equilibrium is:

$$F_m = \frac{\sum (c' \beta R + (N - u \beta) R \tan \phi')}{\sum W_x - \sum N f \pm \sum D d}$$

The factor of safety equation with respect to horizontal force equilibrium is:

$$F_f = \frac{\sum (c' \beta \cos \alpha + (N - u \beta) \tan \phi' \cos \alpha)}{\sum N \sin \alpha - \sum D \cos \omega}$$

The terms in the equations are:

c'	=	effective cohesion
ϕ'	=	effective angle of friction
U	=	pore-water pressure

N	=	slice base normal force
W	=	slice weight
D	=	line load
$\beta, R, x, f, d, \omega$	=	geometric parameters
α	=	inclination of slice base

There are additional terms in these equations, but their definition is not required here for this discussion. The complete equations are presented in the theory chapter.

One of the key variables in both equations is N , the normal at the base of each slice. This equation is obtained by the summation of vertical forces. Vertical force equilibrium is consequently satisfied. In equation form, the base normal is defined as:

$$N = \frac{W + (X_R - X_L) - \frac{c' \beta \sin \alpha + u \beta \sin \alpha \tan \phi'}{F}}{\cos \alpha + \frac{\sin \alpha \tan \phi'}{F}}$$

F is F_m when N is substituted into the moment factor of safety equation and F is F_f when N is substituted into the force factor of safety equation. The literature on slope stability analysis often refers to the denominator as m_α . Later we will return to this term in the discussion on the Bishop method.

An important point to note here is that the slice base normal is dependent on the interslice shear forces X_R and X_L on either side of a slice. The slice base normal is consequently different for the various methods, depending on how each method deals with the interslice shear forces.

The GLE method computes F_m and F_f for a range of lambda (λ) values. With these computed values, a plot such as in Figure 3-2 can be drawn that shows how F_m and F_f vary with lambda (λ). This type of plot is a useful feature of the GLE method. Such a plot makes it possible to understand the differences between the factors of safety from the various methods, and to understand the influence of the selected interslice force function.

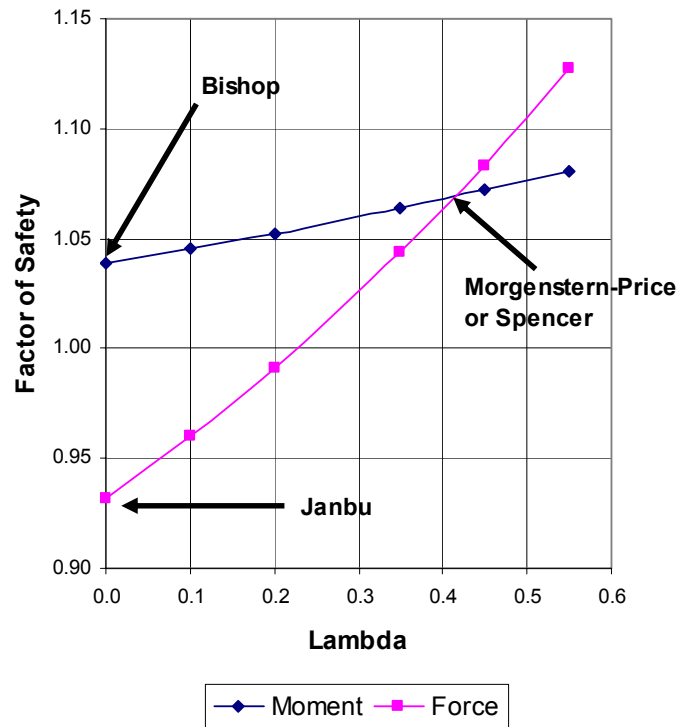


Figure 3-2 A factor of safety versus lambda (λ) plot

Two of the primary assumptions of the Bishop's Simplified method are that it ignores interslice shear forces and satisfies only moment equilibrium. In the GLE terminology, not considering shear forces means λ is zero. As a result, the Bishop's Simplified factor of safety falls on the moment curve in Figure 3-2 where λ is zero. Janbu's Simplified method also ignores interslice shear forces and only satisfies force equilibrium. The Janbu's Simplified factor of safety consequently falls on the force curve in Figure 3-2 where λ is zero. The Spencer and Morgenstern-Price (M-P) factors of safety are determined at the point where the two curves cross. At this point the factor of safety satisfies both moment and force equilibrium. Whether the crossover point is the Spencer or M-P factor of safety depends on the interslice force function. Spencer only considered a constant X/E ratio for all slices, which in the GLE formulation corresponds to a constant (horizontal) interslice force function. The M-P method can utilize any general appropriate function. Methods like the Corps of Engineers and Lowe-Karafiath

factors of safety fall on the force curve, since they only satisfy force equilibrium. The position on the force curve depends on the procedure used to establish the inclinations of the interslice force resultant. This is discussed in further detail below for each of the method.

The GLE method can be applied to any kinematically admissible slip surface shape. By implication, the Bishop method, for example, can consequently be used to analyze non-circular as well as circular slip surfaces. All the methods discussed here are characterized more by the equations of statics satisfied and the manner in which the interslice forces are handled than by the shape of the slip surface. The importance of the interslice force function is related to the slip surface shape, as noted in the previous chapter, but no method is restricted to a particular slip surface shape. As it turns out, the moment factor of safety is not sensitive to the assumed interslice force function when the slip surface is circular. Consequently, the Bishop's Simplified factor of safety for a circular slip surface is often close to a Spencer or Morgenstern-Price factor of safety. In this sense, the Bishop's Simplified method is suitable for a circular slip surface analysis. The assumptions inherent in the Bishop's Simplified method, however, can equally be applied to non-circular slip surfaces. So the GLE method encompasses all the other methods regardless of slip surface shape.

The GLE method in SLOPE/W can accommodate a wide range of different interslice force functions. The following is a summary list.

- Constant
- Half-sine
- Clipped-sine
- Trapezoidal
- Data point fully specified

The GLE method satisfies both moment and force equilibrium by finding the cross-over point of the F_m and F_f curves. The factor of safety versus lambda plots are mirrored for right-left and left-right problems, as illustrated in Figure 3-3. The safety factors are the same (1.283), but lambda has the opposite sign. This is required to keep all the forces in the correct direction. Lambda values can sometimes also take on opposite signs, for example, when large lateral forces are applied.

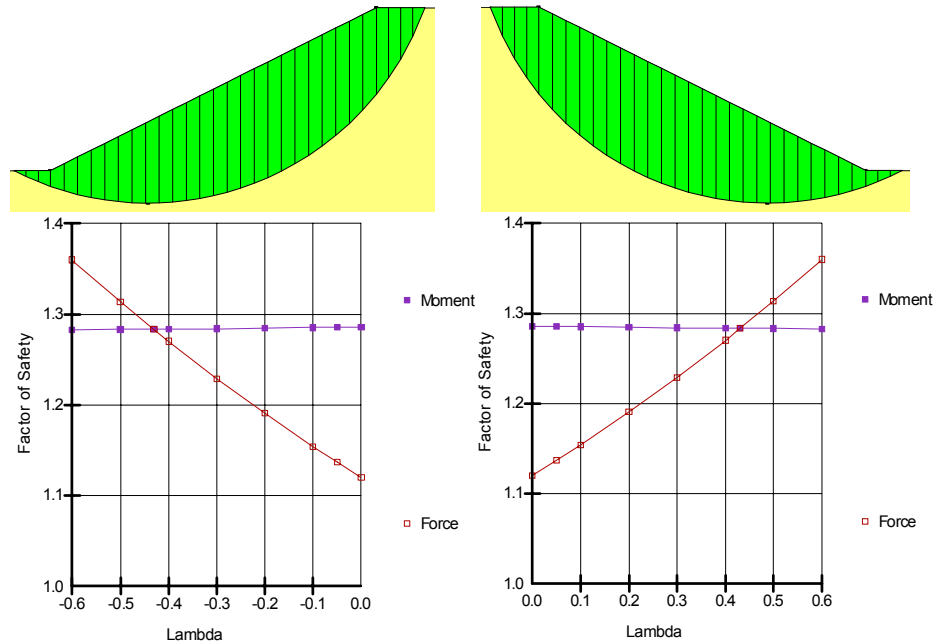


Figure 3-3 Effect of sliding direction on lambda

SLOPE/W by default uses lambda values that varying from -1.25 to +1.25. This range sometimes needs to be narrowed, since it is not always possible to obtain a converged solution at the extremities of the range. For presentation in Figure 3-3 the lambda range was set to a range from 0.0 to 0.6.

The GLE method is very useful for understanding what is happening behind the scenes and understanding the reasons for differences between the various methods. It is not necessarily a method for routine analyses in practice, but it is an effective supplementary method useful for enhancing your confidence in the selection and use of the other more common methods.

3.3 Ordinary or Fellenius method

This method is also sometimes referred to as the Swedish method of slices.

This is the first method of slices developed and presented in the literature. The simplicity of the method made it possible to compute factors of safety using hand calculations.

In this method, all interslice forces are ignored. The slice weight is resolved into forces parallel and perpendicular to the slice base. The force perpendicular to the slice base is the base normal force, which is used to compute the available shear strength. The weight component parallel to the slice base is the gravitational driving force. Summation of moments about a point used to describe the trial slip surface is also used to compute the factor of safety. The factor of safety is the total available shear strength along the slip surface divided by the summation of the gravitational driving forces (mobilized shear).

The simplest form of the Ordinary factor of safety equation in the absence of any pore-water pressures for a circular slip surface is:

$$FS = \frac{\sum [c\beta + N \tan \phi]}{\sum W \sin \alpha} = \frac{\sum S_{resistance}}{\sum S_{mobilized}}$$

where:

c	=	cohesion,
β	=	slice base length,
N	=	base normal ($W \cos \alpha$),
ϕ	=	friction angle,
W	=	slice weight, and
α	=	slice base inclination.

The Ordinary factor of safety can be fairly easily computed using a spreadsheet. Using a spreadsheet is of course not necessary when you have SLOPE/W, but doing a simple manual analysis periodically is a useful learning exercise.

Consider the simple problem in Figure 3-4. There are 14 slices numbered from left to right. The cohesive strength is 5 kPa and the soil friction angle ϕ is 20 degrees.

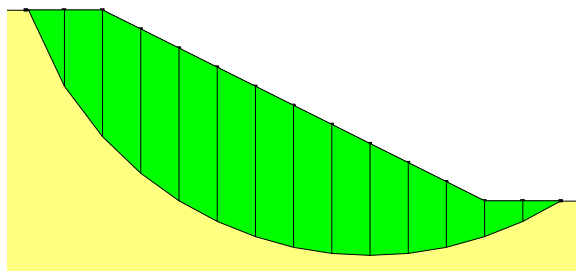


Figure 3-4 Case for hand-calculations

The following two tables illustrate how the Ordinary factor of safety can be easily calculated. The most difficult part is specifying the slice dimensions.

Slice #	Width (m)	Mid-height (m)	Weight (kN)	Alpha (degrees)	β (m)
1	1.9	2.3	86.9	64.7	4.42
2	2.0	5.4	217.8	52.9	3.32
3	2.0	7.2	287.0	43.7	2.77
4	2.0	7.8	313.2	35.8	2.46
5	2.0	8.1	323.3	28.5	2.28
6	2.0	8.0	320.9	21.8	2.15
7	2.0	7.7	307.7	15.4	2.07
8	2.0	7.1	285.1	9.2	2.03
9	2.0	6.3	253.7	3.0	2.00
10	2.0	5.3	213.7	-3.0	2.00
11	2.0	4.1	165.1	-9.2	2.03
12	2.0	2.7	107.7	-15.4	2.07
13	2.0	1.5	60.9	-21.8	2.15
14	2.0	0.6	23.3	-28.5	2.28

Slice #	$C \beta$	N	$N \tan \phi$	$W \sin \alpha$	$C \beta + N \tan \phi$
1	22.12	37.09	13.50	78.56	35.62
2	16.60	131.25	47.77	173.84	64.37
3	13.83	207.49	75.52	198.27	89.35
4	12.32	254.18	92.51	182.98	104.83
5	11.38	284.02	103.37	154.50	114.76
6	10.77	297.88	108.42	119.23	119.19
7	10.37	296.70	107.99	81.67	118.36
8	10.13	281.48	102.45	45.40	112.58
9	10.01	253.30	92.19	13.46	102.21
10	10.01	213.35	77.65	-11.34	87.67
11	10.13	163.01	59.33	-26.29	69.46
12	10.37	103.87	37.81	-28.59	48.18
13	10.77	56.50	20.56	-22.61	31.33
14	11.38	20.49	7.46	-11.15	18.84
Σ	—	—	—	947.93	1116.75

From the summations listed above, the factor of safety can be computed to be:

$$FS = \frac{\sum [c\beta + N \tan \phi]}{\sum W \sin \alpha} = \frac{1116.75}{947.93} = 1.18$$

SLOPE/W gives the same factor of safety as shown in Figure 3-5.

1.18

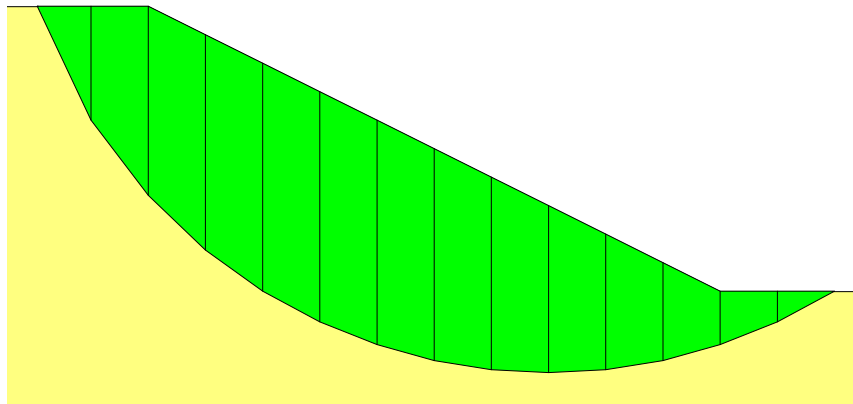


Figure 3-5 SLOPE/W computed Ordinary factor of safety

The most noteworthy aspects of this method are the slice forces and force polygons. Figure 3-6 shows free body diagrams and force polygons for Slice 3 and Slice 13. Slice 3 is just below the slope crest and Slice 13 is just below the slope toe. First of all, note that there are no interslice shear and no interslice normal forces. Secondly, note the extremely poor force polygon closure. The lack of force polygon closure indicates the slices are not in force equilibrium. With no interslice normal forces, there is nothing available to counterbalance the lateral components of the base shear and normal, particularly when the slice base is close to being horizontal.

When interpreting the free body diagram and force polygons, it is important to note that the shear at the slice base is the mobilized shear, not the available shear strength resistance. The available shear resistance is equal to the mobilized shear times the factor of safety. The last column in the above table lists the available shear resistance, which has to be divided by the factor of safety in order to match the base shear values shown on the slice free bodies.

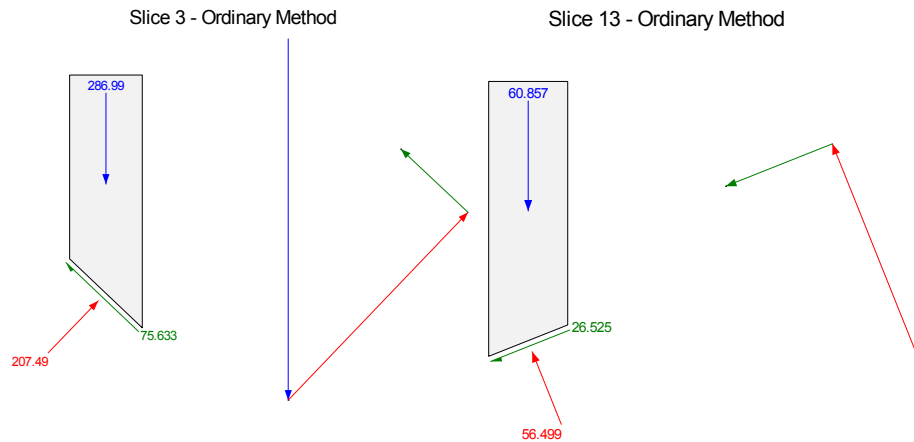


Figure 3-6 Free body diagram and force polygon for the Ordinary method

Due to the poor force polygon closure, the Ordinary method can give unrealistic factors of safety and consequently should not be used in practice. A more realistic Factor of Safety for this simple problem is around 1.36, which is about 15% higher than the 1.18 obtained from the Ordinary method.

The Ordinary method is included in SLOPE/W only for historic reasons and for teaching purposes. It is a useful learning exercise to compare a SLOPE/W analysis with hand calculations. Also, this method is where it all started, so in this sense, it is a good historic reference point.

The Ordinary factor of safety cannot be plotted on a GLE Factor of Safety versus Lambda graph since lambda is undefined.

The Ordinary method should not be used in practice, due to potential unrealistic factors of safety.

3.4 *Bishop's simplified method*

In the 1950's Professor Bishop at Imperial College in London devised a method which included interslice normal forces, but ignored the interslice shear forces. Bishop developed an equation for the normal at the slice base by summing slice forces in the vertical direction. The consequence of this is that the base normal

becomes a function of the factor of safety. This in turn makes the factor of safety equation nonlinear (that is, FS appears on both sides of the equation) and an iterative procedure is consequently required to compute the factor of safety.

A simple form of the Bishop's Simplified factor of safety equation in the absence of any pore-water pressure is:

$$FS = \frac{\sum \left[(c\beta + W \tan \phi) \left\{ \cos \alpha + \frac{\sin \alpha \tan \phi}{FS} \right\} \right]}{\sum W \sin \alpha}$$

FS is on both sides of the equation as noted above. The equation is not unlike the Ordinary factor of safety equation except for the m_α term, which is defined as:

$$m_\alpha = \cos \alpha + \frac{\sin \alpha \tan \phi}{FS}$$

To solve for the Bishop's Simplified factor of safety, it is necessary to start with a guess for FS. In SLOPE/W, the initial guess is taken as the Ordinary factor of safety. The initial guess for FS is used to compute m_α and then a new FS is computed. Next the new FS is used to compute m_α and then another new FS is computed. The procedure is repeated until the last computed FS is within a specified tolerance of the previous FS. Fortunately, usually it only takes a few iterations to reach a converged solution.

Now if we examine the slice free body diagrams and forces polygons for the same slices as for the Ordinary method above, we see a marked difference (Figure 3-7). The force polygon closure is now fairly good with the addition of the interslice normal forces. There are no interslice shear forces, as assumed by Bishop, but the interslice normal forces are included.

In a factor of safety versus lambda plot, as in Figure 3-8, the Bishop's Simplified factor of safety falls on the moment equilibrium curve where lambda is zero ($FS = 1.36$). Recall that

$$X = E \lambda f(x)$$

The interslice shear is not included by making lambda zero.

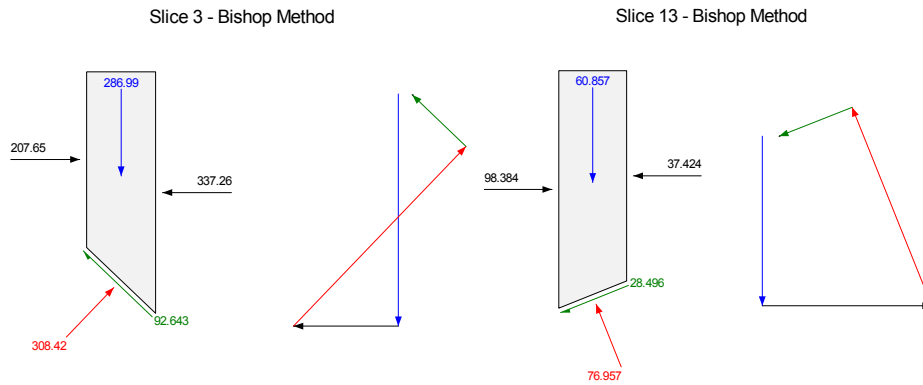


Figure 3-7 Free body diagram and force polygon for the Bishop's Simplified method

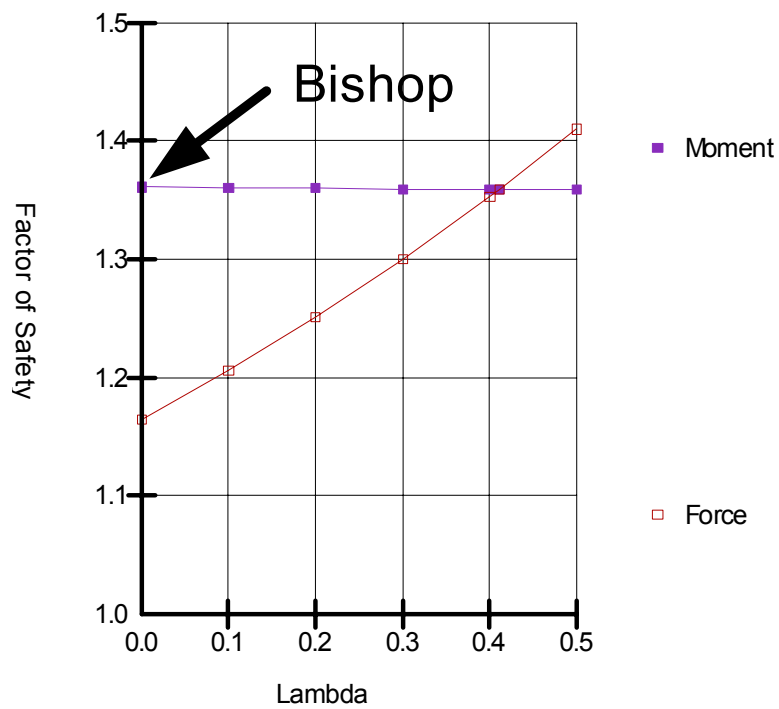


Figure 3-8 Bishop's Simplified factor of safety

Note that in this case the moment factor of safety (F_m) is insensitive to the interslice forces. The reason for this, as discussed in the previous chapter, is that no slippage is required between the slices for the sliding mass to rotate. This is not true for force equilibrium and thus the force factor of safety (Ff) is sensitive to the interslice shear.

In summary, the Bishop's Simplified method, (1) considers normal interslice forces, but ignores interslice shear forces, and (2) satisfies over all moment equilibrium, but not overall horizontal force equilibrium.

3.5 Janbu's simplified method

The Janbu's Simplified method is similar to the Bishop's Simplified method except that the Janbu's Simplified method satisfies only overall horizontal force equilibrium, but not overall moment equilibrium.

Figure 3-9 shows the free body diagrams and force polygons of the Janbu's Simplified method. The slice force polygon closure is actually better than that for the Bishop's Simplified method. The factor of safety, however, is 1.16 as opposed to 1.36 by Bishop's Simplified method. This is a significant difference. The Janbu's Simplified factor of safety is actually too low, even though the slices are in force equilibrium.

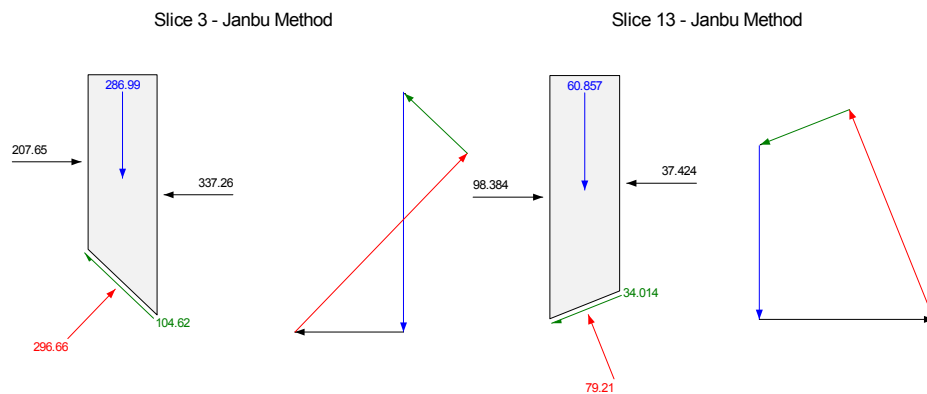


Figure 3-9 Free body diagram and force polygon for the Janbu method

As with the Bishop's Simplified method, lambda (λ) is zero in the Janbu's Simplified method, since the interslice shear is ignored. Therefore, the Janbu's

Simplified factor of safety falls on the force equilibrium curve where λ is zero (Figure 3-10). Since force equilibrium is sensitive to the assumed interslice shear, ignoring the interslice shear, as in the Janbu's Simplified method, makes the resulting factor of safety too low for circular slip surfaces.

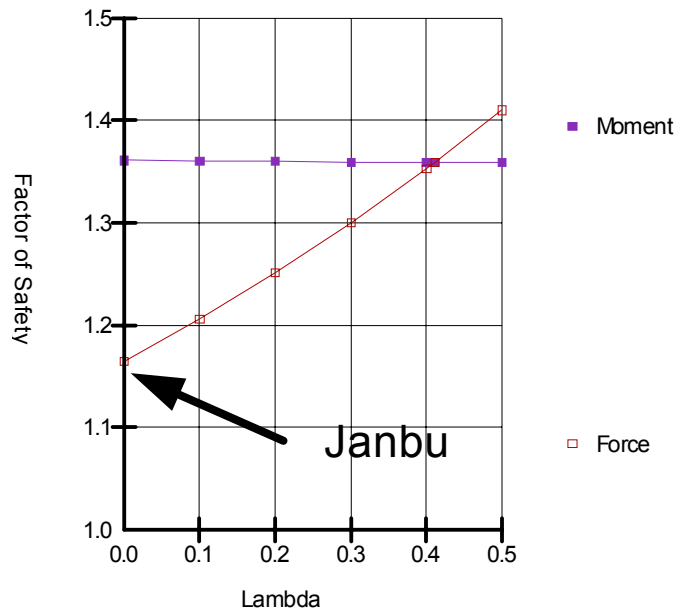


Figure 3-10 Janbu's Simplified factor of safety

In summary, the Janbu's Simplified method, (1) considers normal interslice forces, but ignores interslice shear forces, and (2) satisfies over all horizontal force equilibrium, but not over all moment equilibrium.

3.6 *Spencer method*

As discussed in the previous chapter, Spencer (1967) developed two factor of safety equations; one with respect to moment equilibrium and another with respect to horizontal force equilibrium. He adopted a constant relationship between the interslice shear and normal forces, and through an iterative procedure altered the interslice shear to normal ratio until the two factors of safety were the same. Finding the shear-normal ratio that makes the two factors of safety the same, means that both moment and force equilibrium are satisfied.

SLOPE/W uses the following equation to relate the interslice shear (X) and normal (E) forces.

$$X = E \lambda f(x)$$

In the Spencer method, the function $f(x)$ is a constant; that is, the interslice shear-normal ratio is the same between all slices.

Figure 3-11 shows a typical slope stability situation. The Spencer Factor of Safety is 1.140.

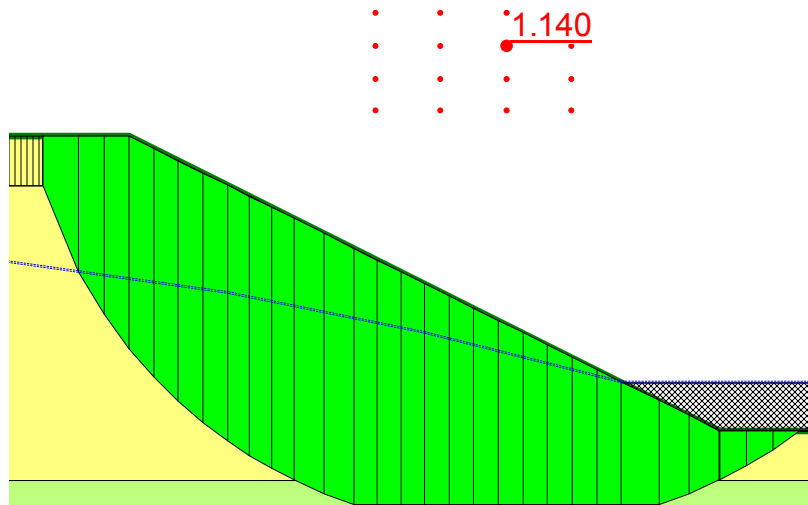


Figure 3-11 Typical slope stability situation

On a Factor of Safety versus Lambda plot as in Figure 3-12 the Spencer factor of safety is where the moment and force equilibrium curves cross.

Lambda at the crossover point is 0.12. The function $f(x)$ is 1.0 for the Spencer method. This means that the equation relating the interslice shear and normal forces is,

$$X = E \times 0.12 \times 1.0$$

$$X = 0.12E$$

A graph of the specified function and the applied interslice function is shown in Figure 3-13. Note that the applied function is a constant at 0.12.

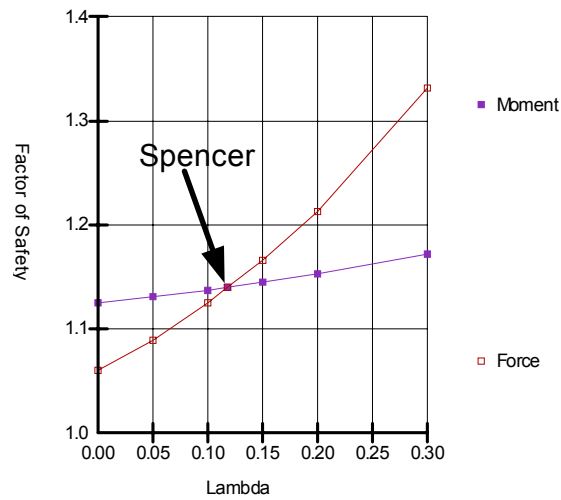


Figure 3-12 Spencer factor of safety

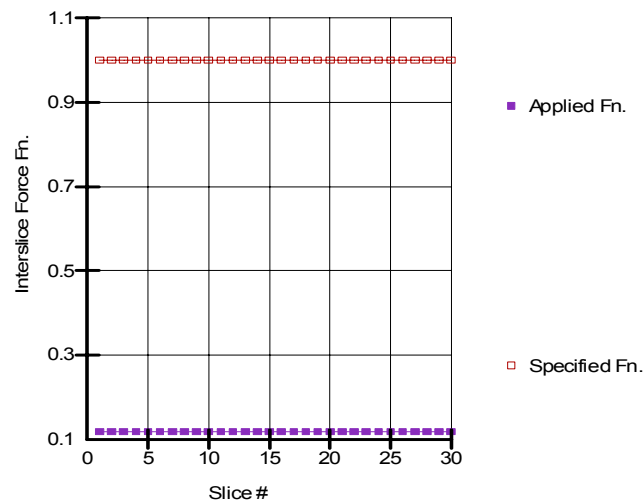


Figure 3-13 Interslice functions for the Spencer method

Further confirmation of the relationship between the interslice shear and normal forces is evident in the slice forces. Figure 3-14 shows a typical slice.

Slice 6 - Spencer Method

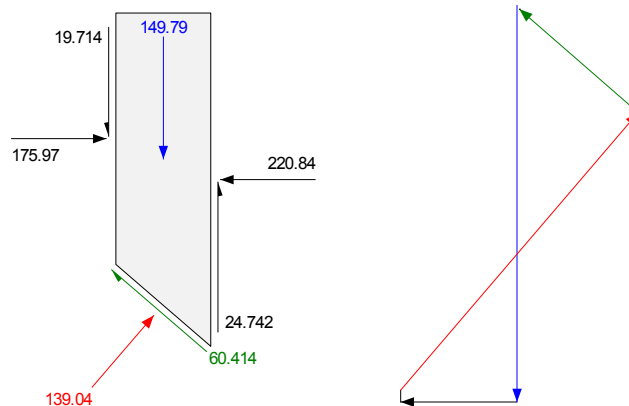


Figure 3-14 Free body diagram and force polygon for the Spencer method

On the left of the slice, the ratio of shear to normal is $19.714/175.97$ which is 0.12. On the right side the ratio is $24.742/220.84$ which is also 0.12.

A shear-normal ratio of 0.12 means that the interslice force resultant is inclined at an angle of $\arctan(0.12)$, which is 6.74 degrees.

Worth noting is that when both interslice shear and normal forces are included, the force polygon closure is very good.

In summary, the Spencer method:

- Considers both shear and normal interslice forces,
- Satisfies both moment and force equilibrium, and
- Assumes a constant interslice force function.

3.7 Morgenstern-Price method

Morgenstern and Price (1965) developed a method similar to the Spencer method, but they allowed for various user-specified interslice force functions. The interslice

functions available in SLOPE/W for use with the Morgenstern-Price (M-P) method are:

- Constant
- Half-sine
- Clipped-sine
- Trapezoidal
- Data-point specified

Selecting the Constant function makes the M-P method identical to the Spencer method.

For illustrative purposes, let us look at a M-P analysis with a half-sine function for the same problem as was used to discuss the Spencer method. The result is presented in Figure 3-15.

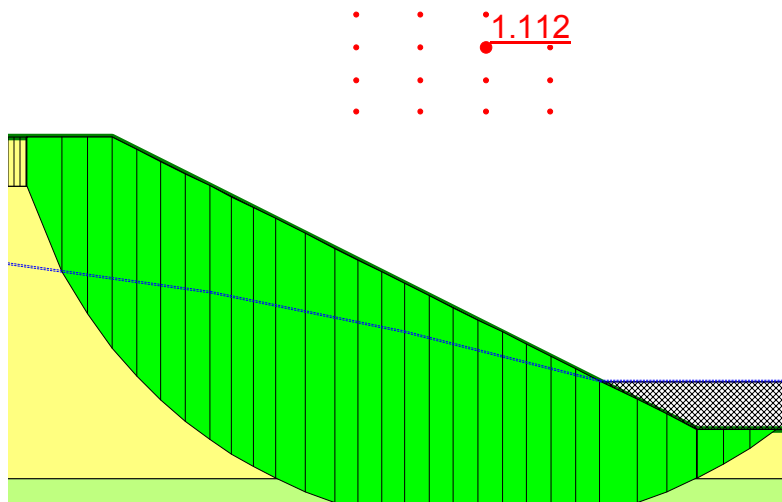


Figure 3-15 Result of Morgenstern-Price analysis

Figure 3-16 shows how the moment and force factors of safety vary with lambda. The M-P Factor of safety occurs where the two curves across.

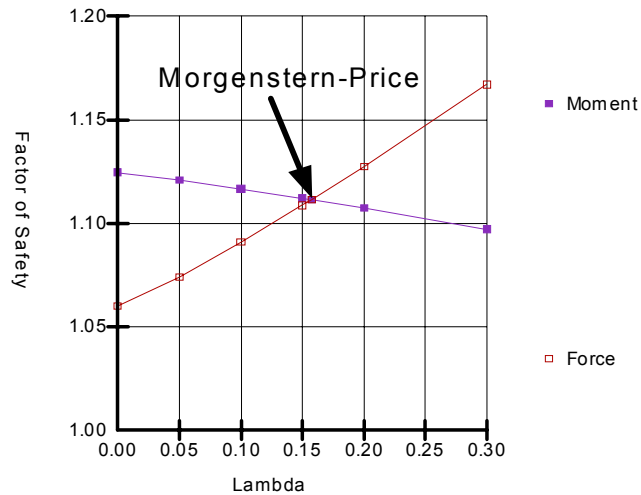


Figure 3-16 Morgenstern-Price safety factors with half-sine function

The specified and applied interslice force functions are shown in Figure 3-17. The specified function has the shape of a half-sine curve. The applied function has the same shape, but is scaled down by a value equal to lambda which is 0.145.

Consider the forces on Slice 10 (Figure 3-18). The specified function at Slice 10 is 0.86 and lambda is 0.146. The normal force on the right side of Slice 10 is 316.62. The corresponding interslice shear then is,

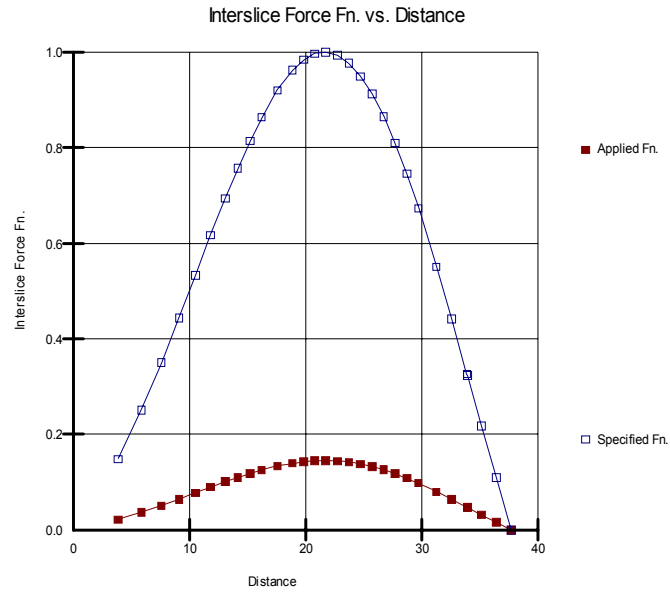
$$X = E\lambda f(x)$$

$$X = 316.62 \times 0.146 \times 0.86$$

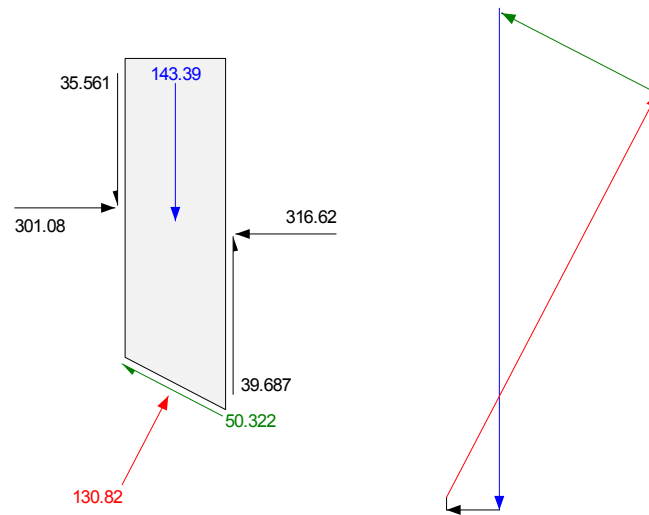
$$X = 39.7$$

This matches the interslice shear value on the free body diagram in Figure 3-18.

As with the Spencer method, the force polygon closure is very good with the M-P method, since both shear and normal interslice forces are included.

**Figure 3-17 Interslice half-sine functions**

Slice 10 - Morgenstern-Price Method

**Figure 3-18 Free body and force polygon for Morgenstern-Price method**

A significant observation in Figure 3-18 is that the M-P Factor of Safety (cross over point) is lower than the Bishop's Simplified Factor of Safety (moment equilibrium $\lambda = 0$). This is because the moment equilibrium curve has a negative slope. This example shows that a simpler method like Bishop's Simplified method that ignores interslice shear forces does not always err on the safe side. A more rigorous method like the M-P method that considers both interslice shear and normal forces results in a lower factor of safety in this case.

Simpler methods that do not include all interslice forces and do not satisfy all equations of equilibrium sometimes can err on the unsafe side.

In summary, the Morgenstern-Price method:

- Considers both shear and normal interslice forces,
- Satisfies both moment and force equilibrium, and
- Allows for a variety of user-selected interslice force function.

3.8 Corps of Engineers method

The Corps of Engineers method is characterized by a specific interslice force function, and the method only satisfies overall horizontal force equilibrium. Overall moment equilibrium is not satisfied.

This method makes two different assumptions about the interslice forces. One uses the slope of a line from crest to toe (slip surface entrance and exit points) and the other uses the slope of the ground surface at the top of the slice.

Interslice assumption one

Figure 3-19 illustrates the first of the interslice force assumption for Corps of Engineers method. The dark line from crest to toe is the assumed direction of the interslice force resultant.

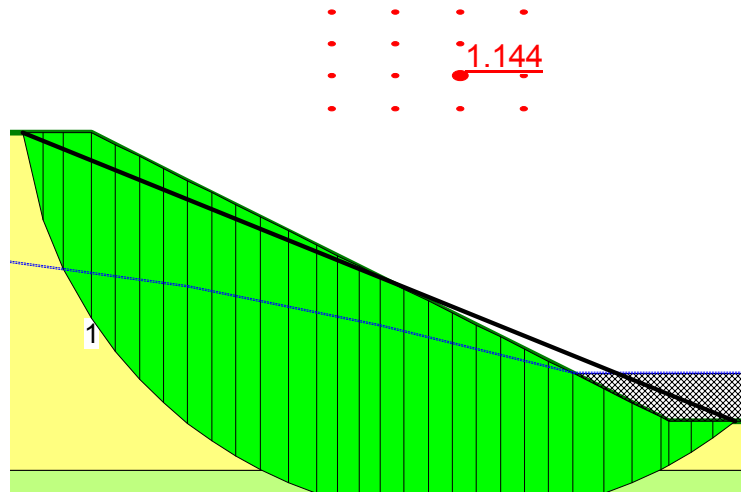


Figure 3-19 Corps of Engineers assumption #1

The slope of the line from crest to toe in Figure 3-19 is about 0.37. The SLOPE/W plot of the interslice force function, as shown in Figure 3-20, indicates a constant function of 0.37. In this case, the applied function is equal to the specified function, since the specified function is computed by the software.

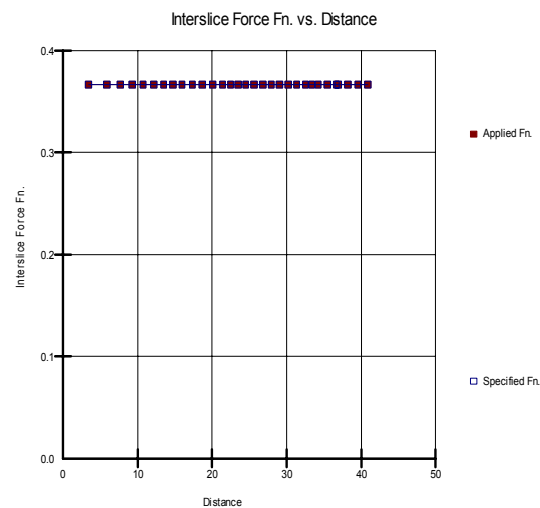


Figure 3-20 Corps of Engineers #1 interslice function

We can check the resultant direction by looking at the slice forces. Figure 3-21 shows the forces for Slice 6. The ratio of shear to normal on the side of the slice is about 0.37, confirming that the direction of the resultant is parallel to the line from crest to toe.

Slice 6 - Corps of Engineers #1 Method

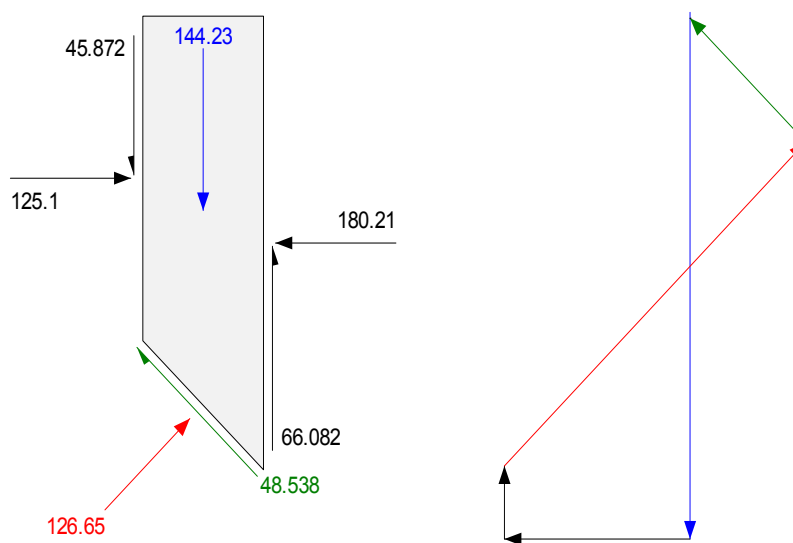


Figure 3-21 Free body and force polygon for Corps of Engineers Method Interslice Assumption One

Interslice assumption two

The second interslice assumption in the Corps of Engineers method is that the interslice resultant is equal to the ground surface slope at the top of the slice. The interslice function for the example in Figure 3-22 is shown in Figure 3-23. Where the ground surface is horizontal, the interslice force resultant is horizontal. Where the ground surface is at an incline, the resultant is parallel to the ground surface slope. The inclination of the slope is at 2:1. This makes the ratio of shear to normal 0.5. This is consistent with the function in Figure 3-23.

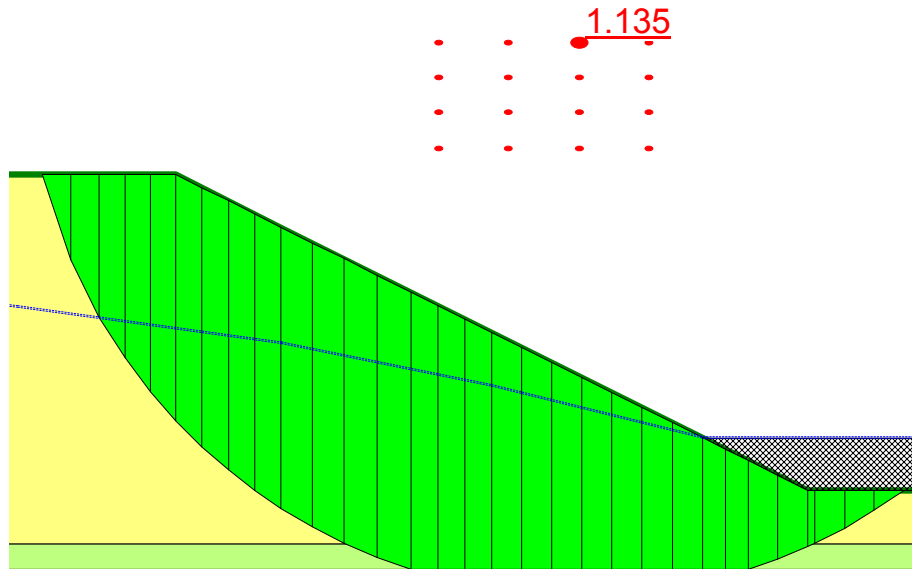


Figure 3-22 Corps of Engineers assumption #2

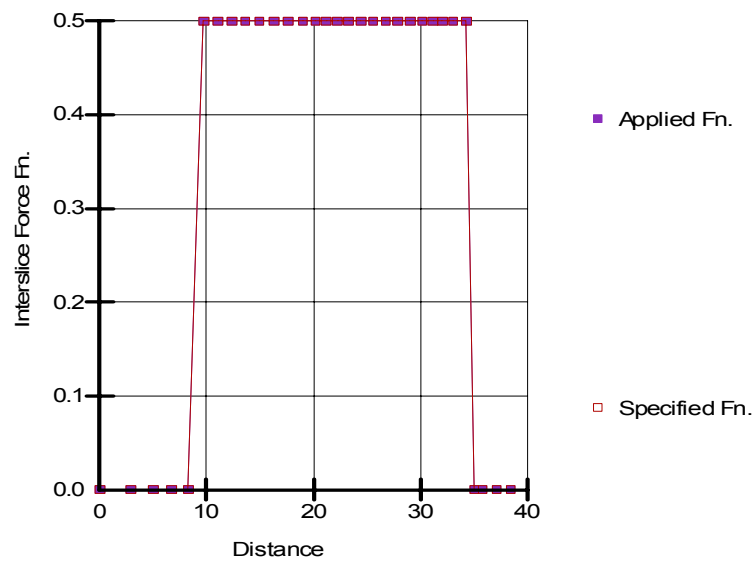


Figure 3-23 Corps of Engineers #2 interslice force function

A consequence of the second Corps of Engineers interslice force assumption is that the interslice shear is zero when the ground surface is horizontal.

Again, we can check the resultant direction by looking at the slice forces. Figure 3-24 shows the forces for Slice 6. The ratio of shear to normal on the side of the slice is about 0.5, confirming that the direction of the resultant is parallel to inclination of the slope.

Slice 6 - Corps of Engineers #2 Method

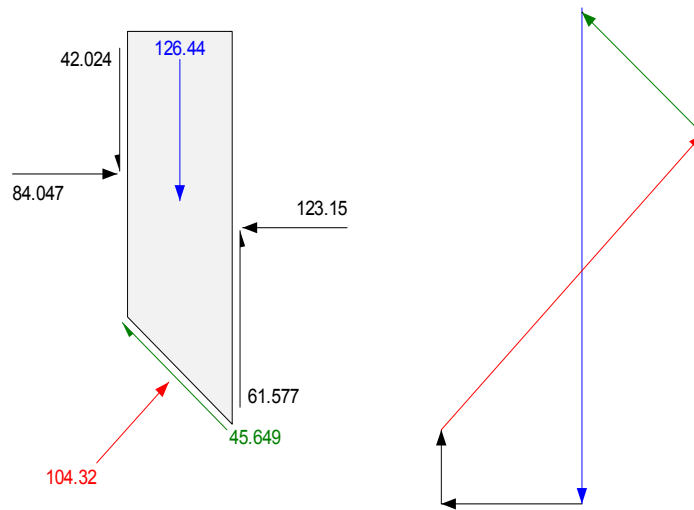


Figure 3-24 Free body and force polygon for Corps of Engineers Method Interslice Assumption Two

The Corps of Engineers factor of safety falls on the force equilibrium curve in a Factor of Safety versus Lambda plot, since this method only satisfies force equilibrium. Placing the computed safety factor on the plot is, however, somewhat misleading. There is no one single lambda value as in the Spencer or M-P method. If a Corps of Engineers factor of safety is plotted on such a graph, the corresponding lambda value would be a representation of an average lambda. Such an average value, however, can not be used to spot check the shear to normal ratio. The computed interslice function is all that is required to spot check that the correct shear forces have been computed.

In Summary, the Corps of Engineers method:

- Considers both interslice shear and normal forces,
- Satisfies overall horizontal force equilibrium, but not moment equilibrium, and
- Uses interslice force functions related to the slope and slip surface geometry.

3.9 *Lowe-Karafiath method*

The Lowe-Karafiath (L-K) method is essentially the same as the Corps of Engineers method, except that it uses another variation on the assumed interslice force function. The L-K method uses the average of the slice top (ground surface) and the base inclination. Figure 3-25 shows a case analyzed using the L-K method, and Figure 3-26 shows the corresponding computed interslice force function. The function is a reflection of the ground surface slope and the slice base inclination. Note that where the slice base is horizontal, the function is around 0.25, which is the average of the surface slope (0.5) and the base inclination (0.0).

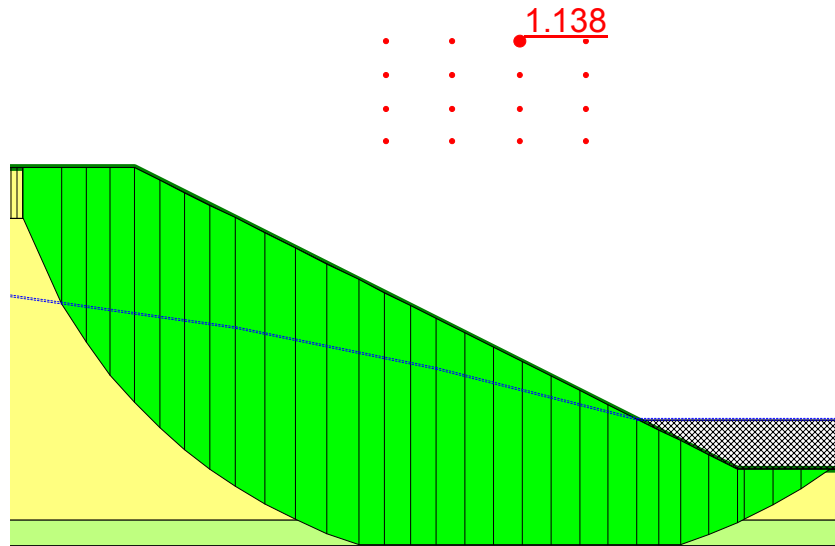


Figure 3-25 Lowe-Karafiath safety factor

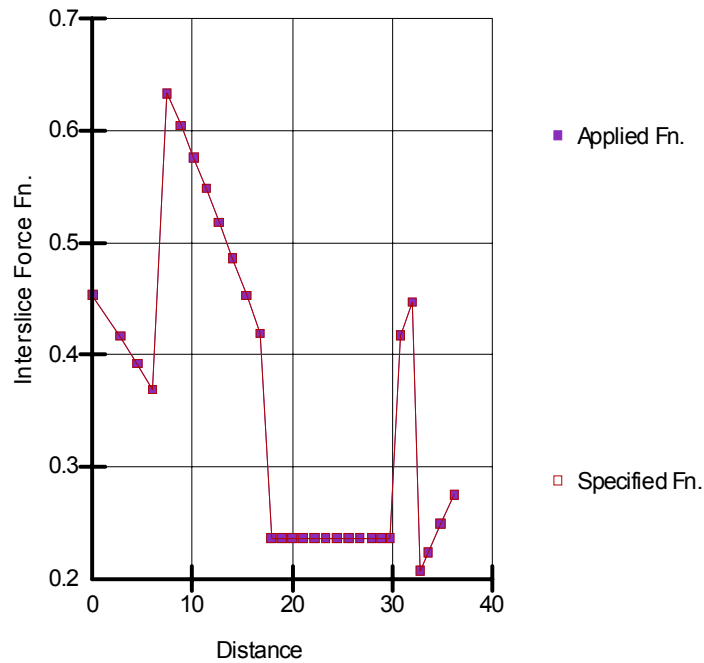


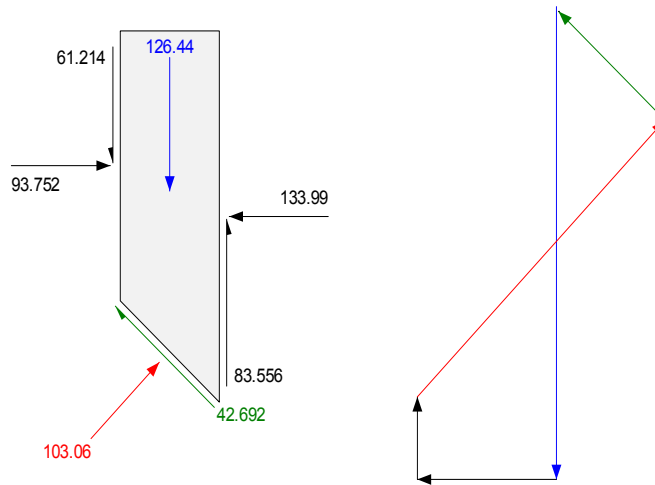
Figure 3-26 Lowe-Karafiath interslice function

We can check the resultant direction by looking at the slice forces. Figure 3-27 shows the forces for Slice 6. The ratio of shear to normal on the side of the slice is about 0.62, confirming that the direction of the resultant is parallel to inclination of the slope.

In Summary, the Lowe-Karafiath method:

- Considers both interslice shear and normal forces,
- Satisfies overall horizontal force equilibrium, but not moment equilibrium, and
- Uses interslice force functions related to the ground surface slope and slip surface inclination.

Slice 6 - Lowe-Karafiath Method

**Figure 3-27 Free body and force polygon for Lowe-Karafiath Method**

3.10 Sarma method

Sarma (1973) developed a stability analysis method for non-vertical slice or for general blocks. Only vertical slices are assumed in the current Sarma method implemented in SLOPE/W. The full Sarma method has as yet not been implemented. The geometric definition of the blocks does not fit into the general method of slices scheme in SLOPE/W for all the other methods, and therefore special software is required to define and visualize the results. The plan is to add the complete Sarma method at a future time.

The approach used by Sarma to relate the inter-block shear and normal forces can also be used to describe the relationship between the interslice shear and normal forces between slice.

Sarma adopted an equation similar to the Mohr-Coulomb shear strength equation to relate the interslice shear and normal forces. The equation (using SLOPE/W terminology) is:

$$X = c \times h + E \tan \phi$$

where, c is a cohesive strength component, h is the slice side height and ϕ is a material friction angle. The material properties are user-specified values.

The attraction of this approach is that the interslice forces are related by material properties that are intuitively perhaps easier to conceptualize than a specified function, but in the end it just another mechanism for specifying the interslice function.

This approach works best when the cohesion is zero or at least very small. When the cohesion is zero, the interslice shear is directly proportional to the normal as with all the other methods. When a cohesion value is specified, the interslice shear starts to become independent of the interslice normal, which can lead to convergence difficulties.

When using the Sarma interslice force approach, you should start with cohesion being zero. Later you can add a small amount to cohesion and investigate the effect of adding this component, but it has to be done care and caution. Considering how insensitive the resulting factor of safety is to interslice forces, it is likely best to always leave the cohesion as zero.

Other than the manner in which the interslice forces are related, the Sarma method in SLOPE/W is the same as the Spencer and the Morgenstern-Price methods. The computed interslice shear forces are adjusted with a global factor (similar to Lambda) until overall force and moment equilibrium are satisfied.

Figure 3-28 shows the free body diagram and the force polygon when $c = 0$ and $\phi = 30$ degrees. The final lambda value when converged is 0.197. The interslice shear force on the right side of the slice is $0.197 \times 221.51 \tan 30 = 25.1$ as shown in Figure 3-28. The force polygon closes, showing force equilibrium in the Sarma method.

In summary, the Sarma method in SLOPE/W:

- Considers both shear and normal interslice forces,
- Satisfies both moment and force equilibrium, and
- Relates the interslice shear and normal forces by a quasi-shear strength equation.

Slice 6 - Sarma Method

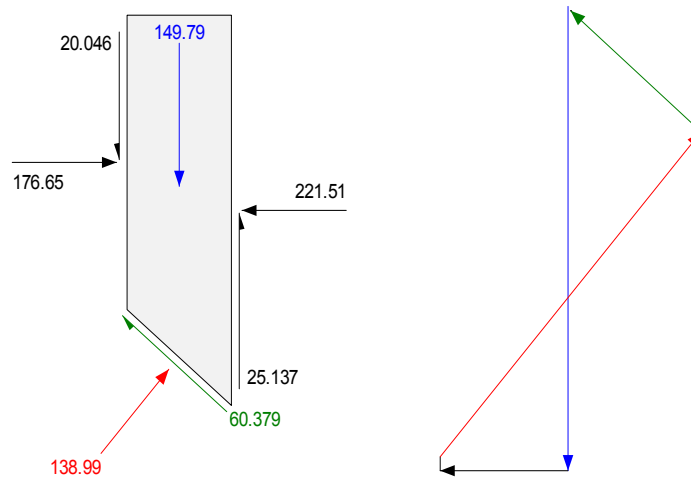


Figure 3-28 Free body and force polygon for Sarma Method

3.11 Janbu's Generalized method

The Janbu Generalized method is somewhat different than all the other limit equilibrium methods discussed above. This method imposes a stress distribution on the potential sliding mass by defining a line of thrust. The interslice shear-normal resultant is assumed to act where the line of thrust intersects the slices, which typically is at the lower $\frac{1}{3}$ point along the sides of the slices to represent a hydrostatic stress distribution. Assuming the position of the resultant makes it possible to compute the interslice shear forces by taking moments about the slice base center, the interslice normals are first computed using the Janbu's Simplified method, which has been discussed earlier. Next the interslice shear forces are determined by taking moments about the base of the slice.

The Janbu's Generalized method only satisfies overall force equilibrium, which is the same as the Janbu's Simplified. Moment equilibrium is only satisfied at the slice level. In SLOPE/W, the Janbu's Generalized method only computes the force equilibrium factor of safety (F_f). The overall moment equilibrium factor of safety (F_m) is not computed.

The Janbu Generalized method is actually similar to the Corps of Engineers and Lowe-Karafiath methods. All these methods consider both interslice shear and normal forces, but satisfy only force equilibrium. The Janbu Generalized method just uses a different technique to relate the interslice shear forces to the normal forces.

The previous chapter on Limit Equilibrium Fundamentals discusses the consequence of imposing a stress distribution on the potential sliding mass. Limit equilibrium formulations do not necessarily result in realistic stress distributions. Limit Equilibrium formulations find the slice forces that ensure force equilibrium of each slice and that ensure a constant factor of safety for each slice. These inherent characteristics can result in unrealistic stresses, and if the stresses are unrealistic, the slice itself may not satisfy moment equilibrium. Numerically this means the application point of the interslice resultant may be outside the slice. Conversely, if we find the slice forces that ensure moment equilibrium of each slice, then it may not be possible to ensure force equilibrium of each slice if the factor of safety is assumed the same for each slice. In a sense, assuming on a constant factor of safety overconstrains the problem at some level. To overcome this difficulty it is necessary to have a variable local factor of safety. In a limit equilibrium formulation, this is not possible. A method such as the Finite Element Stress based method discussed in the next section is required to have a variable local slice factor of safety.

Stress concentrations arising from sharp corners in a piece-wise linear slip surface or from concentrated forces representing reinforcement can create convergence difficulties in the Janbu's Generalized method. Also, the method may exhibit poor force polygon closure. Enforcing slice moment equilibrium means that it is not always possible to achieve slice force equilibrium.

Figure 3-29 shows the free body diagram and the force polygon of a slice using the Janbu's Generalized method. The interslice forces, although shown to be applied to the middle of the slice, are actually applied at the lower 1/3 of the slice sides in SLOPE/W. Although moment equilibrium is achieved in the slice, force equilibrium is not necessarily achieved, as indicated by the force polygon in Figure 3-29.

You will note in publications on the Janbu's Generalized method that the illustrated potential sliding masses are often long relative to the depth. In a relatively long shallow slide, the stress distribution is likely close to being hydrostatic with depth, similar to that assumed in the method. The Janbu's

Generalized method of course works the best when the actual stress distribution is close to the imposed stress distribution.

Slice 6 - Janbu Generalized Method

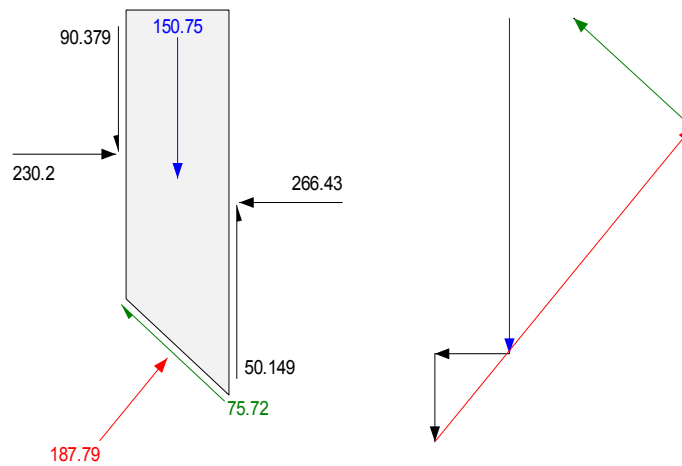


Figure 3-29 Free body and force polygon for Janbu's Generalized Method

So in summary, Janbu's Generalized method is just another approach to a limit equilibrium formulation. It is not necessarily better or worse than any of the other methods, as it has limitations just like all the other methods. The Janbu's Generalized method factors of safety will be similar to those methods that consider both shear and normal interslice forces, particularly if there are no sharp corners along the slip surface or high concentrated loads that cause stress concentrations.

3.12 *Finite element stress-based method*

The chapter on Limit Equilibrium Fundamentals discusses stress distributions obtained from limit equilibrium formulations, and shows that these stress distributions are not necessarily representative of the actual field stresses. To repeat, the limit equilibrium formulations give stresses and forces that:

- Aim to provide for force equilibrium of each slice
- Make the factor of safety the same for each slice

These inherent concepts and assumptions mean that it is not always possible to obtain realistic stress distributions along the slip surface or within the potential sliding mass. Some other piece of physics has to be added to the stability analysis to overcome these limitations. The missing piece of physics is a stress-strain relationship. Including such a relationship means displacement compatibility is satisfied, which in turn leads to much more realistic stress distributions.

One way of including a stress-strain relationship in a stability analysis is to first establish the stress distribution in the ground using a finite element analysis and then use these stresses in a stability analysis. This idea has been implemented in SLOPE/W. The ground stresses can be computed using SIGMA/W, and SLOPE/W uses the SIGMA/W stresses to compute safety factors. The following is a description of the implemented procedure.

Figure 3-30 shows a simple 45-degree slope discretized into finite elements. Using a simple gravity turn-on technique, the stresses in the ground can be computed. Using a linear-elastic constitutive relationship, the vertical stresses are as presented in Figure 3-31. This is typical of the information available from a finite element analysis. The basic information obtained from a finite element stress analysis is σ_x , σ_y and τ_{xy} within each element.

Worth noting at this stage is the 50 kPa contour, which is not a constant distance from the ground surface. The contour is closer to the surface under the toe. This means that the vertical stress is not just influenced by the overburden weight. It is also affected by the shear stress.

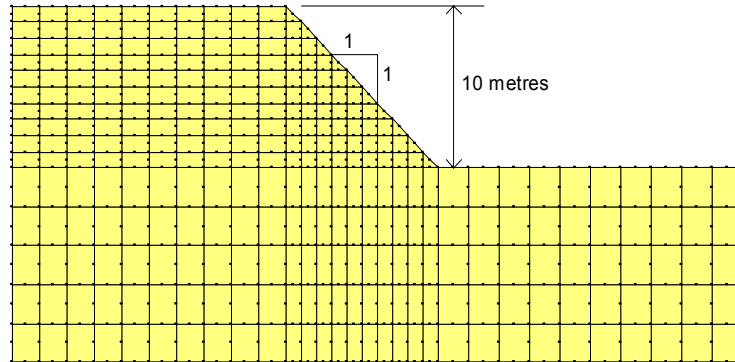


Figure 3-30 Finite element mesh for computing insitu stresses

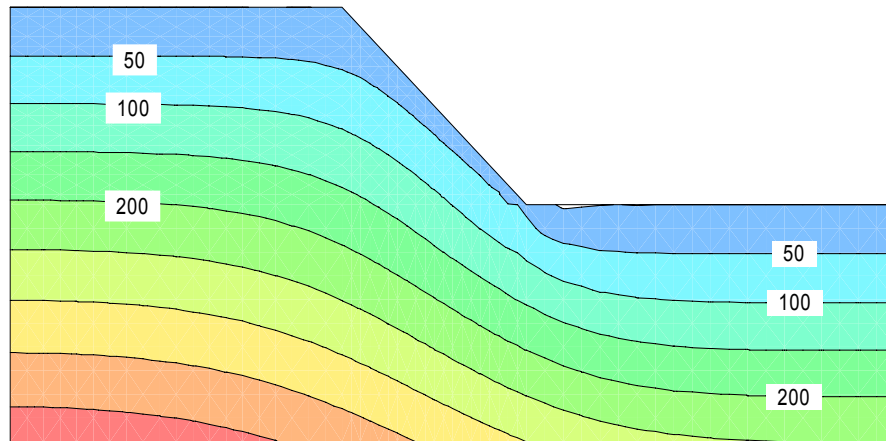


Figure 3-31 Vertical stress contours computed with SIGMA/W

The finite element-computed stresses can be imported into a conventional limit equilibrium analysis. The stresses σ_x , σ_y , τ_{xy} are known within each element, and from this information the normal and mobilized shear stresses can be computed at the base mid-point of each slice. The procedure is as follows:

1. The known σ_x , σ_y and τ_{xy} at the Gauss numerical integration point in each element are projected to the nodes and then averaged at each node. With the σ_x , σ_y and τ_{xy} known at the nodes, the same stresses can be computed at any other point within the element.

2. For Slice 1, find the element that encompasses the x-y coordinate at the base mid-point of the slice.
3. Compute σ_x , σ_y and τ_{xy} at the mid-point of the slice base.
4. The inclination (α) of the base of the slice is known from the limit equilibrium discretization.
5. Compute the slice base normal and shear stress using ordinary Mohr circle techniques.
6. Compute the available shear strength from the computed normal stress,
7. Multiply the mobilized shear and available strength by the length of the slice base to convert stress into forces.
8. Repeat process for each slice in succession up to Slice # n

Once the mobilized and resisting shear forces are available for each slice, the forces can be integrated over the length of the slip surface to determine a stability factor. The stability factor is defined as:

$$FS = \frac{\sum S_r}{\sum S_m}$$

where, S_r is the total available shear resistance and S_m is the total mobilized shear along the entire length of the slip surface. Similar stability factor expressions have been presented by others (Kulhawy 1969; Naylor, 1982).

Figure 3-32 shows a potential sliding mass discretized into slices superimposed on the finite element mesh. Following the procedure listed above, the stability factor for this slip surface is 1.318. This compares with a Morgenstern-Price factor of safety of 1.145 (constant interslice function). This is about a 15% difference.

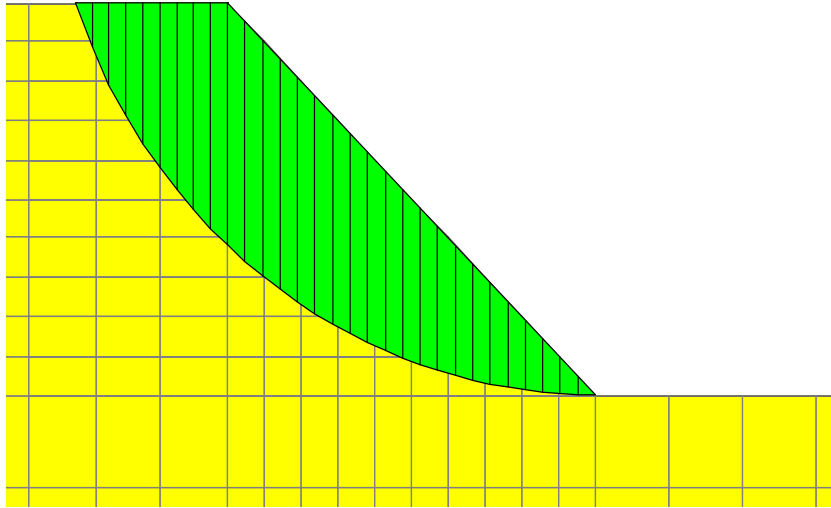


Figure 3-32 Toe slip surface on a finite element mesh

The reason for the difference in the margin of safety is primarily related to the normal stress distribution along the slip surface. The finite element and limit equilibrium normal stress distributions for this particular slip surface were presented earlier in Figure 3-33. The significantly different normal stresses in the toe area result from the shear stress concentration in this part of the section. Localized shear stress concentrations are, of course, not captured in a limit equilibrium formation where the slice base normal is derived primarily from the slice weight. This is one of the limitations of the limit equilibrium method.

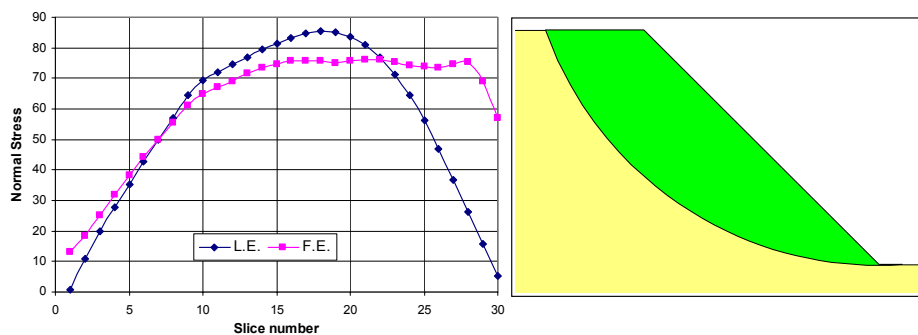


Figure 3-33 Normal stress distribution along a toe slip surface

The situation is somewhat different for a deeper slip, as shown in Figure 3-34. The finite element and limit equilibrium normal stress distributions along the slip surface are much closer for this case. Consequently the stability factor based on finite element stresses is almost the same as the Morgenstern-Price factor of safety. The stress-based stability factor is 1.849 while the Morgenstern-Price factor of safety is 1.804. This shows that, when the normal stress distribution along the slip surface is fairly representative of the actual ground stresses, the limit equilibrium factor of safety is as good as a stress-based factor of safety.

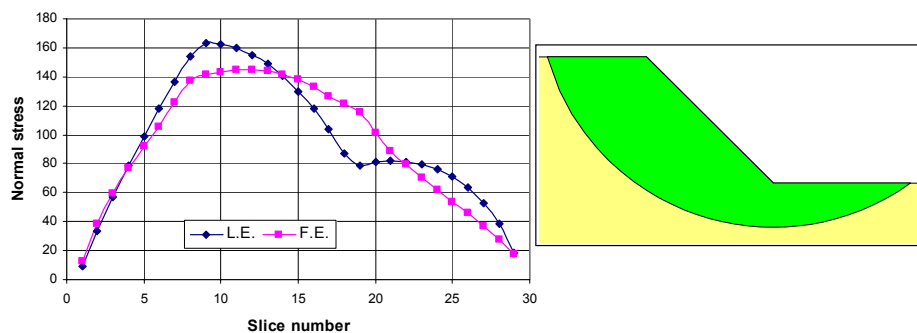


Figure 3-34 Normal stress distribution along a deep slip surface

An added advantage of the finite element stressbased approach is that it creates the possibility of looking at local safety factors for each slice. Figure 3-35 shows the variation of the local safety factor for the toe and deep slip surfaces. Included in the figure is the limit equilibrium factor of safety, which is the same for each slice.

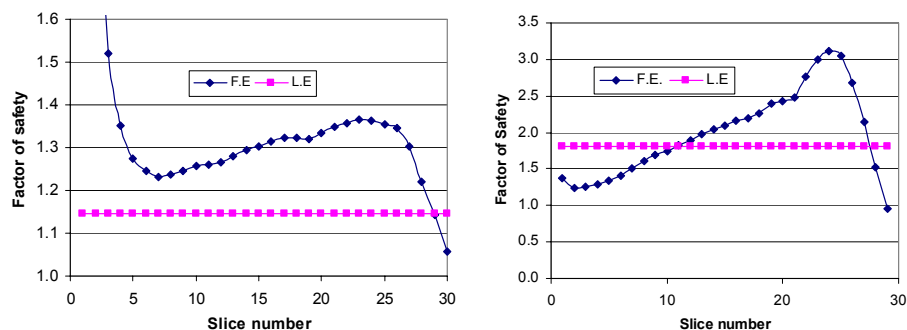


Figure 3-35 Local safety factors for toe (left) and deep (right) slip surfaces

For the deep slip surface the two global factors of safety are almost identical. Locally, however, the safety factors are either smaller or greater than the global value represented in this figure by the constant limit equilibrium factor of safety. Integrating the total available shear resistance and total mobilized shear along the slip surface averages the variation, making the two factors of safety the same.

The finite element stress-based approach overcomes some other limitations, such as highlighted in the previous chapter. Convergence is problematic in a LE formulation, particularly when the critical slip surface is steep, as behind a tie-back wall. Using FE stresses overcomes these convergence difficulties, as is further illustrated in the chapter on analyzing walls and steep slopes with reinforcement. Also, using FE stresses overcomes many of the difficulties with soil-structure problems. One of the very attractive features of doing a stability analysis based on finite element computed stresses is that soil-structure interaction can be handled in a direct manner. The difficulty of dealing with forces outside the sliding mass in a LE analysis was discussed in the previous chapter in the discussion on dealing with sheet piling embedment below the slip surface. Another similar situation is the use of a shear key wall placed across a slip surface to stabilize a slope, as illustrated in Figure 3-36. In this case, there is no need to try and represent the wall resistance with a line load as in a limit equilibrium analysis, and there is no need to independently determine the line load magnitude. The stiffness of the structure is included in the finite element analysis, which alters the stress state and which in turn increases the margin of safety.

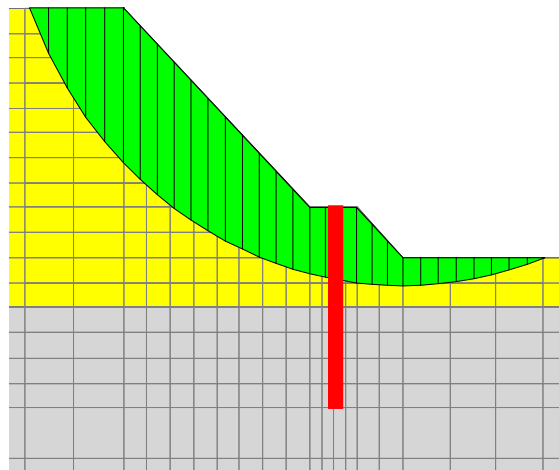


Figure 3-36 A shear-key wall for slope stabilization

The finite element stress-based approach also opens the door to looking at stability variations due to ground shaking during an earthquake. The stresses can come from a QUAKE/W dynamic finite element analysis the same as they can from a static stress analysis. The stresses computed during a dynamic earthquake analysis can be saved at regular intervals during the shaking. A factor of safety then can be computed for each moment in time that the stresses are available, and in the end a plot of factor of safety versus time graph can be created, as shown in Figure 3-38. This type of plot can be readily created for each and every trial slip surface. This is a great improvement over the historic pseudo-static approach still used so routinely in practice. This is discussed further in the chapter on Seismic and Dynamic stability.

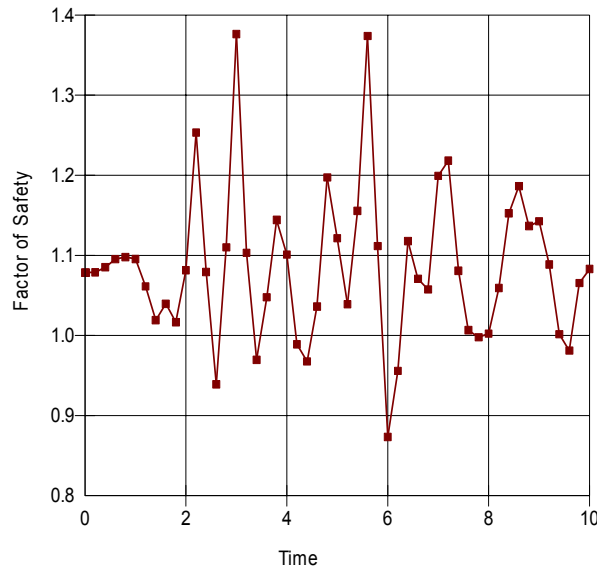


Figure 3-37 Factors of safety variations during earthquake shaking

3.13 Commentary on finite element stress-based method

The use of finite element computed stresses inside a limit equilibrium framework to assess stability has many advantages. Some are as follows:

- There is no need to make assumptions about interslice forces.

- The stability factor is deterministic once the stresses have been computed, and consequently, there are no iterative convergence problems.
- The issue of displacement compatibility is satisfied.
- The computed ground stresses are much closer to reality.
- Stress concentrations are indirectly considered in the stability analysis.
- Soil-structure interaction effects are readily handled in the stability analysis
- Dynamic stresses arising from earthquake shaking can be directly considered in a stability analysis.

The finite element based approach overcomes many of the limitations inherent in a limit equilibrium analysis. At the same time, it does raise some new issues.

It is necessary to first carry out a finite element stress analysis with the proposed approach. Fortunately, the necessary software tools are now readily available and relatively easy to use. However, it does mean that the analyst must become familiar with finite element analysis techniques.

Fortunately, a finite element stress analysis is fairly straightforward if the material properties are restricted to simple linear-elastic behavior. Besides being relatively simple, using only linear-elastic soil models always ensures a solution, since there are no convergence difficulties, which can be a problem with nonlinear constitutive models. A linear-elastic analysis is adequate in many cases to obtain a reasonable picture of the stress conditions. It certainly gives a much better stress distribution picture than that obtained from a limit equilibrium analysis. Nonlinear constitutive relationships are often essential if the main interest is deformation, but not if the main interest is a stress distribution. Furthermore, even approximate linear-elastic properties are adequate to get a reasonable stress distribution and, consequently, not a great deal of effort is required to define the linear-elastic parameters.

The results from a simple linear-elastic analysis may mean that the computed stresses in some zones are higher than the available soil strength. This manifests itself as a local factor of safety of less than 1.0 for some slices, which is not physically possible. Ideally, nonlinear constitutive models should be used to redistribute the stresses such that the applied stresses do not exceed the strength. However, using nonlinear constitutive relationships greatly complicates the analysis, primarily because of the associated numerical convergence issues.

Ignoring local safety factors that are less than unity is not all that serious. Physically, it means that neighboring slices have a local safety factor that is too high. Since all the mobilized and resisting shear forces are tallied along the entire slip surface, local irregularities are smoothed out and therefore have little effect on the total forces which are used in computing the global factor of safety for the entire sliding mass. This is an indirect form of averaging, but not nearly to the extent that is inherent in the limit equilibrium formulation, where the factor of safety is the same for all slices.

Figure 3-38 shows the local factor of safety distribution for a simple 2h:1v slope when the stresses are determined using a linear-elastic analysis and an elastic-plastic analysis. The linear-elastic stresses result in local safety factors less than 1.0. The elastic-plastic analysis redistributes the stresses and then none of the local safety factors are less than 1.0. The global factors of safety are, however, nearly identical. For the linear-elastic case, the global factor of safety is 1.206 and for the elastic-plastic case the global factor of safety is 1.212, less than half a percent difference.

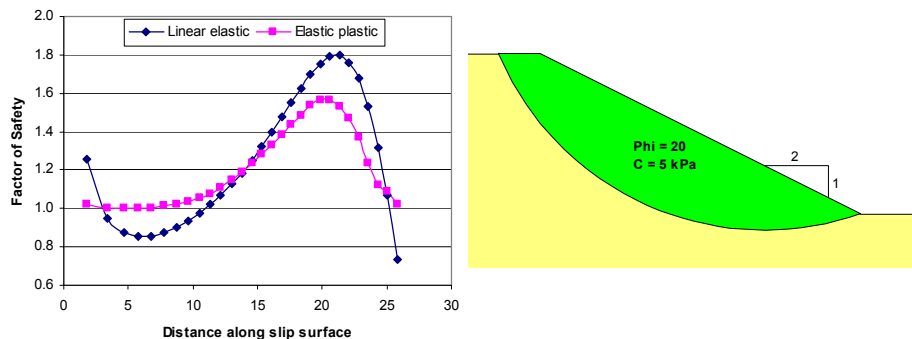


Figure 3-38 Local safety factors for linear-elastic & elastic-plastic stresses

Using the finite element computed stresses means that the stability calculations now involve the horizontal stresses as well as the vertical stresses. This is good and bad. The good part is that various K_o (σ_x / σ_y ratio) conditions can be considered in a stability analysis. The bad part is that the K_o must be defined. In a linear-elastic gravity turn-on analysis, the ratio of σ_x / σ_y is reflected through Poisson's ratio (ν). For level ground, K_o equals $\nu / (1 - \nu)$. Different K_o conditions will give different safety factors. Fredlund et al. (1999) studied the effect of varying Poisson's ratio on the factor of safety. Fortunately, defining appropriate K_o conditions is not an

impossibility. It is certainly not so difficult as to prevent the use of finite element stresses in assessing stability.

3.14 *Selecting an appropriate method*

The limit equilibrium method for analyzing stability of earth structures remains a useful tool for use in practice, in spite of the limitations inherent in the method. Care is required, however, not to abuse the method and apply it to cases beyond its limits. To effectively use limit equilibrium types of analyses, it is vitally important to understand the method, its capabilities and its limits, and not to expect results that the method is not able to provide. Since the method is based purely on the principles of statics and says nothing about displacement, it is not always possible to obtain realistic stress distributions. This is something the method cannot provide and consequently should not be expected. Fortunately, just because some unrealistic stresses perhaps appear for some slices, does not mean the overall factor of safety is necessarily unacceptable. The greatest caution and care is required when stress concentrations exist in the potential sliding mass due to the slip surface shape or due to soil-structure interaction.

A detailed understanding of the method and its limits leads to greater confidence in the use and in the interpretation of the results. Getting to this position means you have to look at more than just factors of safety. To use the limit equilibrium method effectively, it is also important to examine the detailed slice forces and the variation of parameters along the slip surface, at least sometime during the course of a project. Looking at a FS versus lambda plots, for example, is a great aid in deciding how concerned one needs to be about defining an interslice force function.

Also, limit equilibrium analyses applied in practice should as a minimum use a method that satisfies both force and moment equilibrium, such as the Morgenstern-Price or Spencer methods. With the software tools now available, it is just as easy to use one of the mathematically more rigorous methods than to use the simpler methods that only satisfy some of the statics equations.

In practice you should use a method that meets two criteria. One, the method should satisfy all equations of statics, and two, the method should consider both shear and normal interslice forces.

At this stage the SIGMA/W-SLOPE.W integrated method is the most applicable where conventional limit equilibrium methods have numerical difficulties as in vertical or near vertical walls with some kind of reinforcement. The method is perhaps not all that applicable in the stability of natural slopes where it is not easy to accurately determine the stresses in the slope due to the complex geological processes that created the slope. In the analysis of natural slopes where the potential slip surface does not have sharp corners and there are no high stress concentrations, the conventional limit equilibrium method is more than adequate in spite of its limitations.

The tools required to carry out geotechnical stability analyses based on finite element computed stresses are today readily available. Applying the tools is now not only feasible, but also practical. Unforeseen issues will possibly arise in the future, but such details will likely be resolved with time as the method is used more and more in geotechnical engineering practice.

Using finite element computed stresses inside a limit equilibrium framework to analyze the stability of geotechnical structures is a major step forward since it overcomes many of the limitations of traditional limit equilibrium methods and yet it provides an anchor to the familiarity of limit equilibrium methods so routinely used in current practice.

4 Slip Surface Shapes

4.1 *Introduction and background*

Determining the position of the critical slip surface with the lowest factor of safety remains one of the key issues in a stability analysis. As is well known, finding the critical slip surface involves a trial procedure. A possible slip surface is created and the associated factor of safety is computed. This is repeated for many possible slip surfaces and, at the end, the trial slip surface with the lowest factor of safety is deemed the governing or critical slip surface.

There are many different ways for defining the shape and positions of trial slip surfaces. This chapter explains all the procedures available in SLOPE/W, and discusses the applicability of the methods to various situations.

Finding the critical slip surface requires considerable guidance from the analyst in spite of the advanced capabilities of the software. The soil stratigraphy may influence the critical mode of potential failure and the stratigraphy therefore must be considered in the selected shape of the trial slip surfaces. In the case of a tie-back wall, it may be necessary to look separately at a toe failure and a deep seated failure. In an open pit mine the issue may be bench stability or overall high wall stability and each needs to be considered separately. Generally, not all potential modes of failure can necessarily be investigated in one analysis. In such cases the positions of the trial slip surfaces needs to be specified and controlled to address specific issues.

A general procedure for defining trial slips may result in some physically inadmissible trial slip surfaces; that is, the trial slip surface has a shape which cannot exist in reality. Often it is not possible to compute a safety factor for such unrealistic situations, due to lack of convergence. Sometimes, however, safety factors can be computed for unrealistic slips, and then it is the responsibility of the analyst to judge the validity of the computed factor of safety. The software cannot necessarily make this judgment. This is an issue that requires guidance and judgment from the analyst. This issue is discussed further toward the end of the chapter.

Another key issue that comes into play when attempting to find the position of the critical slip surface is the selection of soil strength parameters. Different soil strength parameters can result in different computed positions of the critical slip surface. This chapter discusses this important issue.

Presenting the results of the many trial slip surfaces has changed with time. This chapter also addresses the various options available for presenting a large amount of data in a meaningful and understandable way. These options are related to various slip surface shapes, and will consequently be discussed in the context of the trial slip surface options.

4.2 Grid and radius for circular slips

Circular trial slip surfaces were inherent in the earliest limit equilibrium formulations and the techniques of specifying circular slip surfaces has become entrenched in these types of analyses. The trial slip surface is an arc of circle. The arc is that portion of a circle that cuts through the slope. A circle can be defined by specifying the x-y coordinate of the centre and the radius. A wide variation of trial slip surfaces can be specified with a defined grid of circle centers and a range of defined radii. In SLOPE/W, this procedure is called the Grid and Radius method. Figure 4-1 shows a typical example.

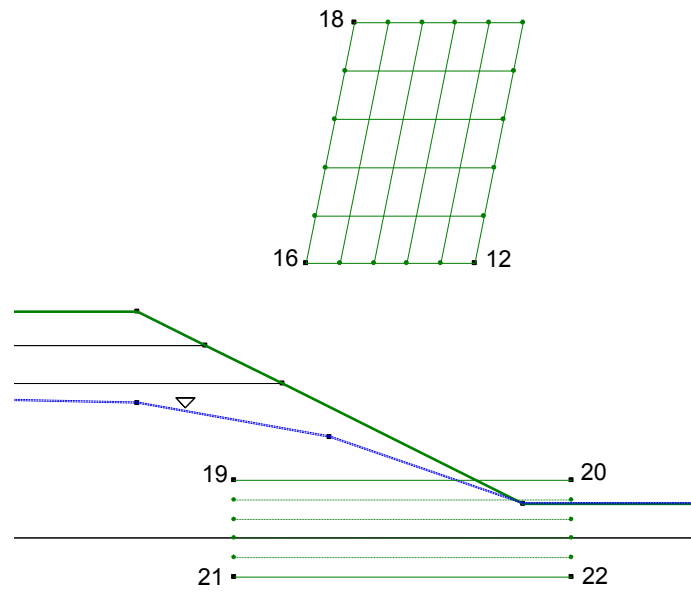


Figure 4-1 The grid and radius method of specifying trial slip surfaces

The grid above the slope is the grid of rotation centers. Each grid point is the circle center for the trial slips. In this example there are 36 (6 x 6) grid points or circle

centers. In SLOPE/W, the grid is defined by three points; they are upper left (18), lower left (16) and lower right (12).

The trial circle radii are specified with radius or tangent lines. The lines are specified by the four corners of a box. In the above example, the four corners are 19 (upper left), 21 (lower left), 22 (lower right) and 20 (upper right). For the SLOPE/W main processor to interpret the radius line specification correctly, the four points need to start at the upper left and proceed in a counter-clockwise direction around the box. The number of increments between the upper and lower corners can be specified. In the above example there are five increments making the total number of radius lines equal to 6.

To start forming the trial slip surfaces, SLOPE/W forms an equation for the first radius line. Next SLOPE/W finds the perpendicular distance between the radius line and a grid centre. The perpendicular distance becomes the radius of the trial slip surface. The specified radius lines are actually more correctly tangent lines; that is, they are lines tangent to the trial circles. Figure 4-2 shows one imaginary circle. Note that the specified radius line is tangent to the circle. The trial slip surface is where the circle cuts the soil section. For this example, SLOPE/W will compute safety factors for 216 (36 x 6) trial slip surfaces.

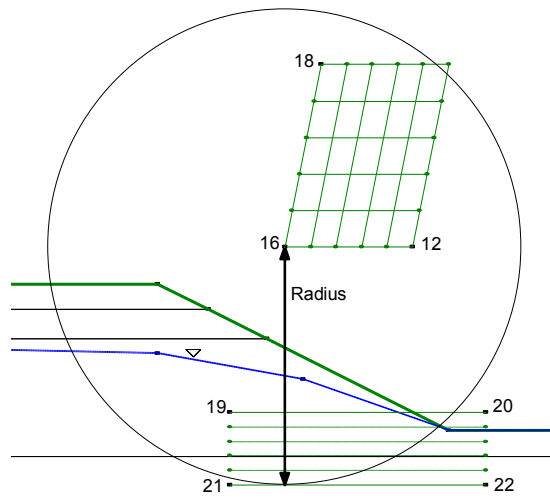


Figure 4-2 Imaginary trial slip surface

The radius line “box” (points 19, 21, 22, 20) can be located at any convenient position and can form any quadrilateral shape. The illustration in Figure 4-3 is entirely acceptable. Also, the position of the radius box does not necessarily need to be on the soil section. Usually it is most convenient for the box to be on the slope section, but this is not a requirement in the SLOPE/W formulation. It becomes useful when the trial slip surfaces have a composite shape as discussed below.

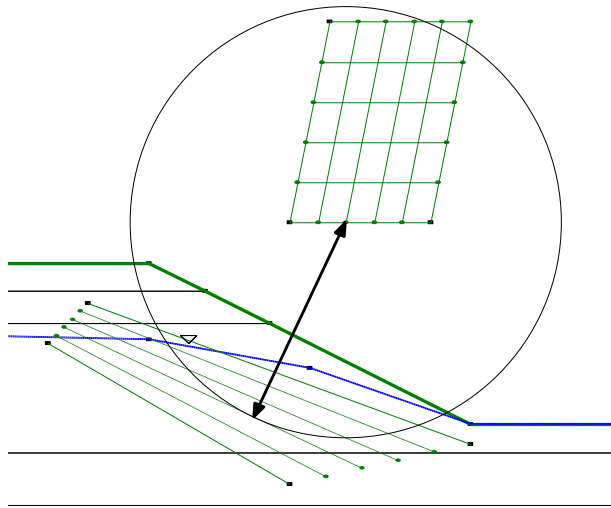


Figure 4-3 Specification of radius lines

Single radius point

The radius line box can be collapsed to a point. All four corners can have the same point or the same x-y coordinate. If this is the case, all trial slip surfaces will pass through a single point (Figure 4-4). This technique is useful when you want to investigate a particular mode of failure, such as the potential failure through the toe of a wall.

The grid of centers can also be collapsed to a single point. This makes it possible to analyze just one slip surface, which can be very useful for doing comparisons of various features or options.

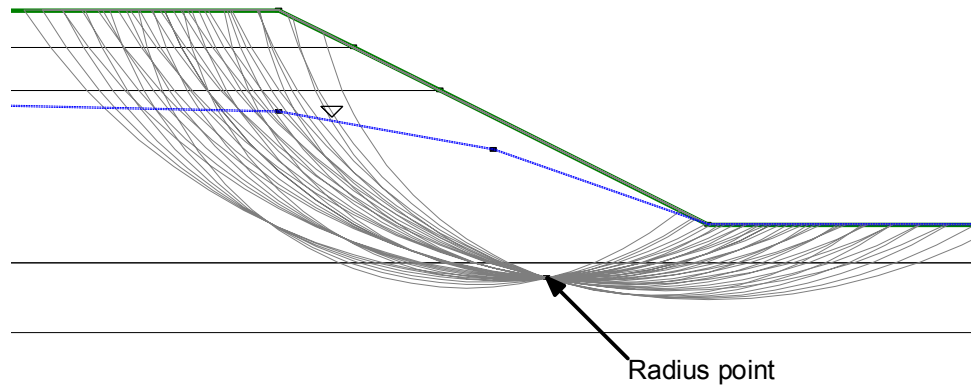


Figure 4-4 All slip surfaces through a point

Multiple radius points

The radius box can also be collapsed to a line with radius increments. This makes it possible to analyze trial slips that pass through a series of points. This can be done by making the upper two corners the same and the lower two corners the same. This is illustrated in Figure 4-5.

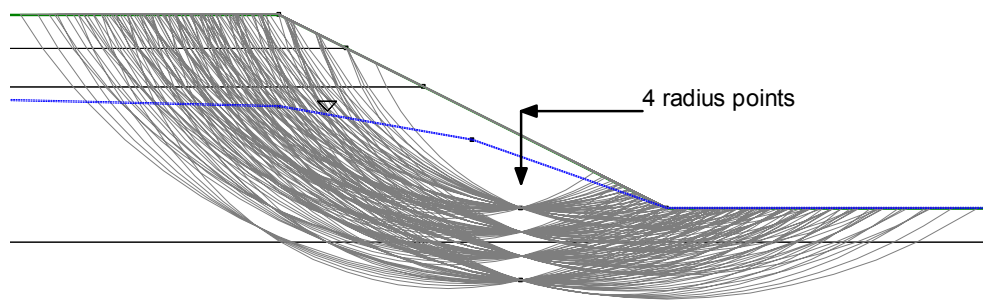


Figure 4-5 Slip surfaces through a series of radius points

Lateral extent of radius lines

The tangent or radius lines in SLOPE/W do not have lateral extents. The tangent lines are used to form the equation of a line, but the equation lines are not limited by the lateral extents of the specified lines. The two cases illustrated in Figure 4-6 result in exactly the same trial slip surfaces. This can sometimes result in unexpected trial slip surfaces that fall outside the intended range. A typical

example may be a shallow slip that just cuts through the crest of the section as in a near vertical wall. This undesired outcome is one of the weaknesses of the Grid-Radius technique and the reason for other options for specifying trial slip surfaces. The Enter-Exit method, for example, discussed below does not have this shortcoming.

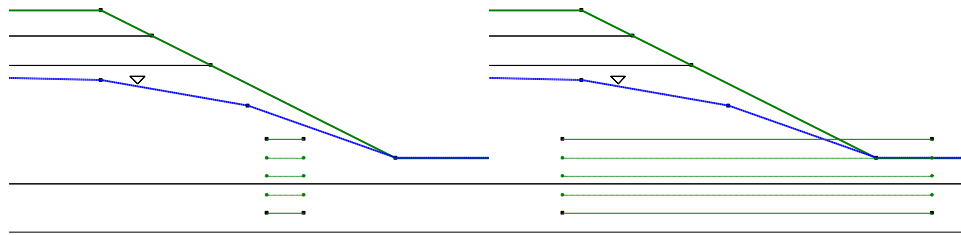


Figure 4-6 Effect of radius line lengths

Another side effect of the Grid-Radius method is that trial slips can fall outside the extents of the geometry. All trial slips must enter and exit along the Ground Surface line. If trial slips enter or exit outside the Ground Surface line, they are considered invalid and no factor of safety is computed. A typical case may be a trial slip that enters or exits the vertical ends of the defined geometry. Such trial slips are invalid. No safety factors are displayed at the Grid centers for which no valid trial slip surface exists.

Factor of Safety contours

In the early days of limit equilibrium stability analyses, the only way to graphically portray a summary of all the computed safety factors was to contour the factors of safety on the Grid, as illustrated in Figure 4-7. The contours provide a picture of the extent trial slip surfaces analyzed, but more importantly the contours indicate that the minimum safety factor has been found. The ideal solution is when the minimum falls inside a closed contour like the 1.240 contour in Figure 4-7.

The technique of contouring the safety factors on the Grid has become deeply entrenched in slope stability analyses. This has come about partly because of early developments and presentations, and partly because all related textbooks present this as an inherent requirement.

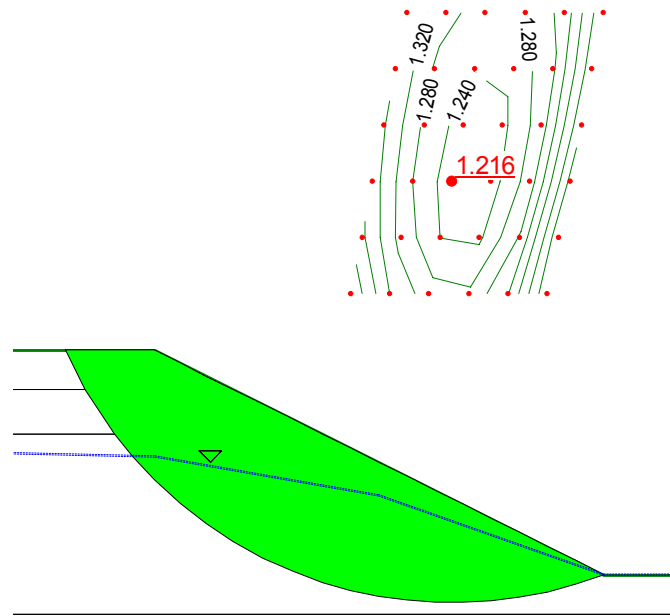


Figure 4-7 Factor of safety contours on grid of rotation centers

Unfortunately, the ideal solution illustrated in Figure 4-7 is not always attainable; in fact the number of situations where the ideal contour picture can be attained is considerably less than the situations where it is not attainable. The ideal solution can usually be obtained for conventional analyses of fairly flat slopes (2h:1v or flatter), with no concentrated line loads, and with c and ϕ effective strength parameters. A common case where the ideal cannot be attained is for purely frictional material ($c = 0$; $\phi > 0$) as discussed in detail further on in this Chapter. Another typical case is the stability analysis of vertical or near vertical walls.

Recognizing that the ideal textbook case of the minimum safety factor falling in the middle of the Grid is not always attainable is vitally important in the effective use of a tool like SLOPE/W.

Now there are other ways of graphically portraying a summary of computed safety factors. One way is to display all the trial slip surfaces as presented in Figure 4-8. This shows that the critical slip surface falls inside the range of trial slips and it shows the extent of the trial slips.

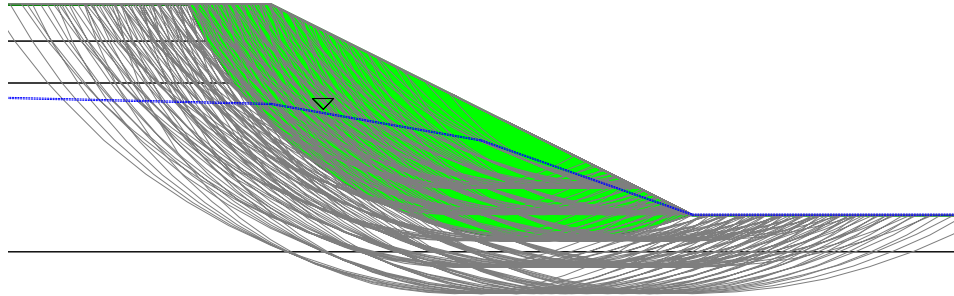


Figure 4-8 Display of multiple trial slip surfaces

Another effective way of graphically viewing a summary of the trial slip surfaces is with what is called a safety map. All the valid trial slip surfaces are grouped into bands with the same factor of safety. Starting from the highest factor of safety band to the lowest factor of safety band, these bands are painted with a different color. The result is a rainbow of color with the lowest factor of safety band painted on top of the rest of the color bands. Figure 4-9 illustrates an example of the safety map.

In this example, the red color is the smallest factor of safety band, and the white line is the critical slip surface. This type of presentation clearly shows the location of the critical slip surface with respect to all trial slip surfaces. It also shows zone of potential slip surfaces within a factor of safety range.

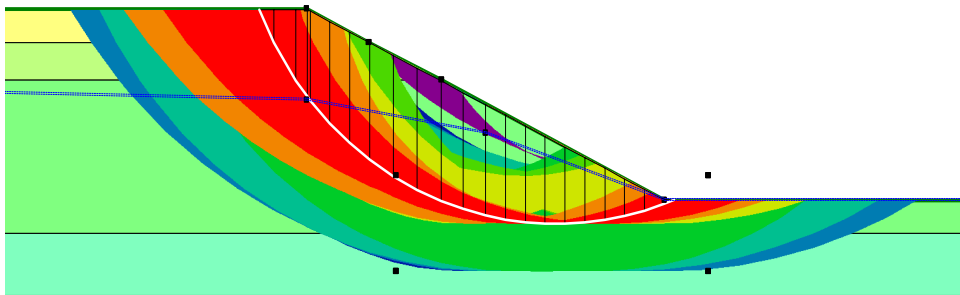


Figure 4-9 Display of safety map

4.3 Composite slip surfaces

Stratigraphic conditions have a major influence on potential slip surfaces. Circular slip surfaces are fairly realistic for uniform homogeneous situations, but this is seldom the case in real field cases. Usually there are multiple layers with varying strength and varying pore-water pressure conditions which can have an effect on the shape of the critical slip surface.

A common situation is where surficial soils overlie considerably stronger material at depth. There is the potential for the surficial soils to slide along the contact between the two contrasting materials. This type of case can be analyzed with what is called a composite slip surface. The stronger underlying soil is flagged as being impenetrable (or bedrock). The trial slip surface starts as an arc of the circle until it intersects the impenetrable surface. The slip surface then follows the impenetrable surface until it intersects the circle, and then again follows the arc of a circle up to the surface as illustrated in Figure 4-10. The circular portion of the trial slip surfaces is controlled by the Grid and Radius method discussed above.

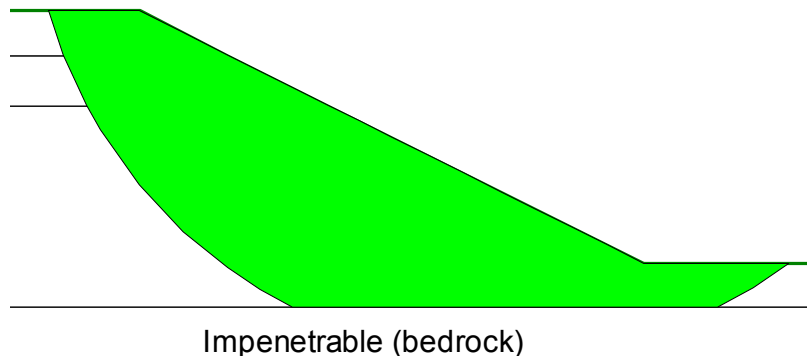
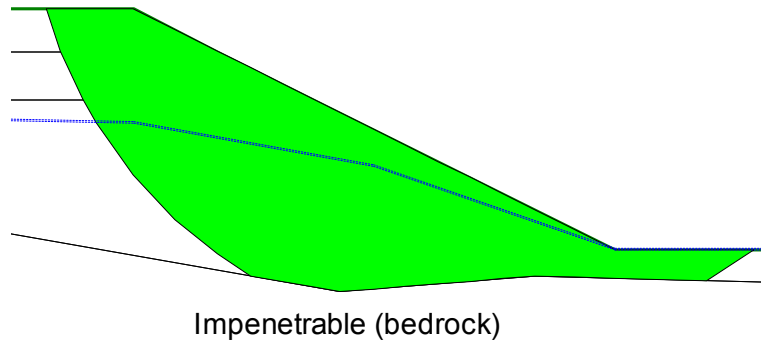


Figure 4-10 Composite slip surface controlled by impenetrable layer

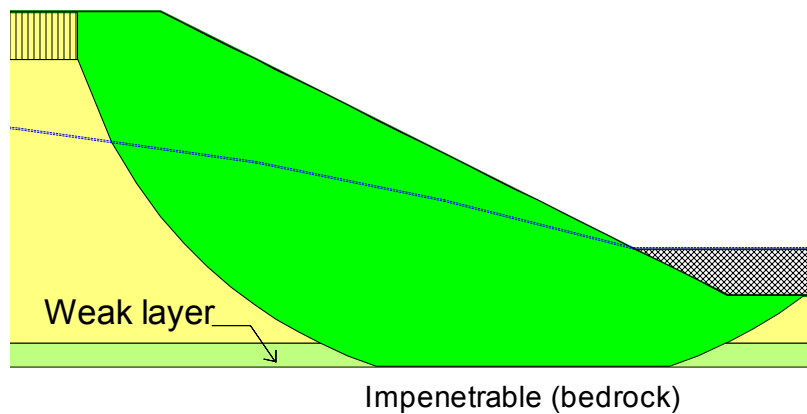
The portion of the slip surface that follows the impenetrable material takes on the soil strength of the material just above the impenetrable layer. This can always be verified by graphing the strength along the slip surface.

The impenetrable surface does not have to be a straight line – it can have breaks as in Figure 4-11. However, extreme breaks may make the slip surface inadmissible, and it usually results in an unconverged solution.

**Figure 4-11 Irregular impenetrable layer**

The impenetrable material feature is useful for analyzing cases with a weak, relatively thin layer at depth. Figure 4-12 shows such an example. In this case, the portion of the slip surface that follows the impenetrable takes on the strength assigned to the weak layer.

For practical reasons, there is no need to make the weak layer too thin. The portion of the slip surface in the weak layer that does not follow the impenetrable contact is relatively small and therefore has little influence on the computed factor of safety. The effort required in making the weak layer very thin is usually not warranted.

**Figure 4-12 Impenetrable layer forces slip along weak layer**

The impenetrable feature can also be used to analyze the sliding stability of cover material on a synthetic liner, as illustrated in Figure 4-13. The impenetrable layer causes the trial slip surface to follow the liner. A thin region just above the impenetrable material has properties representative of the frictional sliding resistance between the cover material and the liner. This is the shear strength along that portion of the slip surface that follows the impenetrable material.

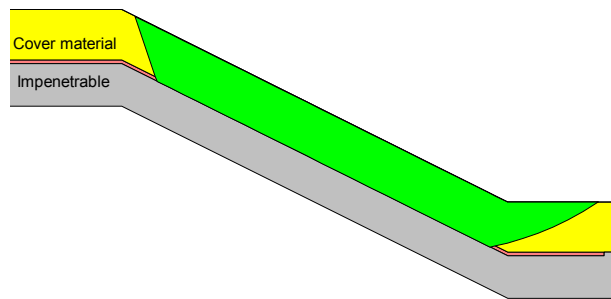


Figure 4-13 Sliding on a synthetic liner

Again this can be verified by graphing the strength along the slip surface. In this illustration the cover material has a friction angle of 30 degrees and the friction angle between the liner and the cover material is 15 degrees. This is confirmed by the SLOPE/W graph in Figure 4-14.

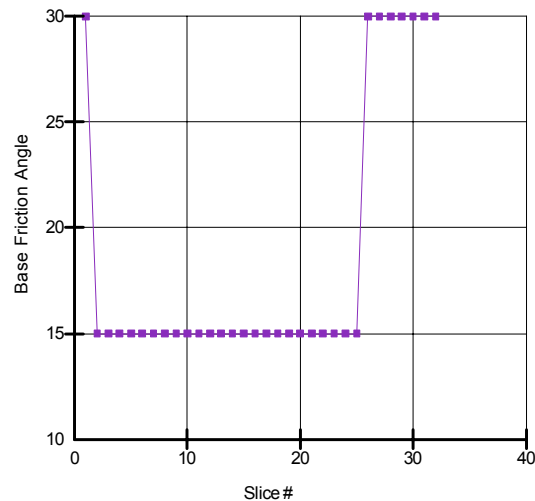


Figure 4-14 Variation of friction angle along slip surface

Note that the tensile capacity of the liner does not come into play in this cover sliding analysis. Considering the tensile strength would require a different setup and a different analysis.

In SLOPE/W, the concept of an impenetrable material is just a mechanism to control the shape of trial slip surfaces – it is not really a material.

4.4 Fully specified slip surfaces

A trial slip surface can be specified with a series of data points. This allows for complete flexibility in the position and shape of the slip surface. Figure 4-15 illustrates a fully-specified slip surface.

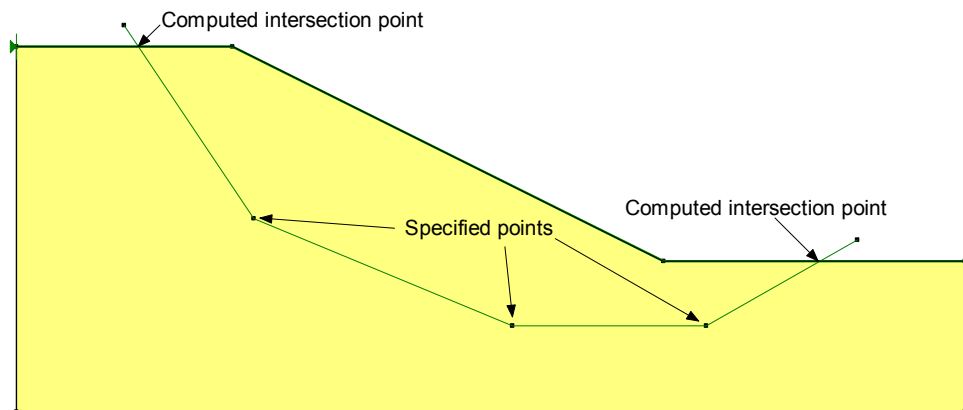


Figure 4-15 Fully specified slip surface

Note that the specified surface starts and ends outside the geometry. SLOPE/W can then compute the ground surface intersection points. Allowing SLOPE/W to compute these intersection points is better than trying to place a point on the ground surface, which can sometimes lead to some numerical confusion.

A point needs to be created about which to take moments. This is called the Axis Point (Figure 4-16). The Axis Point can be specified. If the Axis point is not defined, SLOPE/W will compute an Axis location based on the geometry of the problem.

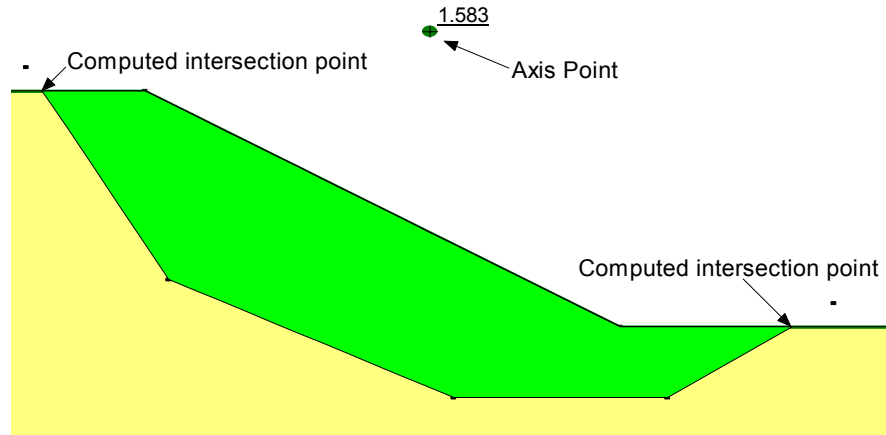


Figure 4-16 Axis point about which to compute moments

The factor of safety calculations are not sensitive to the position of the Axis point, for methods that satisfy both moment and force equilibrium (e.g., Spencer and Morgenstern-Price methods). However, for simplified methods (e.g., Ordinary and Simplified Bishop), the factor of safety calculations can be sensitive to the position of the Axis Point. In general, the Axis Point should be in a location close to the approximate center of rotation of the sliding mass. It is usually somewhere above the slope crest and between the extents of the potential sliding mass.

The Fully Specified method is useful when large portions of the slip surface position are known from slope inclinometer field measurements, geological stratigraphic controls and surface observations.

The Fully Specified option may also be useful for other cases such as the sliding stability of a gravity retaining wall (Figure 4-17).

While the Fully Specified method is completely flexible with respect to trial slip surfaces shapes and position, it is limited in that each and every trial slip surface needs to be specified. The method is consequently not suitable for doing a large number of trials to find the critical slip surface.

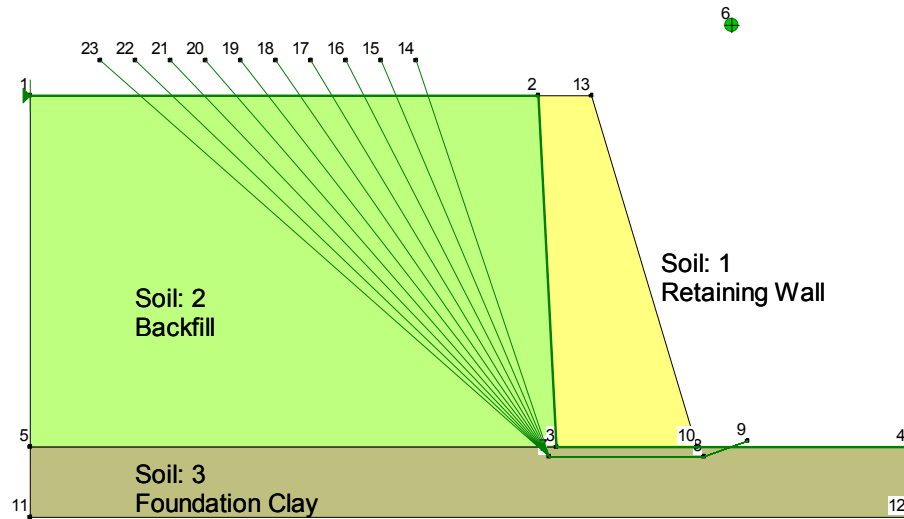


Figure 4-17 Sliding analysis of a gravity retaining wall

4.5 Block specified slip surface

General cross-over form

Block shaped analyses can be done by specifying two grids of points as shown in Figure 4-18. The grids are referred to as the left block and the right block. The grids are defined with an upper left point, a lower left point and a lower right point. In the example here the right block is defined by Points 11, 12 and 13.

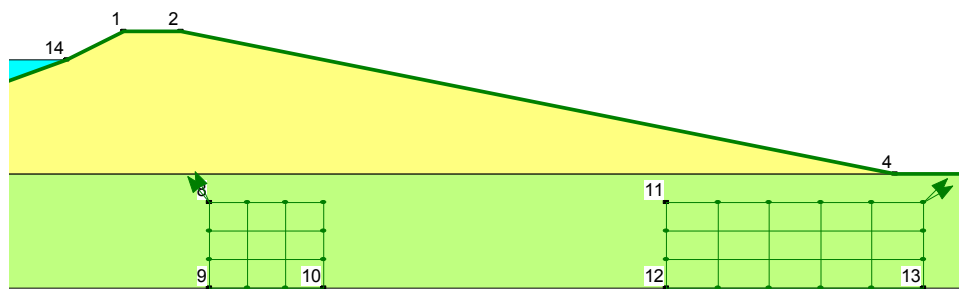


Figure 4-18 Grids in Block Specified method

The slip surface consists of three line segments. The middle segment goes from each grid point on the left to each grid point on the right. The other two segments are projections to the ground surface at a range of specified angles. Figure 4-19 presents the type of trial slip surface created.

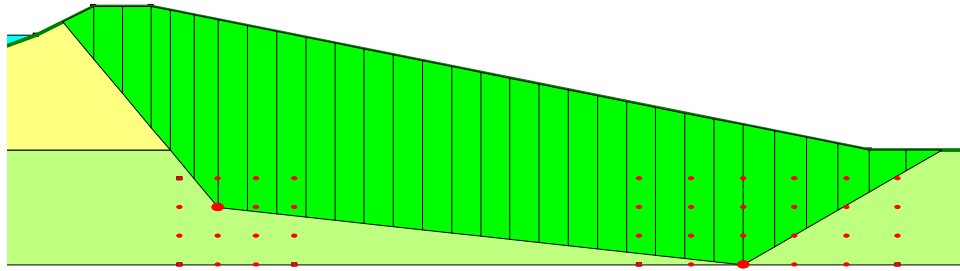


Figure 4-19 Slip surface shape in the Block method

By allowing the middle segments to go from each grid point on the left to each point on the right, the middle line segments cross over each other when multiple slips are viewed simultaneously, and hence the cross-over designation. An option where this is not allowed is also an option available within SLOPE/W that is discussed later in this chapter.

The end projections are varied, depending on the specified angles and the incremental variation in the angles. Arrows are drawn at the upper left and right corners as in Figure 4-20 to graphically portray the specified angles.

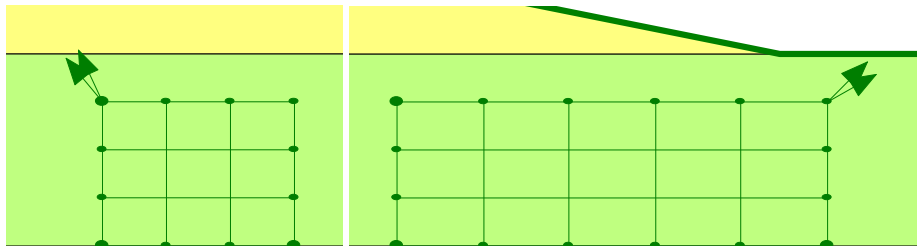


Figure 4-20 Projection angles in the Block method

The situation in the toe area is similar to a passive earth pressure condition where the sliding mass is being pushed outward and upward. In the crest area, the situation is analogous to active earth pressure conditions. From lateral earth pressure considerations, the passive (toe) slip surface rises at an angle equal to

$(45 - \phi/2)$ and the active slip line dips at an angle of $(45 + \phi/2)$. These considerations can be used to guide the selection of the projection angles.

In SLOPE/W, geometric angles are defined in a counterclock-wise direction from the positive x-coordinate axis. An angle of zero means a horizontal direction to the right, an angle of 90 degrees means an upward vertical direction; an angle of 180 degrees means a horizontal direction in the negative x-coordinate direction, and so forth.

In the above example, the right toe (passive) projection angles vary between 30 and 45 degrees, and the left crest (active) projection angles vary between 115 and 130 degrees (between 65 and 50 degrees from the horizontal in the clock-wise direction).

Like the Fully Specified method, the Block method also needs a defined Axis about which to take moments. If the Axis point is not defined, SLOPE/W will compute an Axis location based on the geometry of the problem.

This method of creating trial slip surfaces can lead to a very large number of trials very quickly. For the illustrative example here the left block has 16 (4x4) grid points and the right block has 24 (4x6) grid points. At each end there are three different projection angles. The total number of trial slips is $16 \times 24 \times 3 \times 3$ which equals 3,456. Some caution is consequently advisable when specifying the size of the grid blocks and the number of projection angles.

The Block method is particularly useful in a case such as in Figure 4-19. Here an embankment with flat side slopes rests on a relatively thick stratum of soft foundation soil. The middle segment of the crucial slip surface tends to dip downward as in Figure 4-19 as opposed to being horizontal. Allowing the middle segments to vary between all the grid points makes it possible to find this critical potential mode of sliding.

A difficulty with the Block method is that it is not always possible find a converged solution when the corners along the slip surface become too sharp. A typical situation is shown in Figure 4-21. The break in the slip surface on the left is too sharp and this causes convergence problems.

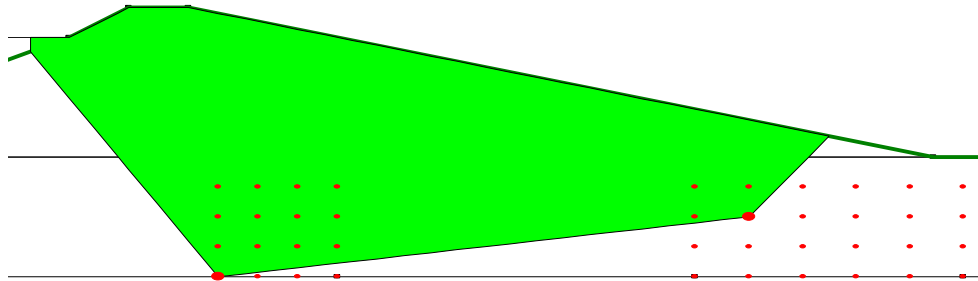


Figure 4-21 Trial slip surface with a sharp corner

The convergence difficulties with the Block method can result in a large number of trial slip surfaces with an undefined safety factor. This is particularly problematic when the grid blocks get close to each other. The Block method works the best and is the most suitable for cases where there is a significant distance between the two blocks. Stated another way, the middle segment line segment should be significantly longer than the two end projection segments.

Slip surfaces seldom, if ever, have sharp corners in reality, which is one of the assumptions made in the Block method. This reality points to another weakness of this method with respect to forming trial slip surfaces. This limitation can sometimes be overcome by the optimization technique discussed below.

Worth noting is that the two grid blocks can be collapsed to a line with points or to a single point. If the two left specified points in the grid block are the same, the block will collapse to a line. If all three points are the same, the grid block will collapse to a single point.

Specific parallel form

There are situations where it is preferable to have all the middle line segments of the trial slip surface parallel. Take, for example, the case of a slope where the material is strongly bedded and the strength along the bedding is less than across the bedding. This is illustrated in Figure 4-22. The grid blocks are placed so that the bases are parallel to the bedding. By selecting the “No crossing” option, the middle segments of the trial slip surfaces will all be along the bedding.

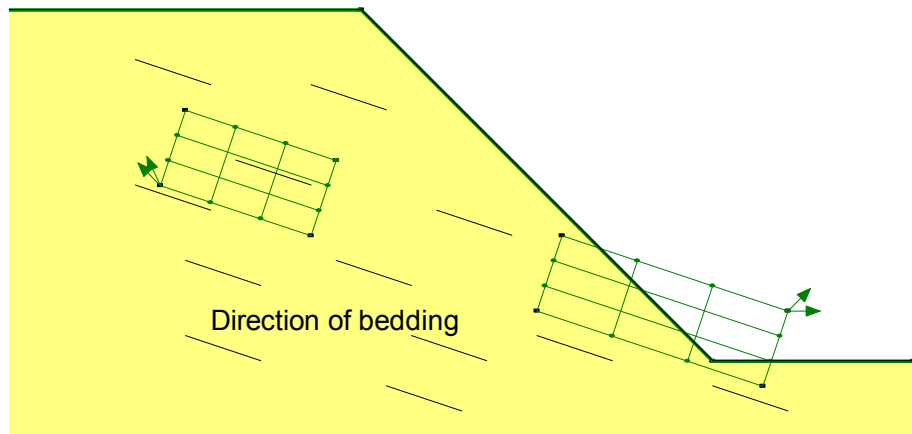


Figure 4-22 Slope with distinct bedding

A typical trial slip surface looks like the one in Figure 4-23.

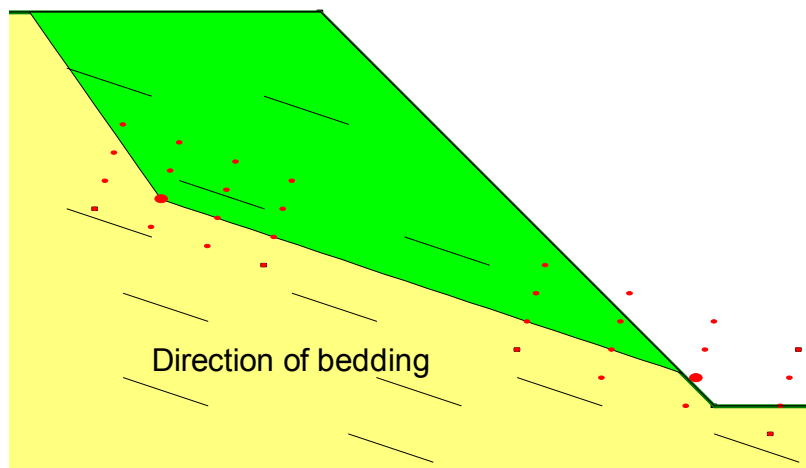


Figure 4-23 Trial slip surface follows the bedding

This approach can be combined with an anisotropic strength function to make the strength across bedding higher than along the bedding. The bedding is inclined at an angle of about 18 degrees. Let us specify the strength parameters along the bedding together with the anisotropic modifier function as in Figure 4-24. When the inclination of the slip surface is 18 degrees, the modifier is 1.0 and therefore

the specified strength is used. Slip Surface inclinations other than 18 degrees will have a higher strength. The specified strength will be multiplied by a factor of 1.15, for example, if the slice base inclination is zero degrees (horizontal).

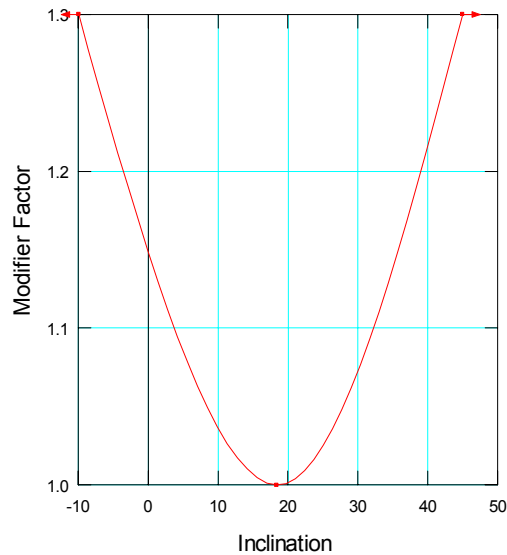


Figure 4-24 Anisotropic function

4.6 Entry and exit specification

One of the difficulties with the historic Grid and Radius method is that it is difficult to visualize the extents and/or range of trial slip surfaces. This limitation can be overcome by specifying the location where the trial slip surfaces will likely enter the ground surface and where they will exit. This technique is called the Entry and Exit method in SLOPE/W.

In Figure 4-25, there are two heavy (red) lines along the ground surface. These are the areas where the slip surfaces will enter and exit. The number of entries and exits can be specified as the number of increments along these two lines.

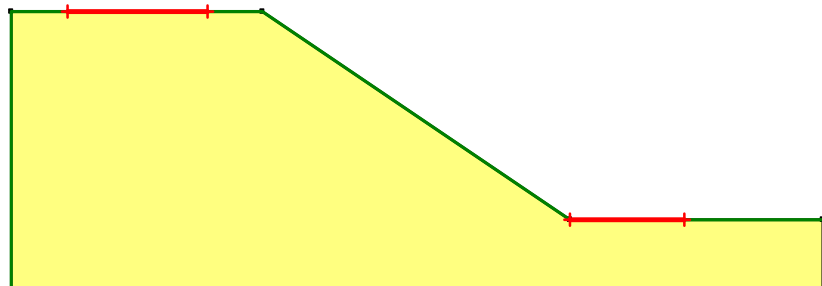


Figure 4-25 Entry and exit areas for forming trial slip surfaces

Behind the scenes, SLOPE/W connects a point along the entry area with a point along the exit area to form a line. At the mid-point of this connecting line, SLOPE/W creates a perpendicular line. Radius points along the perpendicular line are created to form the required third point of a circle (Figure 4-26). This radius point together with the entry and exit points are used to form the equation of a circle. SLOPE/W controls the locations of these radius points so that the circle will not be a straight line (infinite radius), and the entry angle of the slip circle on the crest will not be larger than 90 degrees (undercutting slip circle). The equation of a circle gives the center and radius of the circle, the trial slip surface is then handled in the same manner as the conventional Grid and Radius method and as a result, the Entry and Exit method is a variation of the Grid and Radius method. The number of radius increments is also a specified variable.

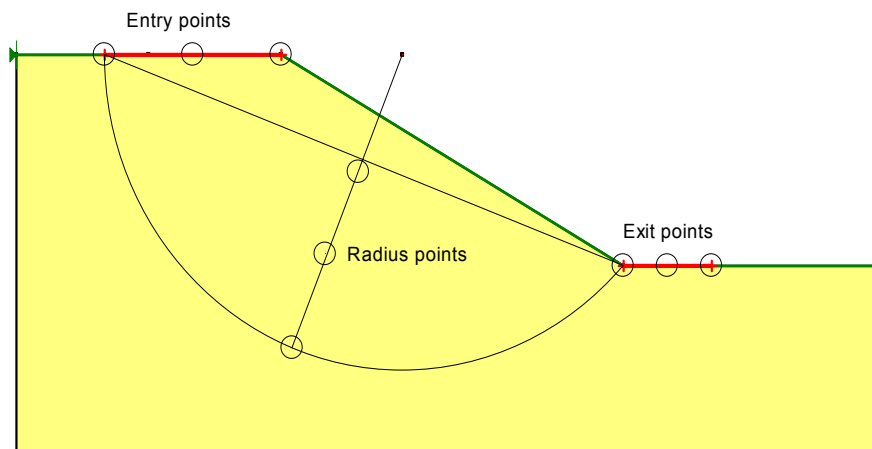


Figure 4-26 Schematic of the entry and exit slip surface

Figure 4-27 shows all the valid slip surfaces when the entry increments, the exit increments and the radius increments are set equal to 5. A total of 216 ($6 \times 6 \times 6$) slip surfaces are generated. The critical slip surface is the darker shaded area.

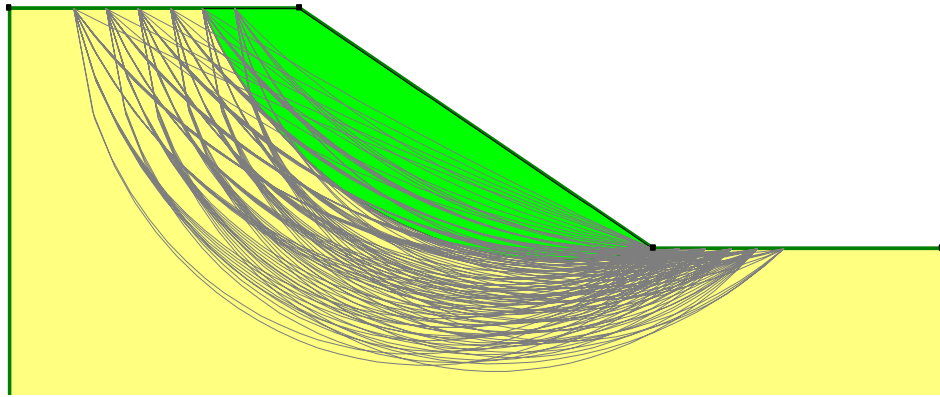


Figure 4-27 Display of all valid critical slip surfaces

4.7 Optimization

All the traditional methods of forming trial slip surfaces change the entire slip surface. Recent research has explored the possibility of incrementally altering only portions of the slip surface (Greco, 1996; Malkawi, Hassan and Sarma, 2001). A variation of the published techniques has been implemented in SLOPE/W. After finding the critical slip surface by one of the more traditional methods, the new segmental technique is applied to optimize the solution.

The first step in the optimization process is to divide the slip surface into a number of straight line segments. The slip surface in essence becomes just like a Fully Specified slip surface. Next, the end points of the line segments are moved to probe the possibility of a lower safety factor. The process starts with the point where the slip surface enters ground surface. This point is moved backward and forward randomly along the ground surface until the lowest safety factor is found. Next, adjustments are made to the next point along the slip surface until again the lowest safety factor is found. This process is repeated for all the points along the slip surface. Next, the longest slip surface line segment is subdivided into two parts and a new point is inserted into the middle. This process is repeated over and over until changes in the computed safety factor are within a specified tolerance or until

the process reaches the specified limits (e.g., the maximum number of optimization trials).

Figure 4-28 presents an optimized slip surface relative to a traditional circular slip surface of a simple slope. The material above the toe is somewhat stronger than the underlying soil below the toe elevation in this example. The factor of safety for this circular slip surface is 1.280, while for the optimized case the factor of safety is 1.240. Of interest is the observation that there is another slip surface that leads to a lower factor of safety than the one obtained for an assumed circular slip surface.

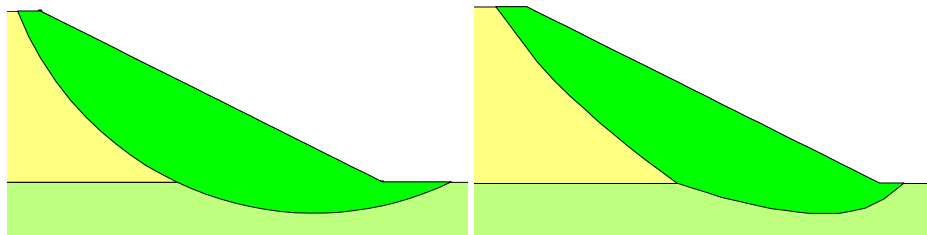


Figure 4-28 Traditional (Left) and Optimized (Right) slip surface

A key element in the optimization procedure is the technique used to move the end points of the line segments. SLOPE/W moves the points within an elliptical search area using a statistical random walk procedure based on the Monte Carlo method. This can be graphically illustrated in Figure 4-29.

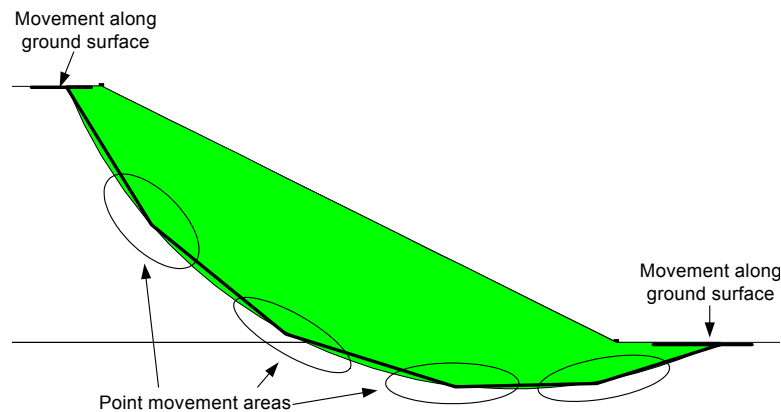


Figure 4-29 Movement areas of points in the optimization procedure

As is readily evident, the optimization is an iterative procedure and consequently some limits and controls are required. These controls include defining a tolerance when comparing safety factor, the maximum number of optimization trials and the number of line segments. These controlling parameters are explained in the online help.

The solution in Figure 4-30 was discussed in the section on the Block method. The optimized solution is presented in Figure 4-31. The Block factor of safety is 1.744 while the Optimized factor of safety is 1.609.

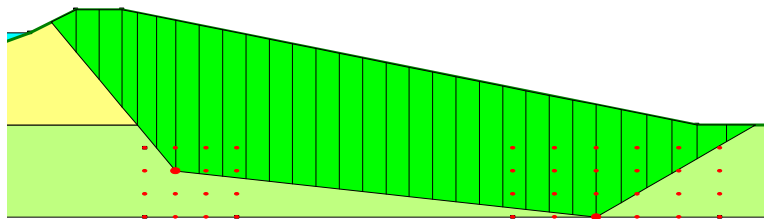


Figure 4-30 Slip surface when using the Block method

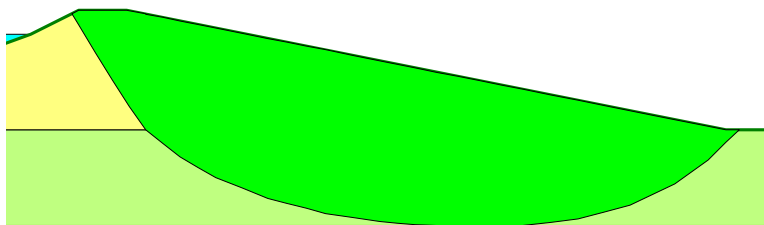


Figure 4-31 Slip surface when Block method optimized

The above two examples discussed here illustrate that slip surfaces do exist that have a lower safety factor than the trial slips that can be created by assumed geometric parameters. This is the attraction of optimization technique. Moreover, the optimized shape, without sharp corners, is intuitively more realistic.

Figure 4-32 shows the difference of a fully specified slip and the slip surface after optimization for geometry with a thin weak layer. The fully specified slip surface does not follow the weak layer and results in a factor of safety of 1.2, but the optimized process was able to locate the weak layer and found a smaller factor of safety 0.96. The Optimization process is appealing in that the trial slip surface is

based on soil properties to some extent. The technique will be biased towards weak layers or weak directions for anisotropic strengths.

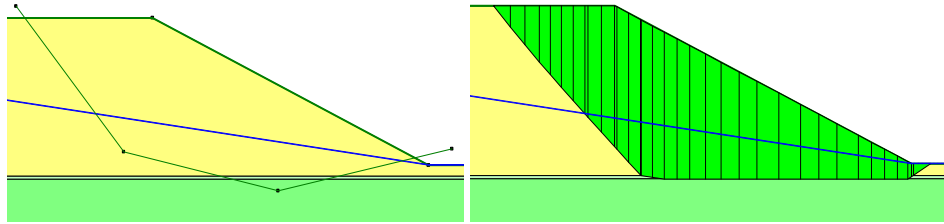


Figure 4-32 Fully specified slip surface (Left) after optimization (Right)

The Optimization procedure is somewhat dependent on the starting slip surface position. The main reason for this is the available elliptical search area during the random walk procedure. Since the elliptical search area is based on the starting slip surface, it is not difficult to understand that the final optimized slip surface can be limited by a poor selection of the starting slip surface.

In the example that had a thin weak layer, depending on the starting position of the slip surface, the optimization process may not be able to locate the critical slip surface along the weak layer (Figure 4-33). In SLOPE/W, the critical slip surface from a regular search is always used as the starting slip surface in the optimization process. In most cases, a smaller factor of safety can be obtained after the optimization.

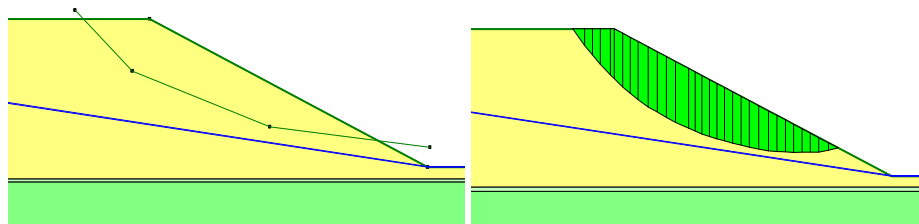


Figure 4-33 Fully specified slip surface (Left) after optimization (Right)

4.8 Auto-search

The Auto-Search technique in SLOPE/W attempts to combine the above-discussed methods and attempts to do some preliminary work for you. Based on the problem geometry, SLOPE/W identifies the Entry and Exit areas along the ground surface and then performs a series of trial analyses using the Entry and Exit method. This

gives an approximate solution. After having established an approximated position of the critical slip surface, SLOPE/W applies the Optimization procedure to find the minimum safety factor.

The Auto-Search method is in essence a combination of the Entry and Exit method with the Optimization procedure, except that SLOPE/W automatically attempts to locate the possible Entry and Exit position in order to find a preliminary approximate solution. The success of the method consequently depends on whether the approximation is realistic. If the behind-the-scenes approximation is realistic, then the Auto-Search final solution should be very similar to the more deliberate Optimization method.

When Auto search is used, SLOPE/W generates 1000 trial slip surfaces to find the most probable minimum slip surface before optimization is applied. As a result, Auto Search will usually lead to a reasonable result. Figure 4-34 shows the result of an example with the traditional grid and radius slip surface search. The critical slip surface is circular and the computed critical factor of safety is 1.211. Figure 4-35 shows the result of the same example with auto search. The critical slip surface is not quite circular and the computed critical factor of safety is 1.196.

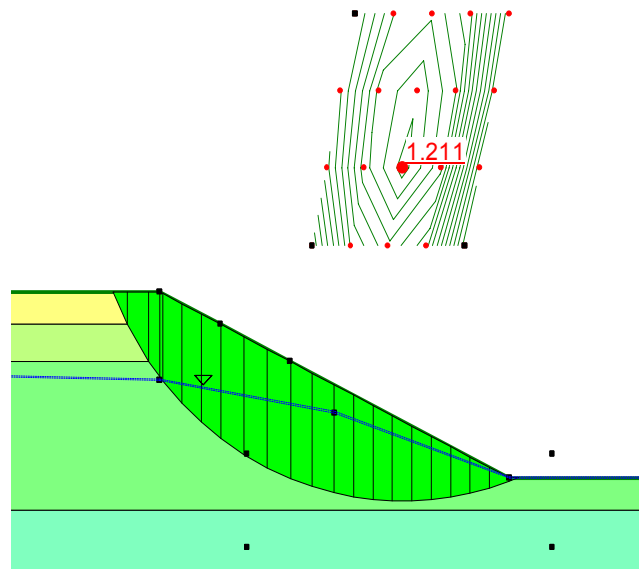


Figure 4-34 Example with grid and radius search

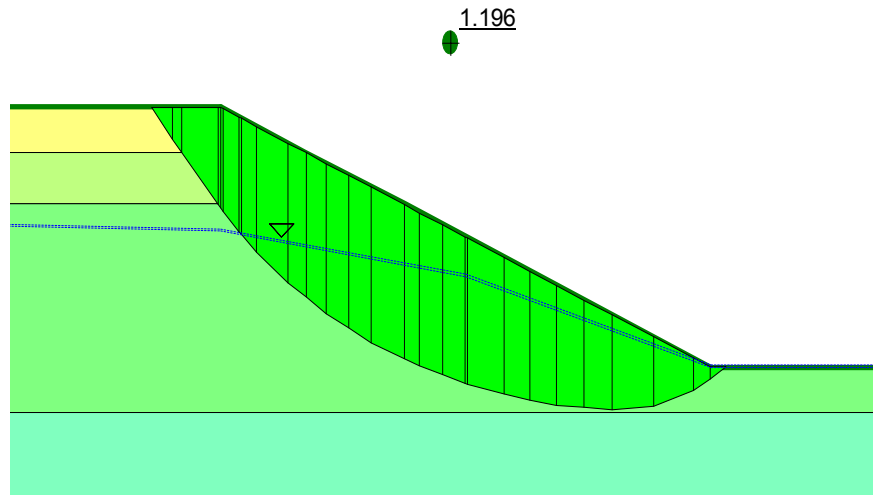


Figure 4-35 Example with auto search

At a first glance, the Auto Search technique appears to be a significant improvement in locating the critical slip surface. Some caution is, however, warranted at this time. It is a new method and has as yet not been used extensively. More time and usage is required before definitive conclusions can be reached that the technique will work in all cases or is applicable in all cases. At this stage we recommended that you start with a traditional analysis and then try the optimization. SLOPE/W makes this very convenient. If the optimized solution appears intuitively more realistic, then perhaps it is acceptable to rely on the new procedure.

4.9 Effect of soil strength

The fact that the position of the critical slip surface is dependent on the soil strength parameters is one of the most misunderstood and perplexing issues in slope stability analyzes. Coming to grips with this issue removes a lot of consternation associated with interpreting factor of safety calculations.

Purely frictional case

When the cohesion of a soil is specified as zero, the minimum factor of safety will always tend towards the infinite slope case where the factor of safety is,

$$F.S. = \frac{\tan \phi}{\tan \alpha}$$

where:

ϕ = the soil friction angle

α = the inclination of the slope.

Figure 4-36 shows a typical situation. The critical slip surface is parallel and immediately next to the slope face. The slope inclination is 26.57 degrees and the friction angle is 30 degrees. The computed factor of safety is 1.203, which is just over the infinite slope factor of safety of 1.15.

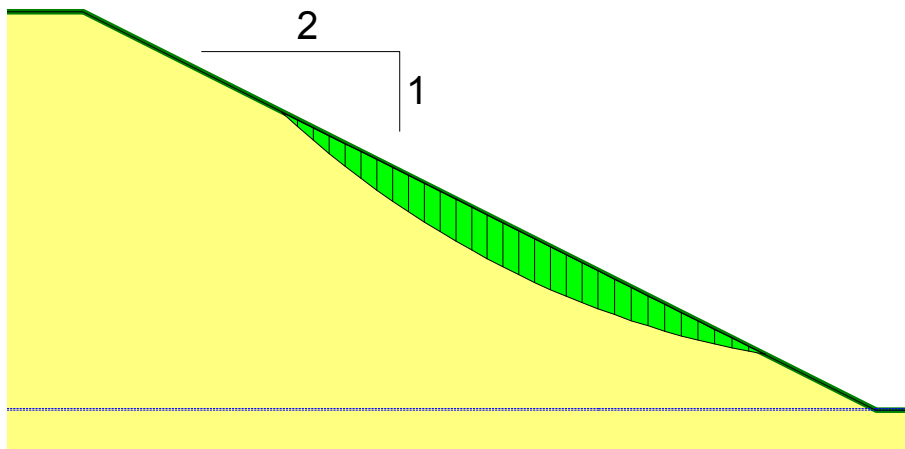


Figure 4-36 Shallow slip for purely frictional (c=0) case

The tendency to move towards the infinite slope case means the radius of the circle tends towards infinity. The minimum factor of safety is therefore usually on the edge of the grid of rotation centers. Figure 4-37 typifies this result. The minimum is right on the grid edge that represents the largest radius. Making the grid larger does not resolve the problem. The minimum occurs when the radius is at infinity, which cannot be geometrically specified. The Grid and Radius method appears to break down under these conditions, and the concept that the minimum factor of safety should be inside the grid is not achievable.

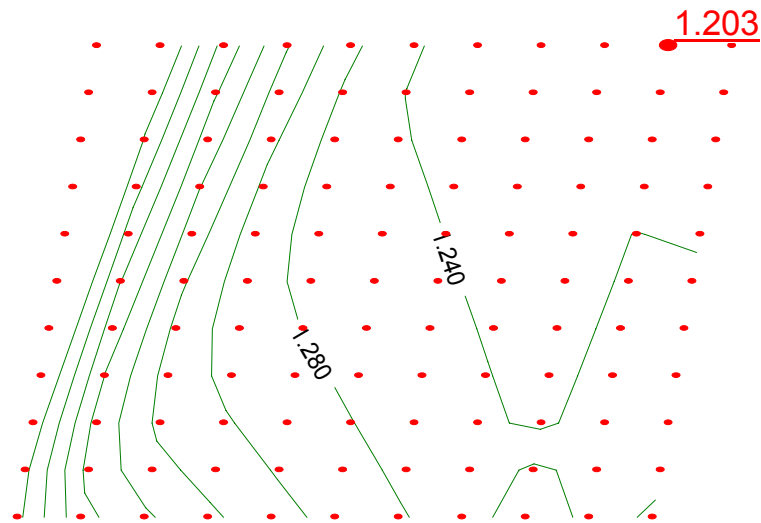


Figure 4-37 Minimum safety factor on edge of grid when c is zero

Undrained strength case

The opposite occurs when the soil strength is defined purely by a constant undrained strength; that is, ϕ is zero. In a case like this the critical slip surface will tend to go as deep as possible as shown in Figure 4-38. In this example the depth is controlled by the geometry. If the problem geometry was to be extended, the critical slip surface would go even deeper.

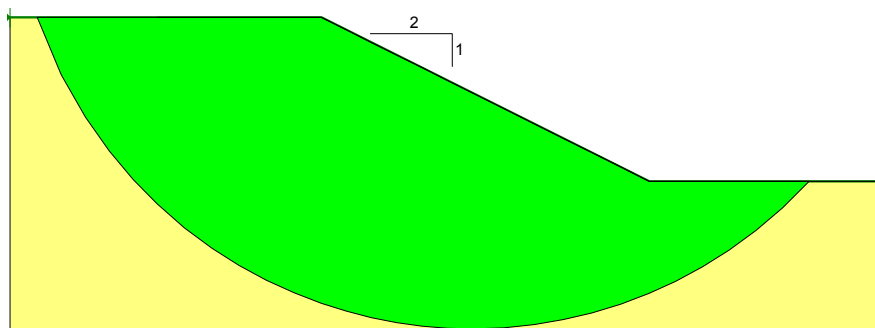


Figure 4-38 Deep slip surface for homogeneous undrained case

Figure 4-39 shows the factor of safety contour plot on the search grid. The minimum factor of safety is always on the lower edge of the search grid. Once again, for this homogenous undrained case it is not possible to define a minimum center inside the search grid.

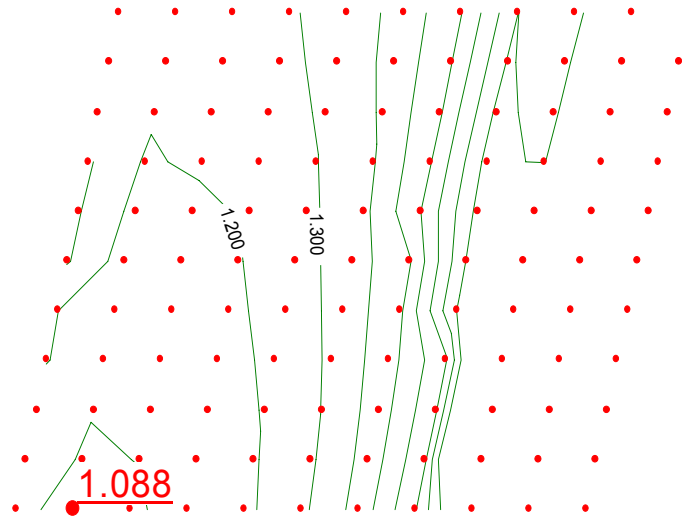


Figure 4-39 Minimum safety factor on edge of grid when ϕ is zero

Cause of unrealistic response

The reason for the unrealistic behavior in both the purely frictional case and the homogeneous undrained case is that the specified strengths are unrealistic. Seldom if ever, is the cohesion completely zero near the ground surface. Almost always there is a desiccated layer near the surface that has a higher strength or there a root-zone near the surface which manifests itself as an apparent cohesion. If the soil strength increases towards the ground surface, the critical slip surface will be at some depth in the slope.

The Shear Strength and Theory Chapter discuss how negative pore-water pressure (suction) increases the shear strength. This can be included in a SLOPE/W analysis by defining ϕ^b . If we make ϕ^b equal to 20 degrees, C equal to zero and ϕ equal to 30 degrees, then the position of the critical slip surface is as in Figure 4-40. Intuitively, this seems more realistic and is likely more consistent with field observations. Moreover, the minimum factor of safety is now inside the grid.

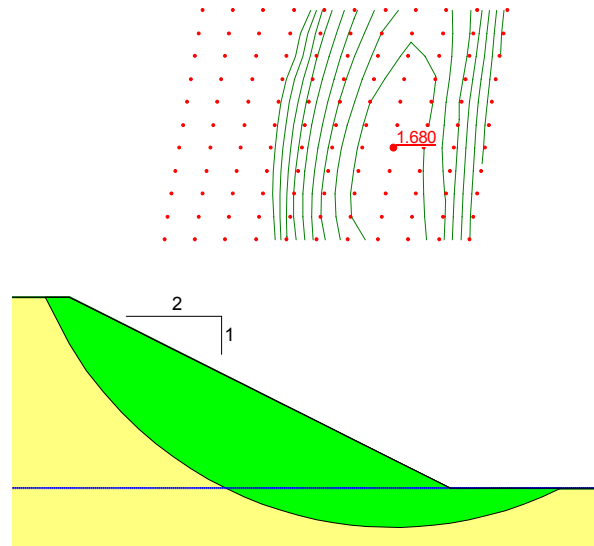


Figure 4-40 Critical slip surface when soil suction is considered

Figure 4-41 presents a plot of strength along the slip surface. Note the additional strength due to the suction and that the cohesion is zero everywhere.

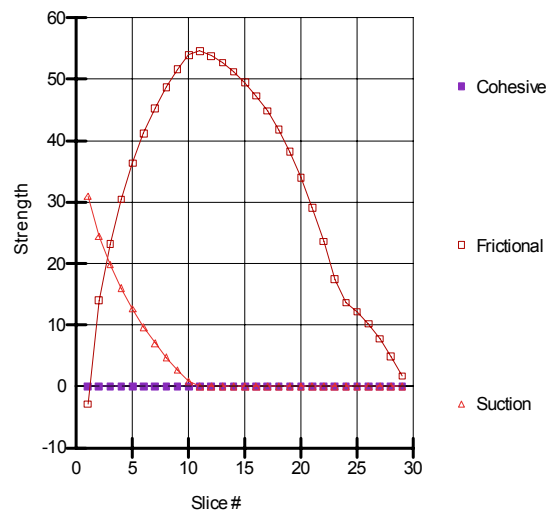


Figure 4-41 Strength components along the slip surface

The problem with the undrained case is that the undrained strength is the same everywhere. Once again, this is seldom, if ever, the case in the field. Usually there is some increase in strength with depth even for very soft soils. If the undrained strength is modeled more realistically with some increase with depth, the critical slip surface position no longer tends to go as deep as possible within the defined geometry. SLOPE/W has several soil models that can accommodate strength increase with depth.

Minimum depth

In SLOPE/W you can specify a minimum sliding mass depth. Say for example, that you specify a minimum depth of one meter. At least one slice within the potential sliding mass will then have a height greater or equal to the specified value. Any trial slips where all slice heights are less than the specified value are ignored.

The minimum depth parameter can be used to prevent SLOPE/W from analyzing very shallow slips. The slip surface with the minimum factor of safety will, however, still be the shallowest one analyzed and the lowest factor of safety will often still be on the edge of the rotation grid. As a result, this parameter does not really solve the underlying inherent problem. The minimum depth parameter should consequently only be used if the implications are fully understood.

Most realistic slip surface position

The most realistic position of the critical slip surface is computed when effective strength parameters are used and when the most realistic pore-water pressures are defined. This includes both positive and negative pore-water pressures.

Someone once said that the main issue in a stability analysis is shear strength, shear strength. The main issue is actually more correctly pore-water pressure, pore-water pressure, pore-water pressure. Effective strength parameters can be fairly readily defined with considerable accuracy for most soils and rocks. This is, however, not always true for the pore-water pressure, particularly for the negative pore-water pressures. The difficulty with the negative pore-water pressures is that they vary with environmental conditions and consequentially vary with time. Therefore the stability can only be evaluated for a certain point in time.

The most likely position of the critical slip surface will be computed when effective strength parameters are used together with realistic pore-water pressures.

Shallow slips near the ground surface actually do happen if the cohesion indeed goes to zero. This is why shallow slips often occur during periods of heavy rain. The precipitation causes the suction near the surface to go to zero and in turn the cohesion goes to zero, and then indeed shallow slips occur as would be predicted by SLOPE/W. Another case is that of completely dry sand. Placing completely dry sand from a point source will result in conical shaped pile of sand and the pile will grow by shallow slips on the surface exactly as predicted by SLOPE/W for a material with no cohesion.

4.10 Tension cracks and exit projections

The steepness of the entrance and exit of the slip surface can have some negative numerical consequences. At the crest, the normal at the base of the first slice will point away from the slice, indicating the presence of tension instead of compression. Generally, this is considered unrealistic, particularly for materials with little or no cohesion. Physically, it may suggest the presence of a tension crack. In the exit area, steep slip surface angles can sometimes cause numerical problems with the result that it is not possible to obtain a converged solution. Both of these difficulties can be controlled with specified angles.

Tension crack angle

In SLOPE/W, it is possible to specify a tension crack angle. What it means is that if the base of a slice in a trial slip exceeds the specified angle, SLOPE/W removes the slice from the analysis. This has the effect and appearance of a tension crack, as shown in Figure 4-42. In this case, the first slice on the left had a base inclination that exceeded the specified allowable; consequently the slice was ignored and replaced with a tension crack.

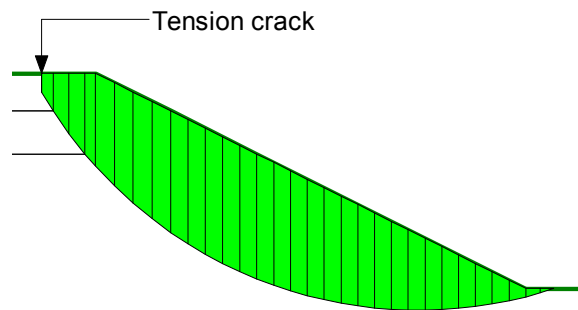


Figure 4-42 Tension crack based on specified inclination angle

Angles are specified in a clockwise direction from the positive x-coordinate axis. In this example the tension crack angle was specified as 120 degrees. So any slice base inclination equal to or greater than 60 degrees from the horizontal is ignored.

The slip surface entrance point is analogous to an active earth pressure situation. Theoretically, the active earth pressure slip line is inclined at $(45 + \phi/2)$ degrees from the horizontal. While this is not strictly applicable, it is nonetheless a useful guide for specifying tension crack angles.

Automatic tension crack search

Another way to include tension crack considerations in an analysis is to allow SLOPE/W to automatically make an adjustment if tension (negative normals) exists at the slice base in the crest area. After a completed analysis, SLOPE/W examines all the slices and looks for any negative slice base normals in the crest area. The first slice with a negative normal is removed from the analysis, and then the analysis is repeated. The whole procedure is repeated until there are no further negative base normals.

As with all automated procedures, this tension crack search option needs to be used with care and caution. It is always a good idea to start an analysis without the tension crack option and then add a tension option later to examine the effect of a tension crack.

Constant tension crack depth

A constant tension crack depth can also be specified as part of the geometry, as discussed earlier.

Tension crack fluid pressures

Tension cracks can be assumed to be dry or filled with water. The extent to which the crack is full of water is expressed by a number between zero and 1.0. Zero means dry and 1.0 means completely full. If there is water in the tension crack, a hydrostatic force is applied to the side of the first element. The value of the lateral fluid force can always be verified by viewing the slice forces.

The idea of a significant fluid pressure in a tension crack is likely not very real. First of all, it is hard to imagine that a tension crack could hold water for any period of time. Secondly, the volume of water in a narrow tension crack is very small, so any slight lateral movement of the sliding mass would result in an

immediately disappearance of the water and the associated lateral force. So considerable thought has to be given to whether a tension crack filled with water can actually exist and if it can exist, will the lateral hydraulic force remain when there is some as movement.

Toe projection

As noted earlier, steep exit angles can sometimes cause numerical difficulties. To overcome these difficulties, the steepness of the exit can be controlled with a specified angle, as illustrated in Figure 4-43. If the slice base has an inclination greater than the specified angle, SLOPE/W reforms the trial slip surface along a projection at the specified angle. Note how, in Figure 4-43, the curvature of the slip surface transforms into a straight line in the exit area.

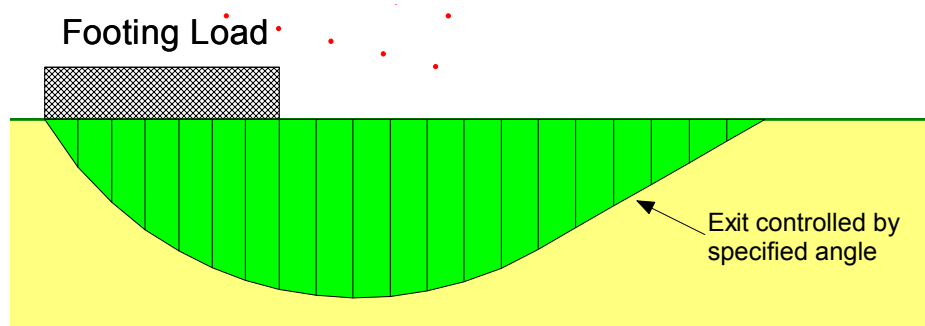


Figure 4-43 Exit angle controlled by specified angle

The toe area of a sliding mass is somewhat analogous to passive earth pressure conditions. In the example in Figure 4-43 the toe area is being pushed up and to the right just in a passive earth pressure case. Theoretically, the inclination of the passive slip line is at an angle of $(45 - \phi/2)$. This can be used as a guide when specifying this exit projection angle.

4.11 Physical admissibility

A consequence of the procedures used to generate trial slip surfaces, is that trial slip surfaces are sometimes formed that are not physically admissible; that is, they cannot exist in reality, or movement cannot possibly take place along the trial slip surface. Fortunately, in many cases it is not possible to obtain a solution for a physically inadmissible trial slip surface due to lack of convergence. Unfortunately, sometimes factors of safety are computed and displayed for cases

where it is highly improbable that the potential sliding mass can slide or rotate as would be dictated by the trial slip surface.

This issue is complicated by the fact that there are no firm criteria to mathematically judge physical inadmissibility. SLOPE/W has some general rules that prevent some unreal cases like, for example, the inclination of the slip surface exit angle. If the slip surface exit is too steep, the results can become unrealistic and so the exit angle is arbitrarily limited to a maximum value. It is, however, not possible to develop similar rules for all potentially inadmissible cases. Consequently, it is necessary for the analyst to make this judgment. While performing limit equilibrium stability analyses, you should constantly mentally ask the question, can the critical trial slips actually exist in reality? If the answer is no, then the computed results should not be relied on in practice.

Some of the more common inadmissible situations are when the slip surface enters the ground at a steep angle and then exits at a steep angle with a relatively short lateral segment as illustrated in Figure 4-44. Described another way, the situation is problematic when the steep enter and exit segments are longer than the lateral segment of the slip surface. The problem is further complicated by very sharp breaks or corners on the trial slip surface. For the example in Figure 4-44 it is not possible to compute a Spencer or Morgenstern-Price factor of safety.

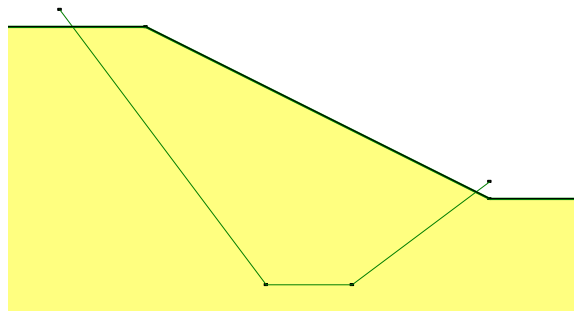


Figure 4-44 An example of a physically inadmissible slip surface

Another example of physical inadmissibility is when a very strong material overlies a very weak material. In the extreme case, if the weak material has essentially no strength, then the upper high strength material needs to sustain tensile stresses for the slope to remain stable. In reality, the soil cannot sustain tensile stresses. Mathematically, this manifests itself in lack of convergence. In other words, the model attempts to represent something that cannot exist in reality.

Sometimes it can be useful to assess the problem in a reverse direction. Instead of finding a factor of safety, the objective is to find the lowest strength of the weak material that will give a factor of safety equal to 1.0; that is, what is the lowest strength to maintain stability? Then the lowest strength required to maintain stability can be compared with the actual shear available. If the actual strength is less than what is required, then the slope will of course be unstable.

As a broad observation, convergence difficulties are often encountered when the model is beyond the point of limiting equilibrium or the sliding mode is physically inadmissible.

In the end, it is vital to remember that while SLOPE/W is a very powerful analytical tool, it is you who must provide the engineering judgment.

4.12 Invalid slip surfaces and factors of safety

A typical analysis may involve many trial slip surfaces; however, some of the slip surfaces may not have a valid solution. In such cases, a factor of safety with a value ranging from 981 - 999 is stored. It is important to realize that these values are not really factors of safety; they actually represent different error conditions of the particular trial slip surface.

The invalid slip surface may be due to convergence difficulties, in which a 999 is stored instead of the real factor of safety. Quite often, the invalid slip surface is also due to the position of the trial slip surface, the position of the grid center in a grid and radius, the pressure line definition, the direction of the sliding mass, the thickness of the sliding mass and overhanging ground surface etc. Although, the Verify feature in SLOPE/W attempts to identify these conditions before the actual computation, many of these conditions can only be detected during the computation inside the solver. In such cases, the solver outputs an error code instead of the true factor of safety. SLOPE/W CONTOUR interprets the error conditions and displays a message concerning the error when you attempt to view the invalid slip surface using the Draw Slip Surfaces command.

The following summarizes the various error conditions:

981 - Slip surface encounters an overhanging ground surface (Figure 4-45). This happens when you attempt to model an overhanging slope or cliff. As you can see, some of the slices in this slip surface will have the slice base exposed to the air. This condition will bring numerical problems in the factor of safety calculations and is therefore not allowed in SLOPE/W.

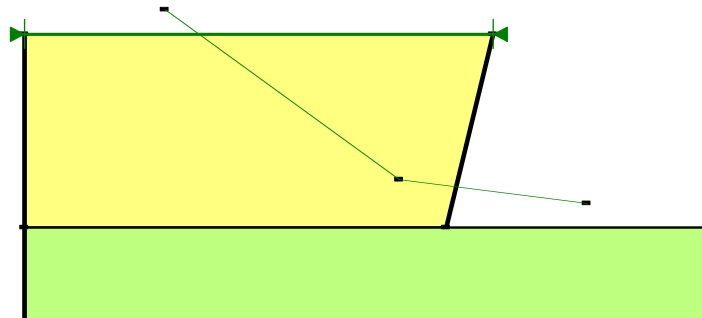


Figure 4-45 Slip surface intersecting an overhanging ground surface

982 - Slip Surface encounters an overhanging or vertical bedrock region (Figure 4-46). When a slip surface intersects an impenetrable material (bedrock), the slip surface will follow the top of the bedrock to form a new slip surface. As a result, an overhanging or a vertical bedrock region will produce an overhanging or vertical slip surface which is not allowed in SLOPE/W.

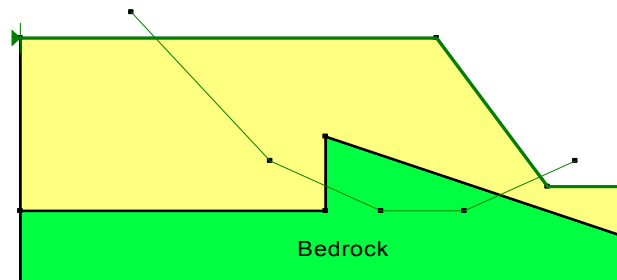


Figure 4-46 Slip surface intersecting an overhanging or vertical bedrock

986 - Slip Surface encounters a pressure line inside a zero strength material (Figure 4-47). This happens when a pressure line is defined on top of a zero strength (water) layer. Pressure lines must be defined above the ground surface to have the loading handled properly. Defining a pressure line on a zero strength layer is physically impossible and confuses the pressure load computation. This is not allowed in SLOPE/W.

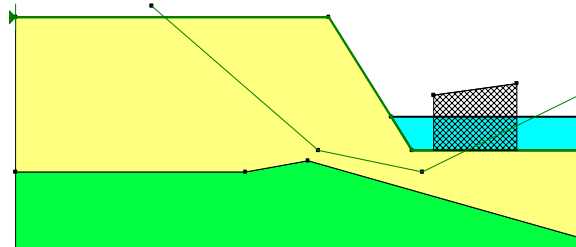


Figure 4-47 Slip surface intersecting a pressure line inside a zero strength material

987 - Slip surface inside a region with an internal pressure line (Figure 4-48). This happens when a pressure line is defined below the ground surface. A pressure line must be defined above the ground surface to have the loading handled properly. A pressure line defined below the ground surface is intuitively impossible and is therefore not allowed in SLOPE/W.

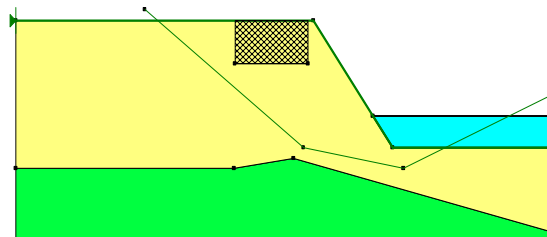


Figure 4-48 Slip surface inside a region with internal pressure line

989 - Slip surface encounters an internal zero strength material (water) (Figure 4-49). A slip surface going through a zero strength material (water) causes numerical problems in the normal force and shear strength computation on some of the slices. This is not allowed in SLOPE/W.

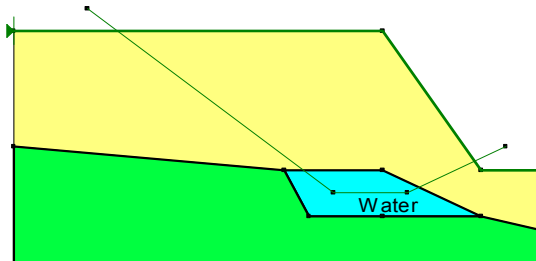


Figure 4-49 Slip surface encounters an internal zero strength material

992 - Slip surface cannot be generated (Figure 4-50). This happens whenever there is a problem in generating a trial slip surface. There may be problems in finding the ground surface line or finding the slip surface intersecting points with the ground surface. This also happens with an overhanging slip surface or when a slip surface is trying to undercut itself. No factor of safety can be computed when a slip surface cannot be generated.

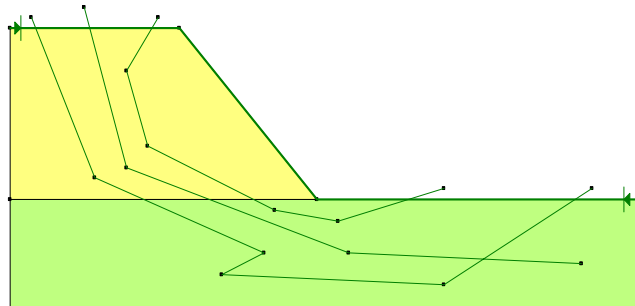


Figure 4-50 Slip surface cannot be generated

993 - Slip surface is too shallow (Figure 4-51). This happens when the thickness of all slices are smaller than the specified minimum slip surfaces thickness. In a purely frictional material, the critical slip surface tends to develop on the shallow ground surface where the normal force is small and the shear strength is low. Although this is theoretically correct and physically admissible, this shallow critical slip surface may not be of any interest to you. SLOPE/W allows you to set a minimum slip surface thickness so that any slip surface shallower than the specified limit will be considered invalid and will not included in the factor of safety calculation.



Figure 4-51 Slip surface with thickness less than specified minimum

994 - No intersecting point is obtained in the factor of safety versus lambda plot for the GLE method (Figure 4-52). This happens when there are convergence difficulties or when the specified lambda values are not sufficient for the factor of safety by moment and factor of safety by force to obtain an intersecting point on the factor of safety versus lambda plot.

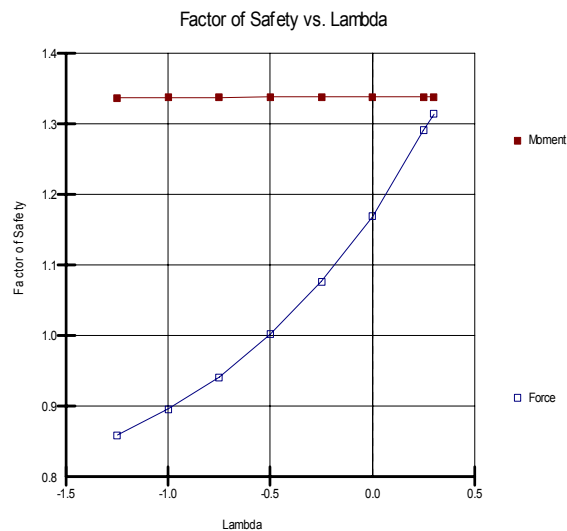


Figure 4-52 No intersecting point in a GLE method

995 - Slip surface could not be analyzed. This happens when all other conditions appear to be fine, but the solver encounters problems in the factor of safety

computation. For example, the mobilized shear resistance is in the opposite direction due to a large negative normal force. This error message could also be related to extreme soil properties or large external forces relative to the sliding mass.

996 - Slip surface is not in the same direction as the specified direction of movement. This happens when the direction of movement is not set properly in SLOPE/W or in a complex geometry where a slip surface has an exit point higher than the entry point.

997 - Slip surface could not be analyzed. This happens mainly when the exit angle of the slip surface is larger than 45 degree. Exit angles larger than the theoretical passive failure surface ($45^\circ - \phi/2$) tend to cause numerical instability to the factor of safety computation. Although a factor of safety may still be obtained in some cases, the computed factor of safety tends to be too small and is therefore consider suspect. SLOPE/W treats all slip surfaces with an exit angle larger than 45 degrees as invalid and no factor of safety is computed.

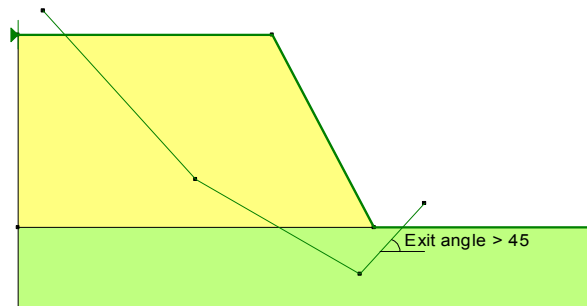


Figure 4-53 Slip surface with exit angle larger than 45 degrees

998 - Slip surface enter and exit beyond the slip surface limit. This happens when the slip surface extends beyond the specified slip surface limits (Figure 4-54). Both of the fully specified slip surfaces in the figure below have at least one exit or entry point beyond the slip surface limits.

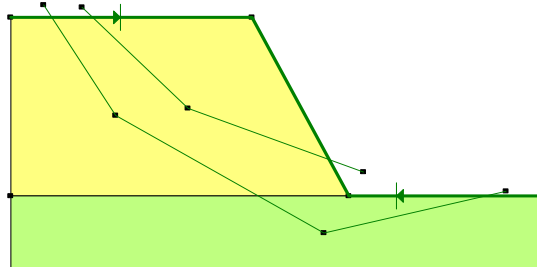


Figure 4-54 Slip surface enter and exit beyond the limits

999 - Slip surface does not have a converged solution. This happens when the solution for the slip surface does not converge. SLOPE/W uses an iterative procedure to solve the nonlinear factor of safety equation until the factor of safety converges within a specified tolerance. The convergence difficulties may be due to conditions with unreasonable soil strength properties, unreasonably large line loads or reinforcement loads, unreasonable seismic coefficient, unreasonable pore water pressure etc. By default, SLOPE/W uses a convergence tolerance of 0.01. While this tolerance is fine for most situations, you may like to relax this tolerance in order to obtain a solution when modeling extreme conditions.

For simplicity, the fully specified slip surface is used to illustrate the various problems with slip surfaces and geometry, however, the same situations would apply to other types of slip surface methods. In a slope stability analysis, it is quite common that some of the trial slip surfaces are invalid especially when using a grid and radius slip surface where the search grid is large and the search radius is long relative to the overall slope. It simply means that many trial slip surfaces are entering or exiting beyond the limits of the slope. Most likely, these invalid slip surfaces are of little interest to you and it is very unlikely that these invalid slip surfaces will be the most critical slip surfaces of the slope. You may choose to ignore these invalid slip surfaces, or you may like to better control the position of the search grid and radius to eliminate these invalid slip surfaces. The Entry and Exit slip surface method is much easier in controlling the position of the trial slip surfaces.

4.13 Concluding remarks

As noted in the introduction, finding the position of the critical slip surface requires considerable guidance from the analyst. SLOPE/W can compute the factors of safety for many trials very quickly, but in the end, it is up to the analyst

to judge the results. Assuming that SLOPE/W can judge the results better than what you as the engineer can do is a perilous attitude. The SLOPE/W results must always must be judged in context of what can exist in reality.

5 Geometry

5.1 Introduction

SLOPE/W uses the concept of regions to define the geometry. Basically this simply means drawing a line around a soil unit or stratigraphic layer to form a closed polygon, similar to what we would do when sketching a problem to schematically explain a particular situation to someone else. In this sense, it is a natural and intuitive approach.

Regions are a beneficial aid for finite element meshing. SLOPE/W by itself does not need a finite element mesh, but regions defined in SLOPE/W can also be used to create a mesh for an integrated finite element analysis. In GeoStudio the objective is to only define the geometry once for use in many different types of analyses. Using regions in SLOPE/W as well as in the finite element products makes this possible even though SLOPE/W uses slice discretization instead of finite element discretization. SLOPE/W can then use the results readily from other analyses, such as SEEP/W and SIGMA/W in a stability analysis.

This chapter describes the basics of regions and shows some examples of how they can be used to define various geometric conditions. Included as well are descriptions and discussions on how to define SLOPE/W specific features including line loads and surface surcharge pressures.

5.2 Regions

Regions are in essence n-sided polygons. Polygons with three sides are triangles and polygons with four sides are quadrilaterals. Figure 5-1 shows some representative basic regions.

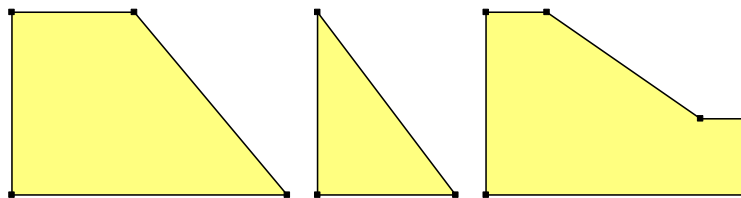


Figure 5-1 Representative basic regions

All regions need to be connected to form a continuum. This is done with the use of Points. The small black squares at the region corners in Figure 5-1 are the points. The regions are connected by sharing the points. In Figure 5-2, Points 6 and 7 are common to the two regions and the two regions consequently behave as a continuum.

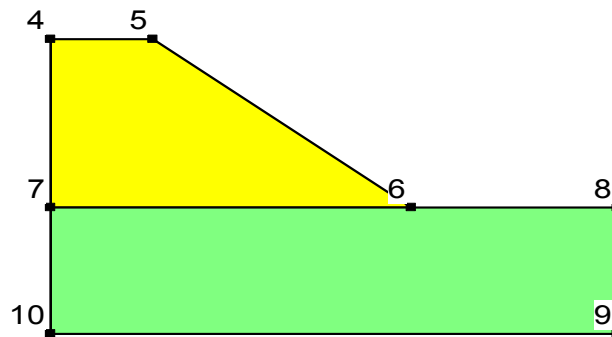


Figure 5-2 Region points

Figure 5-3 shows a typical slope stability case defined with regions. Here Points 2 and 8 are common to the top two regions. Points 3, 7 and 10 are common to the bottom two regions.

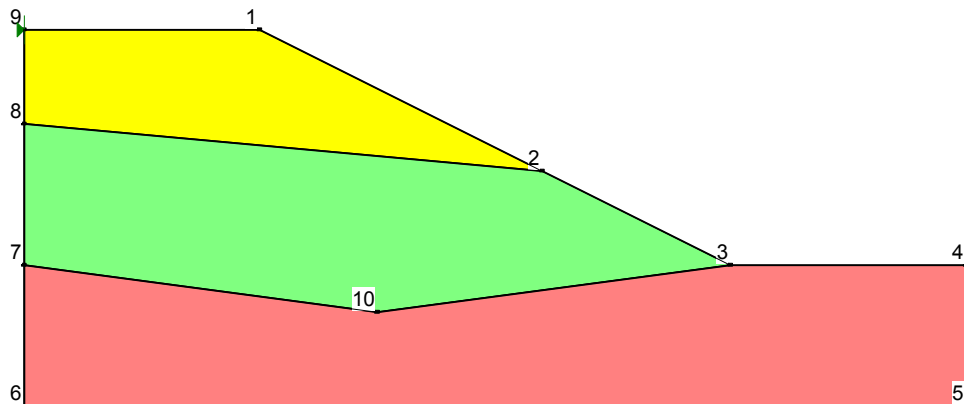


Figure 5-3 Typical regions for a slope stability analysis

Figure 5-4 shows a case where the triangular region on the left represents a soil layer that pinches out in the slope. Region 2-3-11-10 represents water impounded up against the slope.

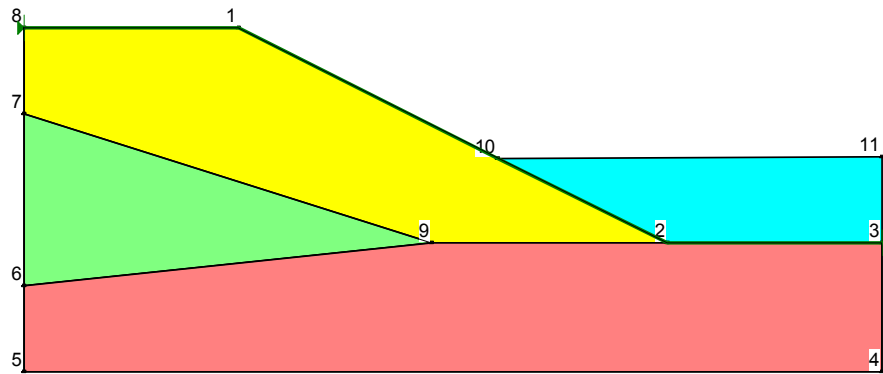


Figure 5-4 Example of pinching out region and water region

Figure 5-5 illustrates a typical tailings impoundment case. The quadrilateral regions on the left represent dykes, and the upper dyke sits on top of tailings; that is, the tailings under-cut the upper dyke.

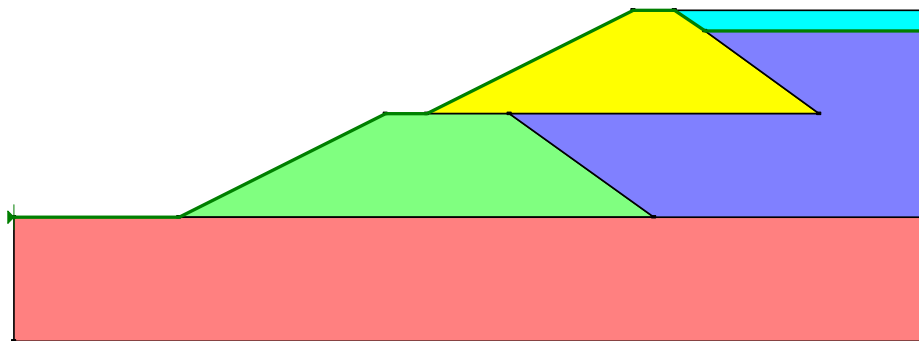


Figure 5-5 Example of an under-cutting region.

From these few examples, it is easy to see how almost any stratigraphic section can be easily and quickly defined with regions.

One of the attractions of regions is that the geometry can be so easily modified by moving the points. The regions do not necessarily have to be redrawn – only the points have to be moved make modification to the geometry.

Regions do have a couple of restrictions. They are:

- A region can have only one material (soil) type. The same soil type can be assigned to many different regions, but each region can have only one soil type.
- Regions cannot overlap.

An island of a particular soil type can be defined by dividing the surrounding soil into more than one region. Figure 5-6 illustrates this. Two regions of the same soil type are drawn such that they encompass the isolated quadrilateral of a different soil type. There may be other ways of defining this particular situation, but at no time can regions overlap. In other words, the pinching out layer in Figure 5-6 cannot be drawn on top of the other soil.

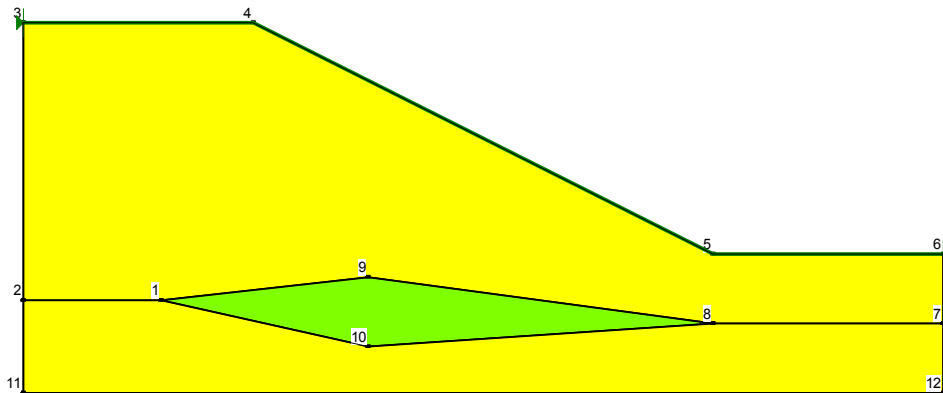


Figure 5-6 Section with an island of soil of a different type

5.3 *Slice discretization*

SLOPE/W uses a variable slice width approach in the sliding mass discretization. In other words, SLOPE/W will discretize the soil mass with slices of varying widths to ensure that only one soil type exists at the bottom of each slice. It is also used to prevent a ground surface break occurring along the top of the slice and to

prevent the phreatic line from cutting through the base of a slice. The objective is to have all the geometric and property changes occur at the slice edges.

Initially SLOPE/W divides the potential sliding mass into section as shown in Figure 5-7. The first section starts on the left where the slip surface enters the ground surface. Other sections occur where (1) the slip surface crosses the piezometric line, (2) the slip surface crosses a stratigraphic boundary, (3) wherever there is a region point, and (4) where the piezometric line crosses a soil boundary. The last section ends on the right where the slip surface exits the ground surface.

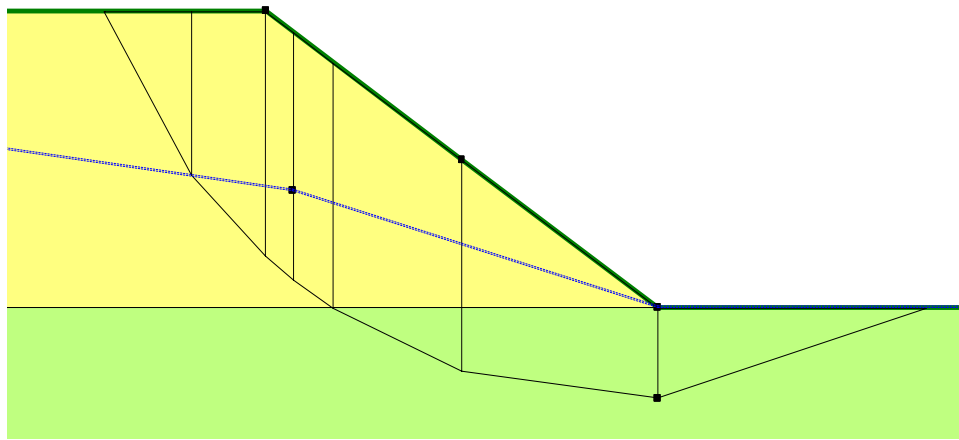


Figure 5-7 Sections in the slice discretization process

As a next step, SLOPE/W finds the horizontal distance from slip surface entrance to exit and divides this distance by the number of desired slices specified by the user (the default is 30). This gives an average slice width. The last step is to compute how many slices of equal width approximately equal to the average width can fit into each section. The end result is as shown in Figure 5-8 when the specified number of slices is 15.

Depending on the spacing of the sections, the variable slice approach will not always lead to the exact number of slices specified. The actual number of slices in the final discretization may be slightly higher or lower than the specified value. In this case, the total number of slices is 16.

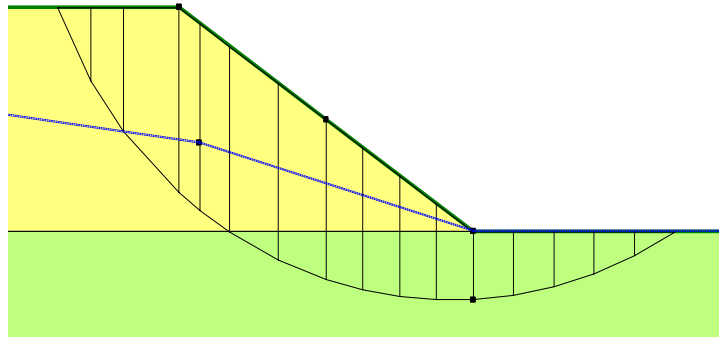


Figure 5-8 Discretization when specified number is 15 slices

The variable slice width approach makes the resulting factor of safety relatively insensitive to the number of slices. Specifying the number of slices to be greater than the default number of 30 seldom alters the factor of safety significantly. Specifying the number of slices lower than the default value of 30 is not recommended unless you want to investigate a specific issue like, for example, comparing the SLOPE/W results with hand calculations. Making the number of slices too high simply creates an excessive amount of unnecessary data without a significant improvement in safety factor accuracy. Figure 5-9 shows the discretization when the number of specified slices is 30.

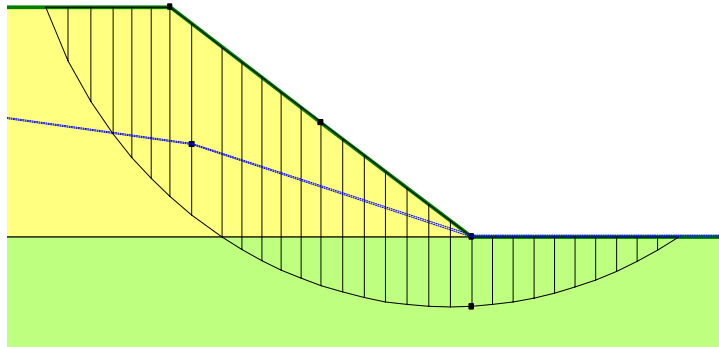


Figure 5-9 Discretization when specified number is 30 slices

5.4 Ground surface line

A special geometric object in GeoStudio is the ground surface line. It is a necessary feature for controlling what happens at the actual ground surface. Climate conditions, for example, can only act along the ground surface.

In SLOPE/W, the ground surface line is used to control and filter trial slip surfaces. All trial slip surfaces must enter and exit along the ground surface. Trial slip surfaces that enter or exit along the perimeter of the problem outside of the designated ground surface are considered inadmissible. Markers indicating the extents of ground surface line can be moved along the ground surface as illustrated on Figure 5-10.

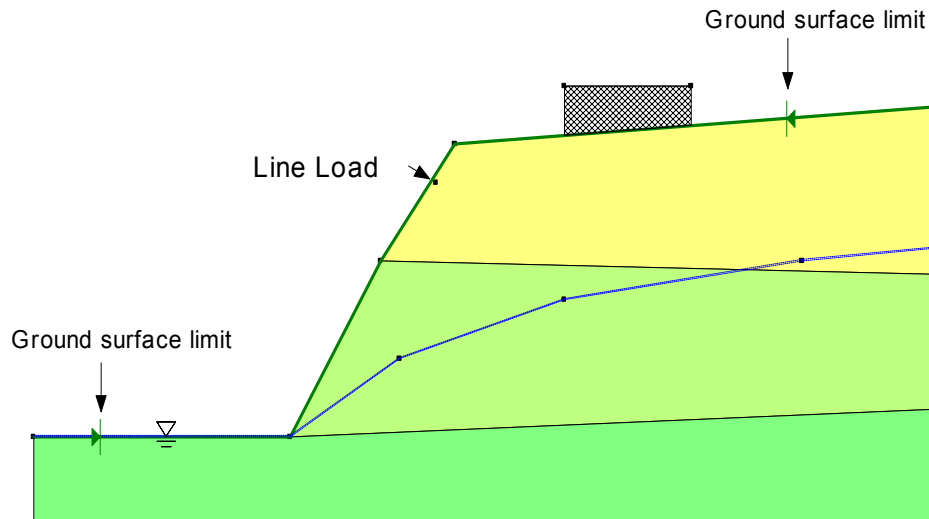


Figure 5-10 Example of a ground surface line and limit markers

SLOPE/W has a particular technique for specifying trial slip surfaces called “enter-exit”. Line segments can be specified which designate specific locations where all trial slip surfaces must enter and exit. These line segments are attached to the ground surface line. The specifics of this technique are discussed in more detail in the chapter on Slip Surface Shapes.

SLOPE/W computes the ground surface line and displays it as a heavy green line. Some care is required in the definition of the geometry to ensure that the computed line is the actual ground surface. For example, if the intended vertical extents of a

problem are not truly vertical, the ground surface line may follow the near vertical ends of the problem. This can happen when there are small numerical differences in the x-coordinates in the points along the ends. The smallest and largest x-coordinates in the problem are used to identify the ends of the intended ground surface line.

5.5 Surface surcharge pressures

Surface surcharge pressures can be simulated with what is known as a pressure line. Figure 5-11 shows two surface pressure lines. The pressure regions are cross-hatched. The pressure at the toe of the slope represents impounded water. Beyond the slope crest the pressure could represent the weight of a building or perhaps some type of equipment.

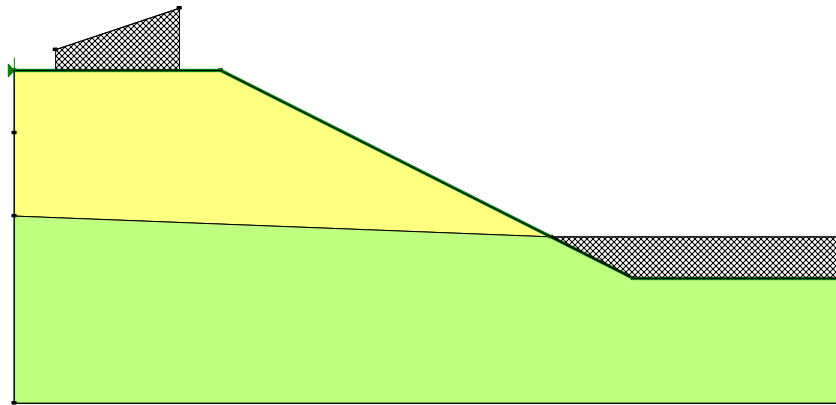


Figure 5-11 Ground surface surcharge pressures

The surface pressure can be applied in a vertical direction or normal to the ground surface. The water impoundment is a typical case of the pressures acting normal to the ground surface.

SLOPE/W creates slices so that slice edges fall at the ends of the pressure regions.

A force representing the surcharge is added to each slice under a pressure line. The force is equal to the vertical distance at mid-slice from the ground surface to the pressure line times the slice width times the specified unit weight.

A useful trick for applying a uniform pressure is to make the distance from the ground surface to the pressure line unity (1.0). The specified unit weight can then

be the applied pressure. This can be useful when simulating situations such as a footing pressure.

The computed surcharge slice forces should always be checked and verified by viewing the slice forces. The surcharge forces are displayed at the top of the slice at the applied direction. The 7.8405 force on top of the slice in Figure 5-12 is a surcharge force.

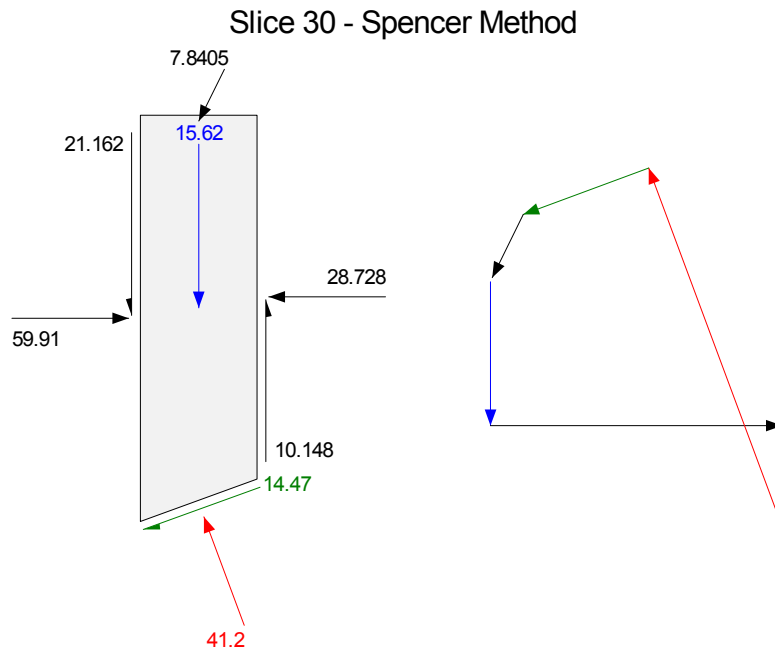


Figure 5-12 Example of a surcharge force at top of slice

Surcharges can only be applied to the tops of slices, not to the sides of slices. Consequently, pressure lines cannot be used to apply lateral forces on vertical walls. Let us say we have ponded water up against a vertical wall as in Figure 5-13. A pressure line cannot be used to simulate the hydrostatic lateral water force acting on the wall.

Care has to be exercised on how to consider this lateral force. If the water is modeled as a no-strength material, the lateral hydrostatic force is automatically included on the last slice where the slip surface exits under the water (Slice 30). The free body diagram of Slice 30 will include the lateral hydrostatic force. The

water will not, however, apply a lateral force on Slice 20. Forces between the water and Slice 20 are interslice forces just like between any other two slices.

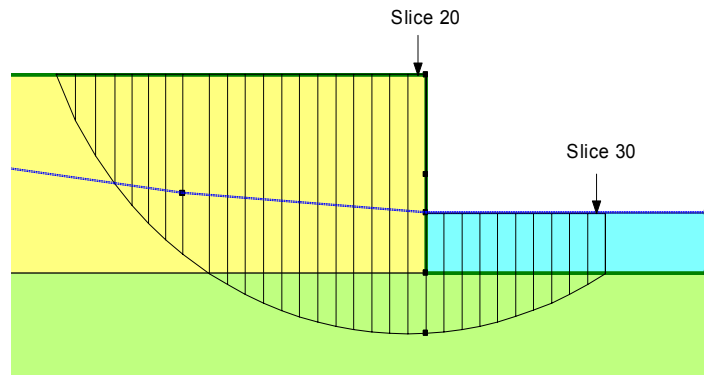


Figure 5-13 Water force included in the last slice

The situation would be different if the slip surface passes through the lower corner of a vertical wall as in Figure 5-14. The water is now external to the sliding mass and external pressures cannot be applied to the sides of slices, only to the top of slices. In this case the lateral water force needs to be specified as a concentrated line load. This is also true when using a pressure line to simulate the ponded water.

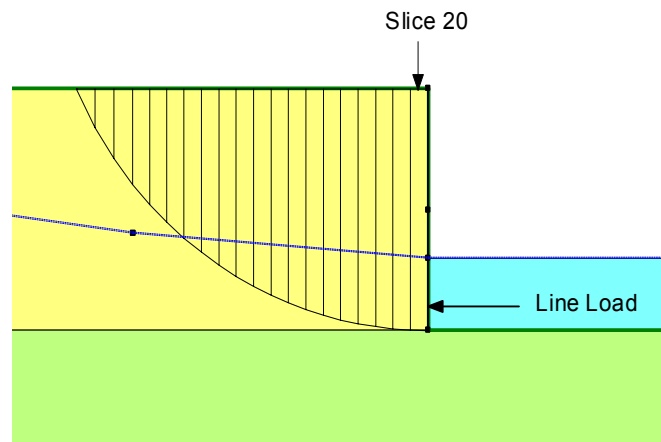


Figure 5-14 Water force not included in the last slice

Whether you simulate ponded water as a surcharge pressure or as a no-strength material comes down to personal preference. In either case, it is important to verify that the appropriate forces have been applied by examining the slice forces.

5.6 *Tension crack line*

A tension crack can be specified with a tension crack line, as illustrated in Figure 5-15. When a tension crack line is specified, the slip surface is vertical in the tension crack zone. The tension crack can have water in it, which results in a lateral force being applied to the end slice. Procedural details on this feature are in the online help. The tension crack line option is discussed here because it is, in essence, a geometric definition.

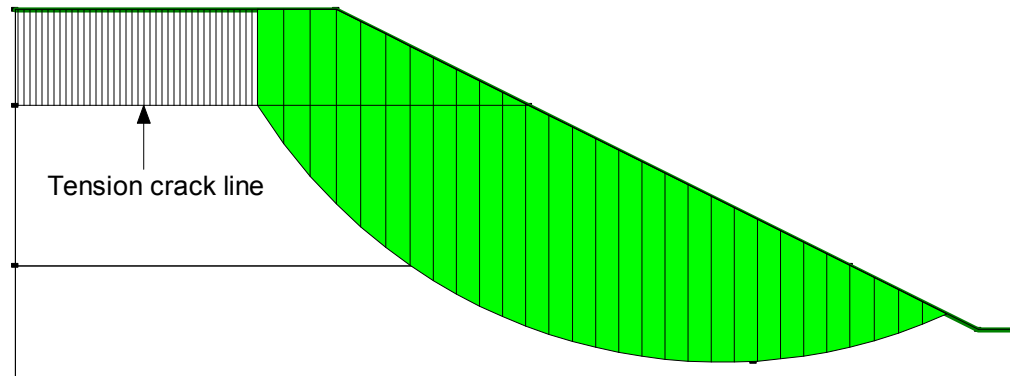


Figure 5-15 Tension crack line

There are other more advanced ways of including the possibility or presence of a tension crack in a stability analysis. A better way is to assume a tension crack exists if the slice base inclination becomes too steep. The angle at which this occurs needs to be specified. Another way is to assume that a tension crack exists if SLOPE/W computes a negative normal at the base of the slice where the slip surface enters the ground. The slice that has a negative base normal is then ignored and the analysis is repeated. The procedure is repeated until negative normals do not exist in the area of the crest.

The tension crack line concept is now somewhat outdated, but is still included for backward compatibility and for historic reasons. The other two options are more recent concepts, and offer more realistic behavior, particularly the angle specification method.

5.7 Concentrated line loads

Like the tension crack line, concentrated line loads are discussed here because they contain a geometric aspect.

Concentrated line loads must be applied inside the potential sliding mass. Intuitively, it would seem that the line loads should be applied on the surface. This is possible, but not necessary. Attempting to apply the line on the surface is acceptable, provided it is done with care. Due to numerical round-off, a line load can sometimes be ignored if the computed application point is slightly outside the sliding mass. The possibility of missing the line load in an analysis can be mitigated by ensuring the application of the line load is inside the sliding mass (Figure 5-16). Remember that a line load is included in the force equilibrium of a particular slice. All that is required is to ensure the line load is inside a slice, and slight differences in precisely where the line loads are placed within the mass are negligible to the solution.

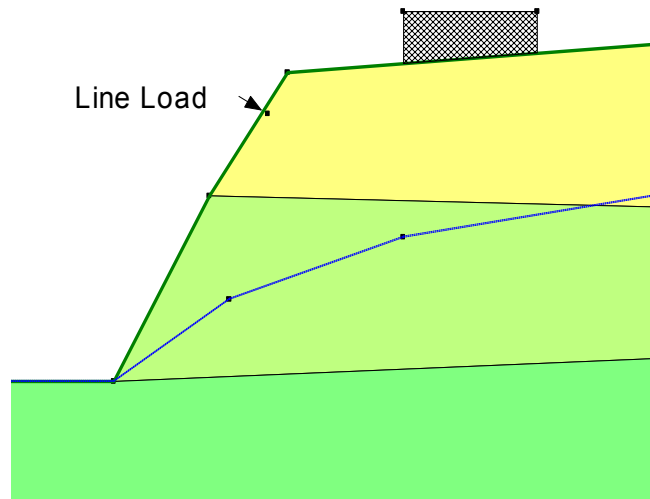


Figure 5-16 Example of a line load on the slope surface

Alternatively, you may add an extra point to the surface of a region and have the line load specified on the same point. This will ensure that the line load will be added to the slice containing the point. However, since there are so many application forces, it is always wise and prudent to check that the line load has been applied as intended by viewing the computed slice forces. Similar to the

surcharge pressure force, a line load is always displayed at the top of the slice at the applied direction. As illustrated on Figure 5-17, the applied line load is 100 lbs on slice 18.

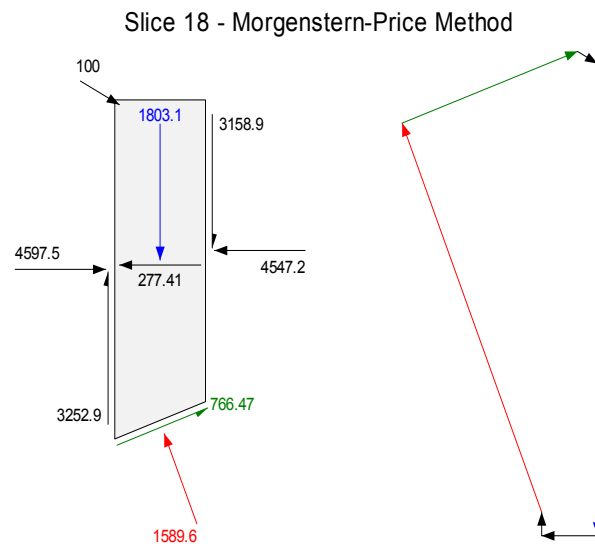


Figure 5-17 Example of a line load force at top of slice

6 Material Strength

6.1 Introduction

There are many different ways of describing the strength of the materials (soil or rock) in a stability analysis. This chapter describes and discusses all the various models available in SLOPE/W.

6.2 Mohr-Coulomb

The most common way of describing the shear strength of geotechnical materials is by Coulomb's equation which is:

$$\tau = c + \sigma_n \tan \phi$$

where:

- τ = shear strength (i.e., shear at failure),
- c = cohesion,
- σ_n = normal stress on shear plane, and
- ϕ = angle of internal friction (phi).

This equation represents a straight line on a shear strength versus normal stress plot (Figure 6-1). The intercept on the shear strength axis is the cohesion (c) and the slope of the line is the angle of internal friction (ϕ).

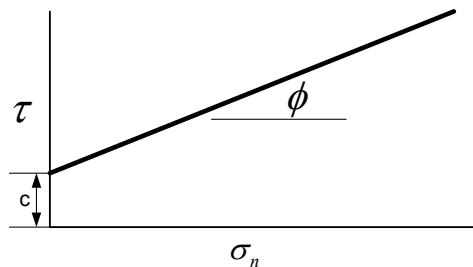


Figure 6-1 Graphical representation of Coulomb shear strength equation

The failure envelope is often determined from triaxial tests and the results are presented in terms of half-Mohr circles, as shown in Figure 6-2, hence the failure envelope is referred to as the Mohr-Coulomb failure envelope.

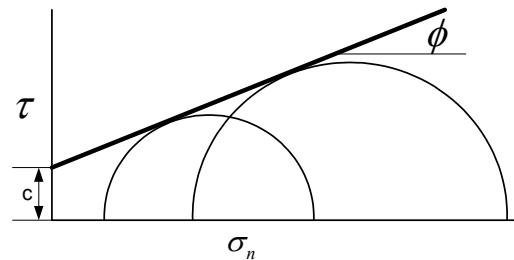


Figure 6-2 Mohr-Coulomb failure envelope

For undrained conditions when ϕ is zero, the failure envelope appears as shown in Figure 6-3. The soil strength then is simply described by c .

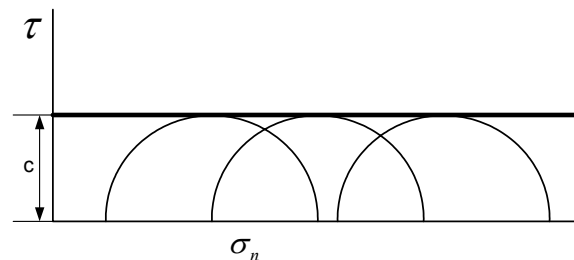


Figure 6-3 Undrained strength envelope

The strength parameters c and ϕ can be total strength parameters or effective strength parameters. SLOPE/W makes no distinction between these two sets of parameters. Which set is appropriate for a particular analysis is project-specific, and is something you as the software user, need to decide. The software cannot do this for you.

From a slope stability analysis point of view, effective strength parameters give the most realistic solution, particularly with respect to the position of the critical slip surface. The predicted critical slip surface position is the most realistic when you use effective strength parameters. When you use only undrained strengths in a slope stability analysis, the position of the slip surface with the lowest factor of safety is not necessarily close to the position of the actual slip surface if the slope

should fail. This is particularly true for an assumed homogeneous section. This issue is discussed further in the Chapter on Slip Surface Shapes and Positions.

The primary strength model in SLOPE/W is called Mohr-Coulomb. With this option you can specify c and ϕ for the soil.

6.3 Undrained strength

The Undrained strength option is a convenient way in SLOPE/W of setting ϕ to zero in the Mohr-Coulomb model (Figure 6-3). With this option, the shear strength of the material is only described by the c value and the pore-water pressure has no effect to the shear strength of the material.

6.4 No strength

The No Strength option simply means c and ϕ are both zero. Selecting this option means SLOPE/W sets c and ϕ to zero in the Mohr-Coulomb model. Selecting No Strength option is just a quick and convenient way of defining c and ϕ as both being zero.

The No Strength option is suitable for assigning the strength of water or any other materials you do not want to contribute to the strength of the soil, but you want the weight of the material to be included in the solution.

6.5 Impenetrable (Bedrock)

The Impenetrable strength option is really not a strength model, but a flag for the software to indicate that the slip surface cannot enter this material. It is an indirect mechanism for controlling the shape of trial slip surfaces. This soil model type is also sometimes referred to as bedrock. The Chapter on Slip Surface Shapes and Positions discusses this soil model option as to how it can be used to simulate certain field conditions.

6.6 Bilinear

Figure 6-4 shows the form of the Bilinear model. The failure envelope is described by two ϕ values, a cohesion value and a normal stress at which the break occurs.

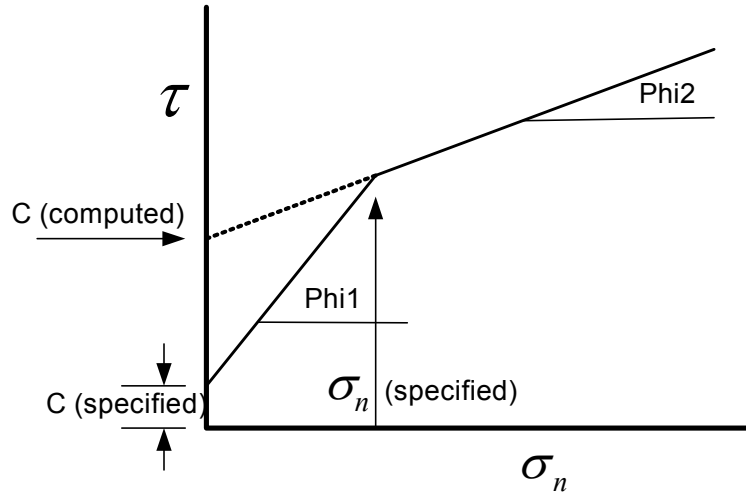


Figure 6-4 Bilinear shear strength envelope

For slice base normal stresses greater than the specified normal stress, SLOPE/W projects the Φ_2 (ϕ_2) line segment back to the shear strength axis and computes an equivalent cohesion intercept. When you look at slice forces or plot strength along the slip surface you will see Φ_2 (ϕ_2) and the computed cohesion intercept. Internally, SLOPE/W treats the Bilinear model as two Mohr-Coulomb models.

The Bilinear strength model was the first attempt in SLOPE/W to accommodate a nonlinear strength envelope. Since then better options have been implemented for specifying nonlinear strength envelopes and the Bilinear model has lost some of its usefulness. The model is still included and available primarily for historic and backward compatibility reasons.

6.7 General data-point strength envelope

A completely general strength envelope can be defined using data points. A smooth spline curve is drawn through the specified points as shown in Figure 6-5.

For each slice, SLOPE/W first computes the normal stress at the slice base. Next SLOPE/W computes the slope of the spline curve at the slice base normal stress. The spline-curve slope (tangent) is taken to be ϕ for that particular slice. The tangent is projected to the origin axis to compute an intercept, which is taken to be c . Each slice consequently has a c and ϕ relative to the slice base normal stress.

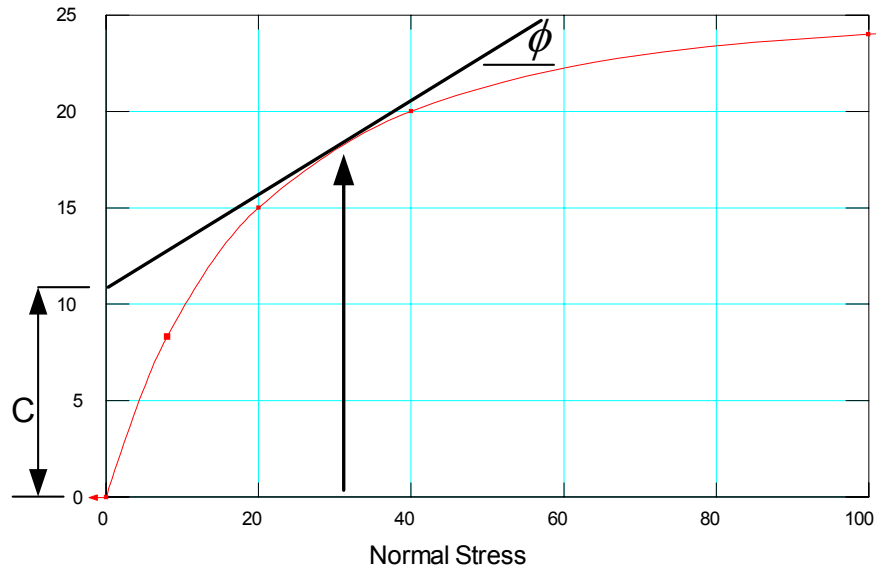


Figure 6-5 General data-point shear-normal function

The c value in this model should not be thought of as a true cohesive strength when the normal stress on the shear plane is zero. The c value in this case is simply an intercept on the shear strength axis. The intercept, together with the tangent, can be used to compute the shear strength at the base of the slice.

This data-point spline curve technique is a more recent development for dealing with curved strength envelopes and is consequently preferred over the Bilinear option.

Techniques for specifying the data and controlling the spline behavior are given in the online help.

The slope (tangent) at the end of the specified curve is used for normal stresses greater than the largest normal stress specified. The small arrow at the end of the curve is a graphical reminder of this behavior. Another point is that c is not allowed to drop below zero.

6.8 *Anisotropic strength*

This strength model uses the following equation for dealing with anisotropy in the soil strength:

$$c = c_h \cos^2 \alpha + c_v \sin^2 \alpha$$

$$\phi = \phi_h \cos^2 \alpha + \phi_v \sin^2 \alpha$$

The subscripts stand for horizontal and vertical. The horizontal and vertical components are specified. Alpha (α) is the inclination of the slice base. In other words, you may enter the c and ϕ in both the horizontal and vertical directions if they are different. This model provides a smooth transition of the c and ϕ based on the inclination angle of the slice base.

Say that the slice base inclination is 25 degrees, that c_h is 20, c_v is 30, $\phi_h = 30^\circ$ and $\phi_v = 35^\circ$. The cohesion and friction angle for this slice then will be:

$$c = 20(\cos 25)^2 + 30(\sin 25)^2 = 21.8$$

$$\phi = 30(\cos 25)^2 + 35(\sin 25)^2 = 30.9^\circ$$

Each slice has a c and ϕ depending on the base inclination angle.

6.9 *Strength using an anisotropic function*

This is a general strength model for anisotropic soil. The variation of c and ϕ with respect to the base inclination angles is described by a general function. The input c and ϕ values are multiplied with the modifier factor obtained from the anisotropic function before use in the shear strength computation

Figure 6-6 shows a typical anisotropic function in which a modifier factor is defined as a function of the inclination angle of the slice base. Let us say the modifier function in Figure 6-6 has been applied to a particular specified undrained strength (c). When the slice base inclination is, for example, 20 degrees, c will be multiplied by 1.08, and if the inclination is -20 degrees, c will be multiplied by 1.1. The maximum modifying factor is 1.3 when the inclination angle is about 45 degrees. When the slice base is horizontal (zero degrees) the modifier factor is 1.0; in other words, the strength remains the same value as was specified.

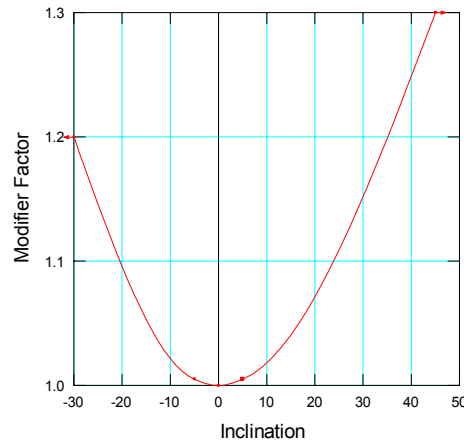


Figure 6-6 Typical anisotropic modifier function

The modifier function can be applied to any c or ϕ specified for a soil.

You can have as many functions as deemed necessary, and/or you can apply the same function to various strength parameters.

The first step in defining the modifier is to decide what strength parameter is known and at what inclination. The modifier factor at the known strength and known inclination is 1.0. The remainder of the function can then be specified relative to this known point.

Figure 6-7 shows the sign convention of the inclination angle used in SLOPE/W. Inclination angles measured from the positive x-axis are positive and negative when measured from the negative x-axis.

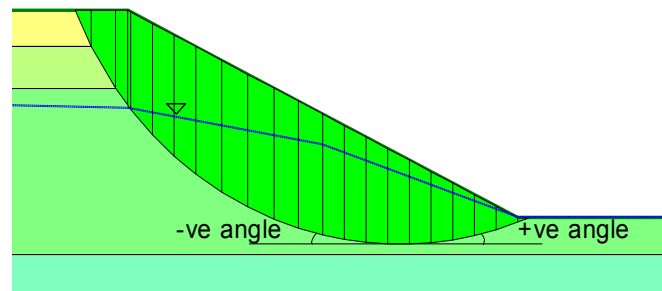


Figure 6-7 Sign convention of inclination angle used in SLOPE/W

6.10 Strength as a function of depth

Soft normally or slightly over-consolidated soil usually exhibits an increase in undrained strength with depth. SLOPE/W has two options for describing this type of strength profile. One is referenced to the top of the soil layer and the other is referenced to a specified datum. The two variations are illustrated below.

Relative to top of soil layer

With this option, it is necessary to specify the undrained strength (c) at the top of the layer and to specify the rate of increase with depth; that is, kPa per meter or psf per foot. In addition, a maximum cohesion can be specified. Figure 6-8 illustrates how this soil model could be used.

The top of the soil layer does not need to be a straight line. SLOPE/W finds the top of layer line for each slice.

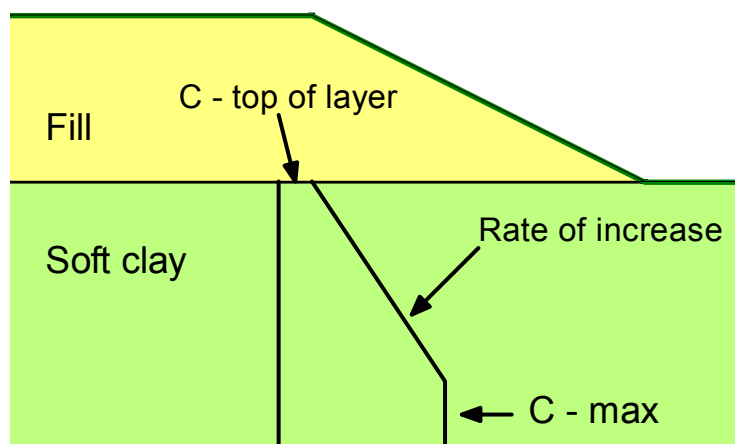


Figure 6-8 Shear strength as function of depth below top of layer

Relative to specified datum

A variation of specifying strength as function of depth is to define the strength parameters relative to a specified datum. This option is illustrated in Figure 6-9.

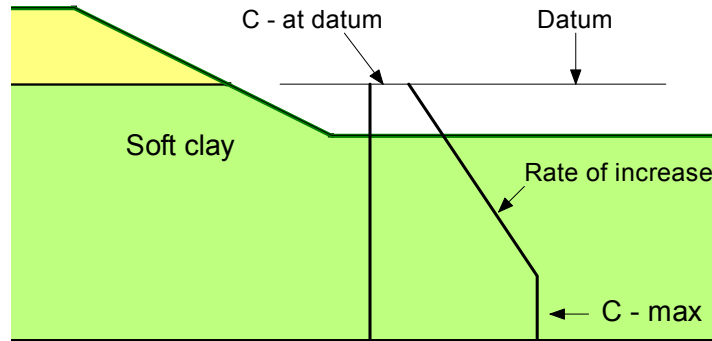


Figure 6-9 Shear strength as a function of depth below a datum

6.11 Frictional-undrained combined models

The frictional-undrained shear strength model was developed and is used in the Scandinavian countries where they have a lot of relatively soft marine clays. The clay is in essence treated as a $c-\phi$ soil, but with a maximum undrained strength as illustrated in Figure 6-10. The model has evolved from strength testing observations.

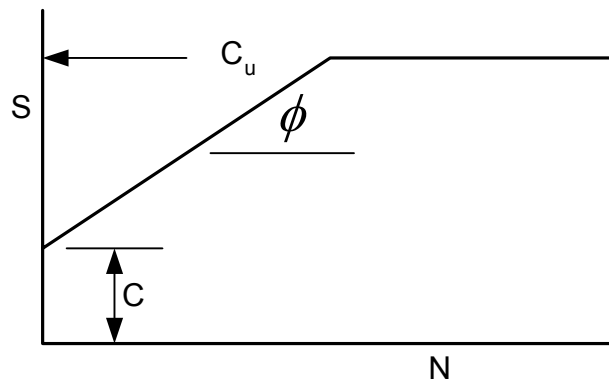


Figure 6-10 Combined frictional-undrained strength model

In addition, the cohesive components of the strength can vary with depth or relative to a specified datum. Either c or c_u can be specified at the top of a layer or at a certain datum together with a rate of increase with depth (kPa/m for example). The concept is similar to that in Figure 6-8 and Figure 6-9.

The c and c_u parameters can also be correlated by specifying a ratio. In SLOPE/W, c is computed from the c/c_u ratio if the ratio is non-zero. If the ratio is zero (undefined), the specified values for c and $c_{rate\ increase}$ are used.

The use of this combined frictional-undrained model is recommended only if you are intimately familiar with the background related to this model.

6.12 SHANSEP or strength = $f(\text{overburden})$ model

The SHANSEP or Strength as a function of overburden model is another strength model for very soft soils. This approach was developed at MIT by Ladd and Foott (1974) and Ladd (1991). The method attempts to normalize the undrained shear strength with respect to the insitu vertical effective stress or effective overburden stress. In SLOPE/W, a τ/σ ratio is specified. The ratio is an indication of the rate of increase in strength with depth (effective overburden). In equation form:

$$C_u \text{ or } S_u = \sigma'_v \times (\tau / \sigma \text{ ratio})$$

Special care is required in using this model to make sure that the pore-water pressure is correct, since the **effective** overburden stress is required.

Consider the case of placing an embankment on soft ground as illustrated in Figure 6-11. The first 2m below the ground is a desiccated layer and the water table is at the contact between the desiccated layer and the underlying soft soil. The weight of the sand fill will increase the pore-water pressure in the clay.

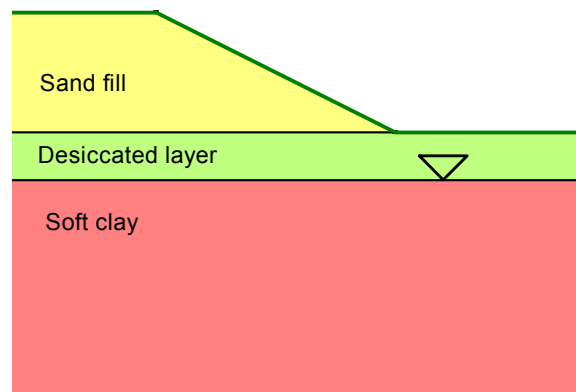


Figure 6-11 Case with SHANSEP model applied to soft clay

To get the correct effective stress in the clay, it is necessary to do the following:

- The soft clay is assigned a B-bar
- A piezometric line (#1 for example) which represents the water table is assigned only to the soft clay.
- The sand fill is flagged as the material that will add pore-water pressure to the piezometric line identified as #1.
- The desiccated layer does not have a B-bar and does not have an assigned piezometric line.

B-bar is defined as:

$$\bar{B} = \frac{u}{\sigma_v}$$

If B-bar is 1.0, all the weight of the sand fill will increase the pore-water pressure. In other words, the additional vertical stress from the fill is added to the initial pore-water pressure represented by the specified piezometric line.

If all of the fill weight goes to increasing the pore-water pressure, then the vertical effective stress in the soft clay does not change. This is the objective in the SHANSEP model so that the undrained shear strength is the same before and after the fill placement.

The pore-water pressures used in the stability calculations should be thoroughly checked and verified by plotting the pore pressure along the slip surface to make sure that appropriate shear strength is being used.

6.13 Hoek and Brown model

The Hoek and Brown model is a nonlinear shear strength model for rock. This model has evolved in stages over a couple of decades. The most recent version is known as the Generalized Hoek-Brown Criterion or the Hoek-Brown Failure Criterion-2002 Edition (Hoek, Carranza-Torres and Corkum, 2002).

Four input parameters are required to compute the shear strength versus normal stress curve. The four parameters are:

σ_{ci} = the uniaxial compressive strength of the intact rock

m_i = a property of the intact rock

GSI = Geological Strength Index (0-100)

D = rock mass disturbance factor (0-1)

The D , GSI and m_i properties are used to compute m_b as follows:

$$m_b = m_i \exp \frac{(GSI - 100)}{(28 - 14D)}$$

Two curve parameters a and s are computed from:

$$a = \frac{1}{2} + \frac{1}{6} \left(e^{-GSI/15} - e^{-20/3} \right)$$

$$s = \exp \left(\frac{GSI - 100}{9 - 3D} \right)$$

For intact rock GSI is 100 and so s is 1.0. In an earlier form of the failure criterion, the coefficient a was assumed to be a constant value of 0.5. It is now considered to be a variable dependent on GSI .

The relationship between the principal stresses at failure is:

$$\sigma_1 = \sigma_3 + \sigma_{ci} \left(m_b \frac{\sigma_3}{\sigma_{ci}} + s \right)^a$$

To establish the strength curve, SLOPE/W computes σ_1 for a range of σ_3 values.

The σ_3 default values range from a negative value representing the rock tensile strength up to a value equal to half the uniaxial compressive strength where the tensile strength is computed as:

$$\sigma_t = -s \frac{\sigma_{ci}}{m_b}$$

Once the $\sigma_1 - \sigma_3$ pairs at failure are known, a series of $\tau - \sigma_n$ data points are computed as follows:

$$\sigma_{ratio} = \frac{\sigma_1}{\sigma_3} = 1 + a m_b \left(m_b \frac{\sigma_3}{\sigma_{ci}} + s \right)^{a-1}$$

$$\sigma_n = \left(\frac{\sigma_1 + \sigma_3}{2} \right) - \left(\frac{\sigma_1 - \sigma_3}{2} \right) \times \left(\frac{\sigma_{ratio} - 1}{\sigma_{ratio} + 1} \right)$$

$$\tau = (\sigma_1 - \sigma_3) \frac{\sqrt{\sigma_{ratio}}}{\sigma_{ratio} + 1}$$

From these data points, SLOPE/W computes a spline curve the same for the General Data Point function discussed above.

Figure 6-12 shows an example strength function when:

$$\sigma_{ci} = 20,000 \text{ kPa (20 MPa)}$$

$$m_i = 10$$

$$GSI = 45$$

$$D = 1.0$$

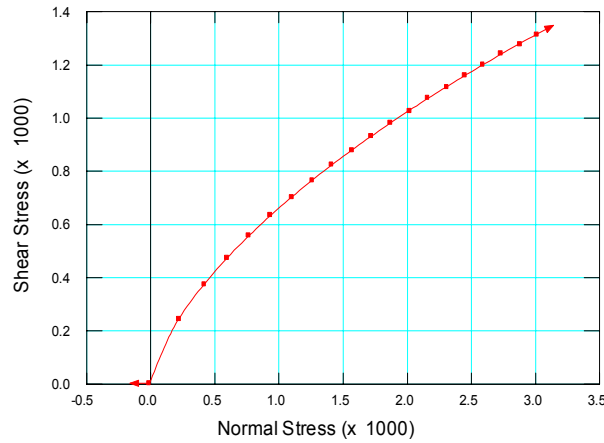


Figure 6-12 Strength function based on generalized Hoek – Brown strength criterion

SLOPE/W computes the normal stress at the base of each slice and then finds the slope of the splined curve, which is taken as the friction angle ϕ . A tangent line to the curve is projected to the τ axis and the intersection point on the τ axis is assumed to be equal to the cohesion. Each slice base consequently will have separate $c - \phi$ parameters depending on the slice base normal.

The following three tables provide some guidelines for selecting and specifying uniaxial compressive strengths, m_i constants and GSI values.

The following tables come from Evert Hoek's course notes entitled Practical Rock Engineering (2000 ed., Chapter 11), and reproduced here simply for convenience reference.

The D parameter is an indication of the amount of disturbance the rock may have undergone during excavation or blasting. A D value of zero means the rock has undergone very little disturbance, while a D value of 1.0 represents a condition where the rock has undergone significant disturbance due to heavy production blasting that may exist in situations such as an open pit mine (Hoek et al, 2002)

Table 6-1 Field estimates of uniaxial compressive strength (After Hoek, 2000)

Grade*	Term	Uniaxial Comp. Strength (MPa)	Point Load Index (MPa)	Field estimate of strength	Examples
R6	Extremely Strong	> 250	>10	Specimen can only be chipped with a geological hammer	Fresh basalt, chert, diabase, gneiss, granite, quartzite
R5	Very strong	100 - 250	4 - 10	Specimen requires many blows of a geological hammer to fracture it	Amphibolite, sandstone, basalt, gabbro, gneiss, granodiorite, limestone, marble, rhyolite, tuff
R4	Strong	50 - 100	2 - 4	Specimen requires more than one blow of a geological hammer to fracture it	Limestone, marble, phyllite, sandstone, schist, shale
R3	Medium strong	25 - 50	1 - 2	Cannot be scraped or peeled with a pocket knife, specimen can be fractured with a single blow from a geological hammer	Claystone, coal, concrete, schist, shale, siltstone
R2	Weak	5 - 25	**	Can be peeled with a pocket knife with difficulty, shallow indentation made by firm blow with point of a geological hammer	Chalk, rocksalt, potash
R1	Very weak	1 - 5	**	Crumbles under firm blows with point of a geological hammer, can be peeled by a pocket knife	Highly weathered or altered rock
R0	Extremely weak	0.25 - 1	**	Indented by thumbnail	Stiff fault gouge

* Grade according to Brown (1981).





** Point load tests on rocks with a uniaxial compressive strength below 25 MPa are likely to yield highly ambiguous results.

Table 6-2 Values of constant m_i for intact rock by rock group; values in parentheses are estimates (after Hoek, 2000)

Rock type	Class	Group	Texture			
			Coarse	Medium	Fine	Very fine
SEDIMENTARY	Clastic		Conglomerate (22)	Sandstone 19 —— Greywacke —— (18)	Siltstone 9	Claystone 4
	Non-Clastic	Organic	—— Chalk —— 7 —— Coal —— (8-21)			
		Carbonate	Breccia (20)	Sparitic Limestone (10)	Micritic Limestone 8	
		Chemical		Gypstone 16	Anhydrite 13	
METAMORPHIC	Non Foliated		Marble 9	Hornfels (19)	Quartzite 24	
	Slightly foliated		Migmatite (30)	Amphibolite 25 - 31	Mylonites (6)	
	Foliated*		Gneiss 33	Schists 4 - 8	Phyllites (10)	Slate 9
IGNEOUS	Light		Granite 33		Rhyolite (16)	Obsidian (19)
			Granodiorite (30)		Dacite (17)	
	Dark		Diorite (28)		Andesite 19	
			Gabbro 27 Norite 22	Dolerite (19)	Basalt (17)	
	Extrusive pyroclastic type		Agglomerate (20)	Breccia (18)	Tuff (15)	

* These values are for intact rock specimens tested normal to bedding or foliation. The value of m_i will be significantly different if failure occurs along a weakness plane.

Table 6-3 Estimates of Geological Strength Index (GSI) based on geological description (after Hoek, 2000)

<p>GEOLOGICAL STRENGTH INDEX</p> <p>From the letter codes describing the structure and surface conditions of the rock mass (from Table 4), pick the appropriate box in this chart. Estimate the average value of the Geological Strength Index (GSI) from the contours. Do not attempt to be too precise. Quoting a range of GSI from 36 to 42 is more realistic than stating that GSI = 38.</p>		<p>SURFACE CONDITIONS</p> <p>VERY GOOD Very rough, fresh unweathered surfaces</p> <p>GOOD Rough, slightly weathered, iron stained surfaces</p> <p>FAIR Smooth, moderately weathered or altered surfaces</p> <p>POOR Slickensided, highly weathered surfaces with compact coatings or fillings of angular fragments</p> <p>VERY POOR Slickensided, highly weathered surfaces with soft clay coatings or fillings</p>	
STRUCTURE		<p>DECREASING SURFACE QUALITY</p>	
 <p>BLOCKY - very well interlocked undisturbed rock mass consisting of cubical blocks formed by three orthogonal discontinuity sets</p>	<p>DECREASING INTERLOCKING OF ROCK PIECES</p>	80	
 <p>VERY BLOCKY - interlocked, partially disturbed rock mass with multifaceted angular blocks formed by four or more discontinuity sets</p>		70	
 <p>BLOCKY/DISTURBED - folded and/or faulted with angular blocks formed by many intersecting discontinuity sets</p>		60	
 <p>DISINTEGRATED - poorly interlocked, heavily broken rock mass with a mixture of angular and rounded rock pieces</p>		50	
		40	
		30	
		20	
		10	

6.14 Unsaturated shear strength

Soil suction or negative water pressures have the effect of adding strength to a soil. In the same way that positive pore-water pressures decrease the effective stress and thereby decrease the strength, negative pore-water pressures increase the effective stress and in turn increase the strength.

The shear strength of unsaturated soil is:

$$s = c' + \sigma_n \tan \phi' + (u_a - u_w) \tan \phi^b$$

where:

- u_a = the pore-air pressure,
- u_w = the pore-water pressure, and
- ϕ^b = an angle defining the increase in strength due to the negative pore-water pressure.

The term $(u_a - u_w)$ is called suction when presented as a positive number. The angle ϕ^b is a material property.

In SLOPE/W, ϕ^b is treated as a constant value, but in actual fact this parameter varies with the degree of saturation. In the capillary zone where the soil is saturated, but the pore-water pressure is under tension, ϕ^b is equal to the friction angle ϕ' . As the soil desaturates, ϕ^b decreases. The decrease in ϕ^b is a reflection of the fact that the negative pore-water pressure acts over a smaller area. More specifically, ϕ^b is related to the soil water characteristic curve (volumetric water content function as discussed at length in the SEEP/W documentation), but relating ϕ^b to the volumetric water content has as yet not been implemented in SLOPE/W. Currently, only a constant ϕ^b can be specified.

For practical purposes, ϕ^b can be taken to be about $1/2 \phi'$.

In SLOPE/W, if ϕ^b is undefined (zero), any negative pore-water pressure is ignored. If ϕ^b is a non-zero specified value, the above equation for unsaturated soil is used in SLOPE/W and an extra strength component dependent on the suction is added to the slice base shear strength.

When you plot shear strength along the slip surface, you will notice three strength components, cohesion, friction and suction. This type of plot should always be created when it is your intention to include the suction strength component in an analysis. The plot should be created to verify that ϕ^b has been used properly and to gain an appreciation as to how significant the suction strength is relative to the cohesive and frictional strength.

6.15 Soil unit weight

The sliding mass weight or gravitational force is applied by assigning the soil a unit weight. The slice cross sectional area times the specified unit weight determines the weight of the slice.

As discussed in the Limit Equilibrium Fundamentals Chapter, SLOPE/W is formulated on the basis of total forces. The unit weight consequently needs to be specified as the **total** unit weight.

SLOPE/W allows for a separate unit weight above the water table, but use of this parameter is seldom necessary.

The soil unit weight is:

$$\gamma = \gamma_w \frac{G + Se}{1 + e}$$

where:

γ_w	=	the unit weight of water,
G	=	specific gravity,
S	=	the degree of saturation, and
e	=	the void ratio.

For illustration purposes, assume that $G = 2.7$, $\gamma_w = 10 \text{ kN/m}^3$, and $e = 0.7$. Below the water table where the soil is saturated ($S = 1$) and the unit weight is 20.0 kN/m^3 . Above the water table where the soil is unsaturated, assume the degree of saturation is 80%, (i.e., $S = 0.8$) the unit weight of water would be 19.2 kN/m^3 , about a 4% difference.

From a stability analysis point of view, the 4% difference in the unit weight is insignificant. First of all there is the capillary zone where S is 100% and the unit weight therefore is the same above and below the water table in the capillary zone. Secondly, factor of safety calculations are not very sensitive to the unit weight. If the slice weight increases, the gravitational driving force increases, but the shear resistance also increases because of a higher normal at the slice base, and vice versa. Therefore, defining different unit weights above and below the water table usually has little effect on the resulting factor of safety.

The unit weight above the water table should certainly not be specified as the dry unit weight. In the field, the soil is seldom completely dry except for perhaps a relatively thin layer near the ground surface.

A situation where the difference in unit weight above and below the water table may be significant is when very coarse rock fill is placed in water to create a water break as illustrated in Figure 6-13.

For this type of situation, assume that e is 1.0, G is 2.7 and γ_w is 10 kN/m^3 . Below the water line where S is 1.0 the unit weight is 18.5 kN/m^3 . Above the water line where S is zero, the unit weight is 13.5 kN/m^3 . This is a significant difference and consequently worth the effort to specify two different unit weights.

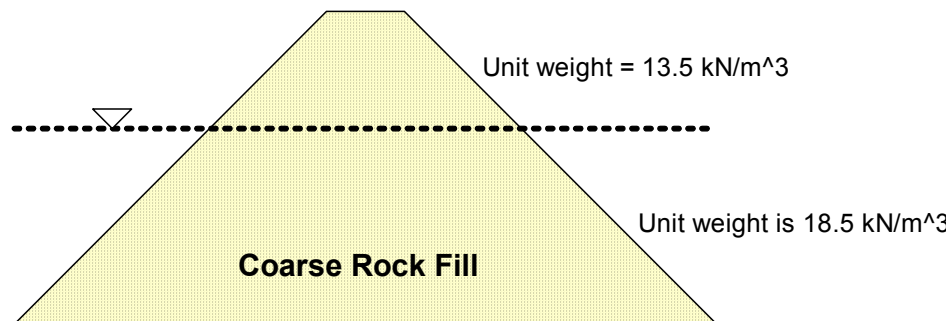


Figure 6-13 Different unit weight above and below the water in rock fill

In the end it is really up to the analyst whether a separate unit weight is specified for the soil above the water table. The option is available in SLOPE/W as an advanced parameter.

6.16 Other soil parameters

There are other soil property parameters, but they will be discussed in the context of their specific application. For example, all the material parameter variability or dispersion are discussed and explained in the Chapter on Probabilistic Analyses. In addition, the residual strength parameters are discussed in connection with Seismic and Dynamic Stability Analyses.

7 Pore-water

7.1 Introduction

In the previous chapter, it was noted that the most realistic position of the critical slip surface is obtained when effective strength parameters are used in the analysis. Effective strength parameters, however, are only meaningful when they are used in conjunction with pore-water pressures. In this sense, the pore-water pressures are as important in establishing the correct shear strength as the shear strength parameters themselves.

Due to the importance of pore-water pressures in a stability analysis, SLOPE/W has various ways of specifying the pore-water pressure conditions. This chapter gives an overview of the options available, and presents some comments on the applicability of the various methods.

7.2 Piezometric surfaces

The most common way of defining pore-water pressure conditions is with a piezometric line. With this option, SLOPE/W simply computes the vertical distance from the slice base mid-point up to the piezometric line, and multiplies this distance times the unit weight of water to get the pore-water pressure at the slice base. This is graphically illustrated in Figure 7-1.

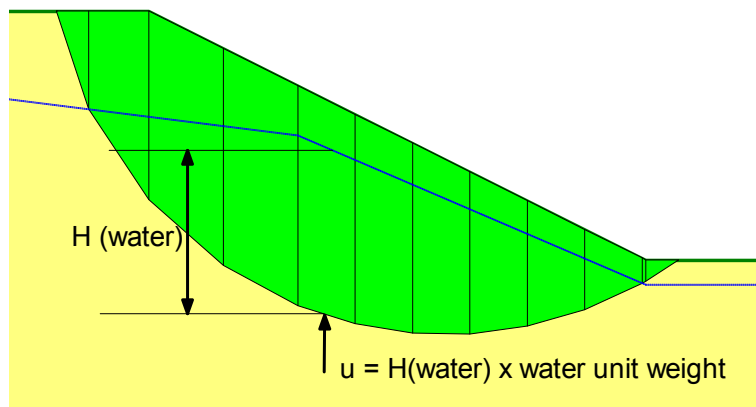


Figure 7-1 Pore pressure from a piezometric line

When thinking about pore-water pressures in SLOPE/W, it is vitally important to recognize that pore-water pressures only come into play in the calculation of the shear strength at the base of each slice – they do not enter into the interslice force calculations.

When the slice base mid-point is located above the piezometric line, the pore-water pressure is taken to be zero unless ϕ^b (Phi B) has been assigned a value. This is explained further in this chapter under the topic of negative pore-water pressures.

Single piezometric line

Usually a profile has only one piezometric line and it applies to all soils. However, sometimes more complex pore-water pressures exist and in SLOPE/W, it is possible to be more selective and precise, if necessary. For example, a piezometric line can be applied only to selected soil layers and not to the entire profile. Consider the case of a sand embankment on soft clay soil as shown in Figure 7-2. Assume we want to make the pore-water pressures equal to zero in the sand, but we want to represent the pore-water pressure in the clay by a piezometric line that exists above the clay surface due to some excess pressure in the clay. A piezometric line can be drawn and assigned only to the clay layer. As a result, pore-water pressures will not exist in the sand layer. This option is useful when it is combined with a R_u or $B\text{-bar}$ value.

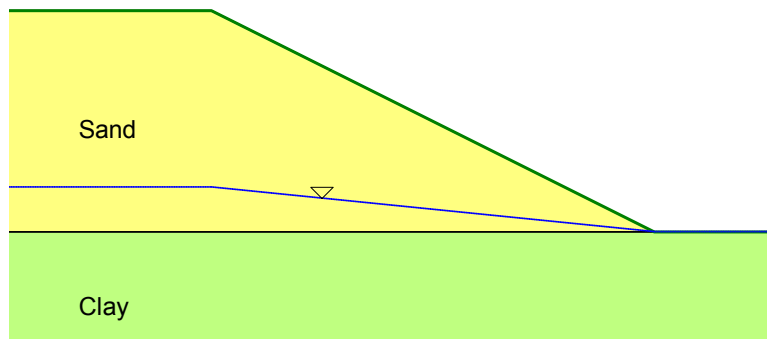


Figure 7-2 Piezometric assigned only to the clay

Multiple piezometric lines

In SLOPE/W, each soil type can have its own piezometric line making it possible to represent irregular non-hydrostatic pore-water pressure conditions. In practice this option is not all that applicable. Highly irregular pore-water pressure

conditions are better specified by one of the other more advanced methods discussed below.

Phreatic correction

In a sloping profile, the flow of water is usually from the uplands towards the slope toe which results in the piezometric surface curving downwards. As we know from flow net design, under these conditions the equipotential lines are not vertical. The assumption in SLOPE/W of relating the pore-water pressure to the vertical distance from slice base to the piezometric line is consequently not strictly correct. A correction factor can be applied to more accurately represent the pore-water pressure, if this is deemed important.

Figure 7-3 illustrates how phreatic correction is applied. The equipotential lines are perpendicular to the piezometric line. The inclination of the phreatic surface is at an angle A. Without phreatic correction, H_w is the height used to compute the pore pressure at the base center of the slice. With phreatic correction, H_w is corrected and H_c is used to compute the pore pressure at the base center of the slice.

$$H_c = H_w \cos^2 A$$

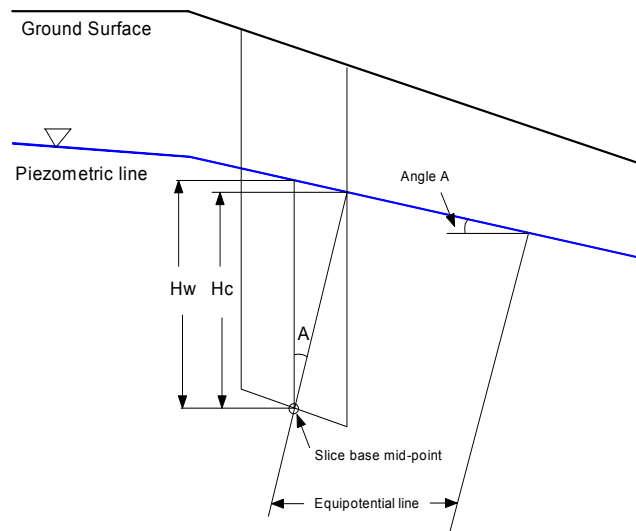


Figure 7-3 Phreatic surface correction

Note that when the piezometric line is horizontal ($A=0$), the phreatic correction factor ($\cos^2 A$) is 1 and H_c is equal to H_w . When the piezometric line is approaching a vertical line, the correction factor is approaching 0. Since the correction factor is always between 0 and 1, applying the phreatic correction always generates a pore water pressure smaller or equal to a non-corrected condition. In other words, the computed factor of safety is always the same or higher when the phreatic correction is applied.

7.3 R_u Coefficients

The pore-water pressure ratio R_u is a coefficient that relates the pore-water pressure to the overburden stress. The coefficient is defined as:

$$R_u = \frac{u}{\gamma_t H_s}$$

where:

u = the pore-water pressure

γ_t = the total unit weight

H_s = the height of the soil column.

By re-arranging the variables, the pore-water pressure u becomes:

$$u = R_u \gamma_t H_s$$

The concept of R_u was in large part developed for use with stability charts (Bishop and Morgenstern, 1960). This pore-water pressure coefficient, together with the stability chart coefficients m and n can be used to quickly estimate the factor of safety for simple slopes from the equation $F = m - n R_u$.

One of the difficulties with the R_u concept is that the coefficient varies throughout a slope if the phreatic surface is not parallel to the ground surface. When the phreatic surface is an irregular distance from the ground surface, it is necessary to establish R_u at a number of points and then by some weighted averaging method to calculate one single overall average value for the slope. The result is that the simplicity of the method is lost.

The variability of R_u within a slope makes it an impractical option in a product like SLOPE/W. The R_u option is included in SLOPE/W mainly for historic reasons. Attempting to make use of the option is not recommended, except in perhaps some simple isolated cases. There are other better options available.

In a multi-layered stratigraphic section, R_u can be applied selectively to each of the soil units.

It is useful to always think about the base of the slice when defining pore-water pressure conditions. If the base of a slice is in a soil with an assigned R_u , then pore-water pressure will be computed based on the *entire* total slice weight. This action is different than B-bar (discussed below). R_u always uses the entire slice weight; B-bar uses only soil layers flagged as adding to the pore-water pressure.

Pore-water pressures based on R_u calculations can be added to conditions represented by a piezometric line. The R_u computed pore-water pressure will be added to the pore-water pressure computed from a piezometric line if the slice base is below the piezometric line and the slice base is in a soil with an assigned R_u .

Consider slice 10 shown in Figure 7-4. The piezometric line is located at the clay-sand contact and the clay has been assigned a R_u value of 0.2. The unit weight for both the sand and clay is 20 kN/m^3 . The vertical distance from the ground surface to the bottom of sand layer is 7.22m. The vertical distance from the slice base center to the piezometric line is 2.14m. The R_u component of the water pressure is $(7.22\text{m} + 2.14\text{m}) \times 20.0 \text{ kN/m}^3 \times 0.2 = 37.44 \text{ kPa}$ (note that both the sand and clay layers are included in the slice weight calculation). The pore pressure from the piezometric line is $2.14\text{m} \times 9.81 \text{ kN/m}^3 = 20.99 \text{ kPa}$. Therefore, the total pore-water pressure at the base center when R_u is used together with the piezometric line is 58.43 kPa.

Combining R_u computed pore-water pressures with piezometric pore-water pressures can be confusing at times. When you attempt to do this, it is highly recommended that you graph the pore-water pressure distribution along the slip surface and spot check that the SLOPE/W pore-water pressures are as intend.

Conceptually, R_u is around 0.5 if the phreatic surface is at the ground surface. This is because the unit weight of water is about half the total unit weight of the soil.

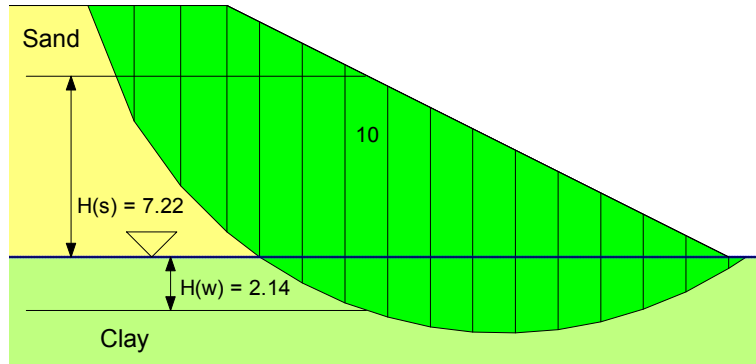


Figure 7-4 Combination of R_u /B-bar with piezometric pore-water pressures

7.4 B-bar coefficients

B-bar (\bar{B}) is a pore-water pressure coefficient related to the major principal stress. In equation form:

$$\bar{B} = \frac{\Delta u}{\Delta \sigma_1}$$

In many situations, the major principal stress is near vertical and, consequently, σ_1 can be approximated from the overburden stress. This approximation is used in the B-bar application in SLOPE/W.

The distinguishing feature about B-bar in SLOPE/W is that individual soil layers can be selected for computing the overburden stress. Consider the same case as shown in the previous section, but now instead of a R_u value, the clay is assigned a B-bar value of 0.2 (Figure 7-4). Only the sand has been flagged as adding to the pore-water pressure. The pore-water pressure from the sand weight is $7.22\text{m} \times 20.0 \text{ kN/m}^3 \times 0.2 = 28.88 \text{ kPa}$. The pore-water pressure from the piezometric line is $2.14\text{m} \times 9.81 \text{ kN/m}^3 = 20.99 \text{ kPa}$. The total pore-water pressure at the base center when B-bar is used together with the piezometric line is 49.87 kPa .

Please note that in this case only the sand weight is added to the pore-water pressure calculations, but the B-bar is assigned to the clay layer.

7.5 Pore-water pressures at discrete points

A powerful and highly flexible option in SLOPE/W for defining pore-water pressure conditions is to specify the actual pressure at discrete points. Figure 7-5 shows an example with pore-water pressure data points. The pore-water pressure is specified at each of the triangular shaped points.

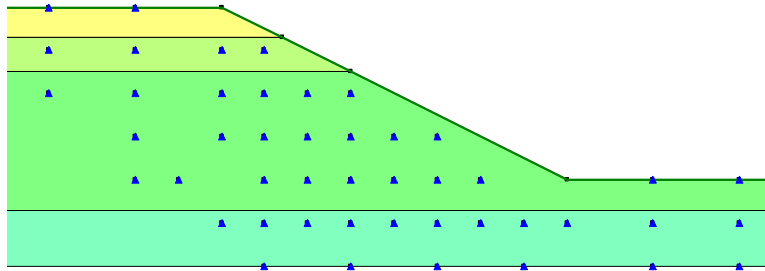


Figure 7-5 Pressure head data points

Using Spline interpretation techniques (see Theory Chapter for details), SLOPE/W constructs a smooth surface that passes through all the specified points. Once the surface has been constructed, the pore-water pressure can be determined at any other x-y coordinate point in the vicinity of the specified data points. For each slice, SLOPE/W knows the x-y coordinates at the slice base mid-point. These x-y coordinates together with the pore-water pressure surface are then used to establish the pore-water pressure at the base of each slice.

The data points can be a grid of R_u values, a grid of pressure heads or a grid of pressures. The best option of these three is the specification of pressure heads. Positive pressure heads are, for example, meters (or feet) of water above the data point. Negative pore-water pressures can also be specified as data points. Pressure heads are generally easier to visualize than R_u values or pressures values.

The Data Point method is useful when the pore-water pressures are fairly irregular or non-hydrostatic. Data points could be used to describe a perched water table. Data points are also useful for directly including field piezometric measurements in an analysis.

When using the Data Point option in SLOPE/W, it is necessary to give careful thought to all the locations the pore-water pressure is known. Say you have an unsaturated zone and you do not wish to consider the suction. Some data points would then be required in the unsaturated zone where the pressure head is zero. If

there is ponded water, a pressure head equal to the depth of the water would need to be specified along the water-soil contact line. On a seepage face where the pore-water pressure is zero, the pressure head would need to be specified as zero. In summary, the pore-water pressure needs to be specified at all locations where the pore-water pressure condition is known with certainty.

The number of data points does not need to be excessively large. The data points can be fairly sparsely spaced except in areas where there are sudden large changes in the pore-water pressures. Also, remember pore-water pressures come into play only along the slip surfaces, and so the data points need to be concentrated in the zone of potential slip surfaces.

As always, it is good practice to graph the pore-water pressure along the slip surface, to spot check that they are a reasonable representation of the intended conditions. A smooth gradual variation in the pore-water pressure along the slip surface usually is an indication that the data is specified correctly. On the other hand, any abrupt changes may indicate there is something wrong with the specified data.

7.6 *Negative pore-water pressures*

SLOPE/W can accommodate negative pore-water pressures just as well as positive pressures. Soil suction (negative pore-water pressure) has the effect of increasing the soil strength, as previously discussed. The additional suction related strength is included if the ϕ^b parameter is specified.

When a piezometric line is used to define pore-water pressures, SLOPE/W computes the negative pressure in the same way as the positive pressures. Where the slice base is above the piezometric line, the vertical distance between the slice base center and the piezometric line is a negative value (y-coordinate of piezometric line minus y-coordinate of slice base center). The pore-water pressure is consequently negative.

Negative pore-water pressure in a material will only be displayed if a ϕ^b is not zero.

7.7 *Finite element computed pressures*

SLOPE/W is fully integrated with the finite element products available in GeoStudio. This makes it possible to use finite element computed pore-water

pressures in a stability analysis. For example, the pore-water pressures can come from a:

- SEEP/W steady-state seepage analysis
- SEEP/W transient analysis at any particular time step
- SIGMA/W analysis where there are excess pore-water pressures due to some kind of loading
- SIGMA/W consolidation analysis
- QUAKE/W dynamic earthquake analysis at any time during the shaking or at the end of shaking
- VADOSE/W ground surface evaporative flux analysis.

In general, the pore-water pressures can come from any finite element analysis that creates a head or pore-water pressure file.

To use the finite element computed pore-water pressures, SLOPE/W first finds the element that encompasses the slice base center. Next, the local element coordinates (r,s) are determined at the slice base. The pore-water pressures are known at the element nodes either directly from the finite element results or by mapping the Gauss point values to the nodes. The nodal pore-water pressures and local r - s coordinates together with the inherent finite element interpolating functions are then used to compute the pore-water pressure at the slice base center. The power of this approach is that the pore-water pressures can have any irregular distribution and represent conditions at various times.

An example of using irregular finite element computed pore-water pressures in SLOPE/W is presented in Figure 7-6 and Figure 7-7. A less permeable layer mid-height in the slope has caused a perched water table to form due to the infiltration. This type of pore-water pressure distribution can be modeled in SEEP/W and then integrated with SLOPE/W.

Figure 7-8 shows the distribution of pore-water pressure along the slip surface. The pore-water pressure starts out negative at the crest, then becomes positive in the perched water zone, becomes negative again in the unsaturated zone and then is positive through the base saturated zone.

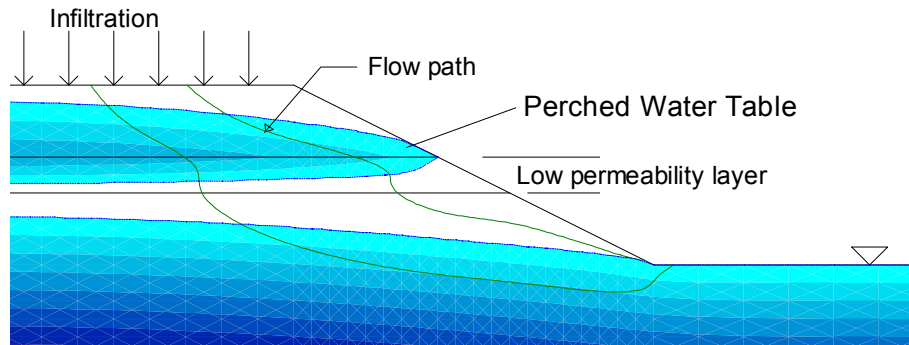


Figure 7-6 SEEP/W computed pore-water pressures

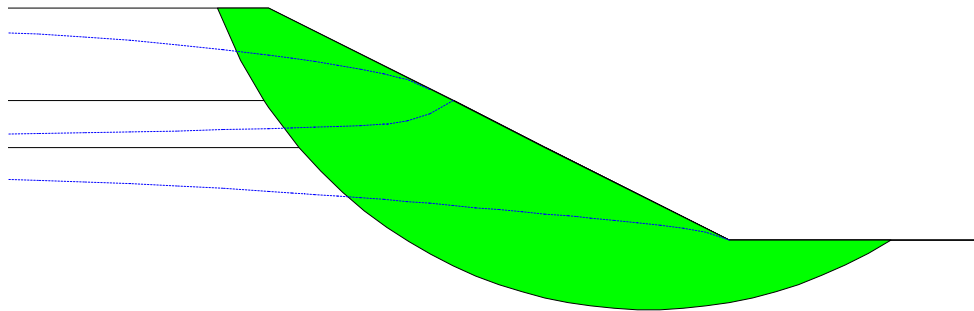


Figure 7-7 SEEP/W pore-water pressures in SLOPE/W

There are few restrictions on using finite element computed pore-water pressures in SLOPE/W. The one thing to be careful about is that all trial slip surfaces must fall within the finite element mesh. No portion of a slip surface can exist outside the mesh.

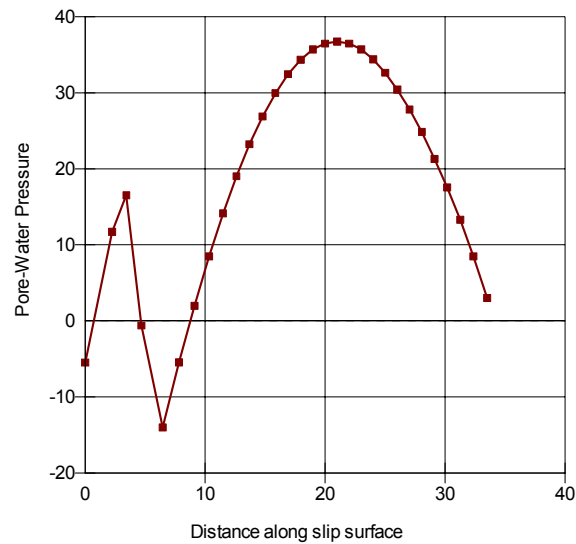


Figure 7-8 Pore-water pressure distribution along slip surface

7.8 Recommended practice

As has been noted several times already, we highly recommend that you graph the pore-water pressure acting along the slip surface, to check that the pore-water pressures used by SLOPE/W are as you expect and are reasonable (Figure 7-8). This should be done periodically throughout a stability analysis.

8 Reinforcement and Structural Components

8.1 Introduction

The limit equilibrium method of slices was initially developed for conventional slope stability analyses. The early developers of the method recognized some of the inherent potential difficulties of determining realistic stress distributions. For example, Lambe & Whitman (1969), in their textbook *Soil Mechanics* point out that the normal stress at a point acting on the slip surface should be mainly influenced by the weight of the soil lying above that point. It seems like they were concerned that other factors could influence the base normal stress and that this may not be appropriate. In spite of the early developers' concerns, over the years concentrated loads were incorporated into the method mainly to simulate equipment or other surcharge loading on the slope crest. Later, thoughts on the subject migrated to the idea that if concentrated surcharge line loads can be included in the method, then why not include lateral concentrated line loads to represent reinforcement. Conceptually, there seemed to be no reason for not doing this, and consequently the simulation of reinforcement with lateral concentrated loads has become common in limit equilibrium stability analyses.

Unfortunately, including lateral concentrated loads in a limit equilibrium analysis has some undesirable side effects. The resulting stress distributions, for example, throughout the potential sliding mass may be totally unrealistic, the critical slip surface may be in an unrealistic position, and the results may be difficult to interpret due to convergence difficulties. In spite of these negative side effects, the concepts can be successfully used in practice provided the procedures are fully understood and applied with considerable care.

This chapter starts with a discussion on some fundamentals related to applying lateral concentrated loads to simulate reinforcement in a limit equilibrium analysis. The numerical issues are the same regardless whether the reinforcement is an anchor, a nail or a fabric. The details of the specified parameters are, however, somewhat different for each of the various types of reinforcement and separate discussions are therefore devoted to each type of reinforcement.

The later part of this chapter deals with using finite element computed stress in the stability analysis of reinforced earth structures.

8.2 *Fundamentals related to concentrated lateral loads*

An important concept that needs to be fully comprehended is that all reinforcement fundamentally is a concentrated line load in a limit equilibrium formulation. The concentrated line loads act on the free body, which is the potential sliding mass, and must therefore be included in the moment and force equilibrium equations. There are fancy and convenient ways of specifying the properties of the reinforcement, as we will see below, but in the end the specified parameters are used to create a concentrated line load in the factor of safety calculations.

Mobilization of reinforcement forces

The effect of reinforcement can conceptually act immediately or develop with some strain. A pre-stressed anchor, for example, acts immediately. The force is induced by the pre-stressing. The force in a geofabric, on the other hand, may develop over time during construction and during stress re-distribution upon completion of the construction. In other words, the reinforcement forces are mobilized in response to straining in the same way that the soil strength is mobilized as the soil strains.

Another way of looking at the reinforcement is that the reinforcement reduces the activating driving forces; that is, the reinforcement forces reduce the destabilizing forces. The reinforcement reduces the gravitational driving force. Alternatively, the reinforcement increases the shearing resistance and thereby increases the safety factor.

The SLOPE/W equilibrium equations are based on the shear mobilized at the base of each slice, and the mobilized shear is the shear strength divided by the factor of safety. In equation form, the mobilized shear S_m is:

$$S_m = \frac{S_{soil}}{F \text{ of } S}$$

If the reinforcement is to be included to increase the shear resistance, then the reinforcement forces must also be divided by the factor of safety. S_m then is:

$$S_m = \frac{S_{soil}}{F \text{ of } S} + \frac{S_{reinforcement}}{F \text{ of } S}$$

A point of significance is that the soil strength and the shear resistance arising from the reinforcement are both divided by the same overall global factor of safety. The implication is that the soil shear resistance and reinforcement shear resistance are developed and mobilized at the same rate. This is likely not entirely correct in reality, but that is the assumption with this approach.

When the reinforcement is considered as contributing to reducing the destabilizing force, then it is assumed that the reinforcement is fully mobilized immediately and the reinforcement forces consequently are not divided by the overall global factor of safety. Safety factors may be specified to limit the allowable loads in the reinforcement, but they do not directly come into the SLOPE/W factor of safety calculations. The specified or the allowable reinforcement forces are directly used in the SLOPE/W calculations.

SLOPE/W allows for both these approaches to include reinforcement in the stability calculations. The option is selected by flagging the reinforcement as “F of S dependent”, Yes or No. The Yes option increases the shear resistance and the reinforcement forces are divided by the global factor of safety to obtain the mobilized reinforcement forces. The No option uses the specified allowable reinforcement forces directly in the analysis.

The “F of S Dependent” Yes option is considered appropriate for ductile reinforcement such as geofabrics. The No option is considered appropriate for pre-stressed anchors or nails that are rigid relative to soil stiffness. By default, SLOPE/W uses the Yes option for fabrics and the No option for anchors and nails. The defaults can, however, be changed and defined as deemed appropriate for each particular design. Earlier versions of SLOPE/W were formulated only for the No option.

The “F of S Dependent” Yes option divides the specified reinforcement forces by the overall global all factor of safety. The “F of S Dependent” No option uses the allowable specified reinforcement forces directly, and the reinforcement is not altered by the global factor of safety.

The two approaches are quite different in that with the “F of S Dependent” No option the specified anchor force is treated as the full mobilized force without consideration of the SLOPE/W computed factor of safety. With the “F of S Dependent” Yes option the computed factor of safety is applied to the reinforcement in the same way as to the soil strength. As shown in the Theory

Chapter, it is the mobilized shear at the base of the slice (S_m) that is used in the equilibrium equations, and S_m is the shear strength divided by the factor of safety (S/F or S). In the same way, it is only the mobilized reinforcement forces that can be included in the summation of the resisting forces, not the specified reinforcement forces. The specified reinforcement force is divided by the SLOPE/W factor of safety to obtain the mobilized reinforcement forces.

The Yes and No approaches will give similar results when the factor of safety is 1.0 or when the reinforcement forces are only a small fraction of the weight of the entire potential sliding mass.

Slice forces and stress distributions

In SLOPE/W a reinforcement load is applied to the slice that has its base intersected with the line of action of the reinforcement. The reinforcement load is treated as a concentrated line load acting at the intersecting point at the base of a slice.

Another important point is that concentrated line loads must become part of the force resolution of one particular slice. The following is the equation for summation of moments about a point as explained in the Theory Chapter. The concentrated load is represented by D .

$$\sum Wx - \sum S_m R - \sum Nf + \sum kWe \pm \sum Dd \pm \sum Aa = 0$$

Now let us look at an example that was introduced earlier in the Limit Equilibrium Fundamentals chapter. The example is a tie-back wall with two rows of pre-stressed anchors (Figure 8-1). Each anchor can apply 150 kN of force

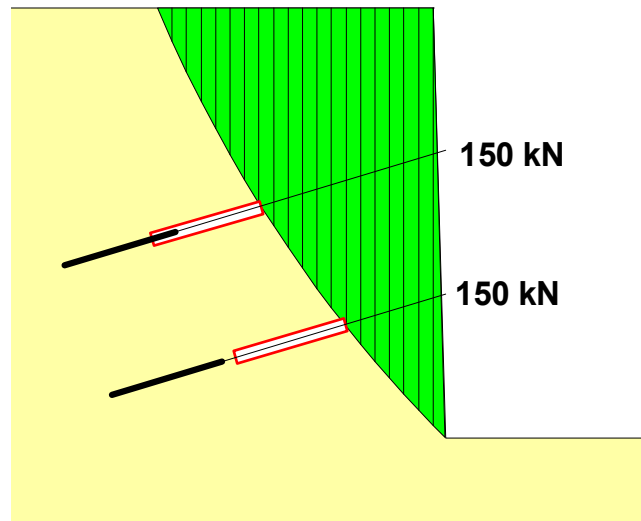


Figure 8-1 Illustration of a tie-back wall

The free body diagrams and force polygons for the two slices that included the reinforcement line loads are presented in Figure 8-2 and Figure 8-3.

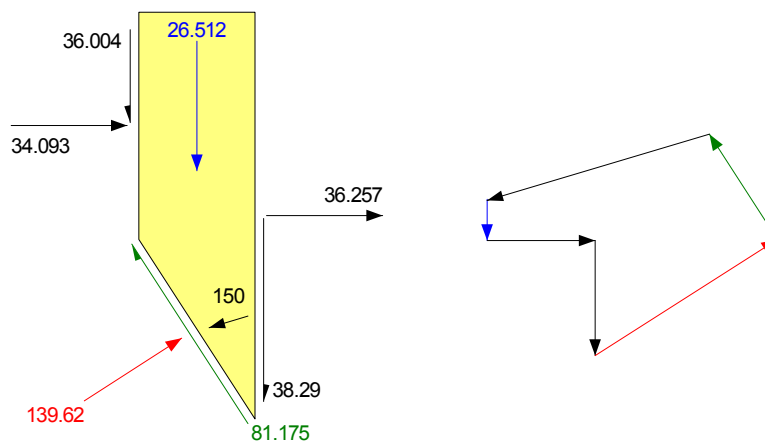


Figure 8-2 Free body and force polygon for upper anchor

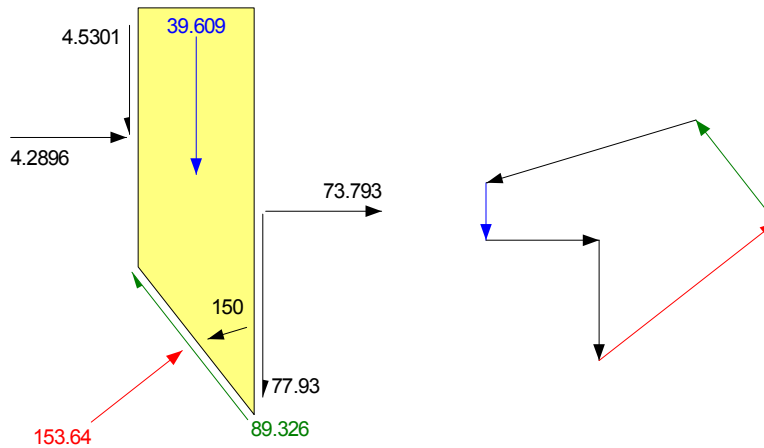


Figure 8-3 Free body and force polygon for lower anchor

The first point to note is that the interslice normals point away from the slice on the right side. This indicates tension between the slides, which is obviously not the case in the field. Plotting the interslice forces as in Figure 8-4 further highlights this difficulty. At each of the anchor locations, the interslice normals become negative and the interslice shear forces reverse direction. Of significance, however, is the fact that the force polygons close, signifying that the slices are in equilibrium. The forces may not be realistic, but they are the forces that provide force equilibrium for the slices, which is the fundamental objective of the method.

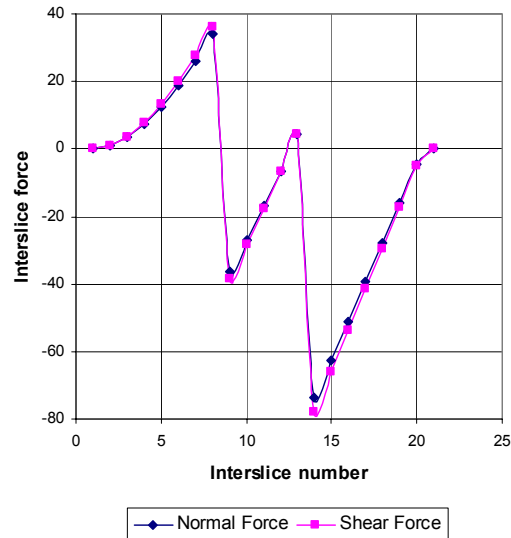


Figure 8-4 Interslice shear and normal forces with anchor loads applied at the slip surface

Now we will model the effect of the anchors by applying equivalent line loads on the wall face. The line loads are now included in the equilibrium of the slice on the right side. The interslice forces are now completely different. Figure 8-5 again shows the interslice shear and normal forces. The normal force increases evenly and gradually except for the last two slices. Of interest is the interslice shear force. The direction is now the reverse of that which usually occurs when only the self weight of the slices is included (simple gravity loading). The shear stress reversal is a reflection of a negative λ .

The large differences in the interslice forces also lead to significantly different normal stress distributions along the slip surface, as shown in Figure 8-6. It is noted in the Theory chapter that the equation for the normal at the base of the slices includes terms for the interslice shear forces. This example vividly illustrates this effect.

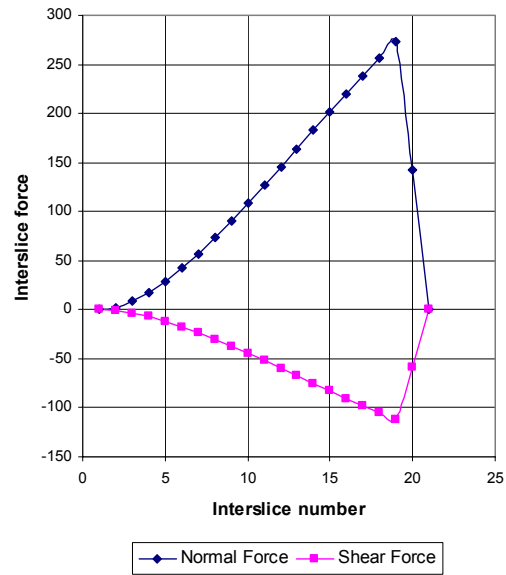


Figure 8-5 Interslice shear and normal forces with anchor loads applied at the face of wall

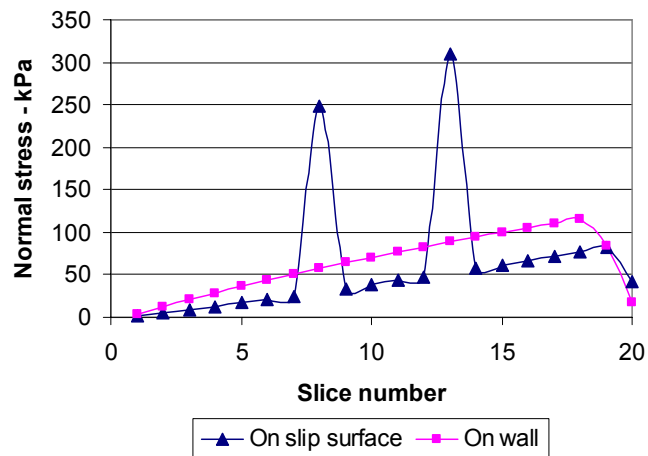


Figure 8-6 Comparison of normal stress distributions

Interestingly, in spite of the vastly different stresses between the slices and along the slip surface, the factors of safety are nearly identical for these two treatments of the concentrated line loads. With the anchors applied at the slip surface location, the factor of safety is 1.075 while when they are applied at the wall, the factor of safety is 1.076. For all practical purposes they are the same. The following table highlights this important and significant result.

Anchor Force Location	Factor of Safety
On slip surface	1.075
On the wall	1.076

The question arises, why do such vastly different stress distributions end up with essentially the same factor of safety? The answer is discussed in detail in the Limit Equilibrium Fundamentals chapter. In summary, there are two main characteristics that lead to this situation which are:

- The forces on each slice are the forces that ensure force equilibrium of each slice.
- They may not be realistic forces, but they do provide for force equilibrium.

The forces on each slice are such that the factor of safety is the same for each slice. Again, this does not represent reality, but it is a symptom of the formulation. The redeeming characteristic of the formulation is that the potential sliding mass (the free body as a whole) is in force and moment equilibrium. The internal stresses may not represent reality, but the sliding mass as a whole is nonetheless in equilibrium. It is for this reason that the method is useful, in spite of its idiosyncrasies.

Convergence

Applying lateral concentrated loads can create considerable convergence difficulties. Reinforcement is required due to the steepness of the slope or wall. This means that portions of the critical slip surface are fairly steep. A steep slip surface, together with the lateral concentrated loads, often makes it difficult to obtain a converged solution.

Not being able to compute a factor of safety is bad enough, but the minimum factor of safety is often located immediately next to the area where non-convergence becomes a problem. Sometimes the minimum factor of safety is among non-

converged slip surfaces. The critical slip surface is often in the proximity of the active wedge line inclined at $45 + \phi/2$, which is also the inclination at which the convergence difficulties frequently start. The difficulty is that the critical factor of safety can be somewhat suspect when its neighbors represent a non-converged case.

A typical situation is portrayed in Figure 8-7. In this example a converged solution could not be obtained for most of the grid rotation centers in the lower right hand triangular area. The grid rotation centers without a factor of safety beside them are the ones where it was not possible to get a converged solution. These non-converged grid centers mostly represent steep slip surfaces. The critical grid rotation centre is represented by the point with the larger dot, and is surrounded by points for which it was not possible to obtain a converged solution.

Furthermore, convergence is a problematic issue when very large lateral concentrated loads are applied; loads that are larger than what would reasonably be mobilized in reality. Convergence becomes particularly troublesome when large lateral line loads are applied near to top of a slope. Care and thought is consequently required when specifying these types of loads. Blindly specifying these lateral loads can lead to unreasonable results.

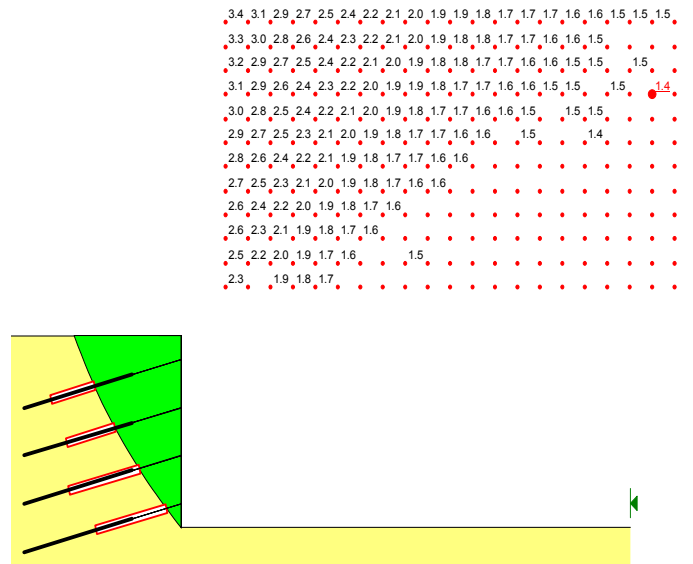


Figure 8-7 Rotation grid with convergence problems in lower right corner

Safety factors of the various components

With the “F of S Dependent” No option, SLOPE/W can only provide the factor of safety against sliding of the potential sliding mass. SLOPE/W cannot directly account for a margin of safety with respect to the reinforcement material or with respect to the bond resistance between the soil and the material. Safety factors associated with these aspects have to be considered separately. It is vitally important to recognize these safety factors are not directly involved in the SLOPE/W factor of safety calculation. This will become clearer as we discuss the details of the various types of reinforcement.

With the “F of S Dependent” Yes option, the SLOPE/W computed factor of safety is used to determine the mobilized reinforcement force. As explained earlier, the computed factor of safety is applied to the reinforcement force as well as to the soil strength.

Recommended analysis approach

In consideration of the limit equilibrium responses when lateral concentrated loads are included, it is often useful to apply some reverse logic. The first step should be to find the force required from the reinforcement that will provide an adequate factor of safety against sliding of the retained soil wedge. Then, once the required reinforcement force is known, the appropriate reinforcement can be selected and sufficient embedment can be computed. This is somewhat opposite of the usual design procedure. The usual procedure is to select the possible materials and create a possible design, and then check the stability. The downside of this approach is that the material strength may be too high, for example, and if the applied lateral concentrated loads are unnecessarily too high, it may not be possible to obtain a converged solution or it may lead to the wrong position of the critical slip surface. To obtain the best SLOPE/W solution, the applied lateral concentrated loads should not be greater than the required mobilized force. The specified reinforcement loads should not necessarily be the capacity of the reinforcement; it should be the portion of the capacity that will be mobilized or needs to be mobilized. You will note that this approach is reflected in the details discussed below on how to use and interpret the results associated with the various types of reinforcement.

Summary

When analyzing problems with reinforcement, it is useful to remember and consider the following:

- Lateral concentrated loads can lead to unrealistic internal stress distribution.
- The overall potential sliding mass can be in equilibrium in spite of poor internal stress distributions.
- The applied lateral loads representing reinforcement should be no greater than the associated expected mobilized force to mitigate convergence problems; it should not necessarily be the reinforcement capacity.
- With the “F of S Dependent” No option, SLOPE/W can only provide the factor of safety with respect to the sliding stability of the retained soil wedge; SLOPE/W does not directly account for safety factors associated with the reinforcement material or the bond between the material and the soil.
- With the “F of S Dependent” Yes option, the SLOPE/W computed factor of safety is applied to the reinforcement forces in the same way as to the soil strength. The mobilized reinforcement forces are the specified forces divided by the factor of safety.
- The best analysis approach often is to first find the forces required from the reinforcement and then detail and dimension the reinforcement, as opposed to detailing and dimensioning the reinforcement and then checking the stability.

8.3 Anchors

An anchor in SLOPE/W is reinforcement that consists of a bar that has a free length and a bonded length, as illustrated in Figure 8-8.

The capacity of the anchor is controlled either by the strength of the bar itself or by the shear resistance between the bonding grout and the soil. The bond pullout skin friction is dependent on the ground conditions and the installation procedure and is therefore a site-specific parameter.

All SLOPE/W analyses are per unit width perpendicular to the section. The reinforcing therefore also has to be resolved into a per unit width force.

Anchors are by default assumed to be tensioned or very rigid relative to the soil, and the load is assumed to be active immediately. This is represented by the “F of

S Dependent” No option. The “F of S Dependent” Yes option can, however, be applied to anchors just like any other reinforcement if this is considered appropriate.

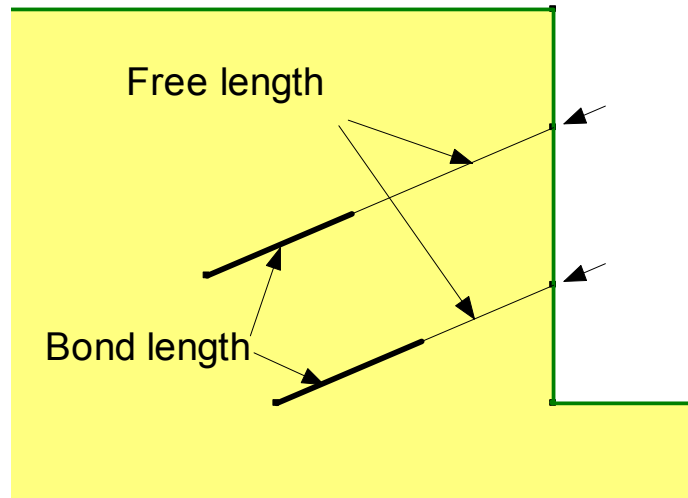


Figure 8-8 Definition of bond and free length

Bar capacity and reinforcement load

SLOPE/W allows you to specify the ultimate breaking capacity of the bar together with a bar safety factor and an anchor spacing. The maximum reinforcement load for a tensioned anchor is computed as:

$$\text{Maximum Reinforcement Load} = \text{Bar Capacity} \div \text{Bar Safety Factor} \div \text{Spacing}$$

Bond resistance

The Bond Resistance is the design pullout resistance per unit length of the bonded zone. The Bond Resistance is a computed value based on the borehole diameter, the unit bond skin friction, a specified bond safety factor and the anchor spacing. In equation form:

$$\text{Bond Resistance} = \text{Unit bond Skin friction} \times \pi \times \text{Bond Diameter}$$

The Bond Resistance is in units of force per unit length (F/L) of bond. The maximum pullout resistance available is the Bond Resistance times the total bonded length. In equation form:

Maximum Pullout Resistance = Bond Resistance \div Bond Safety Factor \div Spacing

Applied load

In SLOPE/W, the applied load is defined as the load that must be mobilized to achieve an acceptable factor of safety against potential failure of the retained soil wedge. The applied load for an anchor can be specified in one of two ways. The anchor behavior can be either “Constant” or “Variable”.

Constant applied load

When the applied load is flagged as “constant”, the same load is applied regardless of the position of the slip surface. The purpose of this option is to provide a means of finding the required working load without giving consideration to the bond resistance or the bar capacity. After the required working loads are known, the bond resistance and bar capacity can be checked to verify that they are adequate to supply the required working load.

Figure 8-9 shows a simple case where the applied load was specified as a “constant” 200 kN. The bond skin friction is 106 kN/m², the borehole diameter is 150 mm (0.15 m), the bond safety factor is 1.0 and the anchor spacing is 1.0 m. The Bond Resistance then is 50 kN/m. In this case it was determined that each anchor has to supply 200 kN per meter of wall to achieve an acceptable factor of safety of 1.3 against possible sliding of the retained soil wedge.

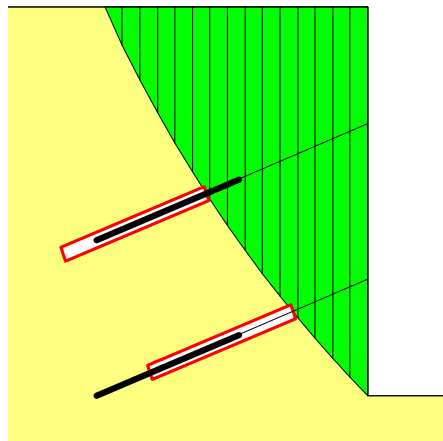


Figure 8-9 Stability results with constant option

Note the (red) box drawn around and along the anchors. These boxes indicate the length of the required bond to supply the required 200 kN. In this example, the required bond length is 4m (200 kN / 50 kN/m). For the upper anchor, the available bond behind the slip surface is inadequate (that is, it is too short). The implication is that the upper anchor would need to be longer to supply the required 200 kN. The lower anchor is long enough to supply the required 200 kN, since the actual bond zone extends past the required bond represented by the box. The implication for the lower anchor is that it could perhaps be shortened for this potential mode of failure.

The upper anchor intersects the base of Slice 6. Figure 8-10 shows the free body diagram and force polygon for this slice. Note the concentrated line load of 200 on the base, which represents the force provided by the anchor.

Slice 6 - Morgenstern-Price Method

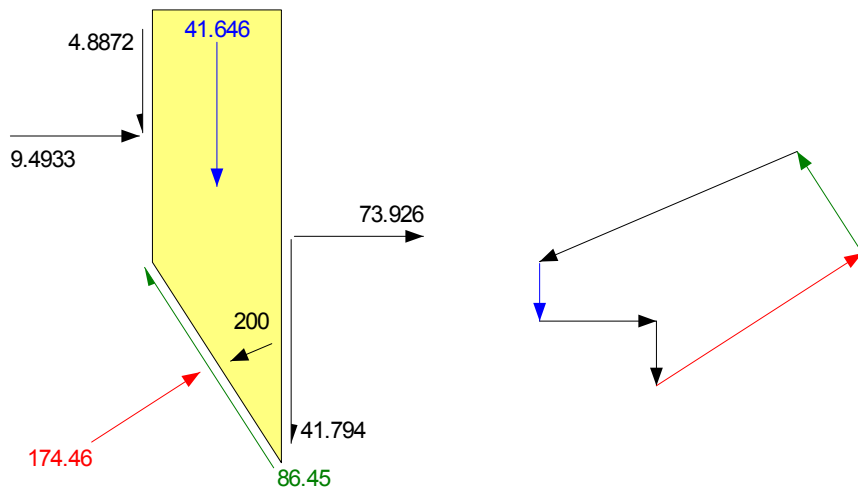


Figure 8-10 Slice free body with constant option

With the “constant” option, SLOPE/W does not use the maximum bond resistance available or the maximum reinforcement load available in the factor of safety calculations. These values are only used for comparative purposes in the presentation of the results, to check that the bond and bar are adequate to supply

the required working load. The only parameter that affects the specified constant working load is the anchor spacing.

Variable working load

When the “variable” option is selected, the working load may vary. The working load could be as low as zero if the slip surface is behind the anchor. The working load can be as high as the maximum available bond resistance or the maximum reinforcement load. The lower of these two governs the maximum available working load.

Figure 8-11 shows the results for when the working loads are flagged as variable. Now the working load for the upper anchor is limited by the bond available behind the slip surface. The available bond is only 2.8 m and the available working load is consequently only about 139 kN, as shown on the slice free body in Figure 8-12. The lower anchor uses the maximum bond resistance of 200 kN available, since the slip surface is in front of the specified bond zone. The maximum reinforcement load is sufficiently high that it does not enter into the calculations.

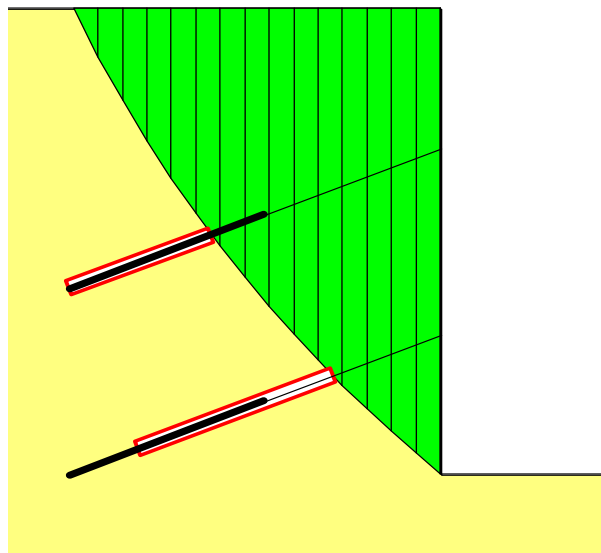


Figure 8-11 Stability results with variable option

Slice 6 - Morgenstern-Price Method

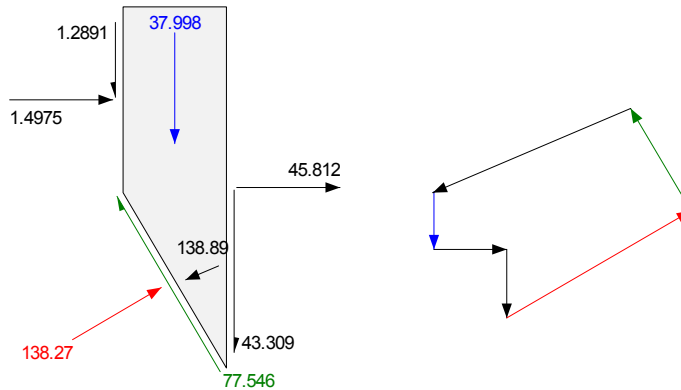


Figure 8-12 Slice free body with variable working load

With the reduced working load available from the upper anchor, the factor of safety is only 1.19. The upper anchor consequently needs to be lengthened to bring the factor of safety back up to 1.3, all else being equal.

Figure 8-13 shows the results when the upper anchor is lengthened slightly. Now the factor of safety is back up to 1.3, since the upper and lower anchors can both provide the required 200 kN to achieve the desired margin of safety.

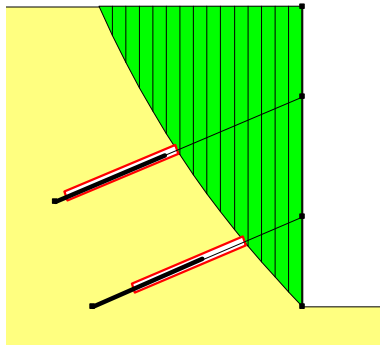


Figure 8-13 Results with variable option for modified design

The best solution is when the factor of safety is essentially the same for the “constant” and “variable” options. The constant approach is useful at the start of an analysis to determine what is required from the reinforcement. The variable option is useful for checking the final design and ensuring that the required reinforcement loading is also available with this alternative approach.

Shear force

SLOPE/W can also accommodate an anchor shear force. The shear force can act perpendicular to the anchor or parallel to the anchor. The direction and magnitude are shown on the slice free body as illustrated in Figure 8-14. In this illustrative case, the shear force is perpendicular to the anchor.

As with all the concentrated loads, the shear force used by SLOPE/W is the shear force per unit width of wall.

Slice 11 - Morgenstern-Price Method

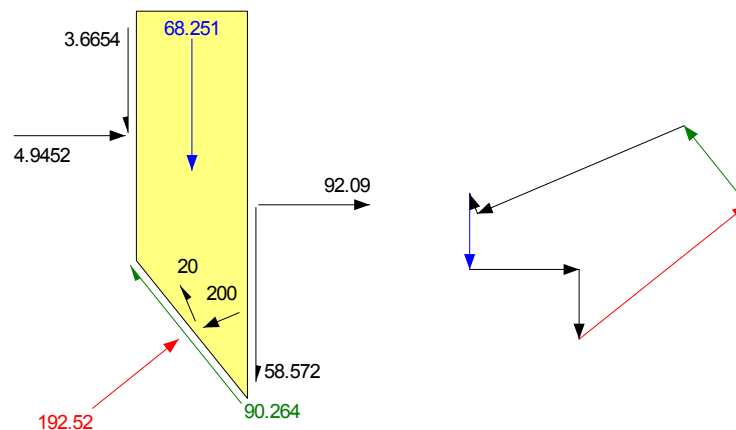


Figure 8-14 Slice free body with a shear force

8.4 Nails

Nails in SLOPE/W behave similar to anchors, except that the bond length is equal to the nail length, the working load is always variable and the nails by default are

considered as being active immediately; that is, the “F of S Dependent” option is No. The specified parameters for nails are:

- Borehole diameter or effective diameter for driven nails
- Bond safety factor
- Bond unit skin friction
- Nail spacing horizontally along the wall
- Bar (reinforcement) ultimate capacity
- Bar (reinforcement) safety factor
- Shear capacity
- Shear safety factor
- Direction of shear – parallel to slip surface base or perpendicular to reinforcement.

Identical to an anchor, the Bond Resistance, the Maximum Pullout Resistance and the Maximum Reinforcement Load are computed as follows:

Bond Resistance = Unit bond Skin friction $\times \pi \times$ Bond Diameter

Maximum Pullout Resistance = Bond Resistance \div Bond Safety Factor \div Spacing

Maximum Reinforcement Load = Bar Capacity \div Bar Safety Factor \div Spacing

Again, the lower of the Maximum Pullout Resistance and the Maximum Reinforcement Load governs the maximum applied load used in the factor of safety calculation.

Figure 8-15 shows a case with four rows of nails. The nails are each 7m long and spaced 2 m horizontally along the wall.

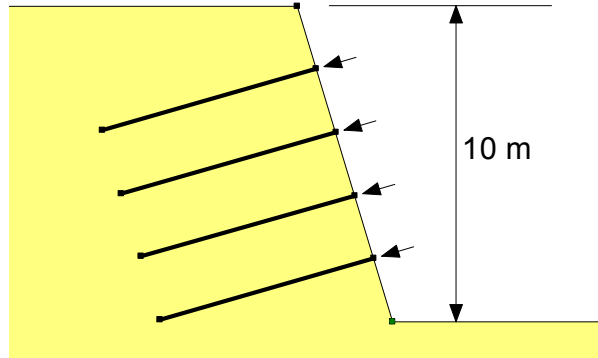


Figure 8-15 Example of retained wall with four rows of nails

The characteristics of the nails were specified such that the maximum allowable working loads are 50 kN due to the capacity of the structural nails.

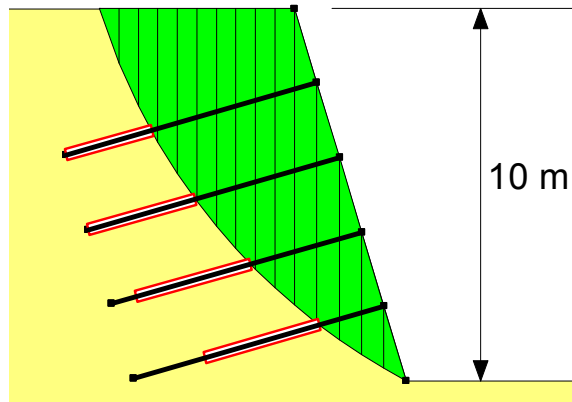


Figure 8-16 Result of nailed wall stability analysis

In this case, the bond governs the resisting force available from the upper two nails. The upper two nails provide loads of 37.4 and 46.7 kN for the critical slip surface. The (red) box encompassing the nail behind the slip surface is equal to the bond length available, indicating that the bond is governing the force available.

The lower two nails each provided 50 kN, the limit of the structural design capacity. The available bond behind the critical slip surface is greater than the design capacity of the bars. The box around the lower two nails is shorter than the bond resistance available, indicating that the structural capacity of the lower two nails is governing the maximum load allowable.

Shear loads can be specified for nails in the same way as for anchors. The specified shear can act perpendicular to the nails or parallel to the slice base.

8.5 *Geo-fabric reinforcement*

With geo-fabric reinforcement, as with nails, the bond length is by default assumed to be equal to the fabric length as illustrated in Figure 8-17. The width of the fabric (distance into the section) is always at unit width (1 m or 1 ft).

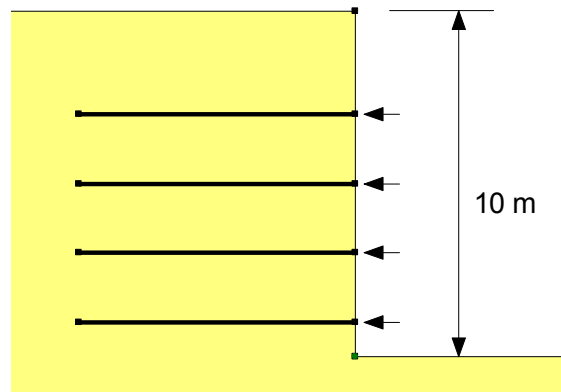


Figure 8-17 Wall reinforced with fabric

The specified parameters for fabrics are:

- Bond skin friction per unit area ($F/L2$)
- Bond safety factor
- Fabric ultimate capacity
- Fabric safety factor
- Load orientation

Bond resistance a specified constant

The bond skin friction is a specified value per unit area. It is a value that includes all effects that contribute to the skin friction, whatever they are. This may include friction on both sides of the fabric or just one side. Whatever the case, the specified value is all-inclusive.

For this example, it is assumed that the fabric is very ductile and that the resistance offered by the fabric will develop with strain at the same rate as is the soil. The fabric is considered as being effective in increasing the shearing resistance, and the SLOPE/W computed factor of safety will consequently be used in establishing the forces available from the reinforcement. The “F of S Dependent” option is set to “Yes” for these nails.

Figure 8-18 presents the results when the maximum Reinforcement Load is 130 kN and the Bond Resistance is 30 kN/m. The computed factor of safety is 1.435. The available bond behind the critical slip surface controls the resisting force for the upper two layers of fabric. The capacity of the fabric itself controls the stabilizing force available from the lower two layers when much longer bond lengths are available behind the slip surface.

For the upper-most layer, the available bond length for this slip surface 1.85 m. The potential available resisting force therefore is 55.5 (1.85 x 30) kN. The actual applied force then is 55.5 divided by 1.435 (the computed factor of safety) which equals 38.7 kN.

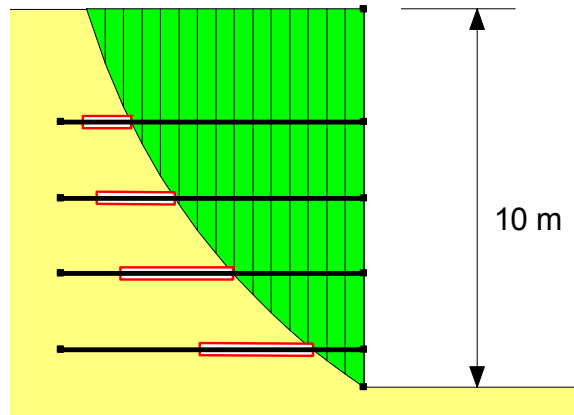


Figure 8-18 Results for fabric reinforcement

For the lowest fabric layer the fabric strength governs. The maximum specified allowable force is 130 kN. This value divided by the factor of safety of 1.435 equals 90.6 kN which is the SLOPE/W analysis. The required bond length is 90.6/30 which equals about 3 m. The available bond is 6.6 m.

Because the resisting force is divided by the factor of safety, the required bond is always less than the available bond if the factor of safety of the slope is greater than 1.0.

Bond resistance a function of overburden stress

The Skin Friction can be a function of the overburden stress, friction parameters, c and ϕ , and an interface factor. With this option, SLOPE/W computes the overburden stress from the slice that includes the reinforcement force; that is, the slice base that intersects the fabric. The Bond Resistance for each fabric then is:

Bond Resistance (F/L^2) = (c + overburden stress $\times \tan \phi$) \times interface factor

Consider the case where c is zero, ϕ is 10 degrees and the interface factor is 1.0. The results are then as shown in Figure 8-19. For the lower two layers, the fabric strength governs. Note that the required bond (size of box) diminishes with depth below the ground surface which reflects the higher Bond Resistance available with depth.

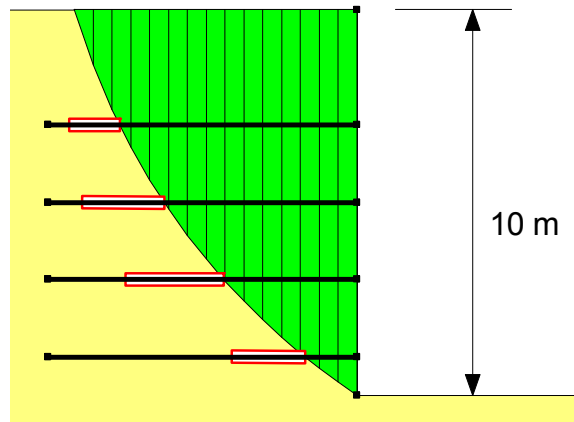


Figure 8-19 Bond resistance a function of overburden

The interface factor reflects how the skin friction is mobilized. Often this is related to whether there is friction on both sides of the fabric or just on one side or something in between. In an ideal situation, an interface factor of 1 means friction only on one side and an interface factor of 2 means friction on both sides. This depends on the nature of the fabric. A solid fabric is different than a mesh of some sort. This is a factor that is likely available from fabric suppliers.

Load orientation

There is belief among some analysts that the stabilizing resisting force from fabrics acts in a direction other than the axial direction. SLOPE/W allows for specifying the load orientation. A specified value of zero (0) means the load is applied in the axial direction parallel to the fabric, and a specified value of 1 means the direction is parallel to the slice base. Any other value between 0 and 1 can be specified. A value of 0.5 means the direction is halfway between the axial direction and slice base inclination. Figure 8-20 shows the slice free body and force polygon for the lowest layer of fabric. Note that the reinforcement force is parallel to the slice base (Load orientation = 1).

Slice 13 - Morgenstern-Price Method

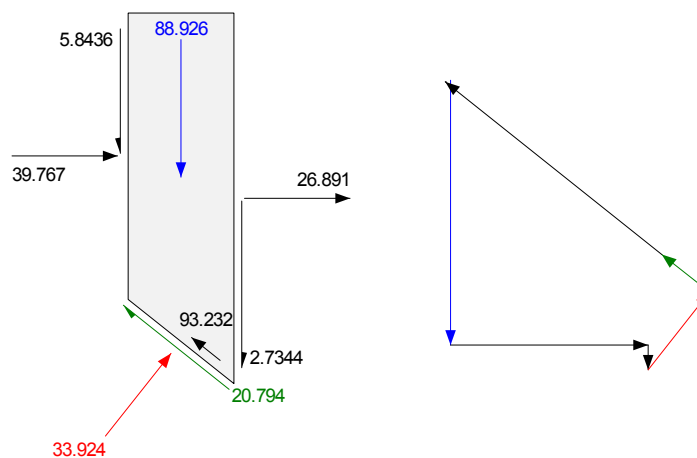


Figure 8-20 Fabric reinforcement force parallel to slice base

8.6 Wall facing

SLOPE/W does not take into account the slope or wall facing. It is assumed that there is some form of facing that prevents the soil from squeezing past the reinforcement. This could be shotcrete, pre-cast panels, wraparound fabric or other component, such that spalling or loss of ground does not occur from the face. In a limit equilibrium formulation, only the resisting forces acting on the potential

sliding mass come into play. Forces associated with the facing consequently do not come directly into the analysis.

This is an important concept, particularly for reinforcement near the wall toe where the critical slip surface is near the front of the reinforcement (close to the wall).

The facing itself can be considered in a finite element analysis, as discussed later in this chapter, but not in a limit equilibrium analysis.

8.7 *Piles and dowels*

A pile or a dowel in SLOPE/W is reinforcement that only provides shear resistance. An example is presented in Figure 8-21. The specified parameters for this type of reinforcement are:

- Dowel or pile spacing
- Shear force
- Shear force safety factor
- Direction of application - parallel to slip surface or perpendicular to reinforcement

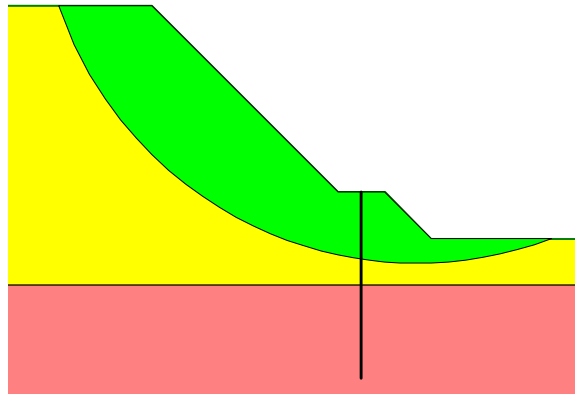
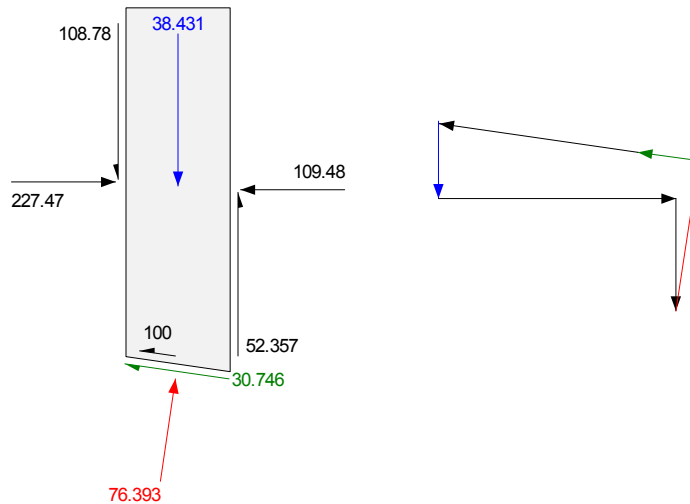


Figure 8-21 Slope reinforced with a pile or dowel

Figure 8-22 shows the slice free body and force polygon for the slice that includes the pile. In this case, the shear force was specified as being parallel to the slice base. The 100 kN force in Figure 8-22 confirms this.

Slice 19 - Spencer Method

**Figure 8-22 Shear force of pile on slice free body**

8.8 Sheet pile walls

The embedment of sheet piling below the base of an excavation offers lateral resistance to a potential toe failure, as illustrated in Figure 8-23. The question is how to represent this lateral resistance. The strength of the piling cannot be included directly in the geometric definition; that is, the piling cannot be represented by a material with a very high strength. Also, forces outside the free body representing the potential sliding mass cannot be included in the equations of statics – only forces acting on the free body can be included in the statics equations.

One way of including the embedment lateral resistance is with a concentrated line load that acts on the potential sliding mass. The concentrated line load arises either from the shear strength of the sheet piling or the passive toe resistance offered by the embedment. The magnitude of the passive toe resistance is:

$$P_p = \frac{\gamma H^2}{2} K_p$$

where:

K_p is the passive earth pressure coefficient.

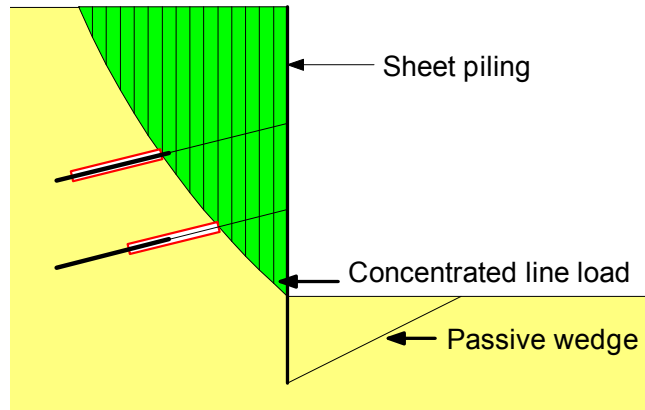


Figure 8-23 Embedded sheet pile

The passive earth pressure K_p coefficient is highly dependent on the friction between the sheet piling and the soil. K_p can vary from approximately 3 to 12, which makes it difficult to make an accurate prediction of the lateral passive resistance. Furthermore, significant displacements are generally required to mobilize the full passive resistance – at least more than what is tolerable for a retaining structure like this. Consequently, it is likely necessary to use a fairly conservative safety factor on the passive resistance – something around 3.0, particularly if there is a heavy reliance on the friction between the piling and the soil.

The impact of the embedment can be considered in a much more realistic way by doing a finite element soil structure interaction analysis and then using the resulting stresses in the stability assessment as discussed in detail below in this chapter. Unfortunately, in a limit equilibrium analysis, the soil interaction component has to be represented by a concentrated line load, even though intuitively it is not a totally satisfactory procedure.

8.9 Deep-seated instability

Deep-seated stability is usually not the most critical potential mode of failure, but it is an issue that needs to be addressed, particularly before the decision is made to shorten the lower reinforcement. Often the lower level reinforcement appears too long for a toe failure, but the deep-seated potential failure needs to be checked as part of the decision to dimension the lower level reinforcement.

Figure 8-24 illustrates a deep-seated analysis. The slip surface passes behind the anchors and underneath the base tip of the sheet piling. All the structural components consequently do not come into the SLOPE/W stability analysis. The structural components simply go along for the ride, so to speak.

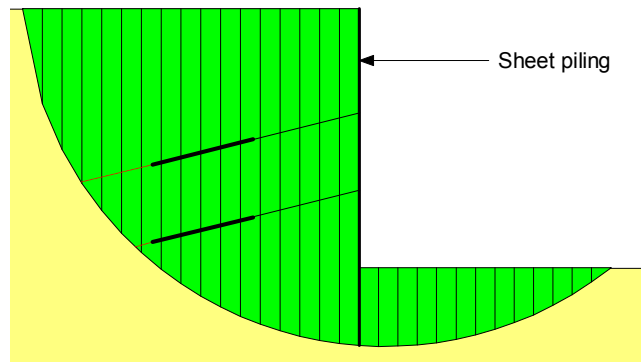


Figure 8-24 Deep seated failure

8.10 Mitigation of numerical problems

Several times in the above discussion, it has been noted that lateral concentrated loads representing reinforcement can cause difficulty with convergence and finding the position of the critical slip surface. A procedure that can be used to mitigate the numerical difficulties is to work with reinforcement forces that give a factor of safety around unity. In other words, what are the forces that represent the point of limiting equilibrium? This tends to give the best numerical behavior. Later when the response of the analysis is better understood, the reinforcement loads can be increased to be more representative of actual conditions.

A point to remember is that the numerical behavior tends to deteriorate as the lateral forces increase relative to the gravitational mobilized shear. Care is also required to make sure that the lateral forces are not so high as to pull (push) the

potential sliding mass uphill. This is another reason to start the analysis with low lateral forces and then increase the magnitude in small stages.

High lateral loads are particularly troublesome when they are applied near the top of a wall. So another trick that can be used to reduce numerical problems is to specify the higher loads near the bottom of the wall and the lighter loads closer to the top of the wall. The total specified for all the reinforcement may be a constant, but the specific forces for each reinforcement can be redistributed sometimes to help out with numerical problems, at least until the wall response is fairly clear.

The convergence tolerance in SLOPE/W can also sometimes be relaxed to obtain more converged solutions. Also, sometimes more converged solutions are available when only moment or only force equilibrium is satisfied, as in the Bishop Simplified and Janbu Simplified methods. Using these simpler methods can sometimes help increase one's confidence as to the position of the critical slip surface.

The concentrated line loads representing reinforcement should always be verified and checked using the View Slice Information tool in SLOPE/W CONTOUR.

The slice free body diagrams and force polygons have been used extensively in the above discussion to illustrate the magnitude and behavior of the concentrated loads. We highly recommend that you use the View Slice Information tool extensively when reinforcement is included in an analysis. It is vitally important to always check the exact concentrated loads used by SLOPE/W to make sure that the applied concentrated loads match your expectations and understanding. The importance of this cannot be overemphasized.

8.11 Finite element stress-based approach

An alternate approach to analyzing the stability of reinforced structures is to use the stresses from a finite element analysis. The interaction between the reinforcement and the soil alters the stress state such that the resulting shear resistance is greater than the mobilized shear force.

Wall with nails

Figure 8-25 shows a vertical wall reinforced with four rows of nails. The nails are modeled as structural elements in SIGMA/W.

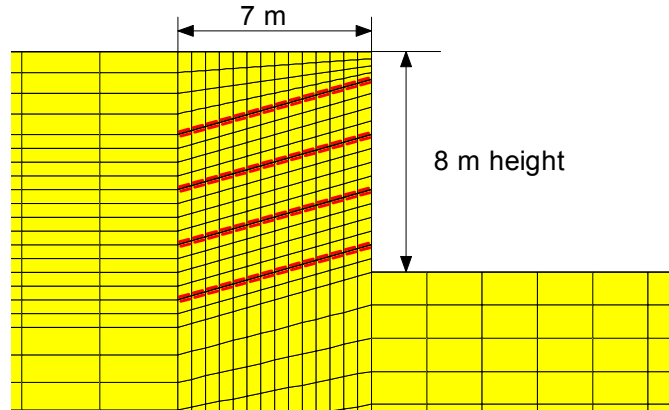


Figure 8-25 A vertical wall retained with nails

One of the possible procedures for computing the stresses in the ground is to do a gravity “turn-on” analysis. Basically, this means that we have constructed the structure and then we turn on gravity to check the performance of the structure. In reality, this is of course not possible, but this is possible with numerical models. The thinking here is that the modeling does not exactly follow the construction procedure, but after the construction is complete the stresses will adjust themselves to something close to that obtained from a gravity turn-on analysis.

The structural elements representing the nails can have both flexural (bending) stiffness and axial stiffness. Any shear in the nails is consequently included in the stress analysis. The flexural stiffness is related to the specified moment of inertia, and the axial stiffness is related to the E , (Young’s Modulus) and the effective cross sectional area.

The SIGMA/W computed stresses can be used in SLOPE/W to compute a safety factor. The safety factors are computed as explained in the Theory Chapter.

The SLOPE/W results are presented in Figure 8-26. There are several significant features in the results. The first is that there is no issue with convergence in a limit equilibrium analysis as discussed earlier in this chapter. A safety factor can be obtained for all trial slip surfaces regardless of how steep the trial slip surfaces become. This confirms that there is a legitimate minimum. The lowest safety factor is nicely encompassed within safety factor contours. Visual inspection of the diagram in Figure 8-26 shows that the position of the critical slip surface is close to the active wedge angle (i.e., $45^\circ + \phi/2$).

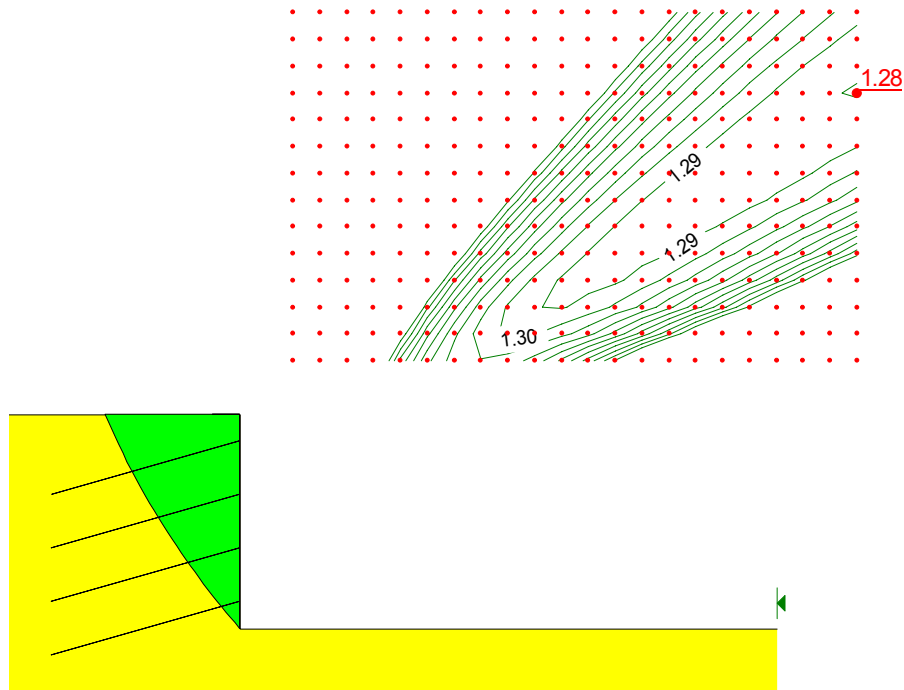


Figure 8-26 SLOPE/W stability analysis results based on SIGMA/W stresses

The nails are not included in the SLOPE/W analysis as concentrated line loads. The effect of the nails is in the SIGMA/W stress distribution and it is the SIGMA/W stresses that give an indication of the safety factor.

Another significant observation is that there are many trial slip surfaces with very similar safety factors. Note all the trial slip surface centres encompassed by the 1.29 safety factor contour. This indicates that there is not one critical slip surface, but a potential failure zone where the safety factors are all very similar.

The integrated approach has the attraction that we can actually look at the stress distributions in the nails. In a limit equilibrium analysis we can only deal with concentrated line loads with the assumption that the nail can somehow provide the load. In a stress analysis we can actually examine the axial, moment and shear distributions in the nails. Figure 8-27 and Figure 8-28 show the axial, moment and shear distributions in the nail third from the top.

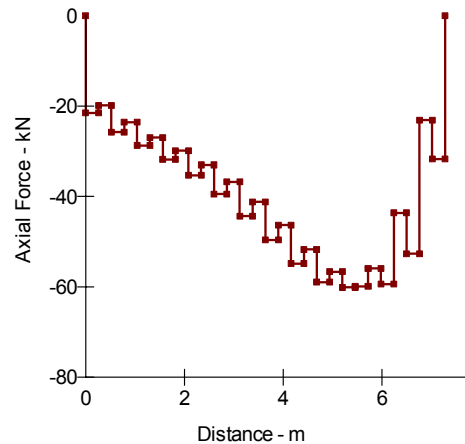


Figure 8-27 Axial force in nail

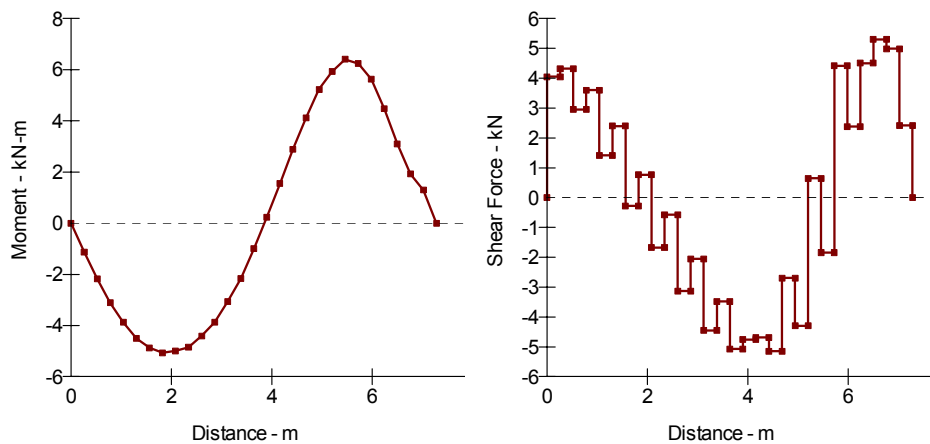


Figure 8-28 Moment and shear distribution in the nail

The acting nail stresses can be compared with the structural capacity of the nails to ensure that they do not exceed safe limits. This assessment needs to be done independently of the SIGMA/W and SLOPE/W analyses.

Examination of the SIGMA/W stresses shows that there is no horizontal tension in the reinforced zone as indicated by a limit equilibrium analysis. Earlier in this chapter it was pointed out that in a limit equilibrium analysis with lateral concentrated loads, tension is required between slices in order to achieve slice

force equilibrium. In reality that is not the case, as we can see in Figure 8-29 which shows the horizontal stress along the slip surface. There is a small amount of tension near the ground surface, but this is as one would expect.

The more realistic stress distribution is possible because the local safety factor is now not limited to be a constant value across the slip surface, as it is in a limit equilibrium analysis. The local safety factor now varies as illustrated in Figure 8-30. Locally the factor of safety varies a lot, but globally the overall the factor of safety is 1.28.

Near the toe there two slices that have a safety factor less than 1.0. This is the result of a linear-elastic analysis, which does not re-distribute stresses in overstressed zones. For stability analyses, the consequence of small overstressed zones is discussed in detail in the Limit Equilibrium Fundamentals Chapter.

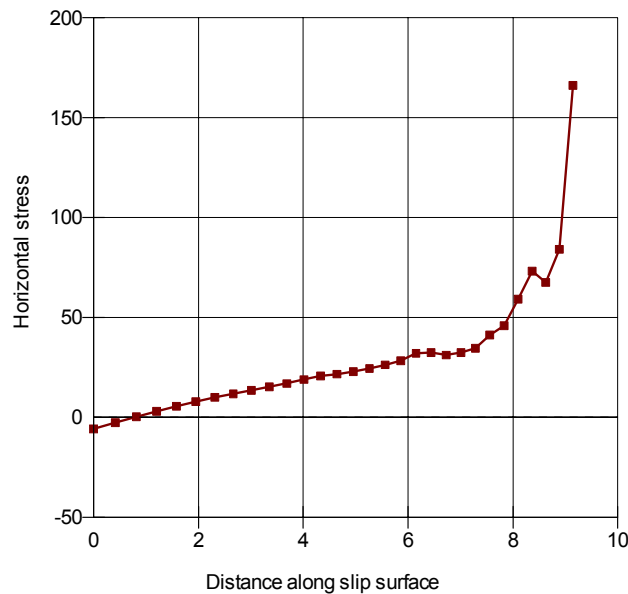


Figure 8-29 Horizontal stress along slip surface

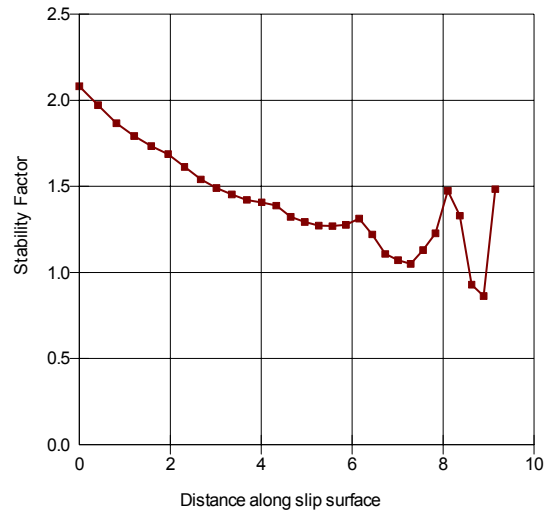


Figure 8-30 Local safety factors along the slip surface

Wall facing has been ignored in the SIGMA/W analysis the same as in a LE analysis. In reality, some form of structural facing is clearly required to prevent spalling and squeezing of the soil past the nails. Structural elements representing the facing could be included in a SIGMA/W analysis, but such added detail is not always necessary for a global stability analysis.

Tie-back wall

Figure 8-31 shows the case of a tie-back retaining structure. The wall is sheet piling and the anchors are pre-stressed at the time of installation. The wall was created in five steps by first excavating to a level below the top anchor. The top anchor was then installed and pre-stressed. Next, the excavation proceeded to a level below the lower anchor, and then the lower anchor was installed and pre-stressed. Finally, the last of the excavation material was removed.

This example is different than the wall with nails discussed above in that the insitu stresses were first established and then the excavation process was simulated by removing elements from the SIGMA/W analysis. The details of this case are included with SIGMA/W as one of the examples.



Figure 8-31 A sheet pile wall with pre-stressed tie-back anchors

When using the stresses computed at the end of construction in a stability analysis, the results are as in Figure 8-32. As with the nailed wall discussed earlier, there is no difficulty with convergence and consequently a true minimum safety factor exists within the grid. The minimum value is nicely encompassed by the 1.5 contour. Also, again there are many trial slip surfaces that have very similar safety factors. Figure 8-33 shows the 20 most critical slip surfaces, and they all fall within a relatively narrow band.

An interesting observation is the position of the critical slip surface. It is well behind the traditional active wedge line as shown graphically in Figure 8-34. The anchors have altered the stresses in the ground such that the critical slip surface is further back from the wall than one would expect from simple earth pressure considerations.

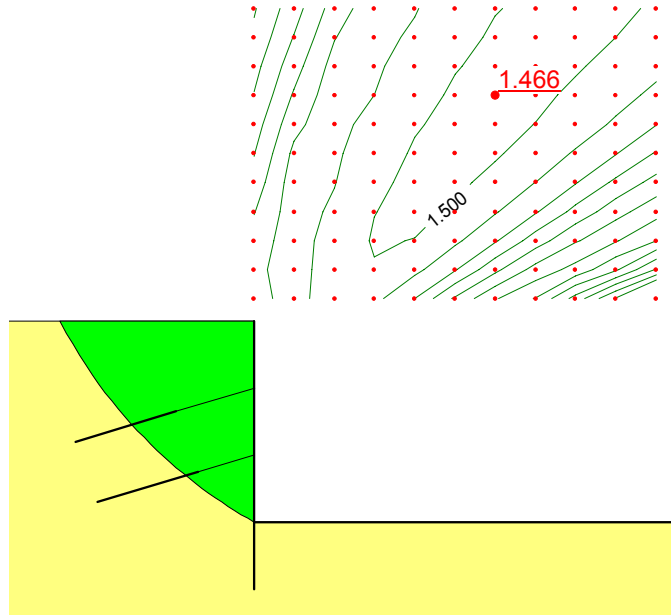


Figure 8-32 Stability analysis based on finite element stresses

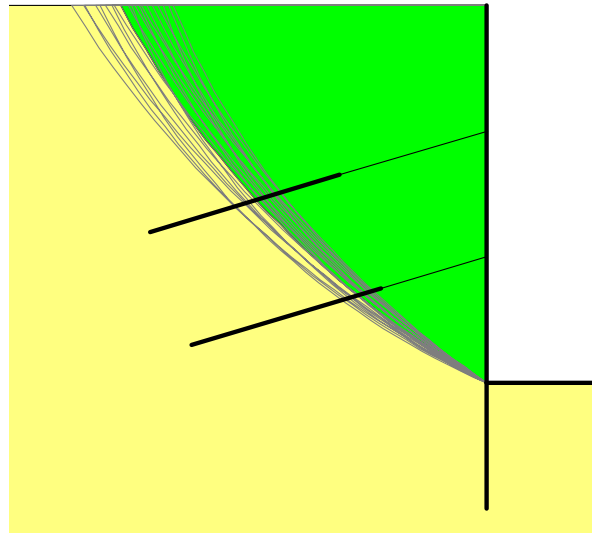


Figure 8-33 Twenty most critical slip surfaces

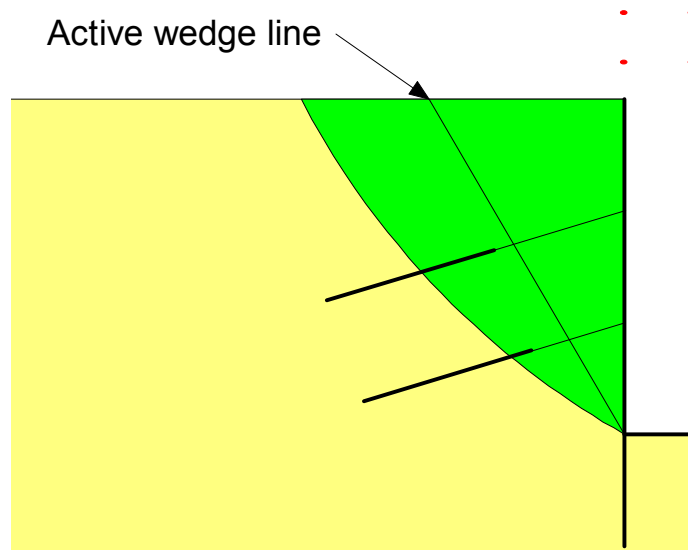


Figure 8-34 Position of critical slip surface relative to active wedge

Now we not only get the stresses in the anchors, but we can also get the stresses in the sheet piling. Figure 8-35 shows, for example, the moment distribution in the wall at the end of construction.

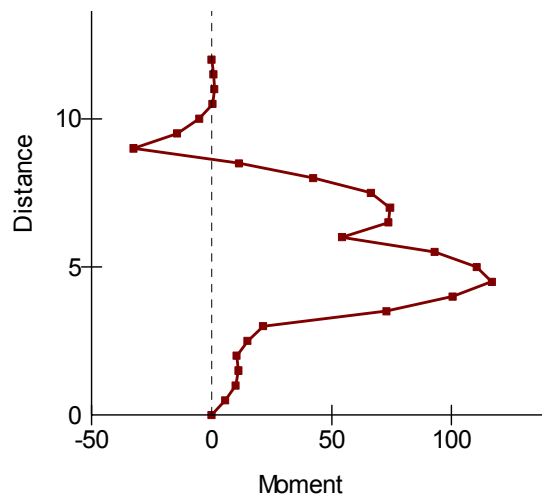


Figure 8-35 Moment distribution in sheet piling

Soil-structure interaction safety factors

Care is required when interpreting safety factors based on finite element computed stresses, particularly if structural components are included.

To start with, let us look at a simple active earth pressure situation (Figure 8-36). The lateral earth pressure is represented by a resultant P_a at the lower third-point on the wall.

The coefficient of active earth pressure is:

$$K_a = \tan^2(45 - \phi/2)$$

So when ϕ is 30 degrees, K_a is 0.33.

Assume that the wall height is 10m and the soil unit weight is 20 kN/m^3 . The theoretical lateral earth pressure resultant then is:

$$P_a = \frac{\gamma H^2}{2} K_a = \frac{20 \times 10^2}{2} \times 0.33 = 330$$

If a line P(a) of 330 kN is applied in SLOPE/W, the resulting factor of safety is very close to 1.0. A factor of safety of unity (1.0) therefore represents the active earth pressure case.

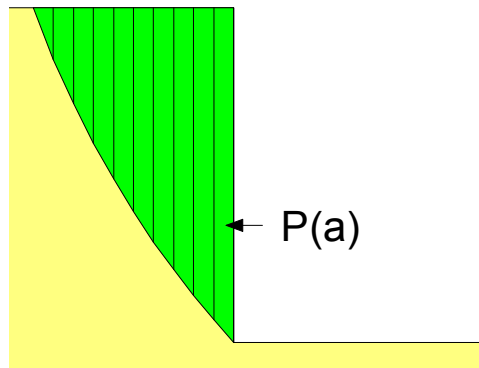


Figure 8-36 Active earth pressure calculation

In both the nailed wall and tie-back wall discussed above the safety factor is greater than 1.0. This means that the structural components are retaining forces that are greater than those represented by the active case. In the case of the tie-back

wall, the sheet piling together with the anchors is stiff enough and strong enough to retain equivalent forces that are greater than those represented by the active case.

The main point here is that the SLOPE/W factor of safety has to be viewed differently than in a conventional slope stability analysis. In the case of the tie-back wall, a factor of safety of 1.0 or less does not mean the structure will necessarily collapse. The structure will maintain its integrity provided the structural components are not overstressed and more resisting capacity can be mobilized from the structural components. In an extreme case like a strutted wall, the material behind the wall could conceptually be a weak fluid-like mass, but if the structural components are intact, the wall and the material would remain stable even though the SLOPE/W factor of safety would be near zero.

Assessing the stability of retaining structures such as those discussed here requires more than just looking at the SLOPE/W factor of safety. SLOPE/W only provides the margin of safety against the potential sliding of the soil wedge that is retained. The structural components need to be assessed separately to check that they are not overstressed.

Perhaps the objective is to design for pressures greater than the active case. Then the SLOPE/W factor of safety would need to be greater than 1.0. That would be a legitimate design objective. In the end, it is vitally important to fully comprehend the significance and meaning of the SLOPE/W factor of safety when the computations are based on finite element soil-structure interaction analyses.

Care is required in interpreting the SLOPE/W safety factors when finite element stresses from a soil-structure interaction analysis are used in the stability assessment.

Shear wall

SIGMA/W computed stresses can also be useful when assessing the effectiveness of a shear wall to improve the stability of a slope. Figure 8-37 shows a slope with a slip surface where the Safety Factor is 1.17. The objective is to attempt to improve the margin of safety by driving piles from the bench through the upper weaker material into the underlying more competent material.

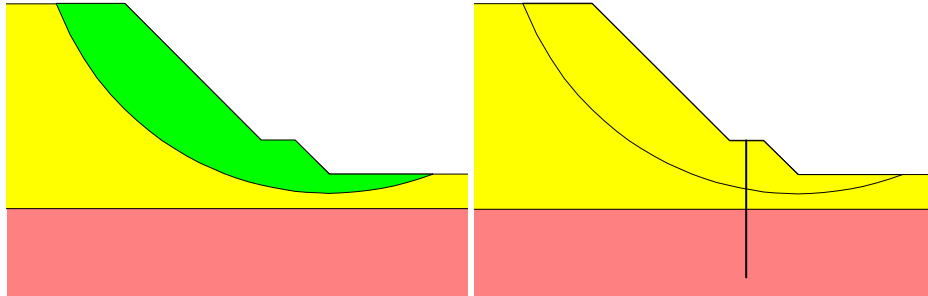


Figure 8-37 Finite element analysis with a shear wall

A SIGMA/W analysis can be done with and without the pile. The pile is modeled as a structural element. If the structural element is assigned a flexural (bending) stiffness, but no axial stiffness, then the stresses can be determined using a gravity “turn-on” approach. If the pile is assigned an axial stiffness, then the surrounding soil hangs-up on the pile when the gravity is turned on. This results in unreasonable stresses around the pile. A more realistic stress distribution can be obtained if the pile axial stiffness is ignored by making $E=0$ or a small number.

The bending stiffness (moment of inertia) alters the stress distribution and in turn improves the margin of safety. When the SIGMA/W stresses with the pile in place are used in SLOPE/W, the Safety Factor is 1.52, as demonstrated in Figure 8-38.

1.522

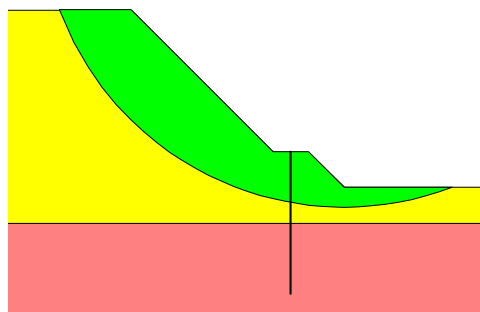


Figure 8-38 Factor of safety with the shear wall in place

Figure 8-39 shows the horizontal stress distributions along the slip surface without and with the pile in place. Note that with the pile in place (right diagram) the horizontal stress peaks at about 90 kPa and then suddenly drops to 40 kPa. In other words, up-slope of the pile, the horizontal stresses are higher and down-slope of the pile, the stresses are lower than when the pile is not present.

In a conventional limit equilibrium analysis, the effect of the pile has to be included as a specified shear value as discussed earlier in this chapter. The difficulty is in knowing the magnitude of the shear.

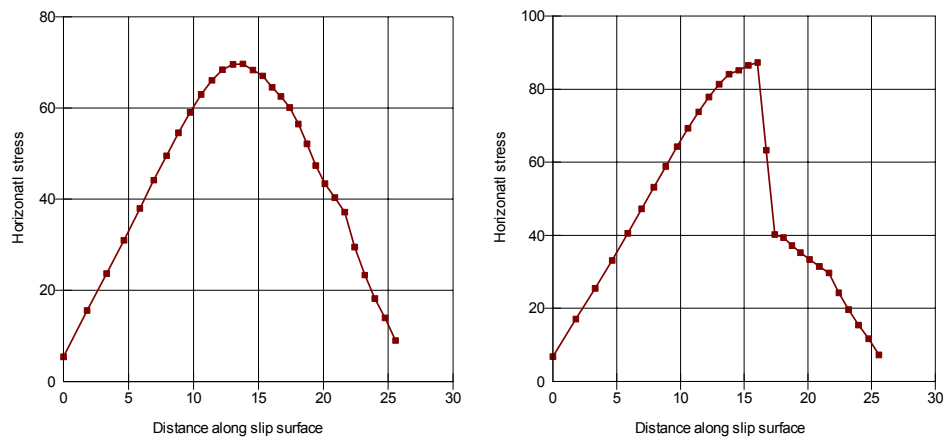


Figure 8-39 Horizontal stresses along slip surface without and with pile

As with any of these soil-structure interaction problems, the structural integrity has to be checked independently. SIGMA/W can provide the moment and shear distributions, as illustrated in Figure 8-40. These data can be used to check that the pile has not been overstressed.

As with the retaining structures discussed above, the factors of safety obtained from a shear-wall analysis need to be interpreted with considerable care. Once again, a factor of safety of less than unity does not necessarily mean the structure will collapse. If the structural components are not overstressed, then the structure may very well be stable even though the SLOPE/W factor of safety is less than 1.0. This is something that needs to be judged in the context of the project requirements and the site-specific design. The important point here is to highlight the need for careful evaluation of the meaning of the SLOPE/W computed factor of safety.

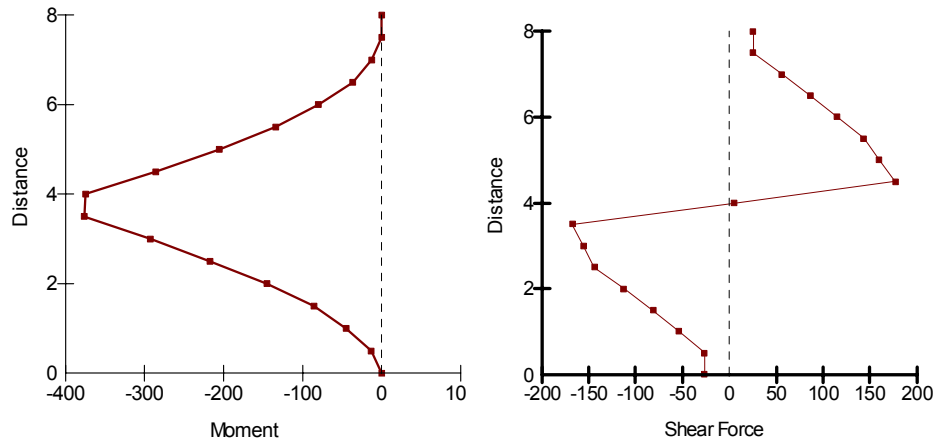


Figure 8-40 Moment and shear distribution in wall

A shear-wall concept can be effective if the structure is founded in competent underlying soil. The underlying soil needs to be able to resist the lateral thrust of the unstable upper soil and the pile needs to transfer this thrust to the competent soil. Without a competent underlying stratum, the shear wall concept is generally not very effective in improving stability.

Key issues

Assessing the stability of geotechnical structures using finite element computed stresses has many attractions and advantages over conventional limit equilibrium types of analyses. It overcomes many of the numerical difficulties associated with limit equilibrium formulations. Unfortunately, establishing the finite element stresses is not all that straightforward. The analyst needs to be intimately familiar with finite element stress-strain types of analyses. Correctly modeling the interaction between the soil and the structural components is a fairly advanced task and needs to be done with considerable care.

Remember, the stress-based approach for assessing the stability of retained structures is only as good as the computed finite element stresses.

Also, it is vitally important to recognize that the actual stresses in the field will be highly dependent on the construction details and procedures. Any stress-based stability analysis needs to be judged and evaluated in light of the actual installation.

Moreover, it is important to remember that using finite element computed stresses in a stability analysis is a fairly new technique. Software tools such as SIGMA/W and its integration with SLOPE/W now makes it possible to do these types of analyses, but the method has as yet not been used extensively in practice, at least not in routine practice as have limit equilibrium types of analyses. Until the industry has more experience with the stress-based approach, it is perhaps prudent to use both the older limit equilibrium methods and the newer stress-based approach to judge and assess the stability of retained earth structures.

9 Seismic and Dynamic Stability

9.1 *Introduction*

This chapter deals with seismic or dynamic forces and how they can be considered in a stability analysis. These types of forces are usually oscillatory, multi-directional, and act only for moments in time. In spite of this complex response, static forces are sometimes used to represent the effect of the dynamic loading. The second concern is that the slope may not completely collapse during the shaking, but there may be some unacceptable permanent deformation.

In SLOPE/W, dynamic effects can be considered in several ways. The simplest is a pseudostatic type of analysis. A more complex way is to use QUAKE/W finite element dynamic stresses and pore-water pressures together with SLOPE/W.

9.2 *Rapid loading strength*

Under certain conditions, it can be argued that the dynamic loading is so rapid that the soil strength behaves in an undrained manner. This may be the case for saturated clayey soils, for example, but not for unsaturated gravels or rock fill.

As discussed in the Limit Equilibrium Fundamentals chapter, a limit equilibrium formulation finds those forces acting on a slice so that the slice is in force equilibrium and so that the factor of safety is the same for every slice. If a dynamic force is applied to a slice, the slice forces will be re-adjusted, which will include a re-adjustment of the base shear strength. SLOPE/W has an option to keep the slice base shear strength unaltered even when the dynamic force is applied.

Consider the simple slope in Figure 9-1. For illustrative and explanation purposes here, only one slip surface is considered. The strength parameters are c equal to zero and ϕ equal to 30 degrees.

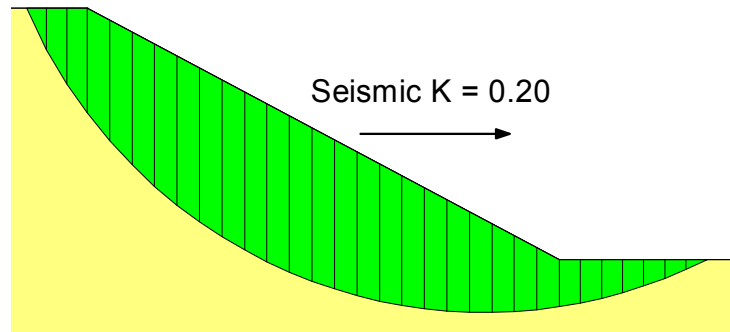


Figure 9-1 Illustrative example with seismic forces

Figure 9-2 compares the shear strength along the slip surface with and without any seismic forces. Applying the seismic forces alters the shear strength profile. This is primarily due to a change in normal stress distribution along the slip surface.

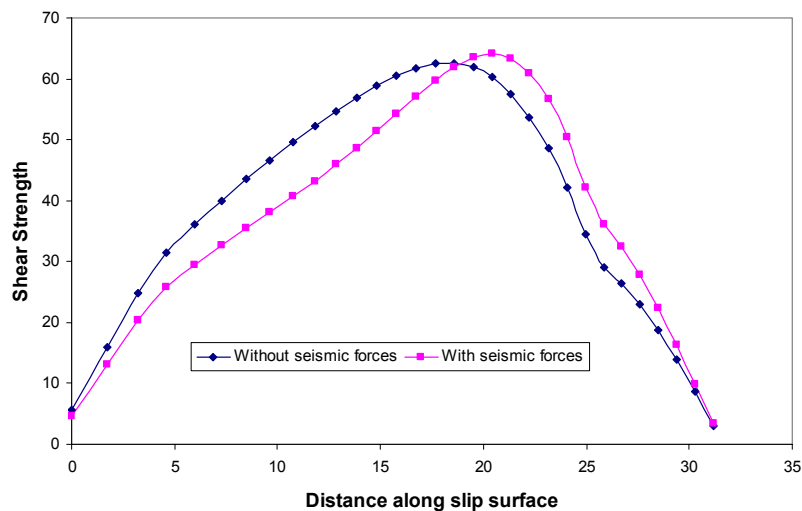


Figure 9-2 Effect of seismic forces on altering the shear strength

If the option to keep the shear strength unaltered due to seismic forces is selected, SLOPE/W first does an analysis without any seismic forces, to establish the strength along the slip surface. The shear strength at the base of each slice is then converted into an equivalent undrained (cohesive) strength. The analysis is then repeated with the seismic loading. The undrained shear strength is not a function of

the normal stress and, consequently, the seismic loads do not alter the shear strength. This is illustrated in Figure 9-3. The graph on the left shows the frictional strength before the seismic forces are applied. The graph on the right shows that the strength was converted into an equivalent cohesive strength. Note that the strengths are the same in both graphs.

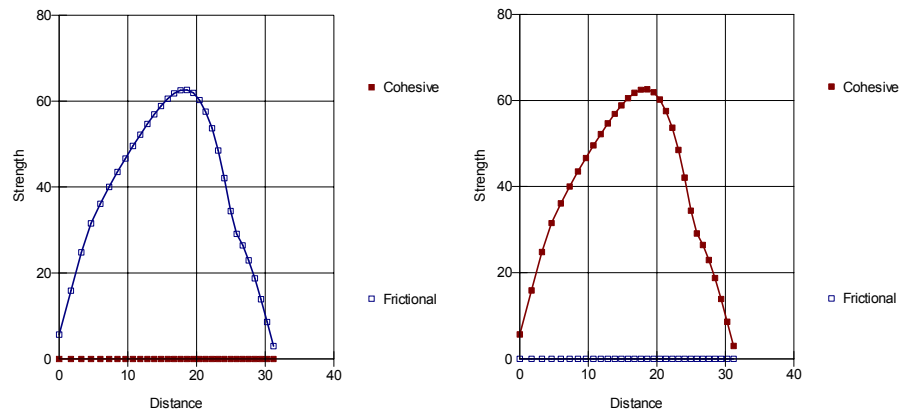


Figure 9-3 Conversion of frictional strength to cohesive strength

Selecting the option to convert to an undrained strength while the seismic forces are applied tends to increase the factor of safety slightly. In this simple illustrative case, the factor of safety increases from 1.102 to 1.150. This suggests that allowing the shear strength to change in response to the seismic forces errs on the safe side.

In the end, the decision to use this option needs to be made in the context of the particulars of each specific project. It is always advisable to do an analysis with and without selecting this option and then make a decision in light of the difference.

9.3 Pseudostatic analysis

A pseudostatic analysis represents the effects of earthquake shaking by accelerations that create inertial forces. These forces act in the horizontal and vertical directions at the centroid of each slice. The forces are defined as:

$$F_h = \frac{a_h W}{g} = k_h W$$

$$F_v = \frac{a_v W}{g} = k_v W$$

where:

a_h and a_v = horizontal and vertical pseudostatic accelerations,
 g = the gravitational acceleration constant, and
 W = the slice weight.

The ratio of a/g is a dimensionless coefficient k . In SLOPE/W, the inertial effect is specified as k_h and k_v coefficients. These coefficients can be considered as a percentage of g . A k_h coefficient of 0.2, for example, means the horizontal pseudostatic acceleration is 0.2 g .

In SLOPE/W, the horizontal inertial forces are applied as a horizontal force on each slice as shown in Figure 9-4. For example, if k_h is 0.2 then the magnitude of the force is 0.2 times the slice weight which equals 22.697.

Vertical inertial forces in SLOPE/W are added to the slice weight. Say that k_v is 0.1. The weight for the same slice as in Figure 9-4 is then 113.48 plus (0.1 x 113.48) which equals 124.83. The diagram in Figure 9-5 confirms this. Note that the horizontal force is based on the actual gravitational weight of the slice and not on the altered weight.

Vertical coefficients can be positive or negative. A positive coefficient means downward in the direction of gravity; a negative coefficient means upward against gravity.

The application of vertical seismic coefficients often has little impact on the safety factor. The reason for this is that the vertical inertial forces alter the slice weight. This alters the slice base normal, which in turn alters the base shear resistance. If, for example, the inertial force has the effect of increasing the slice weight, the base normal increases and then the base shear resistance increases. The added mobilized shear arising from the added weight tends to be offset by the increase in shear strength. Of course this is only true for frictional strength components and not for cohesive strength components.

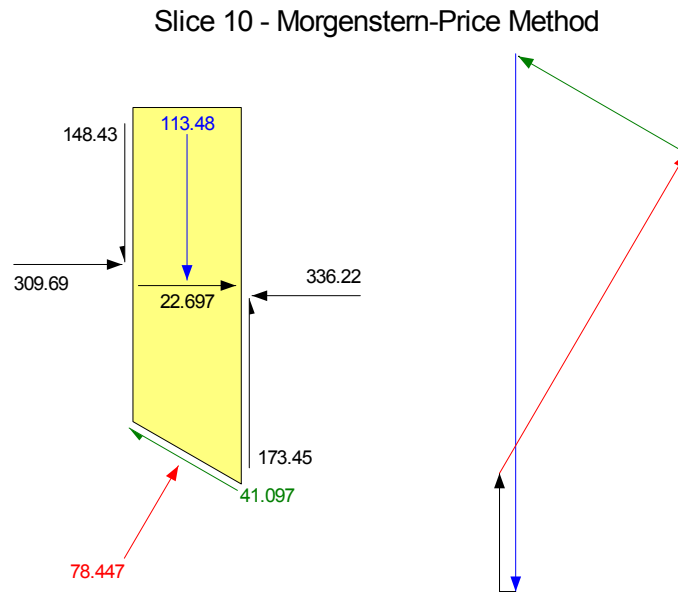


Figure 9-4 Horizontal seismic inertial force at slice centroid

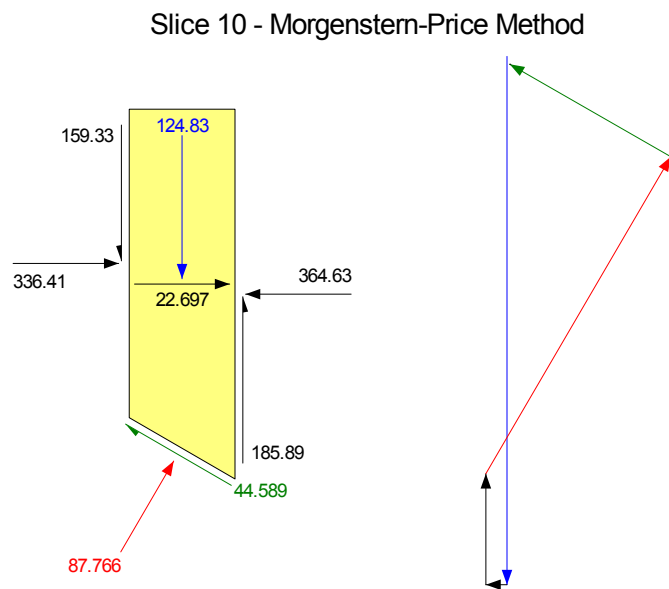


Figure 9-5 Slice forces with a k_v specified

The weight arising from ponded water up against a slope is not included in the calculation of the inertial forces. The thinking is that water (zero strength material) has no shear strength and therefore inertial forces acting on the water do not contribute to destabilizing the slope. Figure 9-6 illustrates a slope with a submerged toe. The inertial forces are now not directly equal to kW , as demonstrated in Figure 9-7. $K_h W$ is 0.2 times 76.474 = 15.29 for Slice 25 which is more than the actual 6.134 applied. The seismic coefficient is only applied to the total slice weight minus the surcharge water weight.

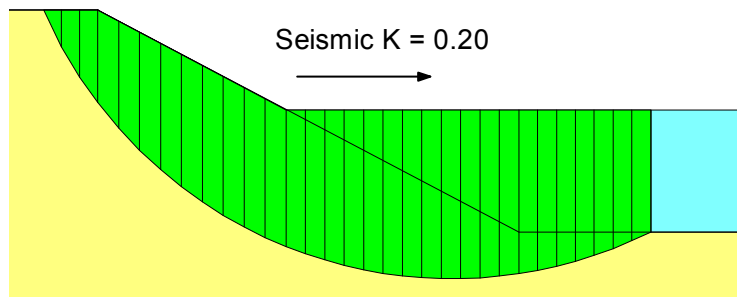


Figure 9-6 Example of slope with a submerged toe

Slice 25 - Morgenstern-Price Method

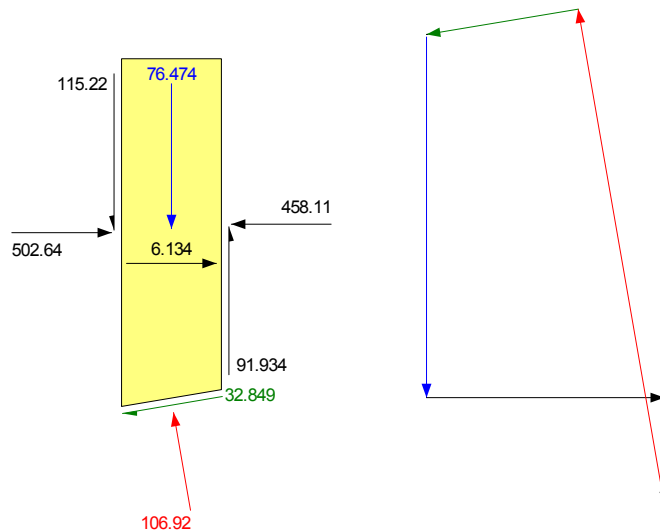


Figure 9-7 Inertial force for slice under water

Horizontal inertial seismic forces can have a dramatic effect on the stability of a slope. Even relatively small seismic coefficients can lower the factor of safety greatly, and if the coefficients are too large, it becomes impossible to obtain a converged solution. It is consequently always good practice to apply the seismic forces incrementally to gain an understanding of the sensitivity of the factor of safety to this parameter. It is often useful to create a graph such as in Figure 9-8. As the seismic coefficient increases, there should be smooth gradual decrease in the safety factor.

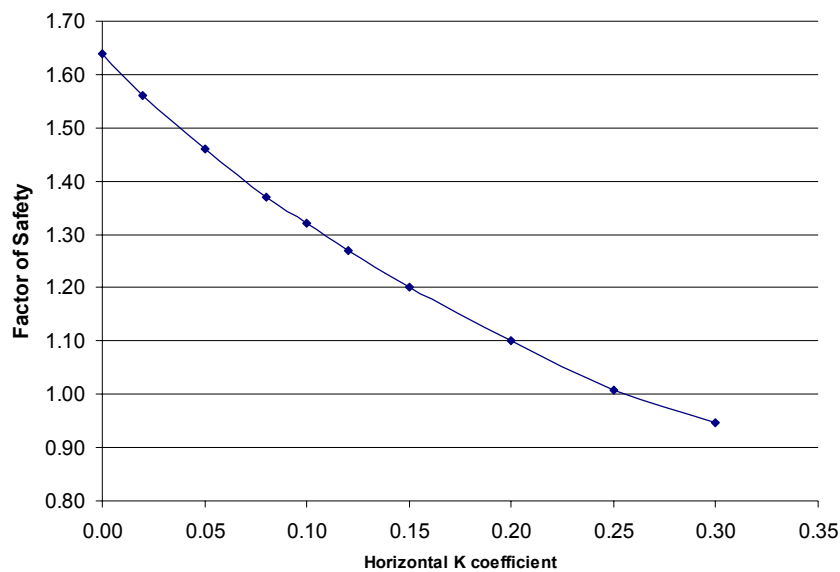


Figure 9-8 Factor of safety as function of k_h

The difficulty with the pseudostatic approach is that the seismic acceleration only acts for a very short moment in time during the earthquake shaking. As we will see in the next section, the factor of safety in reality varies dramatically both above and below static factor of safety. The factor of safety may even momentarily fall below 1.0, but this does not mean the slope will necessarily totally collapse. Looking at this issue more realistically requires knowing something about the shear stress variation during the earthquake shaking. This can be done with a QUAKE/W dynamic finite element analysis.

9.4 Dynamic analysis

Figure 9-9 presents an example of a 10-meter high slope. The slope is subjected to the 10 seconds of shaking arising from the earthquake record in Figure 9-10.

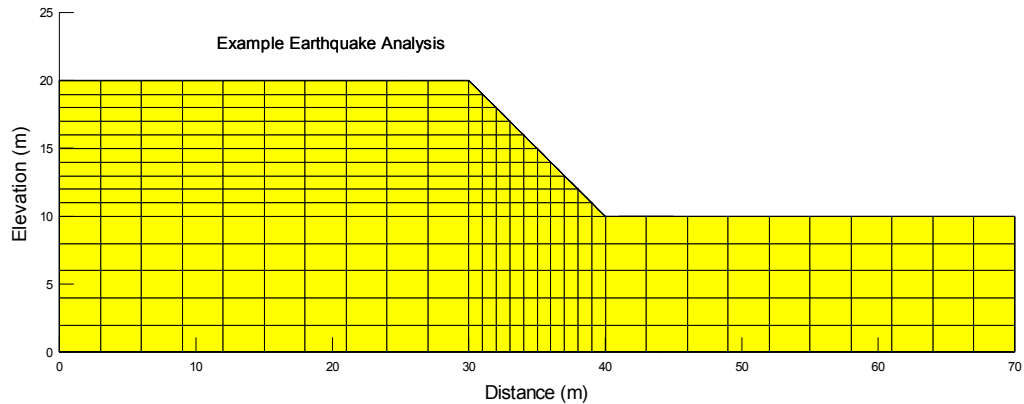


Figure 9-9 Slope subjected to earthquake shaking

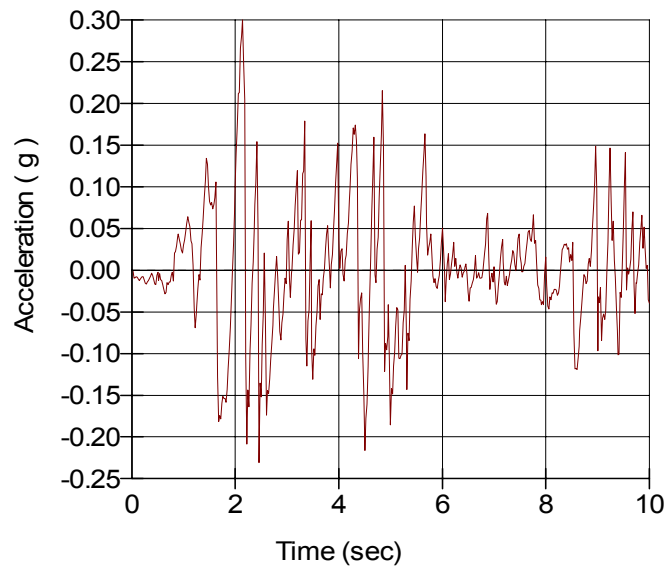


Figure 9-10 Example earthquake record

QUAKE/W can animate the motion of the slope during the entire 10 seconds. The diagrams in Figure 9-11 and Figure 9-12 are two snapshots during the shaking and as is readily evident, the dynamic stresses oscillate dramatically. The condition in Figure 9-11 may cause the factor of safety to decrease while the situation Figure 9-12 may cause the factor of safety to increase. This type of information is available for each time step the results are saved to a file during analysis. In this example, the integration along the earthquake record occurred at an interval of 0.02 seconds. The total of 500 integration steps is consequently required for the 10 seconds of shaking. The results were saved for every 10th time step resulting in 50 sets of output files.

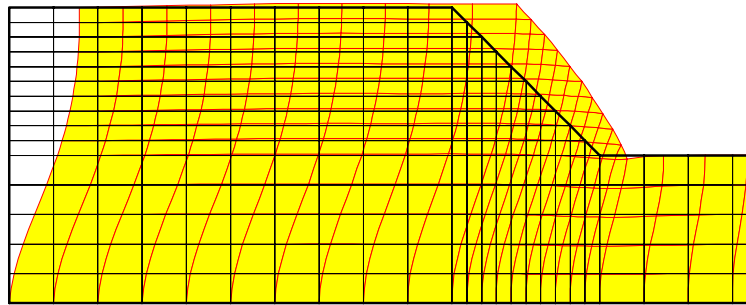


Figure 9-11 A snapshot of the deformation during an earthquake

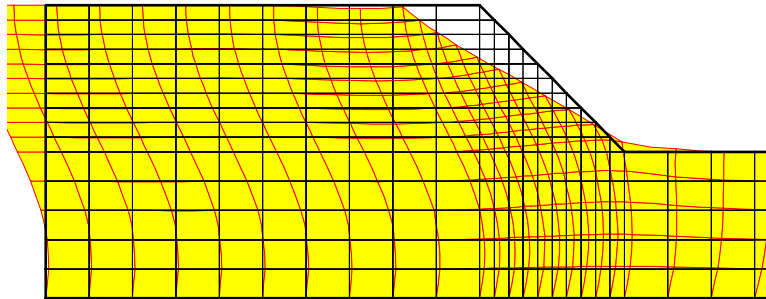


Figure 9-12 A snapshot of the deformation during an earthquake

The earlier chapter on Factor of Safety Methods describes how SLOPE/W can use finite element computed stresses to assess the stability of earth structures. The details will not be repeated here.

SLOPE/W computes a factor of safety for each time step the data is saved to a file. For this example, SLOPE/W computes 50 safety factors. These safety factors can then be plotted versus time as shown in Figure 9-13. The graph vividly illustrates the oscillation in the factor of safety as noted earlier. Note that the factor of safety momentarily falls below 1.0 several times during the shaking.

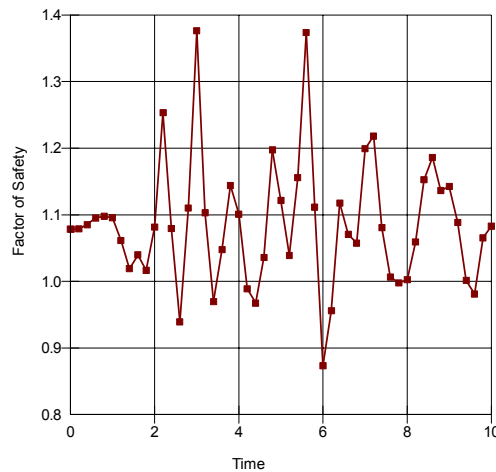


Figure 9-13 Factor of safety versus time

For the factor of safety calculations, the shear strength available along the slip surface is computed based on the initial insitu static stresses and then held constant during the shaking. This has the effect of treating the soil as behaving in an undrained manner during the shaking.

With such a wide variation in factors of safety during the earthquake shaking, it is difficult to say anything meaningful about the slope stability. The issue is more how much movement will take place during the shaking than the total collapse of the slope. An estimate of the resulting deformation can be made from this data, as described in the next section.

9.5 Permanent deformation

The stresses from QUAKE/W are the sum of the static plus dynamic stresses. The static stresses are known from the specified initial insitu stresses. Subtracting the initial static stresses from the QUAKE/W stresses therefore gives the dynamic stresses. In equation form:

$$\sigma_{dynamic} = \sigma_{QUAKE} - \sigma_{static}$$

The dynamic stress can be computed at the base of each slice. Integrating along the entire slip surface then gives the total dynamic mobilized shear. This is the additional shear created by the earthquake shaking.

Dividing the total mobilized dynamic shear by the potential sliding mass provides an average acceleration value. This value is obtained for each time integration step during the shaking and can be plotted against the corresponding factor of safety to produce a plot such as in Figure 9-14. The average acceleration corresponding to a factor of safety of 1.0 is called the yield acceleration, a_y . It is by definition the overall average acceleration that will cause the sliding mass to fail or move. In this example, a_y is 0.048.

The average acceleration obtained at each integration step can also be plotted with time as in Figure 9-15. Where the average acceleration exceeds a_y , the slope will move.

The average acceleration is representative of the resultant of both horizontal and vertical applied accelerations in the QUAKE/W analysis.

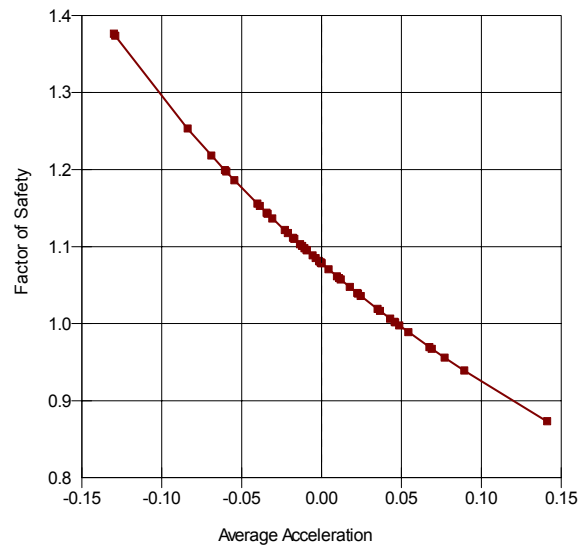


Figure 9-14 Average acceleration versus safety factors

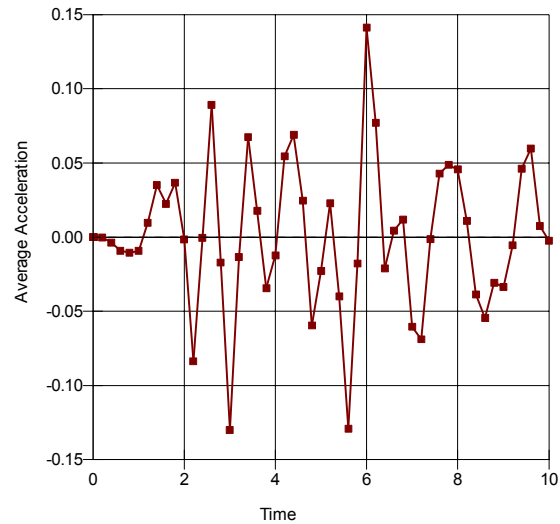


Figure 9-15 Average accelerations versus time during the shaking

Integrating the area under the average acceleration versus time curve where the acceleration exceeds a_y , gives the velocity of the sliding mass during the movement as in Figure 9-16.

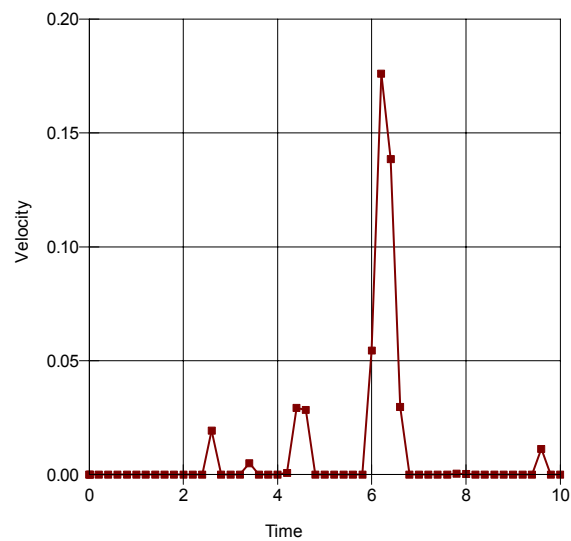


Figure 9-16 Velocity versus time

Integrating the area under the velocity versus time curve gives the cumulative movement during the shaking as in Figure 9-17.

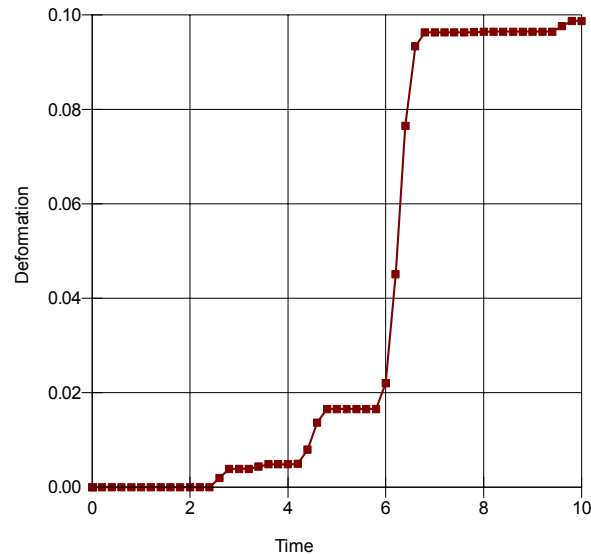


Figure 9-17 Cumulative movement during the shaking

The direction of the movement is parallel to the slip surface. The movement may therefore be both rotational and translational.

You will note that there are negative average accelerations that exceed the yield acceleration. This implies that there is also some up-slope movement, but as is common in these types of analyses, the potential up-slope movement is simply ignored.

SLOPE/W makes this type of calculation for each and every trial slip surface, and this makes it possible to find the trial slip surface with the largest potential movement. For convenience, the trial slip surfaces can be sorted by deformation rather than by factor of safety, to identify the one with the largest movement.

The procedure described here to estimate the permanent deformation is based on the concepts inherent in a Newmark Sliding Block analysis. A Newmark type of analysis is applicable only in certain specific circumstances. The procedure is ideal for cases where there is little or no degradation in the soil shear strength during the dynamic shaking. This may be the case for the rock-fill shells of an earth embankment, steep natural rock slopes or unsaturated, heavily over-consolidated

clayey slopes. This procedure is not applicable to cases where there is a significant potential for a large loss in shear strength due to either the generation of excess pore-water pressures or the collapse of the soil grain structure as may be the case for loose silty and sandy soils. Kramer (1996, p. 437) points out that these types of analyses can be unreliable for situations where there is a large build up of excess pore-water pressures or where there is more than about a 15% degradation in the shear strength during the earthquake shaking.

A useful distinguishing characteristic that can help in deciding whether the Newmark procedure is or is not applicable is to decide if the major destabilizing factor is the inertial forces or the weakening of the soil. The Newmark approach is suitable for cases governed by the inertial forces; it is not applicable if soil weakening is the controlling issue.

9.6 *Liquefaction stability*

In earthquake engineering, there is a line of thinking that says that even under the worst possible conditions the factor of safety should not fall below 1.0. That is to say, even if large pore-water pressures have been generated and the soil strength has fallen from peak to residual, the factor of safety should not be below 1.0 for design purposes. If the factor of safety is below 1.0 under these severe conditions, the thought is that the risk is unacceptably high for a possible catastrophic liquefaction flow failure.

Two pieces of information are available from a QUAKE/W analysis which can be used to assess the possibility of a flow liquefaction failure. One is the pore-water pressure conditions at the end of shaking and the second is the identification of elements where the soil may have liquefied. The elements that have liquefied can then be assigned a residual strength to reflect the weakening associated with the liquefaction.

Figure 9-18 shows an example included with the QUAKE/W software. The shaded elements are ones that have liquefied. Residual soil parameters can be used along portions of trial slip surfaces that pass through the liquefied elements.

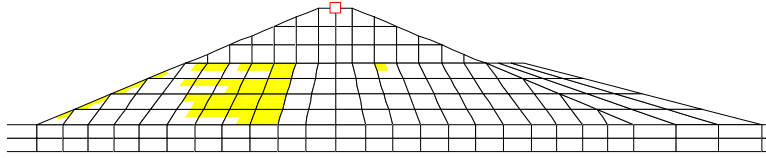


Figure 9-18 Example QUAKE/W analysis showing some liquefied elements

Figure 9-19 shows a trial slip surface. The peak c and ϕ parameters are 200 psf and 30 degrees. The residual parameters are 50 psf and 15 degrees. Figure 9-20 shows how the strength parameters fall from peak to residual along the slip surface. The residual parameters are used when the slice base centre is in a liquefied element, as indicated by the QUAKE/W analysis.

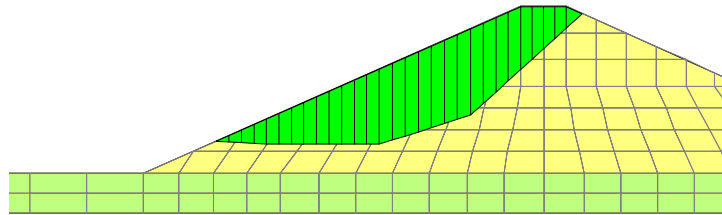


Figure 9-19 A slip surface passing some liquefied elements

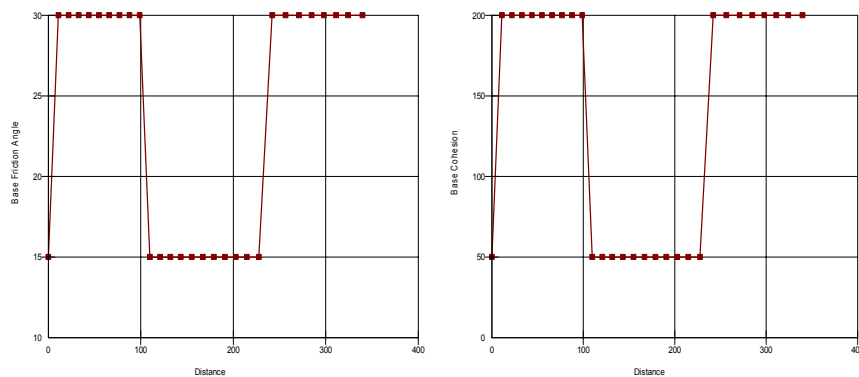


Figure 9-20 Strength parameters (c and ϕ) used along the slip surface

Generally, this analysis is done for stress and pore-water pressure conditions at the end of the shaking. The analysis can, however, technically be done for any time step for which QUAKE/W saved the data.

Using the QUAKE/W liquefaction flags makes the stability analysis relatively straight forward. The downside is that liquefied elements are not necessarily always in a nice cluster. There can be scattered and isolated elements that indicate liquefaction. Numerically this causes the strength parameters to jump back and forth between peak and residual values which may not be all that realistic (Figure 9-20). Furthermore, the system does not provide for any transition between the liquefied and non-liquefied zones. If these undesirable effects are deemed unacceptable in the analysis, then it may be better to use the QUAKE/W results indirectly. Based on interpretation and judgment, a separate stability analysis could perhaps be done by manually including a region in the stability section that is assigned residual strength parameters. The QUAKE/W results are then only used to indirectly identify the region of possible liquefaction.

10 Probabilistic and Sensitivity Analyses

10.1 Introduction

There is an ever-increasing interest in looking at stability from a probabilistic point of view. University research into the area is increasing, as indicated by a recent Ph.D. study at the University of Alberta, Alberta, Canada (El-Ramly, Morgenstern and Cruden, 2002).

SLOPE/W includes a general comprehensive algorithm for probabilistic analyses. Almost all input parameters can be assigned a probability distribution, and a Monte Carlo scheme is then used to compute a probability distribution of the resulting safety factors. Once the probability distribution of the safety factors are known, other quantifying parameters, such as the probability of failure can be determined.

With a uniform probability distribution, the probabilistic scheme in SLOPE/W can also be used to conduct a sensitivity analysis.

This chapter explains the probabilistic capabilities and features available in SLOPE/W and briefly explains the underlying techniques and procedures used in the formulation. More details of the method can be found in the Theory chapter.

10.2 Probability density functions

SLOPE/W includes the following probability density functions (PDF):

- Normal
- Lognormal
- Uniform
- Triangular
- Generalized Spline function

Normal function

As is well known, many natural data sets follow a bell-shaped distribution and measurements of many random variables appear to come from population frequency distributions that are closely approximated by a normal probability

density function. This is also true for many geotechnical engineering material properties. In equation form, the normal probability density function is:

$$f(x) = \frac{e^{-(x-u)^2 / 2\sigma^2}}{\sigma\sqrt{2\pi}}$$

where:

x = the variable of interest,
 u = the mean, and
 σ = the standard deviation.

Figure 10-1 shows a typical Normal distribution for the soil property ϕ when the mean is 28 degrees and the standard deviation is 2 degrees.

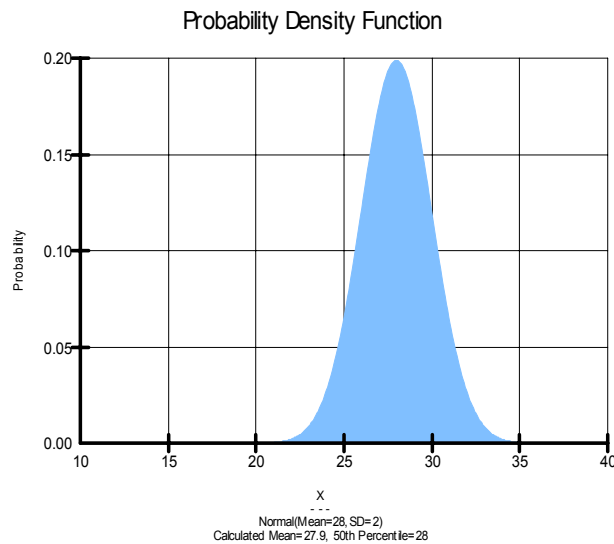


Figure 10-1 Normal probability density function

By default, SLOPE/W uses a range of ± 5 standard deviations. A minimum and a maximum can, however, be specified to truncate or clip the function. Figure 10-2 shows the same probability density function when clipped with a minimum of 23 degrees and a maximum of 33 degrees.

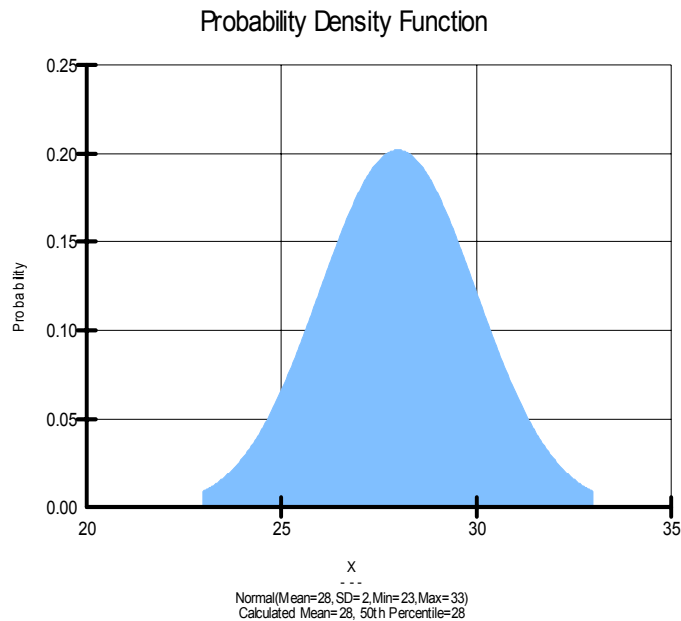


Figure 10-2 A clipped normal probability density function

From the probability density function, SLOPE/W integrates the area under the function to establish a cumulative distribution function and the cumulative distribution function is inverted to form an inverse distribution function or a percent point function.

In SLOPE/W, the inverse distribution function is called a sampling function, since it is this function that is at the heart of sampling the various statistical parameters. The x-axis covers the range of possible random numbers. So, each time a random number is obtained, the parameter is “sampled” using this function. Figure 10-3 presents the resulting sampling function of the clipped normal probability density function.

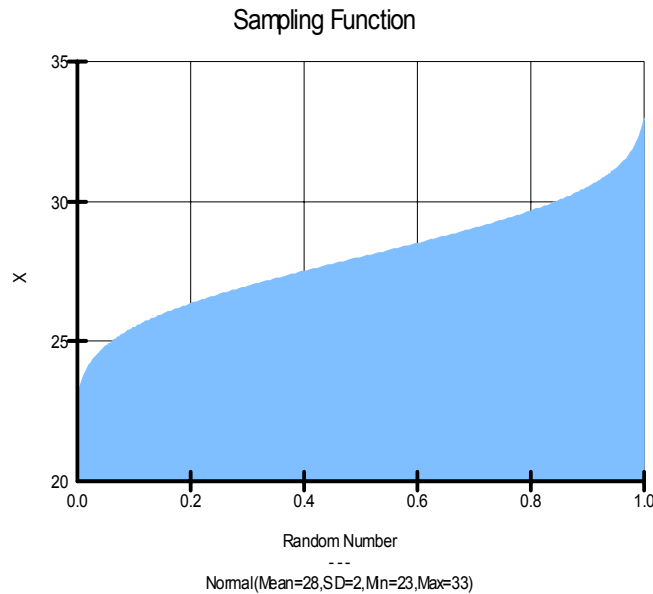


Figure 10-3 A normal sampling function

For the case of a normal probability function, the sampling function has a relatively straight segment in the middle. The implication of this is that parameters around the mean will be sampled more often than values at the extremities of the sampling function.

The normal curve has a convenient property that the area under the normal curve between the mean and any point depends only on the number of standard deviations away from the mean. For example, the area or probability of a value, x , lying between $\pm 1\sigma$ is 68.26%, between $\pm 2\sigma$ is 95.44%, between $\pm 3\sigma$ is 99.72%, between $\pm 4\sigma$ is 99.99% and between $\pm 5\sigma$ is approximately 100.00%.

For example, in SLOPE/W, the mean cohesion of a soil may be specified as 30 kPa with a standard deviation of 5 kPa. This means that for 100 samples, 68.26% of the samples will have a value between 25 and 35 kPa, and 95.44% of the samples will have a value between 20 and 40 kPa.

Lognormal function

With a lognormal function, a variable x is lognormally distributed if the natural log of x (i.e., $\ln x$) is normally distributed. The general formula for a lognormal probability density function is:

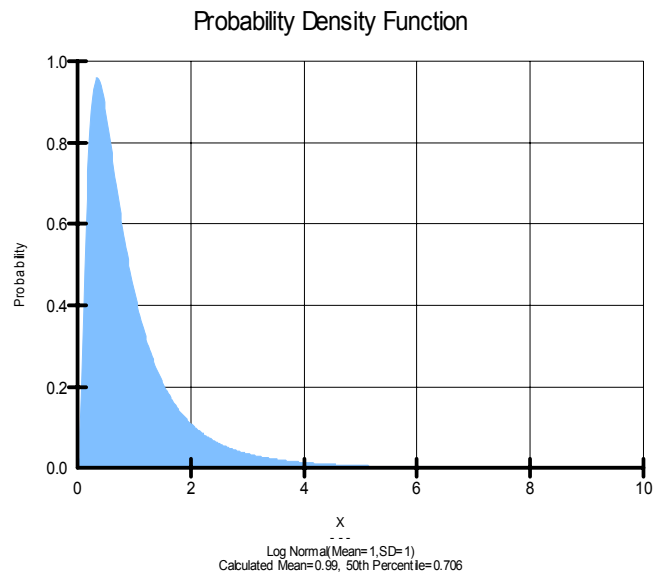
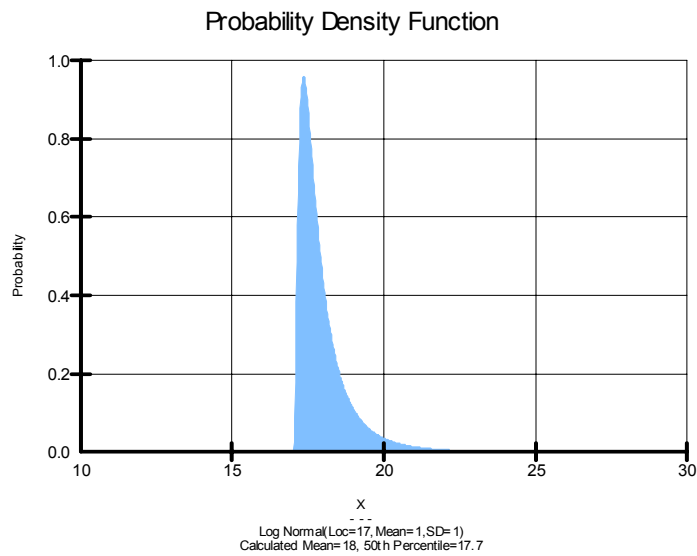
$$f(x) = \frac{e^{-(\ln((x-\theta)/m))^2 / 2\sigma^2}}{(x-\theta)\sigma\sqrt{2\pi}}$$

where:

- σ = the lognormal standard deviation (or shape parameters),
- m = the lognormal mean (or scale parameter), and
- θ = the offset the lognormal mean (or the location parameter).

The standard lognormal probability density function is the special case when there is no offset (i.e., $\theta=0$) and a unit lognormal mean (i.e., $m=1$). Figure 10-4 shows a lognormal probability density function when $\sigma=1$, $m=1$ and $\theta=0$. The function is the same as the standard lognormal probability density function when $\sigma=1$. Since a negative value cannot be supported in log mathematically, the standard lognormal function always has the distribution starting from zero and heavily skewed to the low x range

This special characteristic of the standard lognormal function posts a limitation to the use of the probability density function in modeling actual engineering parameters with a mean value (m) much larger than 1. SLOPE/W uses the general lognormal formula, where an offset value (θ) can be applied to shift the density function to better represent a probability density function. For example, if the actual mean value of the soil parameters is 18, we can apply an offset or location parameter of 17 (i.e., $18-1$) to the general density function. Figure 10-5 shows the density function with the applied offset.

**Figure 10-4 Lognormal probability density function****Figure 10-5 Lognormal probability density function with offset**

The corresponding sampling function is shown in Figure 10-6. The sampling function indicates that when a random number is generated, there is an increased chance of obtaining a value between 17 and 19. This is consistent with the lognormal density function.

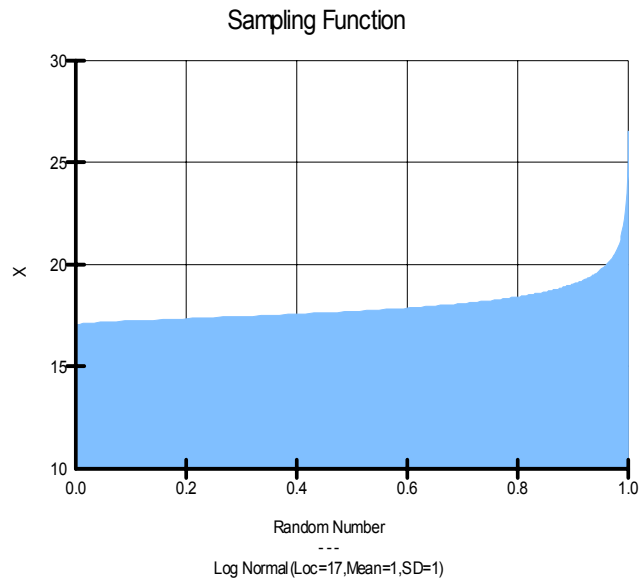
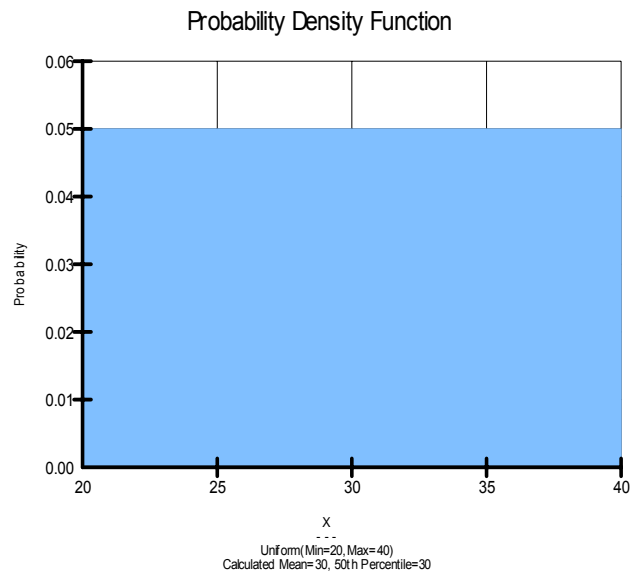
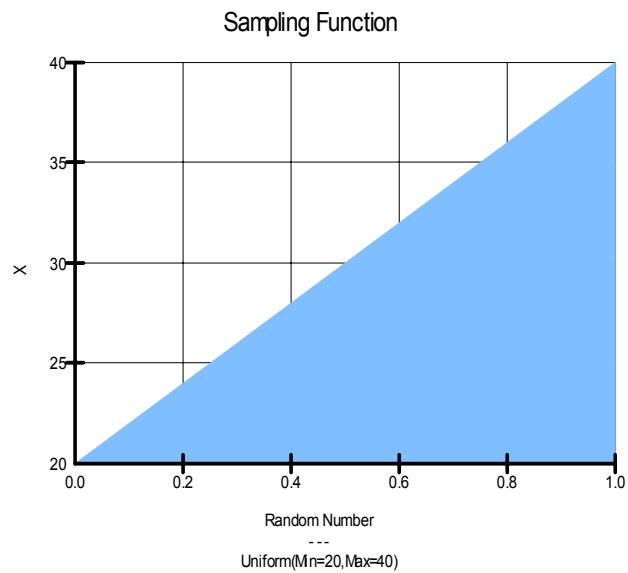


Figure 10-6 A log normal sampling function

Uniform function

A uniform function simply describes a range of values as illustrated in Figure 10-7. The characteristic of a uniform distribution is that all values have an equal probability of occurrence. This is further illustrated by the fact that the sampling function is a straight line as in Figure 10-8.

**Figure 10-7 A uniform probability density function****Figure 10-8 A uniform sampling function**

10.3 *Triangular probability function*

A triangular probability density function can be specified with three points; the min and max values together with the apex value. Figure 10-9 shows a typical triangular probability density function when the mode value is 20, the minimum value is 15 and the maximum value is 45. The associated sampling function of this triangular probability function is shown in Figure 10-10.

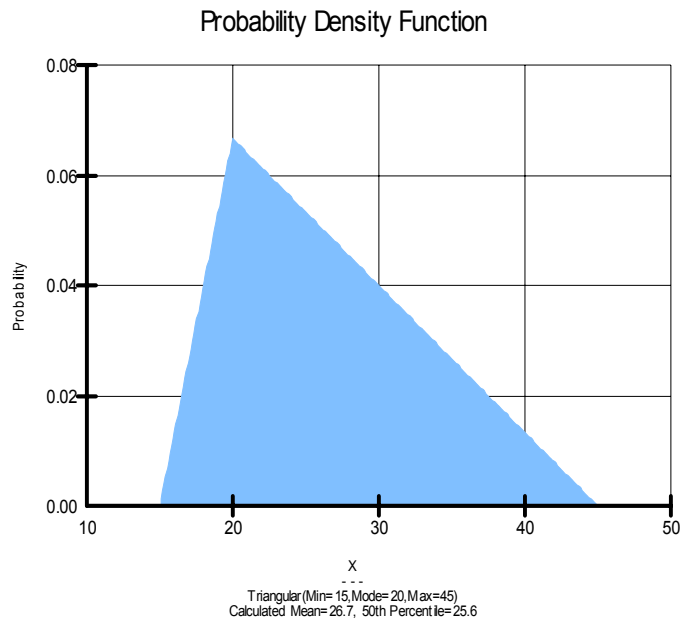


Figure 10-9 A triangular probability density function

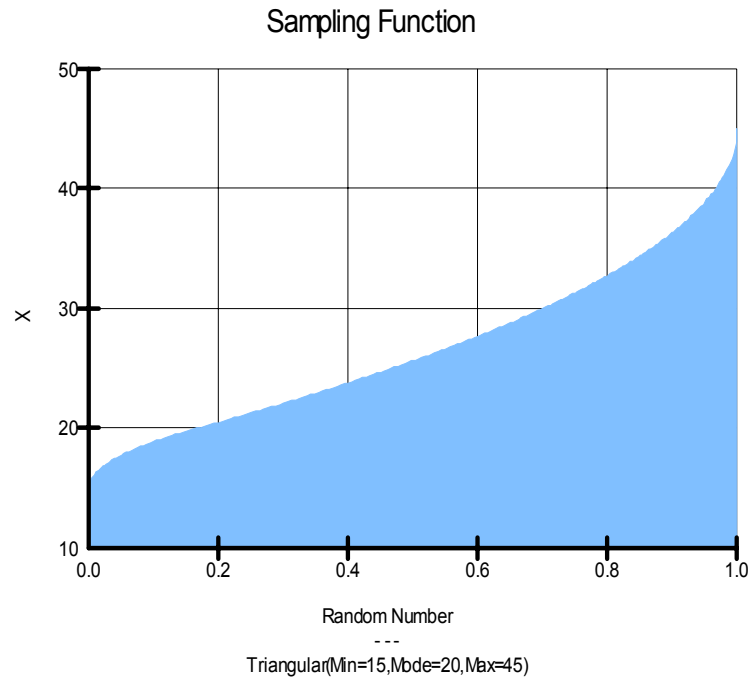


Figure 10-10 A triangular sampling function

10.4 General probability function

Any generalized spline shape function such as the bimodal function shown in Figure 10-11 can be defined in SLOPE/W as in Figure 10-11. This shape function can then be attached to any variable.

Assume that we apply this shape function to a cohesion value that ranges between 10 and 25. The resulting probability density function then is as shown in Figure 10-12 and the associated sampling function is as shown in Figure 10-13. The probability density function is created from the shape function and the minimum and maximum values, so that the area under the function is always 1.0.

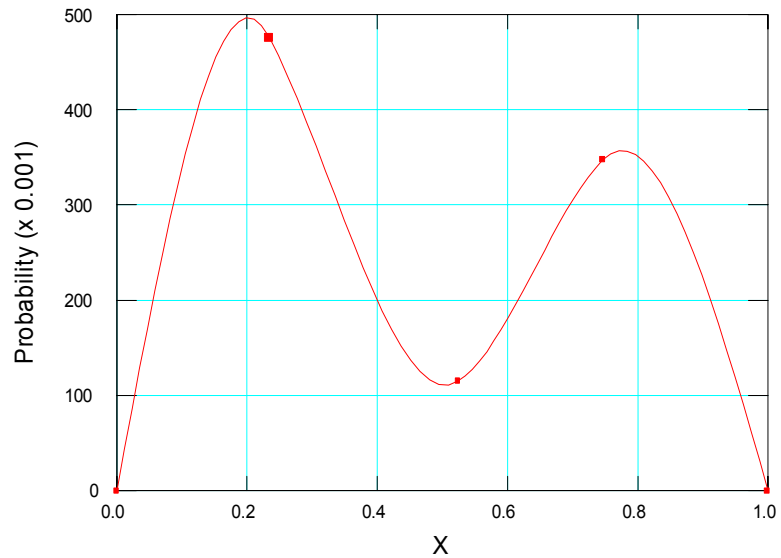


Figure 10-11 A generalized spline shape function

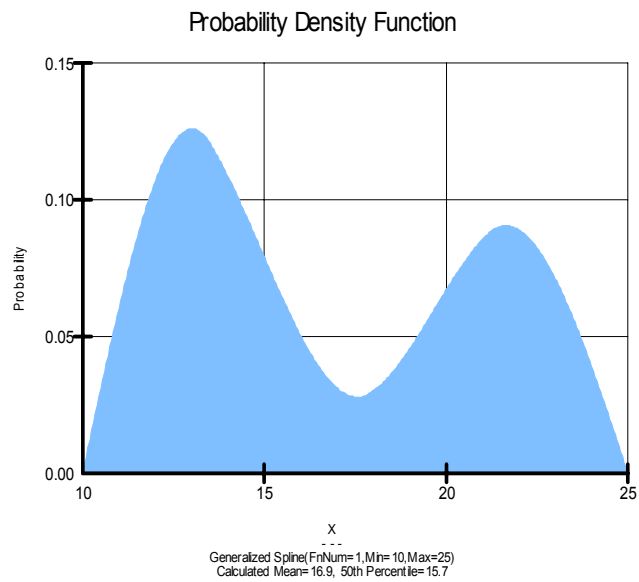


Figure 10-12 A generalized spline probability density function

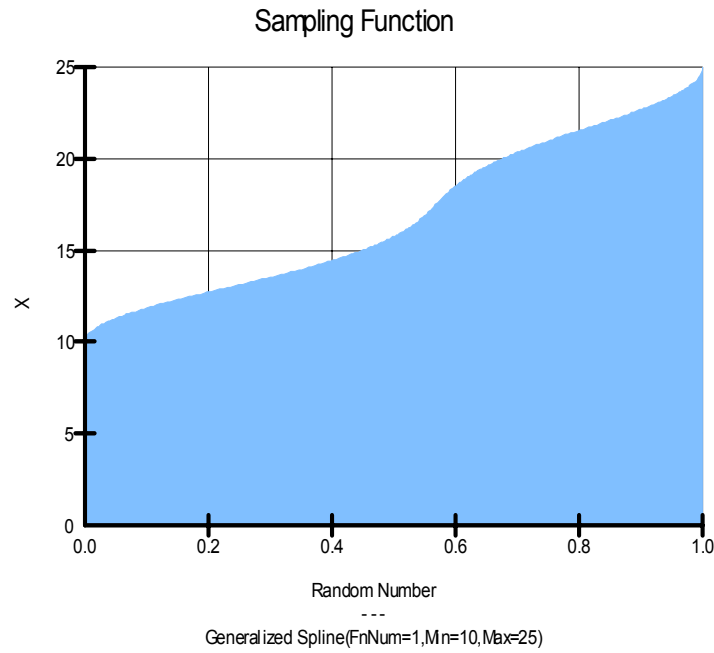


Figure 10-13 A generalized spline sampling function

The generalized spline probability distribution function makes it possible to consider any distribution function. This technique is particularly useful for any irregular distribution of actual measurements.

10.5 $C - \phi$ correlation

A correlation coefficient expresses the relative strength of the association between two parameters. Laboratory tests on a wide variety of soils (Lumb, 1970; Grivas, 1981 and Wolff, 1985) show that the shear strength parameters c and ϕ are often negatively correlated with correlation coefficient ranges from -0.72 to 0.35. Correlation between strength parameters may affect the probability distribution of a slope. SLOPE/W allows the specification of c and ϕ correlation coefficients for all soil models using c and ϕ parameters. Furthermore, in the case of a bilinear soil model, SLOPE/W allows the specification of correlation coefficient for ϕ and ϕ_2 .

Correlation coefficients will always fall between -1 and 1. When the correlation coefficient is positive, c and ϕ are positively correlated, implying that larger values of c are more likely to occur with larger values of ϕ . Similarly, when the correlation coefficient is negative, c and ϕ are negatively correlated which reflects the tendency of a larger value of c to occur with a smaller value of ϕ . A zero correlation coefficient implies that c and ϕ are independent parameters.

10.6 Probability of failure and reliability index

A factor of safety is really an index indicating the relative stability of a slope. It does not imply the actual risk level of the slope, due to the variability of input parameters. With a probabilistic analysis, two useful indices are available to quantify the stability or the risk level of a slope. These two indices are known as the probability of failure and the reliability index.

As illustrated in Figure 10-14, the probability of failure is the probability of obtaining a factor of safety less than 1.0. The probability of failure is determined by counting the number of safety factors below 1.0 and then taking this number as a percentage of the total number of converged Monte Carlo trials. For example, if there are 1000 Monte Carlo trials with 980 converged safety factors and 98 of them are below 1.0. Then the probabilistic of failure is 10%.

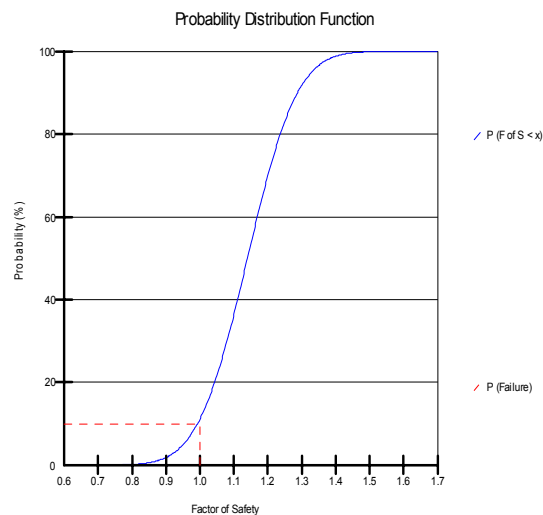


Figure 10-14 Factor of safety probability of failure

The probability of failure can be interpreted in two ways:

- If a slope were to be constructed many times, what percentage of such slopes would fail, or
- The level of confidence that can be placed in a design.

The first interpretation may be relevant in projects where the same slope is constructed many times, while the second interpretation is more relevant in projects where a given design is only constructed once and it either fails or it does not. Nevertheless, the probability of failure is a good index showing the level of risk of instability.

There is no direct relationship between the deterministic factor of safety and probability of failure. In other words, a slope with a higher factor of safety may not be more stable than a slope with a lower factor of safety. For example, a slope with factor of safety of 1.5 and a standard deviation of 0.5 may have a much higher probability of failure than a slope with factor of safety of 1.2 and a standard deviation of 0.1.

Another way of looking at the risk of instability is with what is known as a reliability index. The reliability index (β) is defined in terms of the mean (μ) and the standard deviation (σ) of the trial factors of safety as shown in the following equation:

$$\beta = \frac{(\mu - 1.0)}{\sigma}$$

The reliability index describes the stability by the number of standard deviations separating the mean factor of safety from its defined failure value of 1.0. It can also be considered as a way of normalizing the factor of safety with respect to its uncertainty.

When the shape of the probability distribution is known, the reliability index can be related directly to the probability of failure. Figure 10-15 illustrates the relationship of the reliability index to the probability of failure for a normally distributed factor of safety.

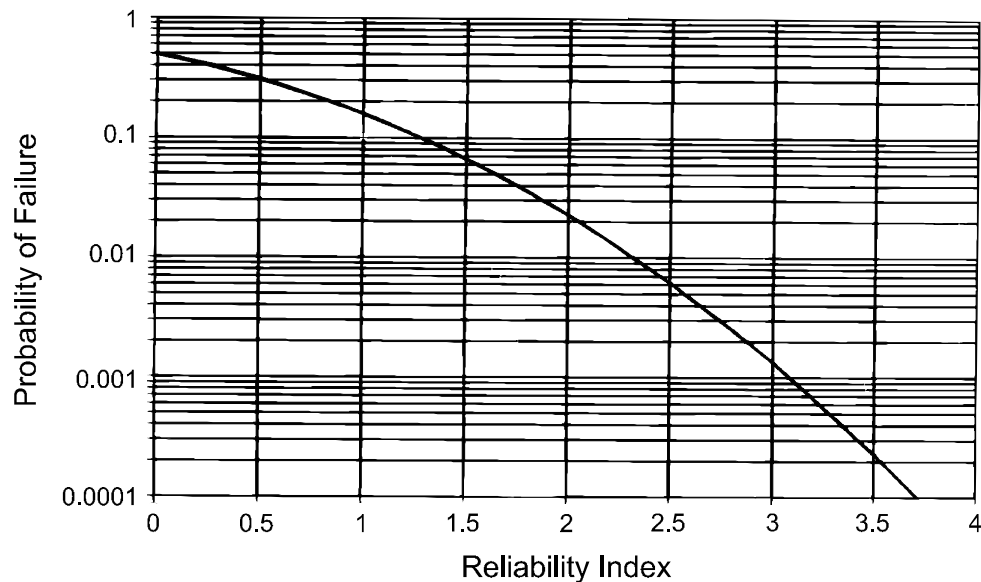


Figure 10-15 Relationship between reliability index and the probability of failure

SLOPE/W computes the reliability index for any and all probability distributions, but the concept is really only meaningful and applicable in SLOPE/W for normal distributions.

10.7 Spatial variability

Spatial variability can be an important issue if a potential slip surface has a significant length within one material. Consider the case in Figure 10-16. A significant portion of the slip surface is in the clay and consequentially it is reasonable to assume that there is some statistical variability in the clay along the slip surface. The length of the potential slip surface in the clay is around 25 m. The horizontal distance is 24 m.

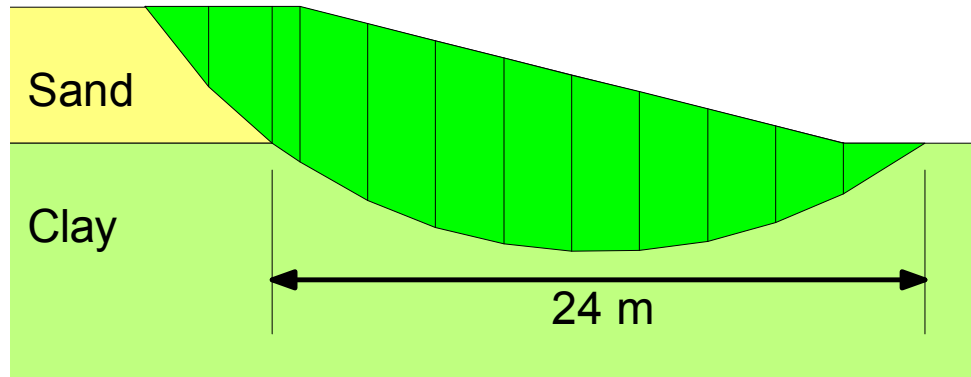


Figure 10-16 Case with statistical variability in the clay

The clay has a mean undrained strength (c) of 15 kPa with a standard deviation of ± 3 . A clipped normal distribution varying between 5 and 25 kPa is assumed as shown in Figure 10-17.

SLOPE/W has 3 options for considering the spatial variability along the slip surface. The options deal with the number of times the soil properties are sampled along the slip surface. The options are:

- Sample the properties only once for each soil for the entire slip surface
- Sample the properties for each slice along the slip surface
- Sample the properties at a specified distance along the slip surface

If the clay strength is sampled only once for each Monte Carlo trial, the strength is constant along the slip surface, as illustrated in Figure 10-18. The graph shows possible strengths for four different Monte Carlo trials.

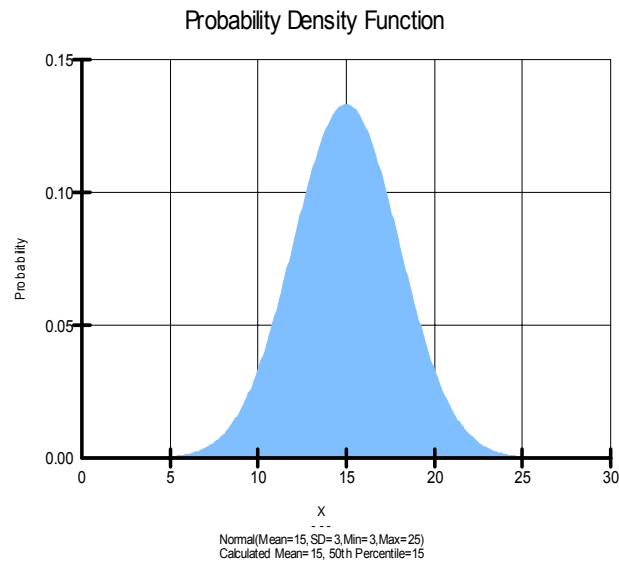


Figure 10-17 Probability density distribution for the clay

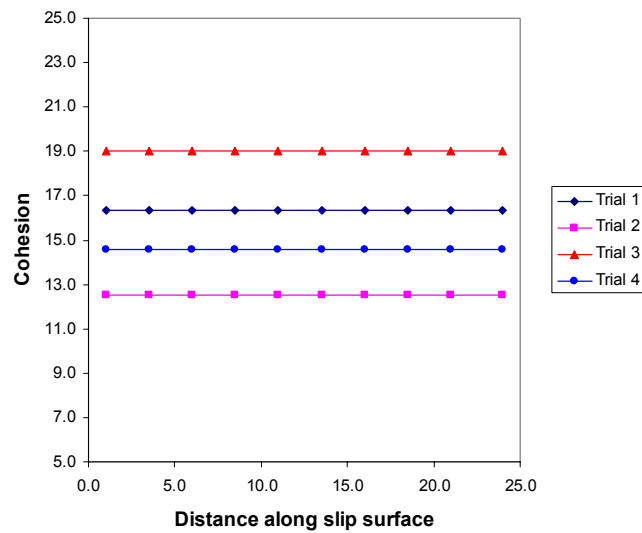


Figure 10-18 Strength variations in the clay when sampled once for each trial run

Statistically, the strength in the clay could be as low as 5 kPa or as high as 25 kPa. Intuitively, it seems unlikely that the strength along the entire slip surface could be at these outer limits, particularly if the slip surface has a significant length. Sampling more than once is likely more appropriate.

Another option is to sample the soil strength for each slice. The variation along the slip surface then could be as illustrated in Figure 10-19 for two trial runs. There are 10 slices in the clay and, consequently, there are 10 different strengths along the slip surface.

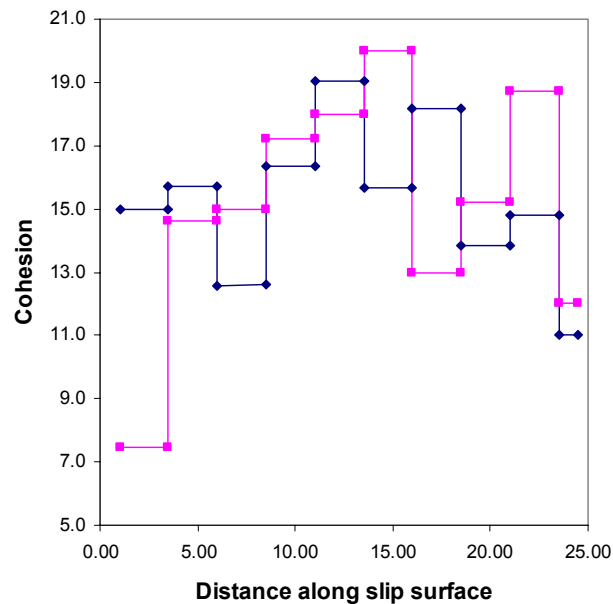


Figure 10-19 Strength variation along the slip surface when soil is sampled for every slice

As indicated on Figure 10-19, to sample the soil strength for each slice in every Monte Carlo trial may result in significant fluctuation of soil strength along the slip surface even within the same material. Although this is statistically possible, it seems quite unlikely in the field.

The third option in SLOPE/W is to sample the soil at a specified distance. For example, if the sampling distance is 10m, then the strength variation along the slip surface for two different Monte Carlo runs could be as shown in Figure 10-20.

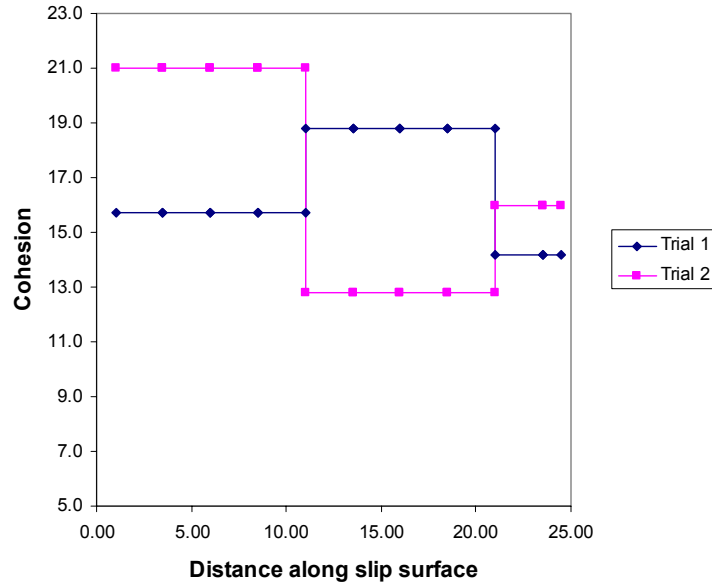


Figure 10-20 Strength variation along the slip surface with a sampling distance of 10 m

At this sampling distance, there are three different strengths along the slip surface.

There are two complete 10-m sampling distances and a third partial sampling distance. A partial sampling distance is considered to be correlated with the immediate preceding sampling distance. The coefficient of correlation between two soil sections can be computed with the equation as proposed by Vanmarcke (1983):

$$\rho(\Delta Z, \Delta Z') = \frac{Z_0^2 \Gamma(Z_0) - Z_1^2 \Gamma(Z_1) + Z_2^2 \Gamma(Z_2) - Z_3^2 \Gamma(Z_3)}{2 \Delta Z \Delta Z' [\Gamma(\Delta Z) \Gamma(\Delta Z')]^{0.5}}$$

where:

- $\Delta Z, \Delta Z'$ = the length between two sections,
- Z_0 = the distance between the two sections,
- Z_1 = $\Delta Z + Z_0$,

$$\begin{aligned}
 Z_2 &= \Delta Z + Z_0 + \Delta Z', \\
 Z_3 &= \Delta Z' + Z_0, \text{ and} \\
 \Gamma &= \text{a dimensionless variance function.}
 \end{aligned}$$

Γ is a dimensionless variance function, which Vanmarcke (1983) showed can be approximated by:

$$\begin{aligned}
 \Gamma(Z) &= 1.0 \text{ when } Z \leq \delta, \text{ and} \\
 \Gamma(Z) &= \delta/Z \text{ when } Z > \delta.
 \end{aligned}$$

The symbol δ is called the scale of fluctuation. It is about twice the autocorrelation distance. In SLOPE/W, when spatial variation is considered, the value of δ is related to the desired sampling distance along the slip surface.

As is evident from the above equations, the correlation is strong when the partial distance is short relative to the specified sampling distance, and the correlation is weak when the partial distance approaches the specified sampling distance.

The probability of failure is related to the sampling distance, especially if there are only a few statistical parameters. The probability of failure is the highest when the soil is sampled only once for each trial run and is the lowest when the soil is sampled for each slice. For the simple case under discussion here, the probabilities of failure for various sampling frequencies are as listed in the following table.

Sampling Frequency	Probability of Failure (%)
Only once	19
Every 15 m	10
Every 10 m	6
Every slice	<1

When the strength is sampled only once there are more trial runs with a factor of safety less than 1.0 and therefore a high probability of failure. Sampling the soil for every slice tends towards an average mean strength and therefore a low probability of failure.

Selecting an appropriate sampling distance is not trivial. Generally, a thorough understanding of the statistical characteristics of the soil stratum is required, and

spatial variability is a factor that can only be assessed in light of the details at each project and the amount of data available.

The two options in SLOPE/W of sampling the soil only once, and sampling the soil strength for each slice are perhaps both unrealistic for some situations, these two options are nonetheless useful. They provide a convenient means of bracketing the possible range of probabilities of failure. Knowing the limits can then help with selecting and evaluating a proper sampling distance.

10.8 Multiple statistical parameters

In SLOPE/W, a wide range of parameters can be assigned a statistical dispersion and included in a Monte Carlo simulation. This includes soil strength parameters, concentrated loads, pore-water pressures, pseudostatic seismic coefficients and so forth. Each of the parameters is sampled for each Monte Carlo run. Using too many statistical parameters together in the same run tends to reduce the distribution of the computed safety factors. That is, the combination of multiple statistical parameters tends to smooth out the extreme of the variability and the probability of failure diminishes. Perhaps this is an appropriate response. The main point here is that it is important to be cognizant of this and to evaluate the results carefully when many parameters are included in a probability analysis.

10.9 Sensitivity analyses

A sensitivity analysis is somewhat analogous to a probabilistic analysis. Instead of selecting the variable parameters randomly, the parameters are selected in an ordered fashion using a Uniform Probability Distribution function.

Consider the simple example in Figure 10-21. A question may be: “Is the stability of the slope more sensitive to the frictional strength of the sand or the undrained strength of the clay?”

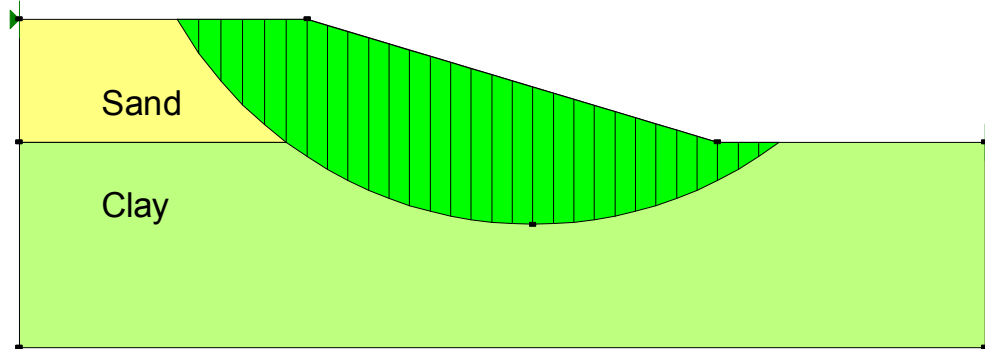


Figure 10-21 Illustrative case for a sensitivity analysis

Let us look at the case where ϕ for the sand is 30 degrees and the variation in ϕ will range from 25 to 35 degrees (11 different ϕ values). The undrained strength of the clay is 20 kPa and the range will be from 15 to 25 kPa.

First SLOPE/W holds the strength of the clay at 20 kPa and computes a factor of safety for each of the 11 trial ϕ values. Next the strength of the sand is kept constant at 30 degrees, and factors of safety are computed for of the 11 different cohesion values.

For presentation purposes, all the strengths are normalized to a value ranging between 0.0 and 1.0. Zero means the lowest value and 1.0 means the highest value. For the example here, zero means a ϕ of 25 degrees and a c of 15 kPa. A value of 1.0 means a ϕ of 35 degrees and a c of 25 kPa.

The results are presented as a sensitivity plot, such as in Figure 10-22. For this case, the stability is much more sensitive to changes in the undrained strength (c) than to changes in the sand friction angle ϕ . This is intuitively correct, since a major portion of the slip surface is in the clay layer.

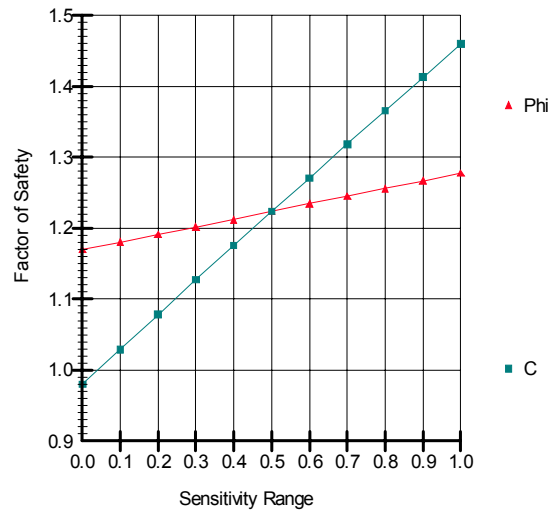


Figure 10-22 Illustration of a sensitivity plot

The point where the two sensitivity curves cross is the deterministic factor of safety or the factor of safety at the mid-point of the ranges for each of the strength parameters.

11 Illustrative Examples

11.1 *Circular slip surface analysis*

Included files

- Circle slip.gsz

The purpose of this illustrative example is primarily to show how to utilize the grid and radius slip surface option to obtain a circular critical slip surface. Other special features include:

- Analysis method: Bishop, Janbu & Ordinary Method (only)
- Multiple soil layers
- Piezometric line
- Imperial units
- Viewing and contouring Factors of Safety

With the grid and radius option, the slip surface that develops within the slope is simply the arc of a circle. A circle can be described by defining the x,y coordinate of the centre point as well as the length of the radius. With the grid and radius slip surface option, you must define a grid of points which are used by SLOPE/W as potential centre points for the circular slip surface. You must also define a range of radii or tangential points. Figure 11-1 shows the placement of the search grid and the radii lines for a multi-layered profile.

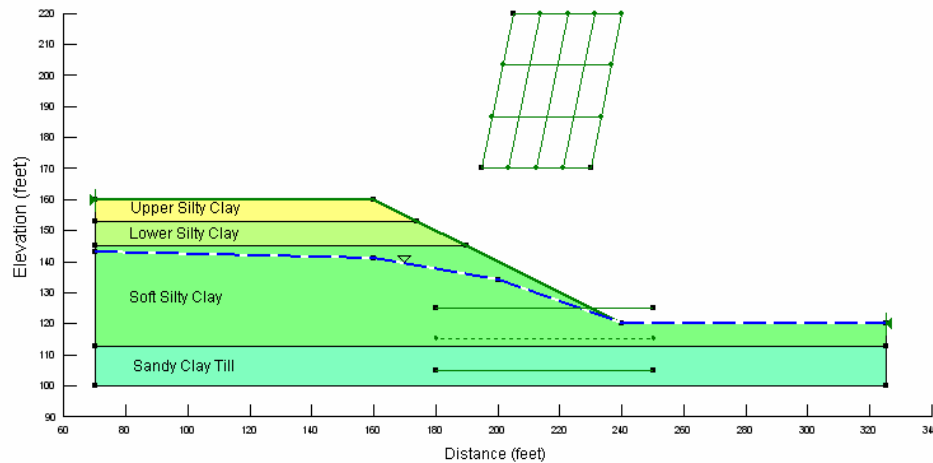


Figure 11-1 Illustrative example using the grid and radius slip surface option

By actually sketching a circle using one of the search grid points as a centre and stretching the circle until it becomes tangent with one of the radius lines, a visual expectation can be developed about whether the grid and radius features have been appropriately defined. This step is not necessary to the solution of the problem. It is simply a visual technique that can be used until placing the grid and radius features become more familiar. Figure 11-2 shows a schematic representation of one of the slip surfaces that will be analysed.

When selecting an analysis method, it is generally recommended that you utilize one of the more rigorous methods such as Morgenstern-Price, Spencer or the GLE method. These methods satisfy both force and moment equilibrium while considering both interslice shear and normal forces; and the additional computational time required is the same as it is for the non-rigorous methods (i.e., Bishop, Janbu and Ordinary). In fact, the default analysis method in SLOPE/W is the Morgenstern-Price method as well as the Bishop, Janbu and Ordinary methods. When the default option is used, the Morgenstern-Price factor of safety is what is initially presented. It is possible, however, to use the simple methods exclusively, which is useful if you know the solution will be appropriate given the profile and conditions being modeled or if you consistently want to use a less rigorous method. By choosing only Bishop, Janbu and Ordinary under the Analysis Method option within SLOPE/W, you are ensured that the Bishop Simplified result is what

is loaded upon first opening CONTOUR. For more information on the differences between methods, please refer to the chapter on Factor of Safety Methods.

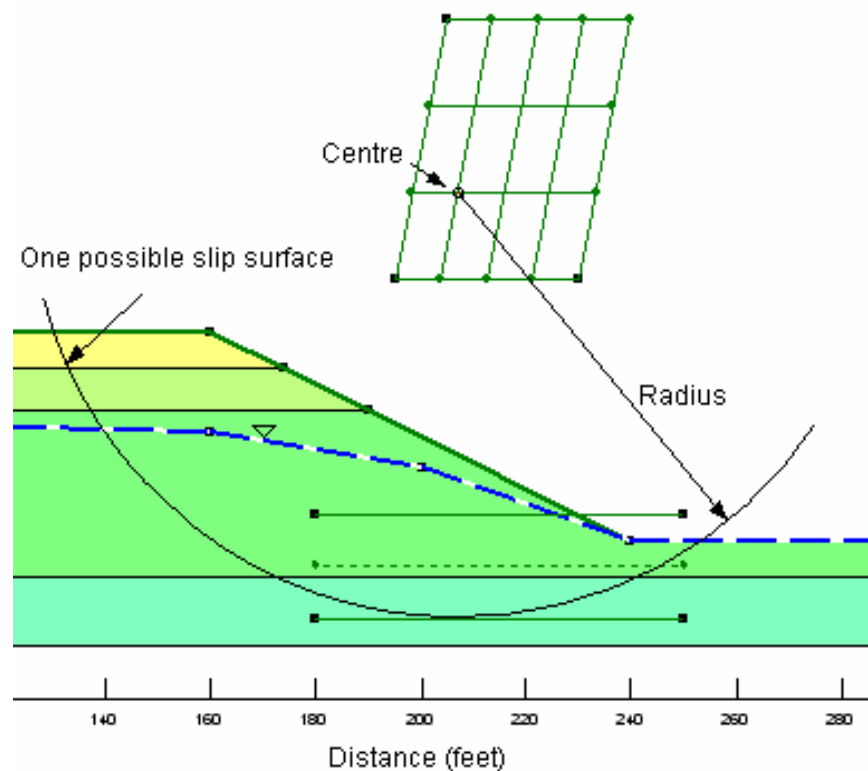


Figure 11-2 Visualization of one potential slip surface

The factor of safety obtained using the Bishop Simplified method is 1.211 and the critical slip surface is as shown in Figure 11-3.

In CONTOUR, you are not limited to simply viewing the most critical factor of safety and the critical slip surface. You can view the shape of all the slip surfaces analysed for every search grid point and view the corresponding factor of safety values on the grid.

Another powerful analyzing feature is the ability to generate factor of safety contours on the search grid. The contours provide a picture of the extent trial slip surfaces analyzed, but more importantly the contours indicate that the minimum

safety factor has been found. The ideal solution is when the minimum falls inside a closed contour as shown in Figure 11-4.

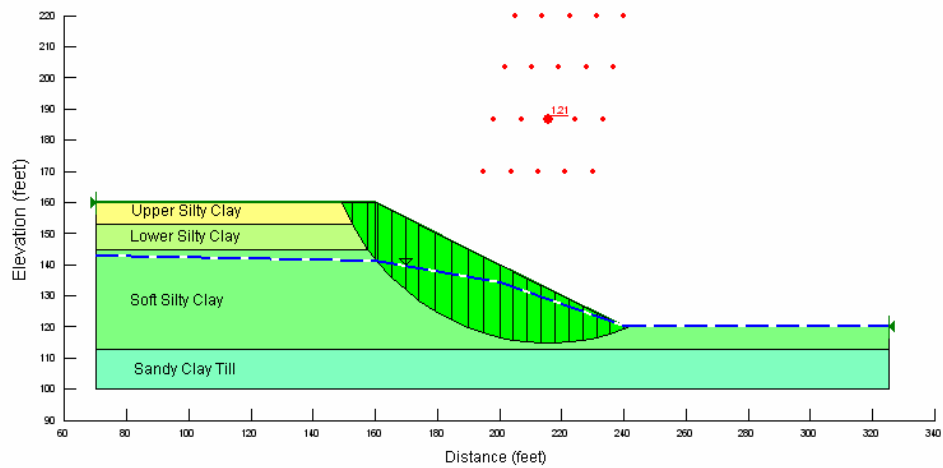
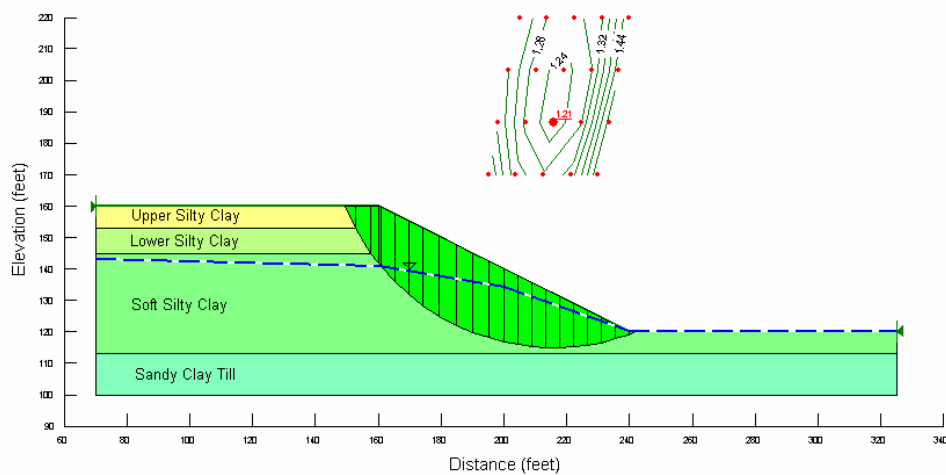


Figure 11-3 Bishop simplified factor of safety and critical slip surface



Viewing slice information and conducting hand calculations to spot check results such as the computed pore-water pressure at the base of a slice can also be very helpful in interpreting the results and ensuring the model was set up the way you intended it to be.

11.2 Composite slip surface analysis

Included file

- Composite slip.gsz

When a surficial soil overlies a considerably stronger material at depth, the potential exists for the surficial soil to slide along the contact between the two contrasting materials. The resulting slip surface is called a composite slip surface. In SLOPE/W you can analyze composite slip surfaces by forcing the slip surface to go below the interface of the two contrasting materials.

The purpose of this example is to show how to analyze a composite slip surface. Features of this simulation include:

- Analysis method: Morgenstern-Price (Constant function)
- Development of a composite slip surface
- Piezometric line
- Water represented by a pressure boundary
- Presence of a dry tension crack
- Hand calculation of the pore-water pressures on a single slice

The features of the profile being analyzed are shown in Figure 11-5.

With a composite slip surface, the slip surface enters the slope on the arc of a circle. When the slip surface intersects the interface between the weak layer and the bedrock, it follows the interface between the two materials until it intersects the circle once again, and then follows the arc of a circle up to the surface. In SLOPE/W, the grid and radius search option is used to develop a composite slip surface. The technique is to force the slip surface to go deep enough to hit the interface between the weak and strong materials by placing the search radii below the weak layer as shown in Figure 11-6.

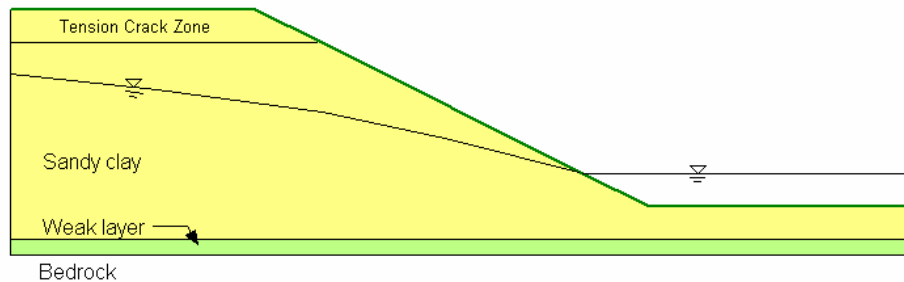


Figure 11-5 Features of a composite slip profile

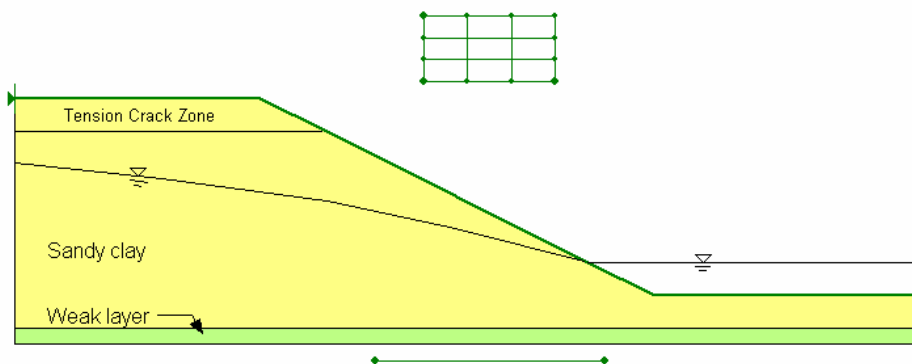


Figure 11-6 Placement of the search grid and radius

There are two different ways of handling the strong or impenetrable soil layer. It can be included in the analysis as a soil layer which has been assigned the bedrock (impenetrable) strength model. A second approach is to leave this soil layer completely out of the analysis since by placing the radii below the weak layer, the slip surface will hit the bottom of the profile and follow the bottom of the weak layer until it re-intersects the circular slip surface and exits the ground surface. For this analysis, the impenetrable layer has been left out of the profile and is assumed to exist directly beneath the soil called “weak layer”.

There are two hydraulic conditions that need to be included in the analysis. The first is the presence of a piezometric surface within the soil profile and the second is a shallow pond that exists at the bottom of the embankment. When a piezometric line is defined, it is used by SLOPE/W to determine the pore-water pressures at the

base of each slice. The stabilizing presence of ponded water at the toe of the embankment can be represented by a pressure boundary. The pressure boundary is used in computing the total weight of a slice and therefore adds a stabilizing weight when placed at the bottom of a slope as shown in Figure 11-7. When modeling a feature such as ponded water at the base of a slope, it is therefore necessary to define both a piezometric line and a pressure boundary to adequately represent both the positive pore-water pressures and the increased weight due to the presence of the ponded water.

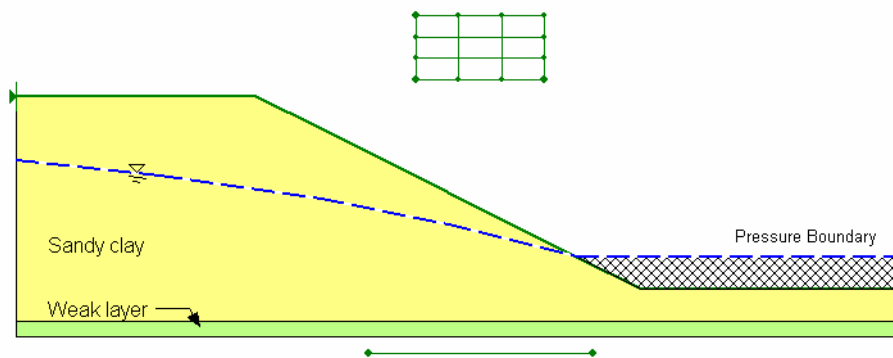


Figure 11-7 Pore-water and pressure conditions

Pore-water pressures at the base of each slice are determined by the relative position of the bottom of the slice to the piezometric line. Hydrostatic conditions are assumed to exist both above and below the piezometric line, but if advanced unsaturated soil parameters are not defined, the negative pore-water pressures that exist above the piezometric surface are set equal to zero.

The last feature to be defined in this example is the presence of a tension crack zone. In this simulation, the tension crack is represented by a tension crack line placed at a depth of 2 m below the ground surface. The implication of this feature is that when the slip surface intersects the tension crack line, the slip surface does not continue along the arc of a circle, but is projected vertically upward to the ground surface. The location of the tension crack is indicated by the vertically hatched area at the top of the embankment as shown in Figure 11-8.

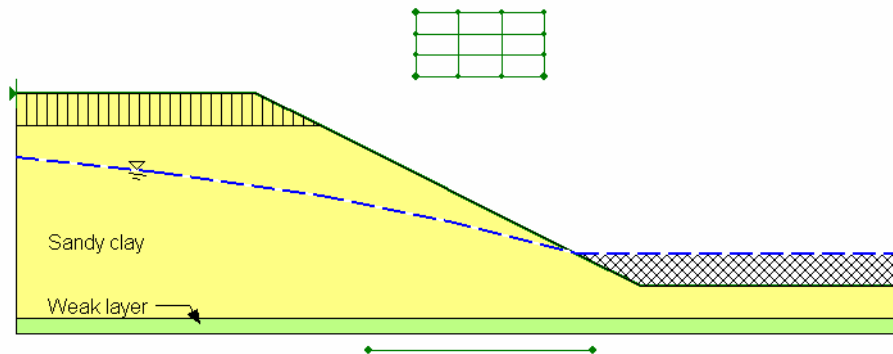


Figure 11-8 Definition of a zone prone to tension cracks

The computed factor of safety for this example is 1.139 and the critical slip surface is as shown in Figure 11-9.

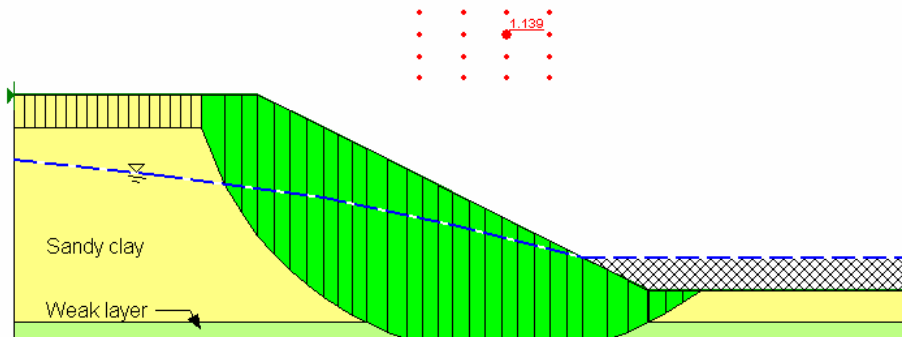


Figure 11-9 Factor of safety and the critical slip surface for Composit.gsz

Note that the shape of the slip surface is generally circular in nature except where it is forced to follow the bottom of the weak layer at the bottom of the profile and where it is forced to become vertical between the tension crack line and the ground surface.

Viewing slice information is particularly useful for verifying to yourself that the presence of the ponded water has been appropriately modeled. Figure 11-10 shows the slice information for slice number 28, which is the third slice from the right, on

horizontal ground under the ponded water. The line load at the top of the slice is 21.063 kN per unit depth. By hand calculation, given a slice width of 1.0739 m, the pressure associated with the pressure line (9.807 kN/m^2) and a water depth of 2 m, the water force should be $2 \text{ m} \times 9.807 \text{ kN/m}^2 \times 1.0739 \text{ m} = 21.063 \text{ kN}$ per unit depth.

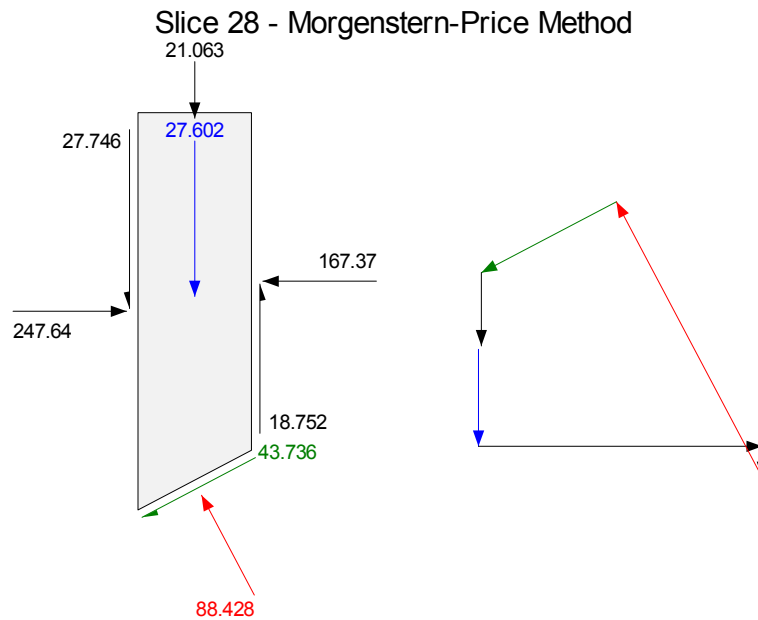


Figure 11-10 Slice forces and force polygon closure for Slice 28

The pore-water pressure at the base of the slice is provided for each slice in the slice information dialogue box. For slice 28, the pore-water pressure is 36.419 kPa (kN/m^2) and the slice mid-height is 1.7135 m. Given a ponded depth of 2 m above the top of the slice, the total height of water is 3.7135 m. Therefore the pore-water pressure should be $3.7135 \text{ m} \times 9.807 \text{ kN/m}^3 = 36.418 \text{ kN/m}^2$ or 36.418 kPa.

For more information on drawing and defining pore-water pressure options, please refer to the online help.

11.3 Hand calculation comparison of SLOPE/W

Included file

- Hand calculate.gsz

Some of the illustrative examples included with the SLOPE/W software have been developed not necessarily to highlight a specific feature, but rather to compare SLOPE/W results with benchmark studies. Comparing computed results with these benchmark studies can be used to verify the program. Other features of this analysis include:

- Analysis method: Bishop, Janbu & Ordinary Method (only)
- Homogeneous material
- Left to right slip surface
- Piezometric line
- Imperial units

Lambe and Whitman's solutions

In the textbook entitled *Soil Mechanics* by Lambe and Whitman (1969), the authors present a hand-calculated factor of safety for a simple slope with an underdrain as shown in Figure 11-11. The slope is 20 feet high, with a slope of 1 vertical to 1.5 horizontal. The material of the slope is homogenous with $c = 90$ psf, $\phi = 32$ and $\gamma = 125$ pcf. The slip surface is assumed to be circular with a radius of 30 feet from the center, as shown in Figure 11-11. The pore-water pressure conditions for the slope are characterized by a flow net.



Page 267

Table 11-1 Lambe and Whitman weight computations

Slice	Width (ft)	Average Height (ft)	Weight (kips)
1	4.5	1.6	0.9
2	3.2	4.2	1.7
2A	1.8	5.8	1.3
3	5.0	7.4	4.6
4	5.0	9.0	5.6
5	5.0	9.3	5.8
6	4.4	8.4	4.6
6A	0.6	6.7	0.5
7	3.2	3.8	1.5
			W=2.65

Table 11-2 presents Lambe and Whitman's calculation for determining the Ordinary factor of safety. The hand-calculated factor of safety is 1.19.

Table 11-2 Lambe and Whitman calculation of the Ordinary factor of safety

Slice	W_i (kips)	$\sin\theta_i$	$W_i \sin\theta_i$ (kips)	$\cos\theta_i$	$W_i \cos\theta_i$ (kips)	u_i (kips/ft)	Δl (ft)	u_i (kips)	N_i (kips)
1	0.9	-0.03	0	1.00	0.9	0	4.4	0	0.9
2	1.7	0.05	0.1	1.00	1.7	0	3.2	0	0.1
2A	1.3	0.14	0.2	1.99	1.3	0.03	1.9	0.05	0.25
3	4.6	0.25	1.2	1.97	4.5	0.21	5.3	1.1	3.4
4	5.6	0.42	2.3	1.91	5.1	0.29	5.6	1.6	3.5
5	5.8	0.58	3.4	1.81	4.7	0.25	6.2	1.55	3.15
6	4.6	0.74	3.4	1.67	3.1	0.11	6.7	0.7	2.4
6A	0.5	0.82	0.4	1.57	0.3	0	1.2	0	0.3
7	1.5	0.87	1.3	1.49	0.7	0	1.3	0	0.7
			12.3				41.8		17.3

$$F = \frac{0.09(41.8) + 17.3 \tan 32^\circ}{12.3} = \frac{3.76 + 10.82}{12.3} = \frac{14.58}{12.3} = 1.19$$

Lambe and Whitman also compute the Bishop's Simplified factor of safety using a trial and error approach. The computations and results are presented in Table 11-3.

Table 11-3 Lambe and Whitman calculation of the Bishop Simplified factor of safety

(1)	(2)	(3)	(4)	(5)	(6)	(7)	(8)		(9)	
Slice	Δx (ft)	$c\Delta x_i$ (kips)	$ui\Delta x_i$ (kips)	$W_i - ui\Delta x_i$ (kips)	$(5)\tan \phi$ (kips)	$(3)+(6)$ (kips)	Mi		(7) + (8)	
							F = 1.25	F = 1.35	F = 1.25	F = 1.35
1	4.5	0.40	0	0.9	0.55	0.95	0.97	0.97	1.0	1.0
2	3.2	0.29	0	1.7	1.05	1.35	1.02	1.02	1.3	1.3
2A	1.8	0.16	0.05	1.25	1.80	1.95	1.06	1.05	0.9	0.9
3	5.0	0.45	1.05	3.55	2.25	2.70	1.09	1.08	2.5	2.5
4	5.0	0.45	1.45	4.15	2.55	3.00	1.12	1.10	2.7	2.75
5	5.0	0.45	1.25	4.55	2.7	3.15	1.10	1.08	3.85	2.9
6	4.4	0.40	0.50	4.1	2.63	3.05	1.05	1.02	2.9	2.95
6a	0.6	0.05	0	0.5	2.30	0.35	0.98	0.95	0.35	0.4
7	3.2	0.29	0	1.5	2.95	1.25	0.93	0.92	1.3	1.35
									15.8	16.05

For assumed $F = 1.25$ $F = \frac{15.8}{12.3} = 1.29$

$F = 1.35$ $F = \frac{16.05}{12.3} = 1.31$

As shown in the above calculations, a trial factor of safety of 1.25 results in a computed factor of safety of 1.29, and a trial factor of safety of 1.35 results in a computed value of 1.31. Since the trial value of 1.25 is too low and the trial value of 1.35 is too high, the correct value using the Bishop Simplified method is between 1.25 and 1.35.

SLOPE/W Solutions

The same problem is analyzed using SLOPE/W. Figure 11-12 shows the same slope as modeled by SLOPE/W.

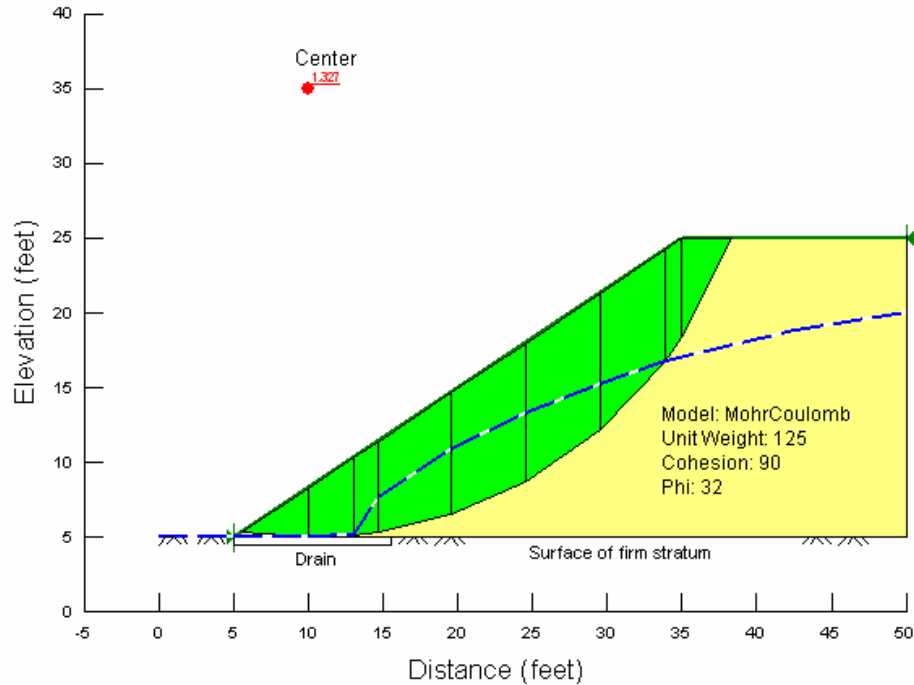


Figure 11-12 Stability of slope with an underdrain using SLOPE/W

Nine slices are also used in the analysis. The computed slice width, average height and weight of the sliding mass are tabulated in Table 11-4. The total weight of the sliding mass is 26,711 lbs. The slices modeled by SLOPE/W are very similar, but not precisely the same as those used by Lambe and Whitman.

Table 11-5 presents the hand calculated factor of safety for the Ordinary method using the slice quantities computed by SLOPE/W. The slice quantities in Table 11-4 and

Table 11-5 are taken from the forces file **HAND CALCULATE.FRC01** and can be displayed using the View Slice Forces command for the **HAND CALCULATE.GSZ** file under SLOPE/W CONTOUR.

Table 11-4 SLOPE/W weight computations

Slice Number	Width (ft)	Average Height (ft)	Weight (lbs)
1	4.49	1.75	983.65
2	3	4.30	1610.90
3	1.70	5.65	1201.00
4	4.80	7.21	4328.60
5	5	8.83	5518.00
6	5	9.39	5865.70
7	4.35	8.52	4636.60
8	1.15	7.04	1009.90
9	3.28	3.79	1556.40
			26710.75

Table 11-5 SLOPE/W calculation of the Ordinary factor of safety

Slice Number	Weight	α	Weight $\times \sin \alpha$	Normal	Water	Normal - Water	Base Length
1	983.7	-4.31	-73.9	980.9	0	980.9	4.51
2	1610.9	2.87	80.6	1608.9	7.1	1601.8	3.01
3	1201.0	7.38	154.2	1191.1	123.5	1067.6	1.711
4	4328.6	13.74	1027.9	4204.8	1059.4	3145.4	4.95
5	5518.0	23.68	2216.4	5053.3	1575.5	3477.8	5.47
6	5865.7	34.72	3341.1	4821.1	1532.6	3288.5	6.09
7	4636.6	46.60	3368.9	3185.7	708.0	2477.7	6.35
8	1009.9	54.55	822.7	585.7	0	585.7	1.98
9	1556.4	63.49	1392.7	694.8	0	694.8	7.38
Total	26710.8		12330.6			17320.2	41.44

$$F = \frac{90 \times 41.44 + 17320.2 \tan 32}{12330.6} = 1.180$$

The SLOPE/W computed value is 1.186. Except for a slight difference due to rounding errors, SLOPE/W gives the same factor of safety as the Lambe and Whitman hand calculated value of 1.19.

The Bishop Simplified factor of safety computed by SLOPE/W is 1.327, which is within the 1.25 to 1.35 range calculated by Lambe and Whitman (Table 11-3). This value is shown in Figure 11-12.

11.4 Comparison with stability charts

Included file

- Stability chart.gsz

In the 1960's, bishop and Morgenstern developed a series of stability charts that can be used to estimate the factors of safety for simple homogeneous earth slopes. The purpose of this detailed example is to compare and verify the SLOPE/W solution with a factor of safety estimated using stability charts. Features of this simulation include:

- Analysis method: Morgenstern-Price (Constant function))
- Use of Ru coefficients
- SI units

Bishop and Morgenstern's solution

Figure 11-13 shows a 4:1 slope with $c' = 12.5 \text{ kN/m}^2$, $\phi' = 20^\circ$, $\gamma = 16 \text{ kN/m}^3$, and $R_u = 0.35$.

The height of the slope from crest to toe is 31 m. Therefore, the dimensionless parameter is:

$$\frac{c'}{\gamma H} = \frac{12.5}{16 \times 31} = 0.025$$

The appropriate D factor for $R_u = 0.35$ is 1.25. The stability coefficients from the Bishop and Morgenstern charts are $m = 1.97$ and $n = 1.78$. Therefore, the factor of safety of the slope using stability charts is calculated to be 1.35.

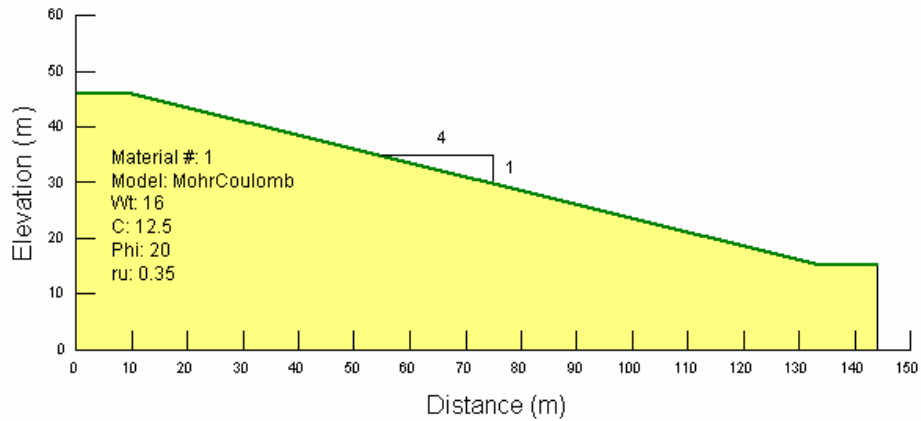


Figure 11-13 Homogeneous slope example

SLOPE/W solution stability chart

The same slope is analyzed with SLOPE/W. The sliding mass contains 30 slices. Figure 11-14 illustrates the slope modeled with SLOPE/W.

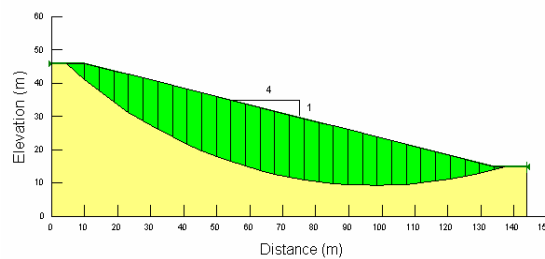
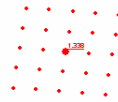


Figure 11-14 Critical slip surface of homogeneous slope

The factor of safety computed by SLOPE/W is 1.34 for both the Bishop Simplified method and the Morgenstern-Price method. This is in close agreement with 1.35 as estimated from the stability charts.

11.5 Comparison with closed form solutions for an infinite slope

Included file

- Infinite slope.gsz

Another way to verify a numerical modeling program such as SLOPE/W is to compare computed results with those computed with closed form solutions. For this detailed example, three cases of an infinite slope are considered. In all cases, the factors of safety computed by SLOPE/W are identical to the closed form solutions. The information provided below shows how to modify the included file to represent the 3 cases highlighted in this illustrative example. Other features of this analysis include:

- Analysis method: Morgenstern-Price (Constant function))
- Homogeneous material
- Use of fully-specified slip surface
- Presence of a dry tension crack
- Use of R_u coefficients
- SI units

Closed form solution for an infinite slope

Consider the case of a 2:1 slope, as illustrated in Figure 11-15. The sliding mass is assumed to be parallel to the slope surface (infinite slope).

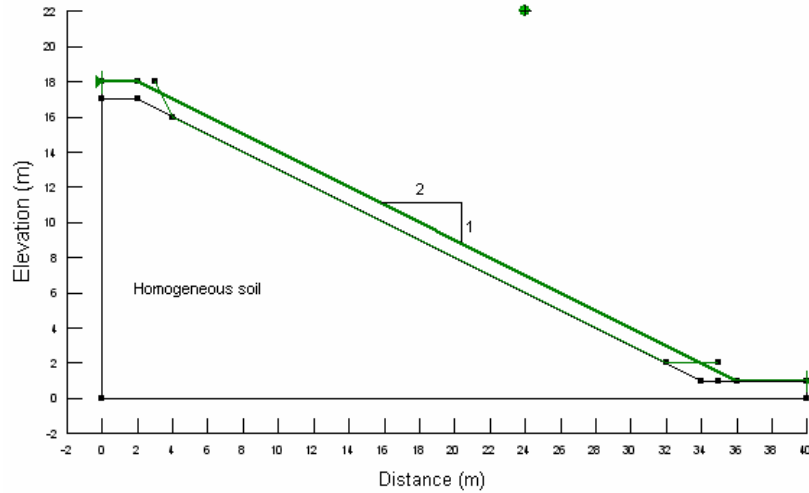


Figure 11-15 Homogeneous infinite slope

Three cases of the closed form solutions are considered. The factors of safety for the three cases are calculated assuming the parameters shown in Table 11-6.

Table 11-6 Parameter values used for infinite slope analyses

Parameter	Values Used		
	Case 1	Case 2	Case 3
Frictional Angle, ϕ (degrees)	35	35	35
Cohesion, c' (kPa)	0	0	5
Pore-water Coefficient, r_u	0	0.25	0.25
Unit Weight, γ (kN/m ³)	19.62	19.62	19.62
Steepness, α (degrees)	26.565 (2:1 slope)	26.565 (2:1 slope)	26.565 (2:1 slope)
Vertical Height, H (m)	1.0	1.0	1.0

Case 1: Dry Frictional Material with No Cohesion

For a dry infinite slope consisting of a frictional material with no cohesion, the factor of safety is:

$$\text{Factor of Safety} = \frac{\tan \phi'}{\tan \alpha} = \frac{\tan 35^\circ}{\tan 26.565^\circ} = 1.400$$

Case 2: Wet Frictional Material with No Cohesion

For a frictional material with no cohesion under the conditions of flow parallel to the slope (i.e., pore-water pressure characterized by R_u), the factor of safety is:

$$\begin{aligned} \text{Factor of Safety} &= (1 - R_u \sec^2 \alpha) \frac{\tan \phi'}{\tan \alpha} \\ &= (1 - 0.25 \times \sec^2 26.565^\circ) \times 1.400 \\ &= 0.963 \end{aligned}$$

Case 3: Wet Frictional Material with Cohesion

For a frictional material with cohesion under the conditions of flow parallel to the slope, the factor of safety is:

$$\begin{aligned} \text{Factor of Safety} &= \frac{c'}{\gamma H \cos \alpha \sin \alpha} + (1 - R_u \sec^2 \alpha) \frac{\tan \phi'}{\tan \alpha} \\ &= \frac{5.0}{19.62 \times 1.0 \times \cos 26.565^\circ \times \sin 26.565^\circ} + 0.963 \\ &= 1.600 \end{aligned}$$

SLOPE/W solution closed form

The three cases of the infinite slope are analyzed using SLOPE/W. Figure 11-16 illustrates the solution for Case 1, where the Morgenstern-Price method is used. A fully specified slip surface was used to compare the same slip surface. The vertical edges of the slip surface were created by defining a tension crack zone, which results in the slip surface being projected vertically up to the surface when intersected. The sliding mass is simulated with 30 slices.

The associated SLOPE/W files for Case 1 is provided with the software, and the data file for Case 2 can be achieved by changing the pore-water coefficient(R_u) value of the soil in Case 1 from 0.0 to 0.25. Case 3 can be obtained by changing the cohesion (c) value in Case 2 from 0.0 to 5.0.

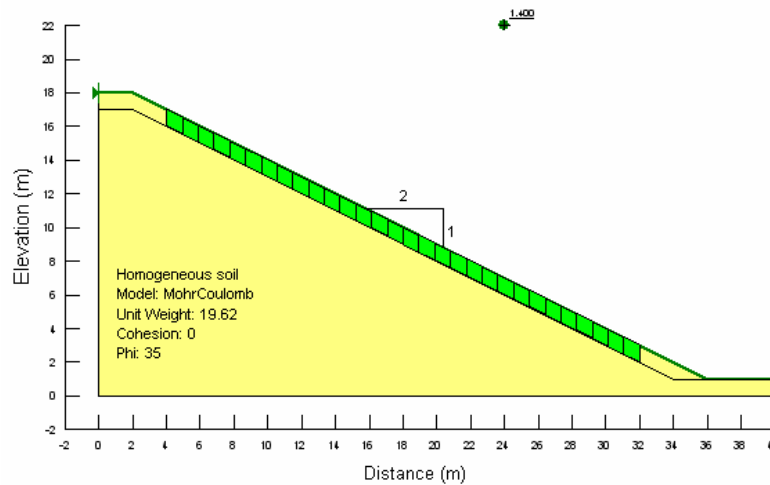


Figure 11-16 SLOPE/W solution of the infinite slope case

Table 11-7 tabulates the comparison of the three cases between the closed form solutions and the SLOPE/W solutions. Factors of safety for the Bishop Simplified method and the Morgenstern-Price method are presented. In all cases, SLOPE/W gives essentially the same factors of safety as the closed form solutions.

Table 11-7 Comparison of SLOPE/W solutions with closed form solutions for an infinite slope

Case	ϕ'	c'	R_u	Factor of Safety		
				Closed Form Solution	SLOPE/W Bishop Simplified	SLOPE/W Morgenstern-Price
1	35	0.0	0.0	1.400	1.402	1.400
2	35	0.0	0.25	0.963	0.965	0.963
3	35	5.0	0.25	1.600	1.601	1.600

11.6 Comparison study

Included file

- Compare.gsz

The purpose of this detailed example is to compare the SLOPE/W program with different computer programs as part of a verification exercise. Features of this simulation include:

- Analysis method: Spencer
- Development of a composite slip surface
- Grid and Radius: Using a single slip surface for comparison purposes
- Imperial units

The information contained in this comparison study is an extension of a detailed study conducted by Fredlund and Krahn, 1977. Fredlund and Krahn analyzed the problem presented in Figure 11-17 as part of a comparison study of slope stability methods. They used the original Morgenstern-Price computer program, as modified at the University of Alberta, (Krahn, Price and Morgenstern, 1971), and compared it with a slope stability program developed by Fredlund, 1974, at the University of Saskatchewan.

The problem shown in Figure 11-17 was re-analyzed with SLOPE/W. The soil properties and the pore-water pressure conditions of the slope were varied to simulate several different cases. Table 11-8 presents the factors of safety and lambda values as computed by the University of Alberta, University of Saskatchewan and the SLOPE/W computer programs with constant side force functions.

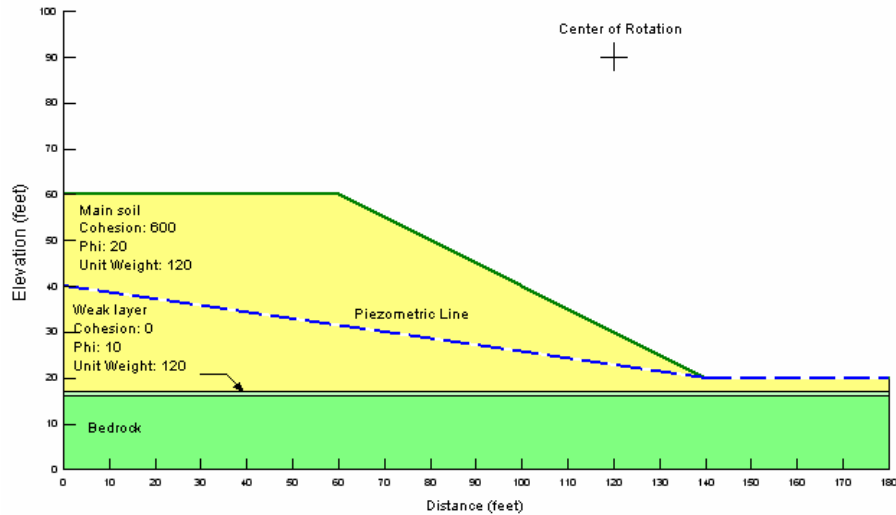


Figure 11-17 Example problem for comparison of different computer programs

The associated SLOPE/W files for Case 6 (with piezometric line, weak layer and bedrock) are included with the software. The data file for Case 1 can be obtained by making all soil properties the same as Soil 1 and selecting no pore-water pressure. The data file for Case 2 can be obtained by adding the soil properties of the weak layer (Soil 2) and the soil properties of the bedrock (Soil 3) to Case 1. The data file for Case 3 can be obtained by changing the pore-water coefficient (R_u) value of the soil in Case 1 from 0.0 to 0.25. The data file for Case 4 can be obtained by changing the pore-water coefficient (r_u) value of the soil in Case 2 from 0.0 to 0.25. The data file for Case 5 can be obtained by adding the piezometric line to Soils 1 to 3 in Case 1.

SLOPE/W gives essentially the same factors of safety as the University of Alberta and University of Saskatchewan computer program. The small differences are principally due to slight differences in geometric interpretation of the sections and different procedures for subdividing the potential sliding mass into slices.

Table 11-8 Comparison of SLOPE/W with other computer programs

Case	Description	U of A		U of S		SLOPE/W	
		F of S	λ	F of S	λ	F of S	λ
1	No pore-water pressure, no weak layer, no bedrock	2.085	0.257	2.076	0.254	2.071	0.262
2	No pore-water pressure, with weak layer & bedrock	1.394	0.182	1.378	0.159	1.338	0.182
3	With $ru = 0.25$, no weak layer, no bedrock	1.772	0.351	1.765	0.244	1.756	0.253
4	With $ru = 0.25$, with weak layer & bedrock	1.137	0.334	1.124	0.116	1.081	0.157
5	With piezometric line, no weak layer, no bedrock.	1.838	0.270	1.833	0.234	1.827	0.245
6	With piezometric line, with weak layer & bedrock	1.265	0.159	1.250	0.097	1.211	0.129

In this analysis, it was critical to conduct multiple analyses on a single slip surface, which is often important when comparing results. To create a single slip surface, the grid and radius slip surface option was utilized, but the search grid was represented by a single center of rotation and the search radii were reduced to a single radius as shown in Figure 11-18.

Normally, when defining a search grid, the top left corner, bottom left corner and bottom right corner need to be identified and then the number of increments of the grid are selected. For this simulation, the search grid was collapsed and represented by one point by clicking in a single location three times (marked center of rotation above). Likewise, one search radius was defined by clicking in a single location four times forcing a fixed radius point (also shown above). By projecting the arc of a circle on the profile, we can see what the circular slip surface will look like for Case 1. The resulting composite slip surface for Case 6 is shown in Figure 11-19.

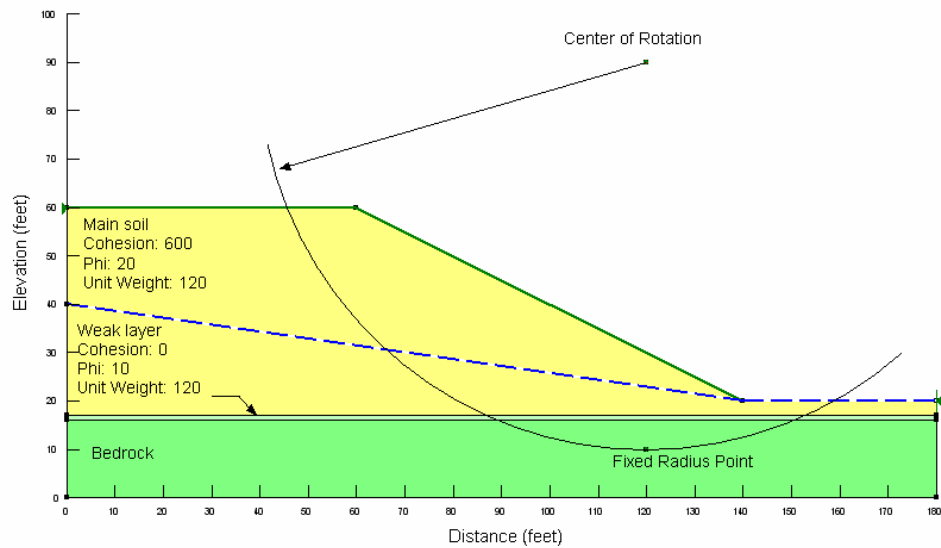


Figure 11-18 Location of the search center and fixed radius point

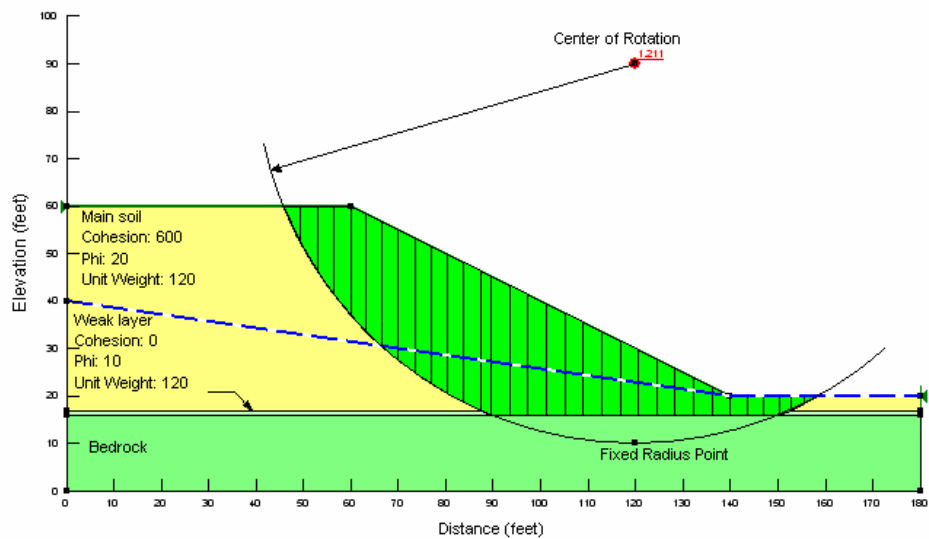


Figure 11-19 Projected slip surface and actual composite slip surface

11.7 Fully specified slip surface analysis

Included file

- Specify slip.gsz

The purpose of this example is to outline and describe an appropriate procedure for analyzing the stability of the gravity retaining wall as shown in Figure 11-20. Features of this simulation include:

- Analysis Method: Spencer
- Use of a no-strength soil model to represent non-water materials
- Fully specified slip surface
- Optimization of the slip surface
- SI units

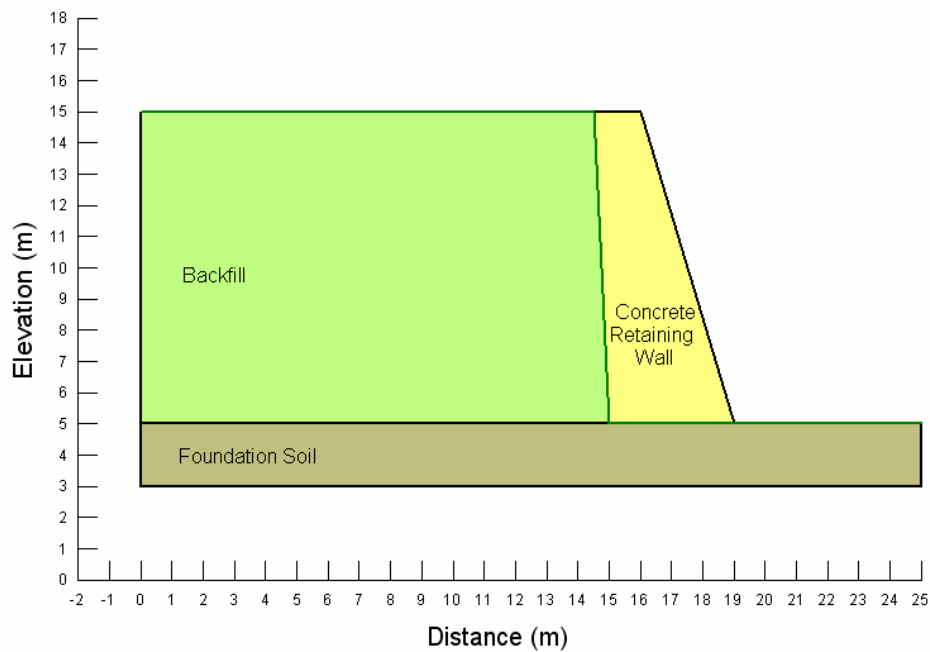


Figure 11-20 Profile used for fully specified slip surface simulation

The difficulty with retaining walls is that they are often concrete or a similar material which, compared to soil, are extremely strong. It is not advisable to include the actual strength of the retaining wall in the analysis, due to potential convergence difficulties. Consider also that failure of retaining walls is usually a result of undercutting of the retaining wall, not shearing of the concrete itself. For this mode of failure, the strength of the retaining wall itself becomes inconsequential, but the weight of the wall acting as a stabilizing force is critical.

By defining a series of fully specified slip surfaces that pass beneath the gravity retaining wall, an undercutting failure mechanism can be analyzed and the actual strength of the wall (i.e., c' and ϕ') does not need to be quantified. The gravity retaining wall should be modeled as a no-strength soil model with an appropriate unit weight that ensures that the weight of the wall is included in the analysis. The strength parameters of the concrete do not need to be quantified.

In this example, a series of fully specified slip surfaces that pass underneath the gravity retaining wall are specified and an axis of rotation is defined as shown in Figure 11-21. When using an axis of rotation, it is important to ensure that a rigorous analysis method that satisfies both force and moment equilibrium is used (i.e., Spencer, Morgenstern-Price, GLE) as the solution is insensitive to the location of the axis.

Note that all seven of the fully specified slip surfaces start and end outside the geometry of the profile. The slip surfaces have different projection angles behind the retaining wall, but coalesce to a single failure plane under the wall itself.

The material properties used in this analysis are shown in Table 11-9.

Table 11-9 Material properties used for the fully specified slip surface example

Material	Unit Weight	c'	ϕ'
Retaining Wall	22	—	—
Backfill	18	10	35
Foundation Soil	18	10	25

The critical slip surface and factor of safety is shown in Figure 11-22.

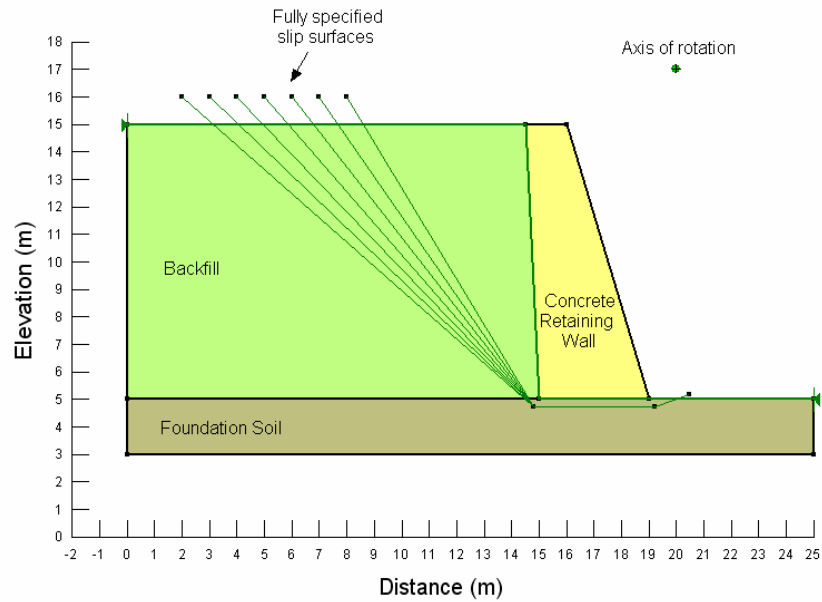


Figure 11-21 Location of the fully specified slip surfaces and the axis of rotation

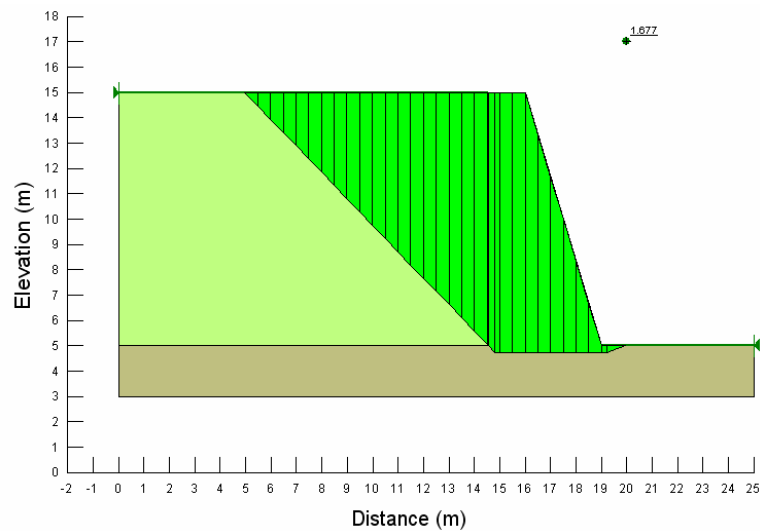


Figure 11-22 Factor of safety and location of the critical slip surface

Since a slip surface with angular corners is not physically realistic, optimization of the critical slip surface was performed, which resulted in a lower factor of safety and a slip surface as shown in Figure 11-23. For this particular situation, the optimized slip surface analysis becomes an enhancement to the original critical slip surface analysis.

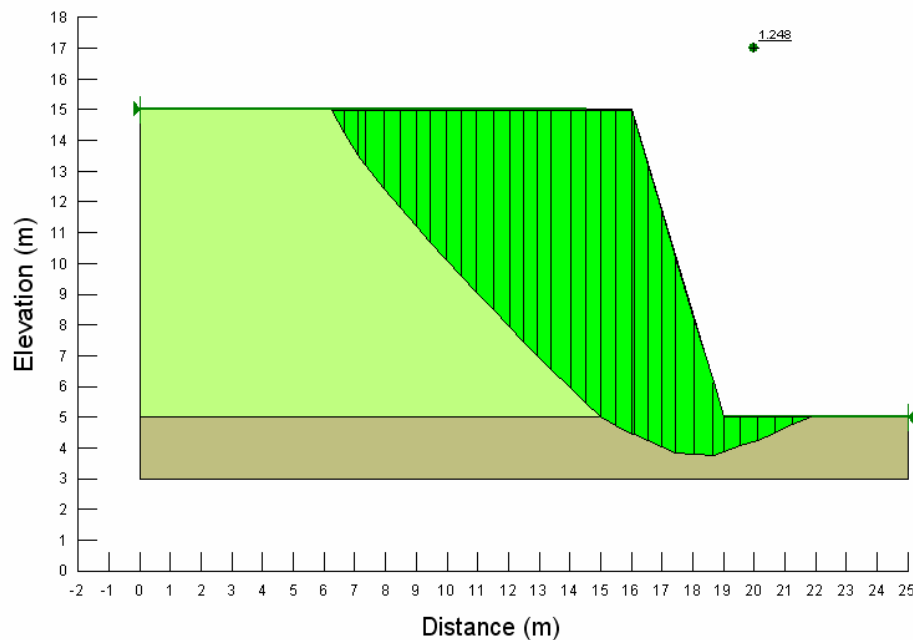


Figure 11-23 Shape and factor of safety of the optimized slip surface

It is important to note that while the optimized slip surface presented for this particular simulation appears to be reasonable, it is possible that the optimized slip surface might have been significantly different in shape than the original fully specified critical slip surface. For example, it is possible that during the optimization procedure, a slip surface with an even lower factor of safety may have been found, which resulted in a slip surface that cut through the gravity retaining wall. Since the purpose of this analysis was specifically to study a mode of failure that undercut the wall, this would have to be interpreted and dismissed as an invalid solution. Care should be used when using optimization with a fully specified slip surface analysis to ensure that the primary objectives are not compromised.

11.8 Block specified slip surface analysis

Included file

- Block.gsz

The purpose of this example is to show how to use the block specified slip surface option. Features of this simulation include:

- Analysis method: Morgenstern-Price (Half-sine function)
- Block specified slip surface
- Water modeled as a no-strength material
- Piezometric line
- Wet tension crack
- SI units

Block searches are especially useful when an embankment rests on a relatively thick stratum of weak material as shown in Figure 11-24. In this particular example, other features include the presence of water at the toe of the embankment, a piezometric line and a desiccated clay layer, which is assumed to have tension cracks that are fully saturated.

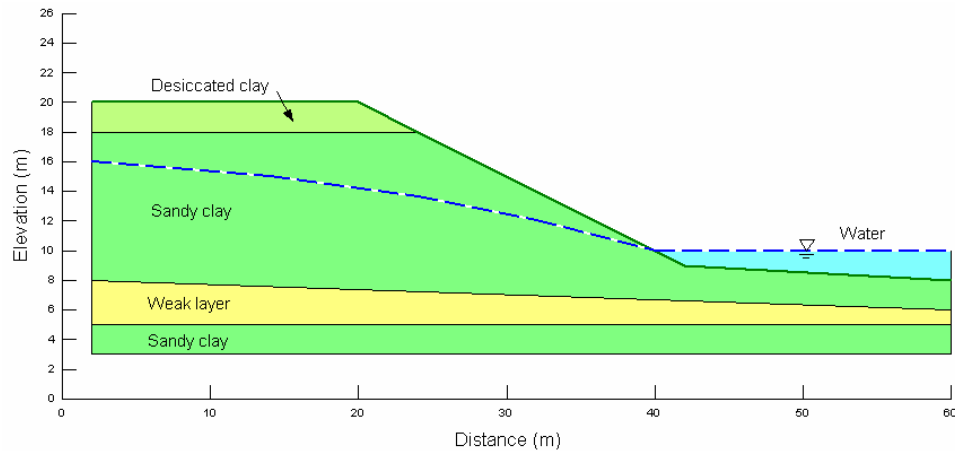


Figure 11-24 Profile used for the block specified slip search example

The material properties of the materials used in this analysis can be found in Table 11-10.

Table 11-10 Material properties for the block specified analysis

Description	Soil Model	Unit Weight	c'	ϕ'
Water	No Strength (e.g., water)	9.807	–	–
Desiccated clay	Mohr-Coulomb	15	10	25
Sandy clay	Mohr-Coulomb	18	20	30
Weak layer	Mohr-Coulomb	18	0	10

There are two ways that the weight contributed by free standing water can be modeled in SLOPE/W. One way is to use a pressure boundary as was shown earlier in the Composite Slip Surface Analysis detailed example and another is to model it as a separate material which is assigned a no-strength soil model. The unit weight of the no-strength material is then set to be equal to the unit weight of water (i.e., 9.807 kN/m³). For both of these options, you also must say something about the pore-water pressures in addition to the pressure boundary or no-strength soil, i.e., piezometric line, pressure contours etc. In this particular example, a piezometric line was drawn through the profile and over the surface of the ponded water. The piezometric line is then used to determine the pore-water pressures at the base of each slice.

For a block search analysis, an axis of rotation is defined in addition to a left and right grid of points. A series of slip surfaces are developed that consist of three line segments. One of the segments is a line that extends from a grid point in the left block over to a grid point in the right block. The other two line segments are projections to the ground surface at a range of specified angles from each block. These three line segments define a single slip surface. All the grid points in the right block are connected to all the grid points in the left block, resulting in a large number of potential slip surfaces to be analysed. Although a range of projection angles can be specified, for this particular example, a single projection angle was defined for each block as shown by the green arrows in Figure 11-25.

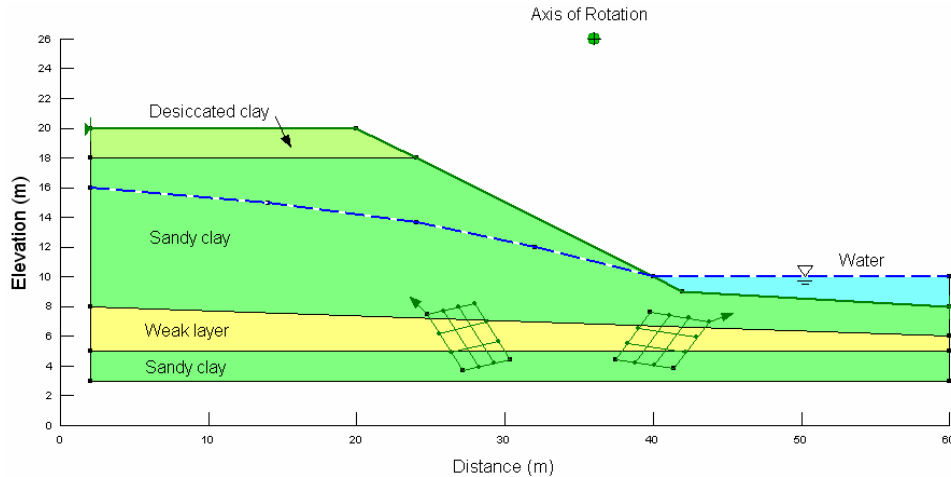


Figure 11-25 Location of the axis of rotation and blocks

While an axis of rotation is required for this type of analysis, the solution will not be overly sensitive to the location of the axis, as long as a rigorous solution method is being used (i.e., Morgenstern-Price, Spencer, GLE).

In this example, a tension crack zone is defined by drawing tension crack line and indicating that the tension crack is completely filled with water. The presence of water in the tension crack results does not affect the pore-water pressure existing at the base of the slice, but it does result in a small hydrostatic pressure being applied to the outermost slice existing at the top of the embankment.

Figure 11-26 shows the resulting factor of safety (1.070) and the location of the critical slip surface. Note that while the slip surface is comprised of three lines, the direction of the two projection lines is altered by the presence of the tension crack zone in the desiccated clay layer and the no-strength water layer. The vertical projection of these lines indicates that no resisting strength is contributed by these two materials.

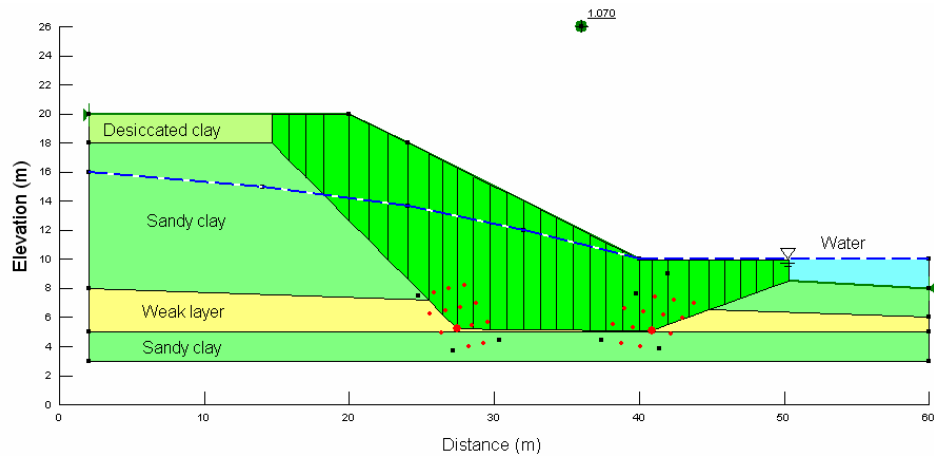


Figure 11-26 Factor of safety and location of the critical slip surface

The presence of the water in the tension crack can be confirmed by viewing slice force information for the left-most slice in the slip surface. Figure 11-27 shows the slice forces acting on this slice and the presence of a left side force (water pressure acting over the side area of the slice) equal to 19.6 kN.

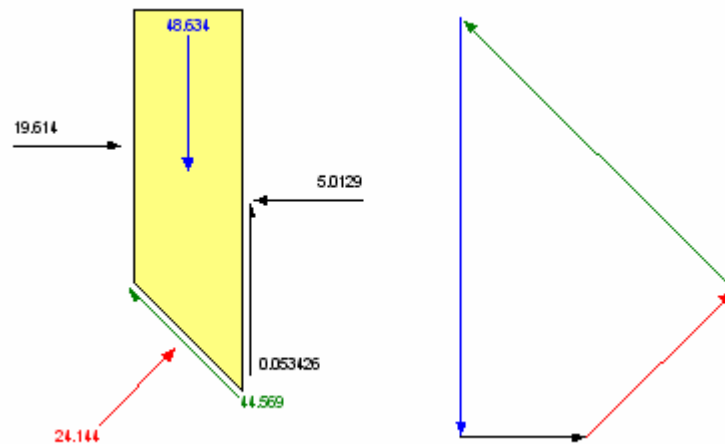


Figure 11-27 Slice forces for the left most slice at the top of the embankment

You can also use view slice forces to verify that the ponded water has been appropriately modeled. Figure 11-28 shows the slice forces for the right most slice of the critical slip surface. Note that the slice extends all the way up to the surface of the water and therefore the weight of the water has been incorporated into the weight of the slice, not represented as a line load acting on the top of the slice as would happen if a pressure boundary was used to model the water (refer to the Composite Slip Surface detailed analysis to view slice results where a pressure boundary has been used). The pore-water pressure at the base of the slice as reported in the detailed slice force information is 16.316 kPa (kN/m^2). Given that the depth of water to the mid-point at the base of the slice is 1.6637 m and the unit weight of water is 9.807 kN/m^3 , the pore-water pressure is correct as calculated.

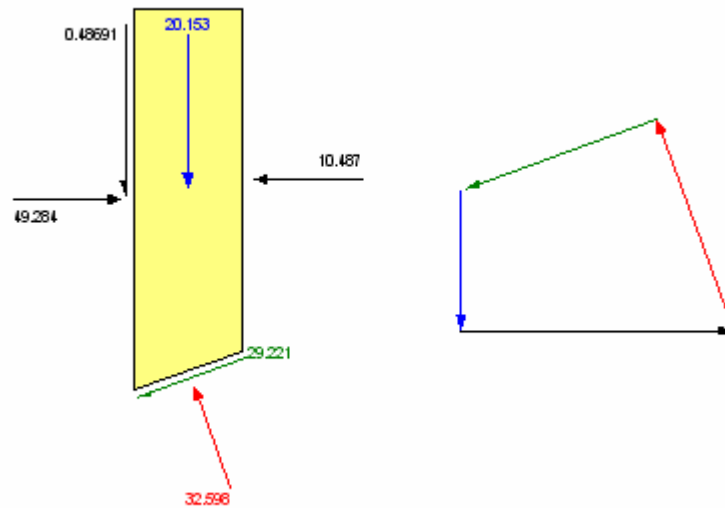


Figure 11-28 Slice forces for the right most slice at the bottom of the embankment

Figure 11-29 shows a plot of the shear strength available and the shear strength mobilized along the slip surface. Note that the two curves are very similar to each other, which is reflected in the factor of safety being very close to unity (i.e., 1.07).

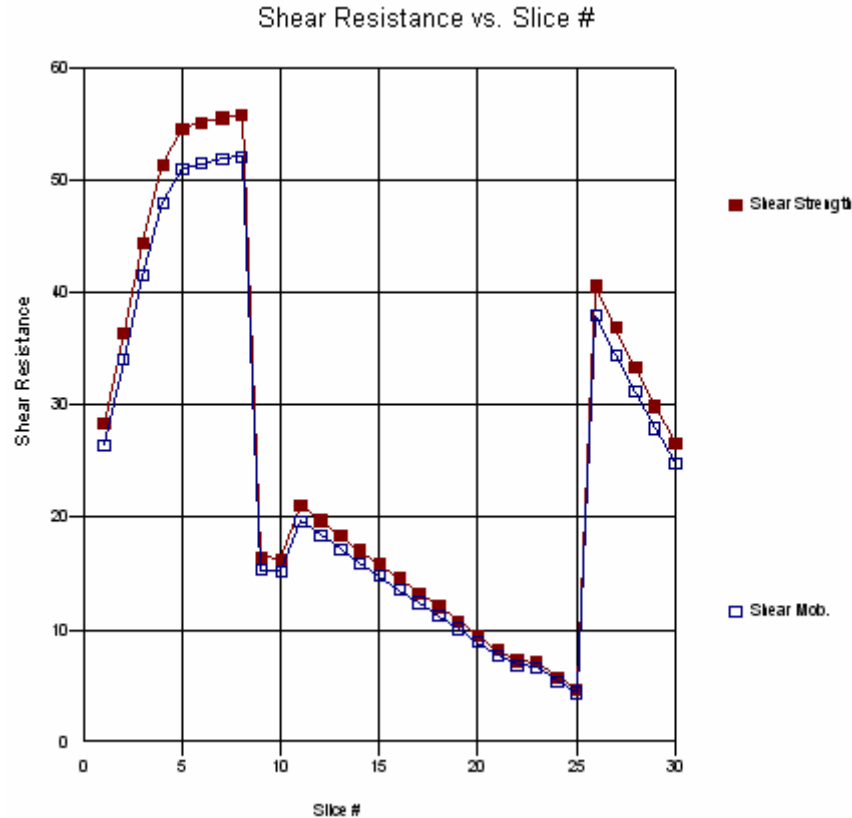


Figure 11-29 Graph of the shear strength available and the shear strength mobilized along the slip surface

11.9 Pore-water pressures defined by pressure data points

There are several different ways that pore-water pressures can be defined within SLOPE/W. For the most simple of scenarios, a piezometric line can easily be drawn with hydrostatic conditions assumed both above and below the piezometric line. For more complex pore-water pressures situations, you may want to integrate results from a SEEP/W finite element analysis where the total heads at each node are computed and used by SLOPE/W (see the SEEP/W computed pressures detailed example). Another option is to specify different pore-water pressures at discrete points within the SLOPE/W profile using the grid of pressure head (or pressures) option.

The purpose of this example is to highlight the use of the grid of pressure head option. Features in this analysis include:

- Analysis method: GLE method (Half-sine function)
- Surface entry and exit slip surface option
- Grid of pressure head option
- Tension crack angle
- Imperial units

Figure 11-30 shows the profile and material property information used to develop this simulation. The embankment is approximately 40 feet high and the associated data file can be found in the SLOPE/W examples folder (if installed) called **POINT PWP.GSZ**.

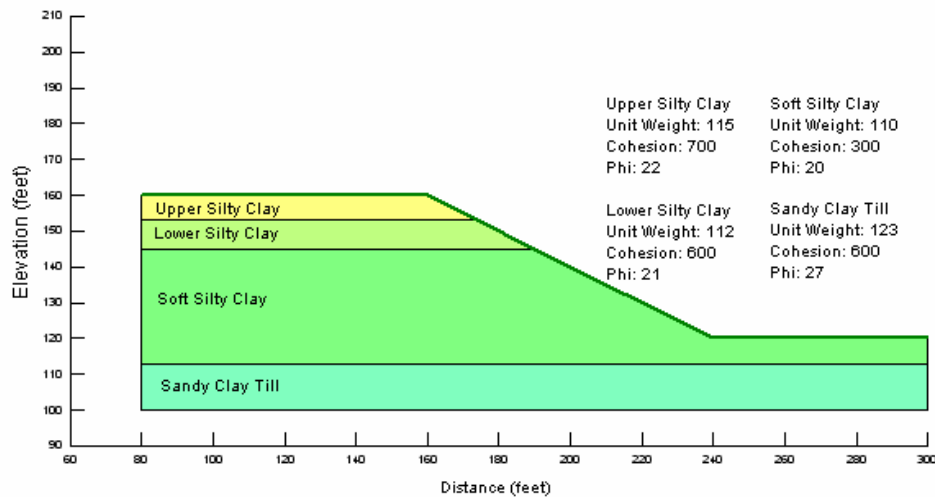


Figure 11-30 Profile and material property information

For this detailed example, pore-water pressure heads are known at a large number of locations and each location is assigned a pressure head value as shown in Figure 11-31.

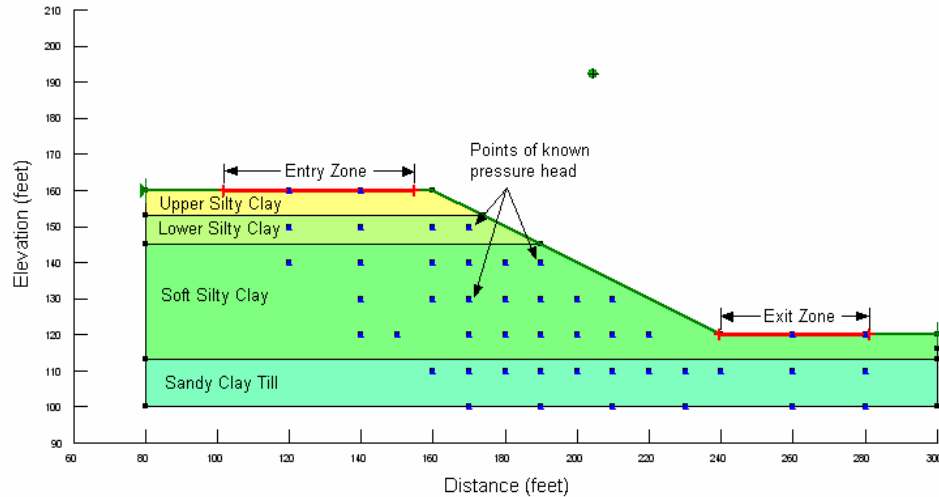


Figure 11-31 Series of points representing pore-water pressure heads within the profile

Using Spline interpretation techniques (see Theory Chapter for details), SLOPE/W constructs a smooth surface that passes through all the specified points. Once the surface has been constructed, the pore-water pressure can be determined at any other x-y coordinate point in the vicinity of the specified data points. For each slice, SLOPE/W knows the x-y coordinates at the slice base mid-point. These x-y coordinates together with the pore-water pressure surface are then used to establish the pore-water pressure at the base of each slice.

There are a couple of other interesting features which have been included in this example, namely the entry and exit slip surface option and a tension crack angle. With the slip surface option, both an entry and exit zone are identified on the ground surface and all analysed slip surfaces are controlled by the location of these zones. The entry and exit zone for this simulation is identified in Figure 11-31.

When a tension crack angle is defined, the program will project vertically to the surface any slip surface that exceeds this limiting angle. If the angle at the base of the slice does not exceed the tension crack angle, a tension crack will not form. The tension crack angle for this simulation has been set equal to 120 degrees. In addition, if a tension crack forms, it is assumed to be water-filled.

For this simulation a GLE method was used with a half-sine interslice force function. The resulting factor of safety of 1.209 and critical slip surface are shown in Figure 11-32.

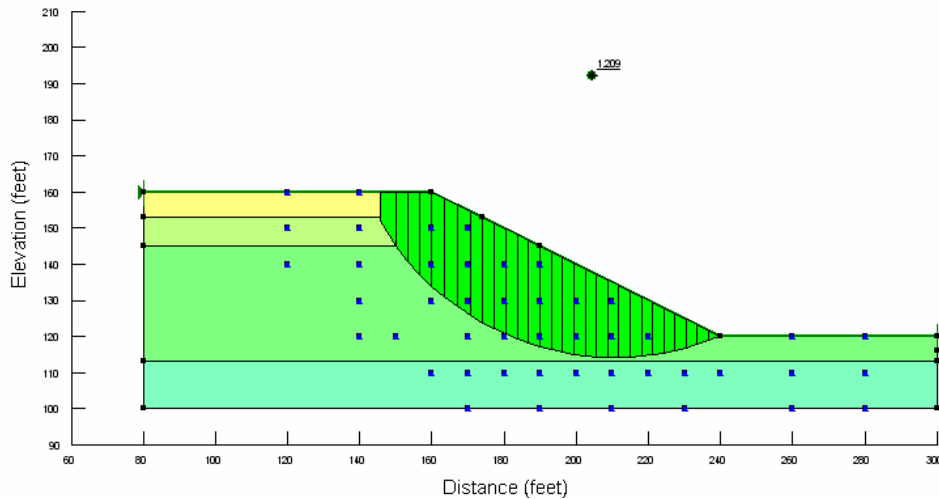


Figure 11-32 Critical slip surface and factor of safety

You can see the development of a tension crack on the top of the embankment where the slip surface is projected vertically upward. Viewing the slice force information for the top left slice shows the presence of a water pressure force acting on the left side of the slice equal to $\gamma H^2/2$ which is the water pressure acting against the wall of the slice.

When conducting a GLE method, you can also generate the Factor of Safety versus Lambda plot shown in Figure 11-33. Looking at this graph helps identify why a particular solution appears to be sensitive to force or moment equilibrium. For this particular example, the Factor of Safety with respect to moment curve is almost horizontal, which explains why the Bishop result is almost the same as the GLE result. For more information about this graph, please refer to the chapter that outlines the various factor of safety methods.

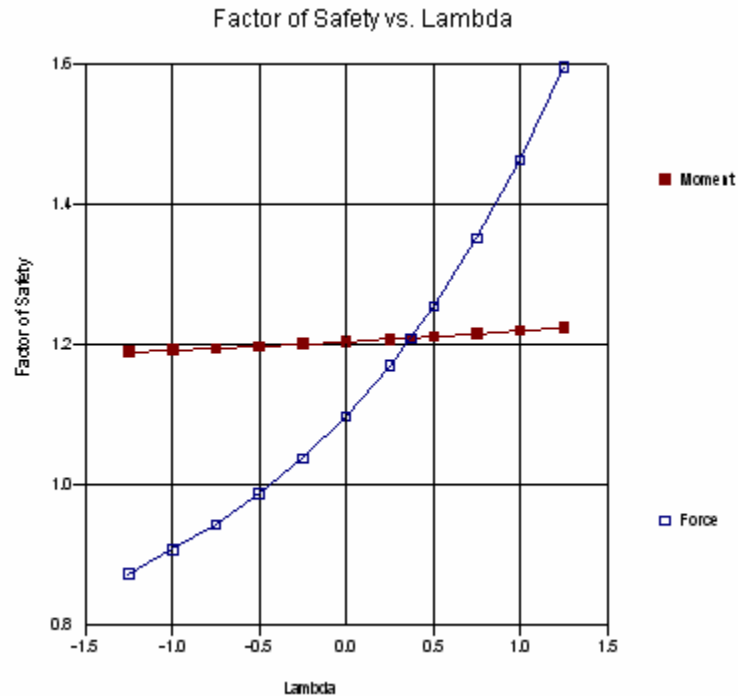


Figure 11-33 Factor of safety versus lambda

11.10 Example with slip surface projection under a footing

The purpose of this example is to illustrate the use of the slip surface projection feature to simulate the slip surface that develops under a footing load. The associated data file for this example can be found in the SLOPE/W examples folder (if installed) called **FOOTING.GSZ**. Other features of this example include:

- Analysis method: Spencer
- Pressure boundary
- Use of Ru coefficients
- Grid and radius slip surface with a limited projection exit angle
- Imperial units

Terzaghi's bearing capacity formula makes the assumption that the slip surface that develops under a strip footing exits the ground surface at an angle of $45^\circ - \phi/2$, which is the angle of passive earth pressure. With the grid and radius slip surface, you have the option of defining active or passive projection angles which are especially useful when you know the slip surface will not follow the arc of a circle throughout the soil profile.

In Figure 11-34, the anticipated failure surface under the strip footing has been sketched on the simple profile. Since this is a left to right failure, the right projection angle is the passive earth pressure projection angle. We know that the slip surface will include the bottom left corner of the footing. This is the location where the search radius is defined as a single point. For this simulation, the friction angle, ϕ , is equal to 30° . When defining the single point radius, a right (passive) projection angle will also be defined as $45^\circ - \phi/2 = 45 - 30/2 = 30^\circ$.

Pressure lines are used to simulate a pressure applied over a portion of the soil surface (e.g., to model a footing on the ground surface). Unlike line loads, which are a concentrated force applied at one point, pressure lines are applied over an area. The pressure over the applied area is then converted into a line load (i.e., a force per unit depth) for each slice that exits underneath the pressure boundary.

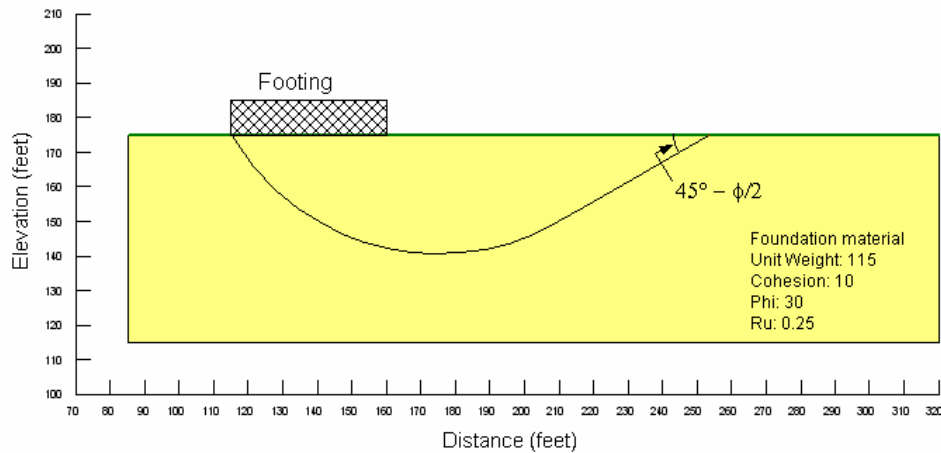


Figure 11-34 Schematic failure surface under a footing load

The location of the single point radius, the search grid and the pressure boundary representing the footing load are shown in Figure 11-35.

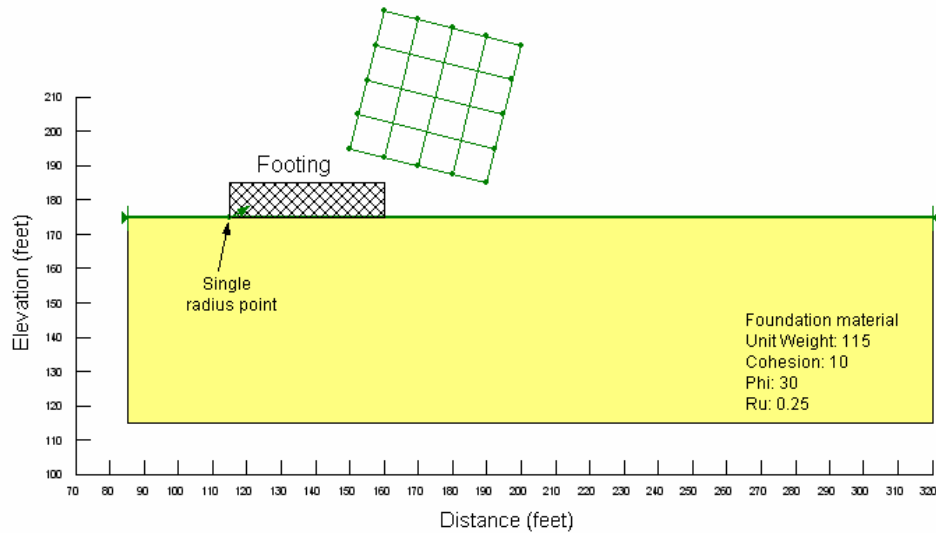


Figure 11-35 Location of the grid and radius

The critical slip surface and factor of safety, as well as factor of safety contours, for the strip footing are presented in Figure 11-36.

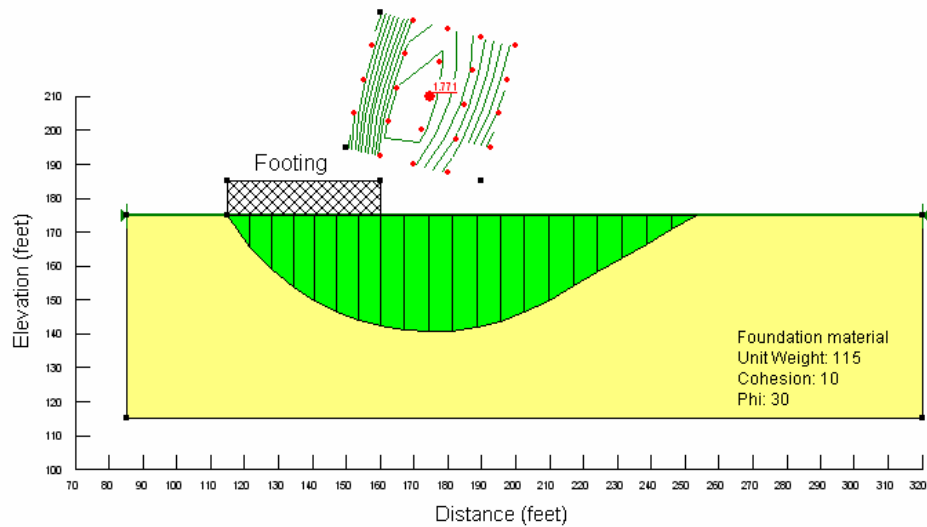


Figure 11-36 Location of the critical slip surface and the resulting factor of safety for a strip footing

In CONTOUR under view slice information, the base angle of the slices is reported. For this slip surface, which consists of 20 individual slices, slices 15 - 20 have base angles equal to 30° , which indicates that the defined projection angle of 30° was maintained for slices in the passive wedge.

Hand calculations can also be completed to spot check that the pressure boundary was appropriately defined. Note the presence of a line load of 64286 lbs/ft acting on the top of slice #5 shown in Figure 11-37.

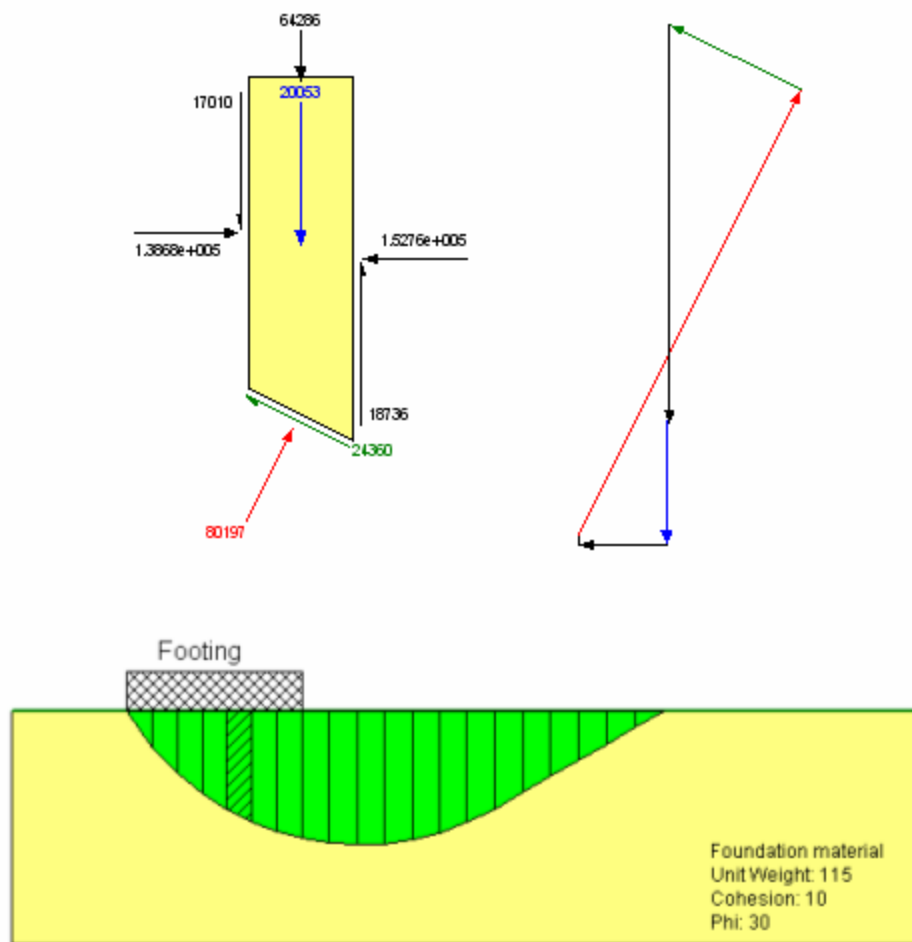


Figure 11-37 View slice information showing the presence of a line load on slice 5

Since the applied pressure is 1000 lbs/ft², the height of the pressure boundary is 10 ft and the width of slice #5 is 6.4286 ft, the applied line load force is as follows:

$$1000 \text{ lbs/ft}^2 \times 10 \text{ ft} \times 6.4286 \text{ ft} = 64,286 \text{ lbs (per unit depth)}$$

Similarly, for slice #5, the reported pore-water pressure acting at the base of the slice is equal to 779.85 lbs/ft². The pore pressure ratio R_u is a coefficient that relates the pore pressure to the overburden stress. The coefficient is defined as:

$$R_u = \frac{u}{\gamma_t H_s}$$

For slice #5, which has a slice height equal to 27.125 ft, the pore-water pressure (u) calculation is:

$$u = 0.25 \times 115 \text{ lbs/ft}^3 \times 27.125 \text{ ft} = 779.85 \text{ lbs/ft}^2$$

11.11 Use of anisotropic features

The purpose of this example is to highlight the use of some of the other strength models that are available for use within SLOPE/W. In this example, the features include:

- Analysis method: Spencer
- Single circular slip surface
- Piezometric line
- Strength Models: Anisotropic, Anisotropic Function & $S=f(\text{overburden})$
- Presence of a dry tension crack
- SI units

The associated data file for this example, **ANISOTROPIC.GSZ** can be found in the SLOPE/W examples folder (if installed).

The profile shown in Figure 11-38 has three different soil layers and each layer has been assigned a different strength model.

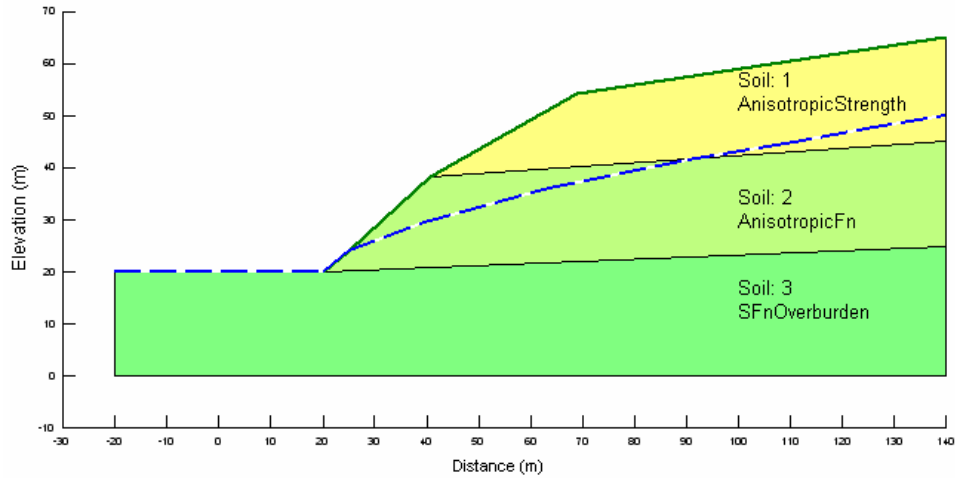


Figure 11-38 Profile for the anisotropic example showing the soil layers

The strength model specifies how the soil strength is defined. For this example, Soil # 1 uses an anisotropic strength soil model which is used to designate anisotropic soil strength. Both vertical and horizontal c and ϕ values are specified. The c and ϕ values are first adjusted for anisotropy before they are used in the shear strength computation. For more information on this strength model, refer to the chapter on material strength. The input parameters defined for the anisotropic strength of soil #1 are as shown in Table 11-11.

Table 11-11 Input parameters for soil #1

Parameter	Value
Unit weight, γ	18 kN/m ³
Horizontal cohesion, c_H	20 kN/m ²
Vertical cohesion, c_V	25 kN/m ²
Horizontal friction angle, ϕ_H	30°
Vertical friction angle, ϕ_V	35°

Soil #2 uses the anisotropic function model in which, depending on the base inclination angle, both the strength parameters c and ϕ are multiplied by a modifier factor. The input c and ϕ values are multiplied with the modifier factor obtained from the function before use in the shear strength computation.

The general function is defined by the user and Figure 11-39 shows how the modifier factor defined for this particular example varies with respect to base inclination angle for soils #2 and #3.

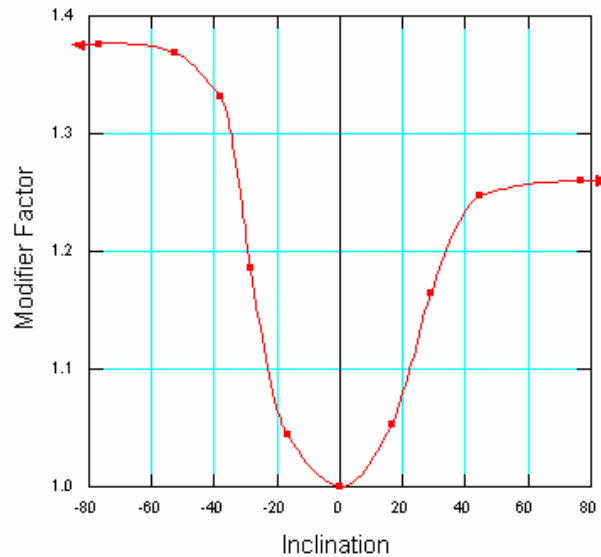


Figure 11-39 Anisotropic modifier function for soil #2 and #3

The required input parameters defined for soil #2 are as shown Table 11-12.

Table 11-12 Input parameters for soil #2

Parameter	Value
Unit weight, γ	18 kN/m ³
Cohesion	20 kN/m ²
Friction angle, ϕ	30°

Soil #3 uses a strength model that estimates the shear strength as a function of effective overburden at the base of a slice. The effective overburden is computed from the weight of the slice and the pore-water pressure acting at the bottom of the slice.

In this example, the Tau/Sigma ratio is 0.55 and the unit weight of water is 18 kN/m³. To account for anisotropy, the shear at the base of a slice is adjusted using the advanced parameters feature according to the specified anisotropic

function, which in this example is the same function used for Soil #2, as shown in Figure 11-39.

For this example, a single slip surface is analyzed by collapsing both the search grid and radius to single points. In addition, a piezometric line is defined and a tension crack angle of 62° is defined, as shown in Figure 11-40. A tension crack angle of 62° means that if the angle of the slip surface becomes greater than 62° , the slip surface will be forced vertically to the surface.

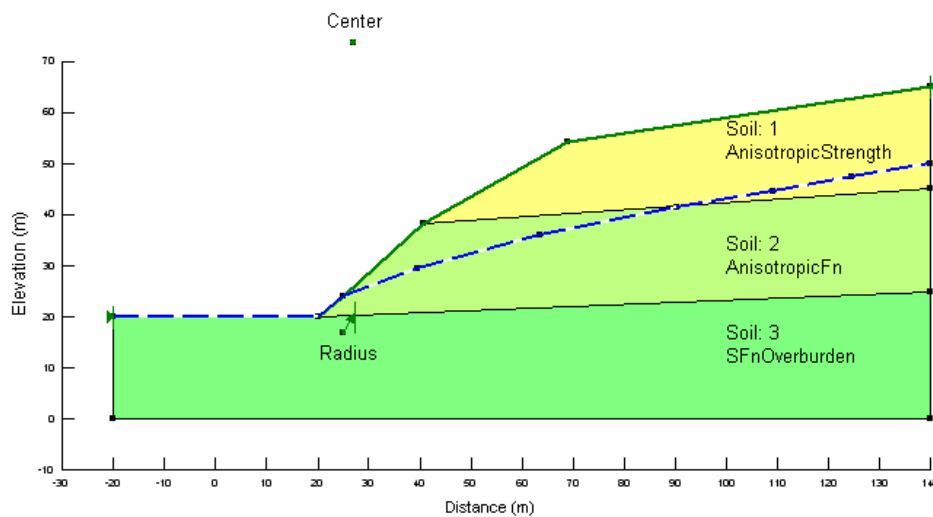


Figure 11-40 Slip surface definition

The critical slip surface and the factor of safety of 1.140 are presented in Figure 11-41.

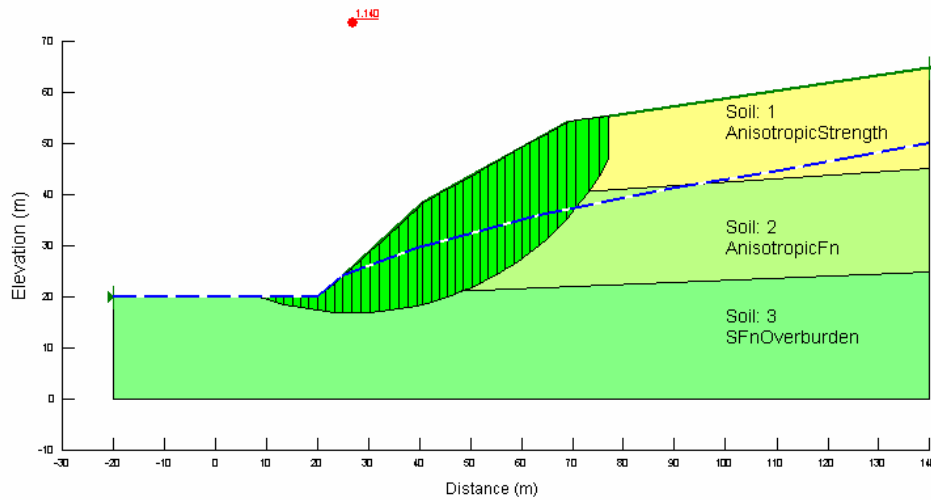


Figure 11-41 Factor of safety and the location of the critical slip surface

To see how the three different strength models were used in this example, we will use some of the slice information available to verify the strength parameters that were used in the analysis.

Soil #1 – anisotropic strength model

Soil #1 uses an anisotropic strength model in which the strength parameters c and ϕ in both the horizontal and vertical directions are defined. The bottom of slice 40 is within Soil #1, located above the piezometric line and the base inclination angle is 59.97° as reported in the view slice information dialogue box. The input c value is 20 in the horizontal direction and 25 in the vertical direction. The input ϕ value is 30 in the horizontal direction and 35 in the vertical direction. Based on the inclination angle, the c and f values at the base of each slice are adjusted according to:

$$c = c_h \cos^2 \alpha + c_v \sin^2 \alpha = 20 \cos^2 59.97 + 25 \sin^2 59.97 = 23.748$$

$$\phi = \phi_h \cos^2 \alpha + \phi_v \sin^2 \alpha = 30 \cos^2 59.97 + 35 \sin^2 59.97 = 33.748$$

From the view slice information for slice 40, the base normal stress (σ_n) is given as 61.514 kN/m^2 and the pore-water pressure (u) is 0. The Mohr-Coulomb equation for shear stress can then be solved as follows:

$$\tau = c + (\sigma_n - u) \tan \phi = 23.748 + (61.514 - 0) \tan 33.748 = 64.847$$

The base length of slice 40 is 4.0248 m and the resisting shear force (S_r) is computed by multiplying the base length by the shear stress:

$$S_r = \tau \times \ell = 64.847 \text{ kN/m}^2 \times 4.0248 \text{ m} = 260.996$$

The shear force mobilized is then determined by dividing the resisting shear by the factor of safety (i.e., 1.140), therefore:

$$S_m = \frac{260.996}{1.140} = 228.944$$

This computed value of the shear force mobilized is equal to the reported shear mobilized force that appears at the base of slice 40 on the free body diagram in Figure 11-42. Round-off errors in the hand-calculation account for the slight difference in the numbers.

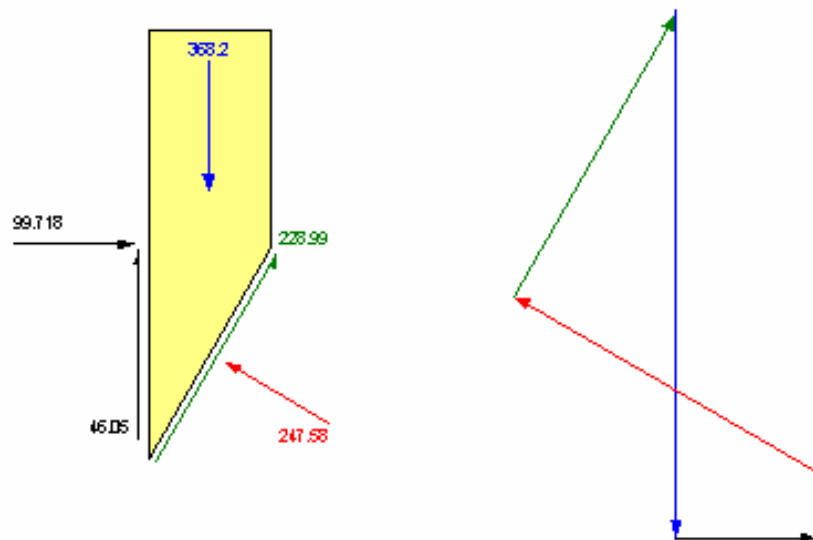


Figure 11-42 Free body diagram and force polygon of slice 40

Soil #2 – anisotropic function

The bottom of slice 30 is in Soil #2, which used the anisotropic function. For this particular slice, the base inclination angle is 32.66. Using the anisotropic function shown in Figure 11-39, the modifier factor for this slice is approximately 1.192. The input parameters were $c=20$ and $\phi = 30$, therefore, the modified c and ϕ values used in the shear strength calculation become $c = 23.842$ and $\phi = 35.763$. From the view slice information for slice 30, the base normal stress (σ_n) is 285.69 kN/m² and the pore-water pressure (u) is 83.30 kN/m². The Mohr-Coulomb equation for shear stress can then be solved as follows:

$$\tau = c + (\sigma_n - u) \tan \phi = 23.840 + (285.69 - 83.30) \tan 35.760 = 169.60$$

The base length of slice 30 is 1.9482 m and the resisting shear force (S_r) is computed by multiplying the base length by the shear stress:

$$S_r = \tau \times \ell = 169.60 \text{ kN/m}^2 \times 1.9482 \text{ m} = 330.41$$

The shear force mobilized is then determined by dividing the resisting shear by the factor of safety (i.e., 1.140), therefore:

$$S_m = \frac{330.41}{1.140} = 289.83$$

This computed value of the shear force mobilized is equal to the reported shear mobilized force that appears at the base of slice 30 on the free body diagram in Figure 11-43. Round-off errors in the hand-calculation account for the slight difference in the numbers.

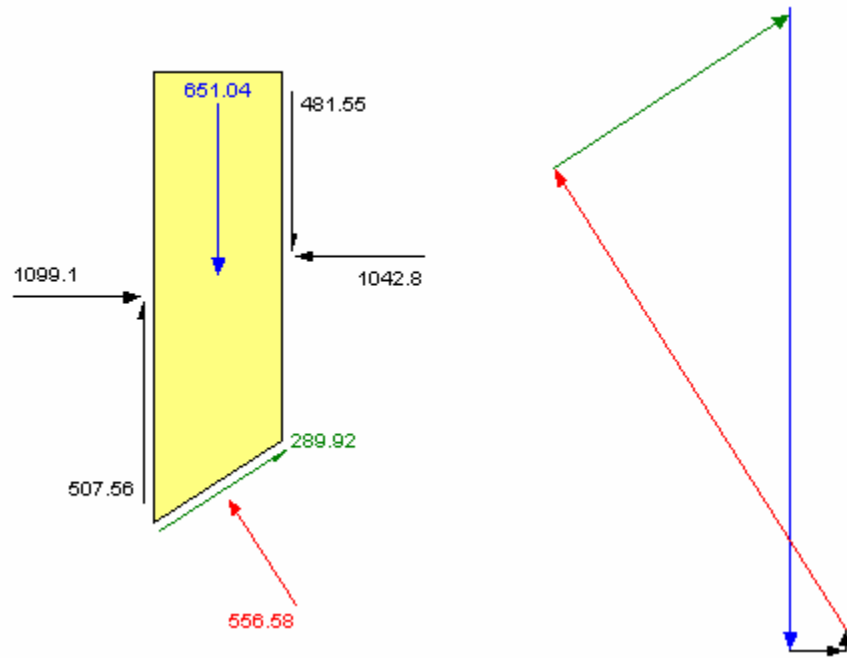


Figure 11-43 Free body diagram and force polygon of slice 30

Soil #3 – $S = \text{function (overburden)}$

Soil #3 uses the model that estimates the shear strength as a function of effective overburden at the base of the slice. Consider slice 20 which is in soil #2. The effective overburden pressure is the total vertical stress minus the pore-water pressure or:

$$\sigma'_v = H_s \gamma_s - H_w \gamma_w = (20.016 \times 18) - (11.205 \times 9.807) = 250.40$$

The input Tau/Sigma Ratio is 0.55, therefore the shear strength can be computed from the following equation:

$$\text{Shear strength} = \sigma'_v \times (\tau / \sigma \text{ ratio}) = 250.40 \times 0.55 = 137.72$$

Using the base inclination angle of 14.815 and the modifier function as shown in Figure 11-39, the modifier factor is determined to be approximately 1.0435.

Therefore, the modified shear strength (τ_{mod}) is $137.72 \times 1.0435 = 143.71$.

The shear resistance along the base of the slice, given a slice length of 1.6292 is:

$$S_r = \tau_{\text{mod}} \times \ell = 143.71 \times 1.629 = 234.105$$

The shear force mobilized is then determined by dividing the resisting shear by the factor of safety (i.e., 1.140), therefore:

$$S_m = \frac{234.105}{1.140} = 205.4$$

This computed value of the shear force mobilized is equal to the reported shear mobilized force that appears at the base of slice 20 on the free body diagram in Figure 11-44 and Figure 11-42. Round-off errors in the hand-calculation account for the slight difference in the numbers.

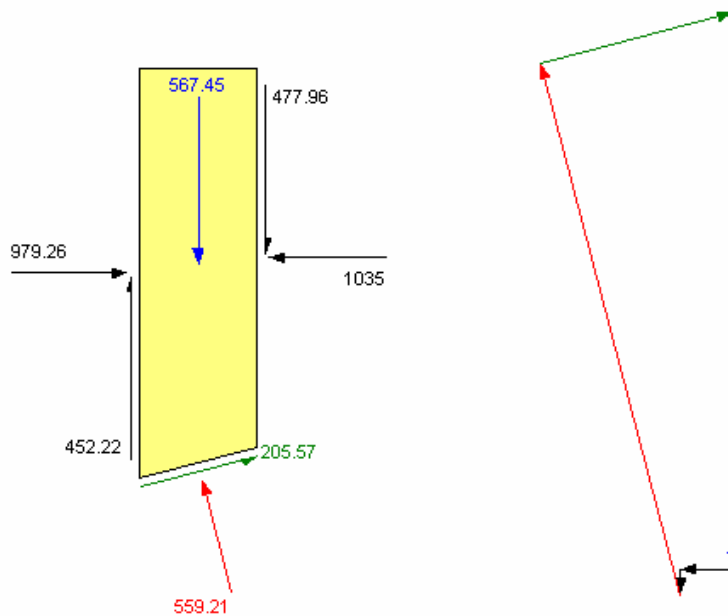


Figure 11-44 Free body diagram and force polygon of slice 20

11.12 SEEP/W pore-water pressures used in a stability analysis

Included file

- Seep pwp.gsz

The objective of this example is to highlight the use of SEEP/W total heads in a stability analysis. Other features of this analysis include:

- Analysis Method: Spencer
- SEEP/W total heads
- Grid and single-point radius
- No-strength material
- Advanced parameters: ϕ^b

One of the most powerful features of GeoStudio is the smooth integration that exists between all the individual programs. For simple pore-water pressure situations, there are several different options that can be used in SLOPE/W. However, if the pore-water pressures become more complex, it is sometimes necessary to use SEEP/W to conduct a finite element seepage analysis to determine the total heads that exist at every node in the profile. Once the finite element equations have been solved, SLOPE/W can be used to determine the critical slip surface by using the pore-water pressures that exist within the finite element mesh at the base of each slice

A schematic picture of the earth dam being modeled is shown in Figure 11-45.

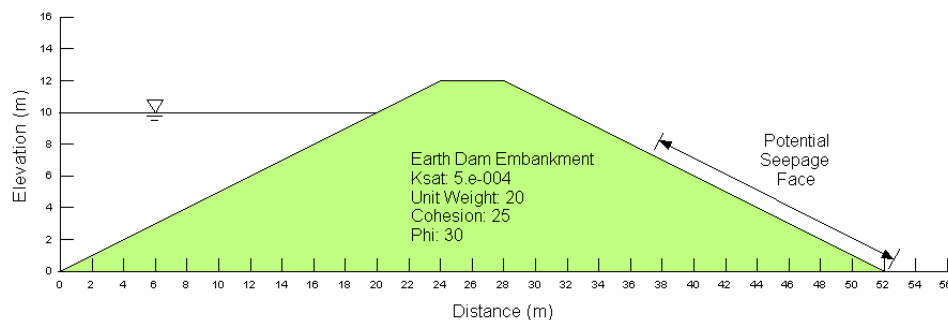


Figure 11-45 Profile and material properties

It is possible to develop the profile in either the SEEP/W or SLOPE/W module; however, the SEEP/W finite element equations need to be solved before the total head results are available for use within SLOPE/W. In the associated data files for this example, two regions have been used to ensure consistency between the two modules. In SLOPE/W the upstream reservoir has been defined as a no-strength material, which provides the weight of the water on the upstream embankment. In SEEP/W, the presence of an upstream reservoir is usually reflected in the boundary condition assigned to the upstream face of the embankment. The water region, which is present in the SLOPE/W analysis appears within the SEEP/W module as well, but the region does not have a mesh generated within it and therefore it is not included in the seepage analysis. The presence of the upstream reservoir is reflected in SEEP/W by the total head boundary condition of 10 m. A potential seepage face is also included on the downstream face by defining a total flux boundary of $Q=0$ (potential seepage face).

The conductivity function defined in SEEP/W for the embankment material is shown in Figure 11-46.

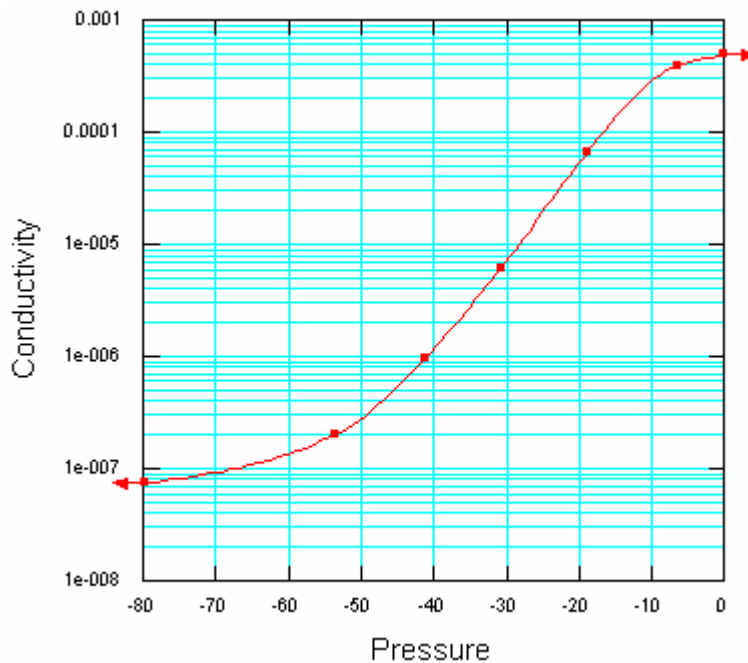


Figure 11-46 Conductivity function defined in SEEP/W for the embankment

Figure 11-47 shows the results of the seepage analysis, including the location of the phreatic surface and the development of a downstream seepage face; the velocity vectors and the pressure head contours. Note the presence of negative pore-water pressures above the phreatic surface ($P=0$ contour).

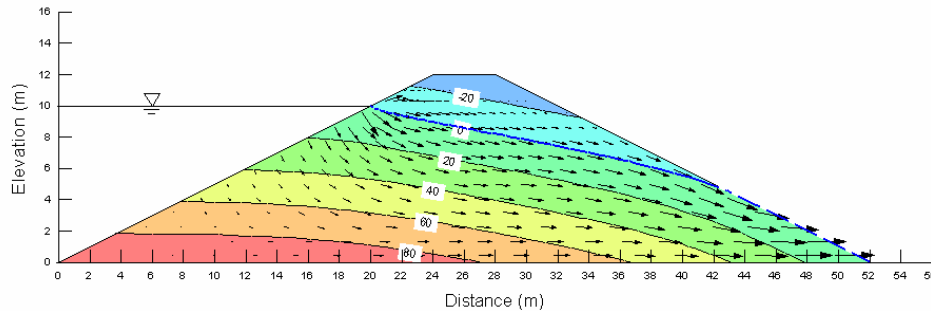


Figure 11-47 Results obtained from the finite element simulation

Now that the total heads have been computed for every node within the profile, a stability analysis can be completed to determine the stability of the downstream face. Figure 11-48 shows the location of the search grid and the location of a single radius point for the stability analysis. Note that the water appears as a material within the SLOPE/W module.

The water is assigned a no-strength material and the embankment is assigned a Mohr-Coulomb strength model. The material property parameters defined for the two materials within SLOPE/W are as shown in Table 11-13.

Table 11-13 Material property parameters used in SLOPE/W

Parameter	Water	Embankment
Frictional angle ϕ' , (degrees)	-	30
Cohesion c' , (kPa)	-	25
Unsaturated ϕ^b , (degrees)	-	10
Unit weight γ , (kN/m^3)	9.807	20

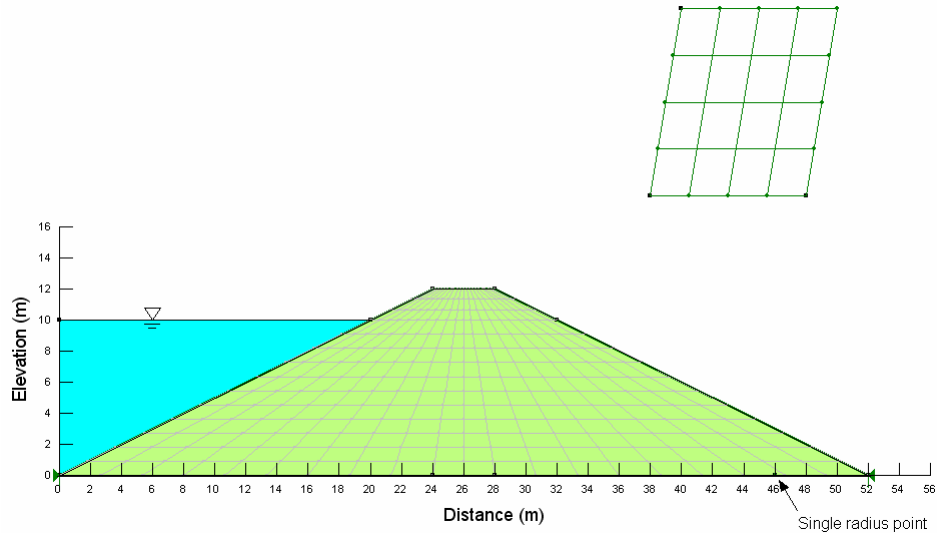


Figure 11-48 Earth dam embankment as defined in SLOPE/W

The finite element mesh still appears within the SLOPE/W module, but the finite element equations are not solved as part of the stability analysis. The pore-water pressures at the base of each slice will be determined from the heads computed at the finite element nodes. It is for this reason that a piezometric line is NOT drawn within SLOPE/W. The stabilizing weight of the water is modeled by including the water as an actual material, and the piezometric information is contributed by the SEEP/W results. If SEEP/W total heads were not being used, both a water material and a piezometric line would be required to appropriately represent the upstream reservoir.

Figure 11-49 shows the location of the critical slip surface and the factor of safety for the downstream face. Note that a phreatic surface is drawn within the embankment, even though a piezometric line was not defined with SLOPE/W. The phreatic surface is part of the SEEP/W results, superimposed on the critical slip surface. Also note that the critical slip surface has passed through the single radius point at the bottom of the embankment.

In assigning the material properties for the embankment material, an advanced parameter, $\phi^b = 10^\circ$ was also defined. In SLOPE/W, if you want to include the increase in cohesion that develops above the phreatic surface due to the presence of suction (negative pore-water pressures), you must define a ϕ^b parameter. If ϕ^b is

not defined, the negative pore-water pressures above the phreatic surface are set equal to zero.

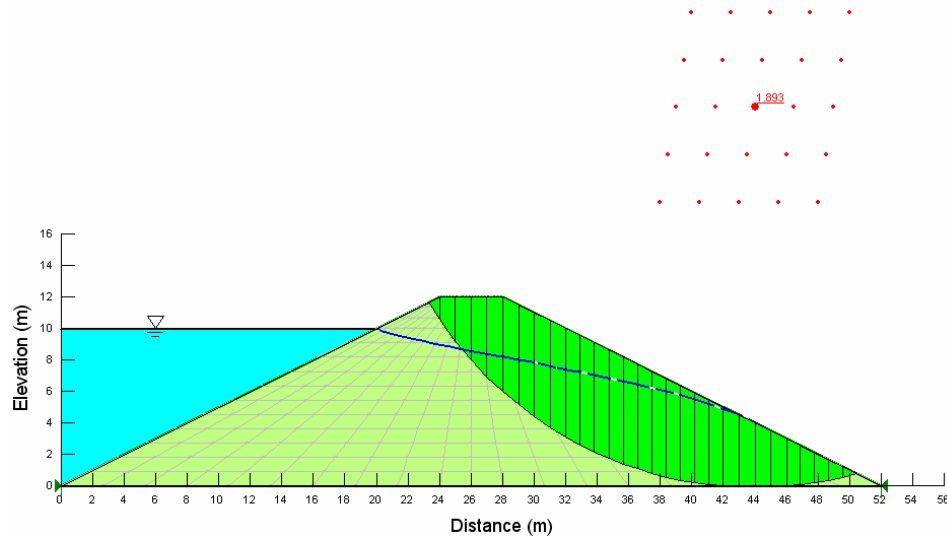


Figure 11-49 SLOPE/W results including the location of the phreatic line

A graph of strength versus slice number (Figure 11-50) can be developed within SLOPE/W which shows that for the two slices that exist above the phreatic surface (slices 1 and 2), there are actually three strength components; cohesion, friction and suction.

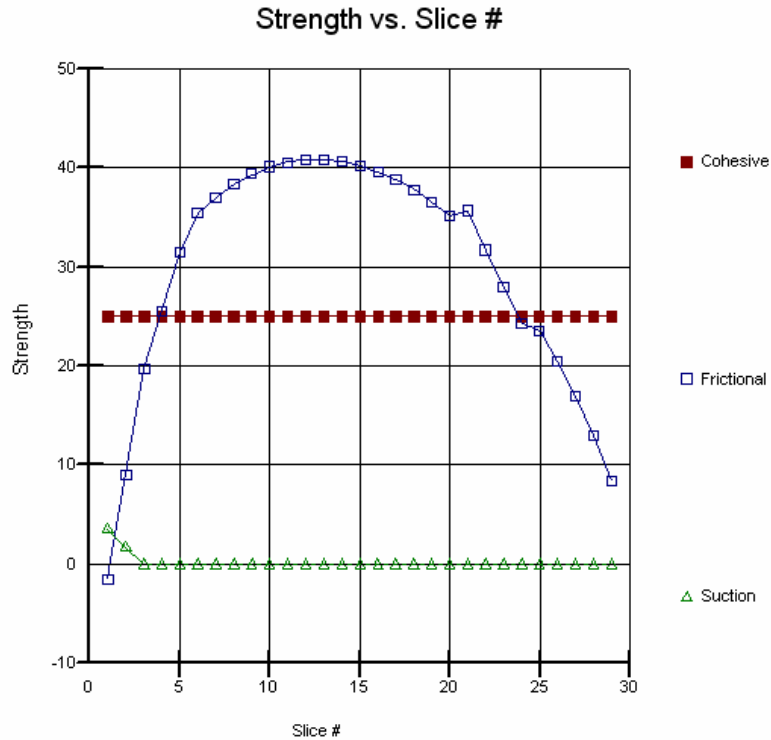


Figure 11-50 Graph of strength versus slice number showing the presence of a strength component due to suction

11.13 Finite element slope stability method

In the finite element slope stability method, the stresses in the ground can be computed using SIGMA/W and then SLOPE/W uses the SIGMA/W stresses to compute safety factors. This is a completely different approach than the limit equilibrium method. The purpose of this example is to highlight the use of the finite element stability method using the SIGMA/W and SLOPE/W modules to obtain a stability factor for the embankment shown in Figure 11-51. Features of this example include:

- Analysis Method: Finite element
- Grid and radius

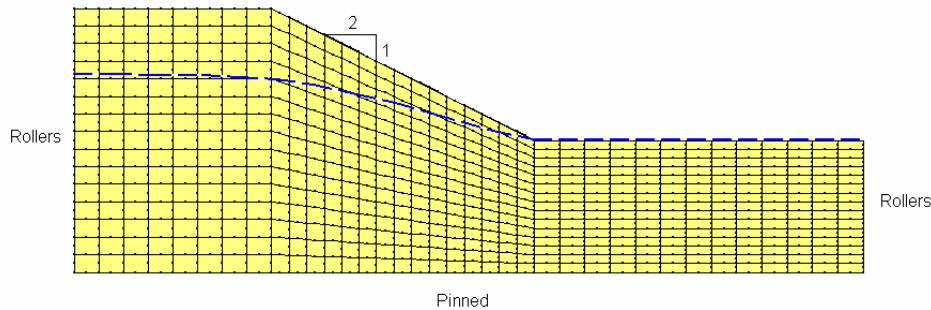


Figure 11-51 SIGMA/W mesh used to determine stresses in the ground

To establish the stresses in the ground using SIGMA/W, the Insitu 2 analysis type is used and an initial water table is drawn to determine pore-water pressures within the ground. By defining an initial water table, both the total and effective stresses can be determined. The bottom boundary condition is pinned and rollers are used along the vertical extents of the finite element mesh. A structured mesh is used in the analysis.

The material property parameters required for the SIGMA/W analysis are presented in Table 11-14.

Table 11-14 Material property parameters used in the SIGMA/W analysis

Parameter	Value
Young's modulus, E (kPa)	100,000
Cohesion, c (kN/m ²)	8
Poisson's ratio, ν	0.4
Friction angle, ϕ , (degrees)	30
Unit weight, γ , (kN/m ³)	20

The computed total stress contours computed by the SIGMA/W analysis are shown in Figure 11-52. In addition, a Mohr circle has been drawn for one of the Gauss regions.

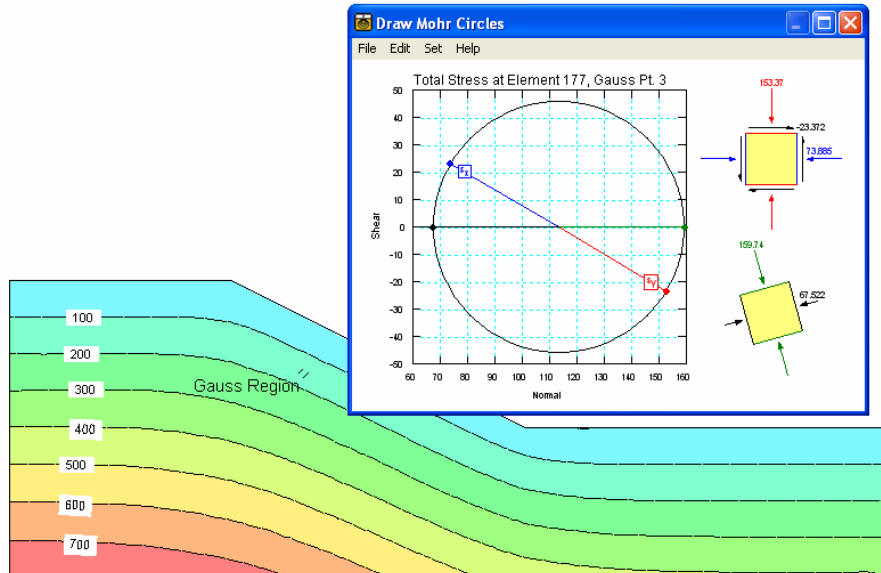


Figure 11-52 Total stress contours within the embankment

The effective vertical stresses versus y-coordinate are shown in Figure 11-53.

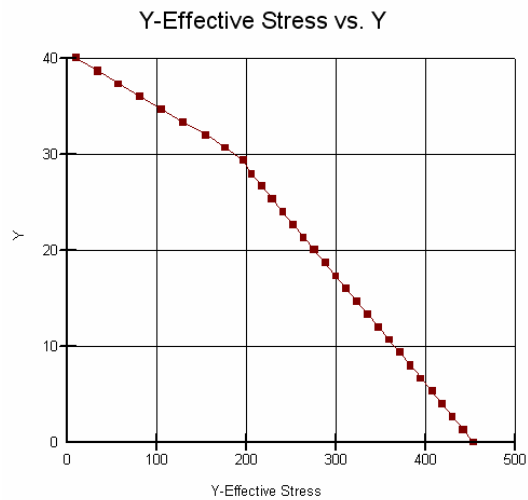


Figure 11-53 Y-Effective stresses through the embankment

Now that the actual stresses in the ground have been computed, the results of the SIGMA/W analysis can be used within SLOPE/W to determine a stability factor for the embankment. Since the material properties of c and ϕ are used both in a stress analysis and a stability analysis, the material property parameters already exist within the SLOPE/W module and do not need to be defined again. SLOPE/W simply needs to be told that the stress profile and pore-water pressures are to be taken from the internal SIGMA/W file and not from an external source.

For this example a single search center and a line of radii has been defined. During the solve process within SLOPE/W, the stability factor is determined by dividing the total available shear resistance (S_r) by the total mobilized shear (S_m) along the entire length of the slip surface as shown in the following equation:

$$FS = \frac{\sum S_r}{\sum S_m}$$

The critical slip surface and stability factor is shown in Figure 11-54. Note the presence of the phreatic line developed within SIGMA/W is now being used within SLOPE/W.

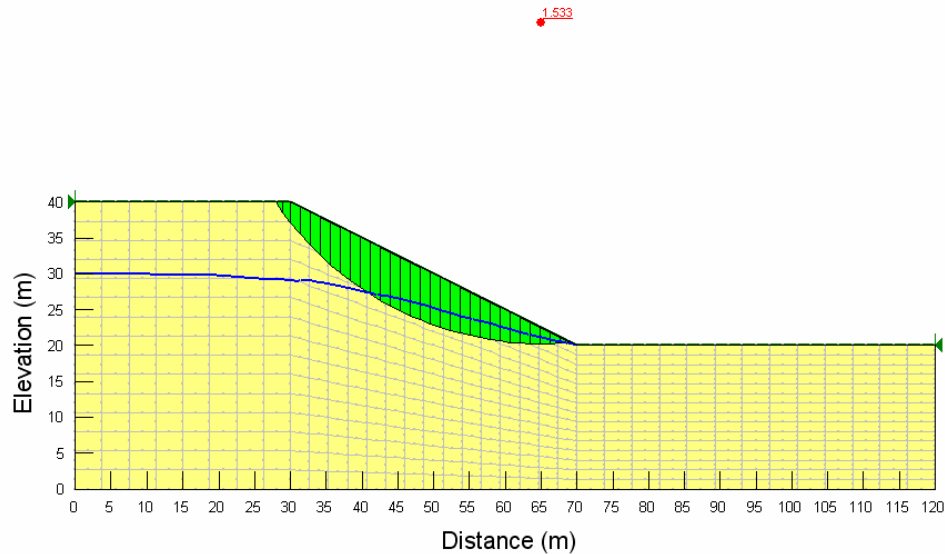


Figure 11-54 Stability factor and critical slip surface for the finite element method

One of the primary assumptions with a limit equilibrium analysis is that the global factor of safety is the same as the factor of safety for every slice. In a limit equilibrium analysis, the factor of safety does not change with position across the slip surface. In a finite element stability analysis the same condition does not need to be satisfied and the stability factor varies across the slip surface as shown in Figure 11-55.

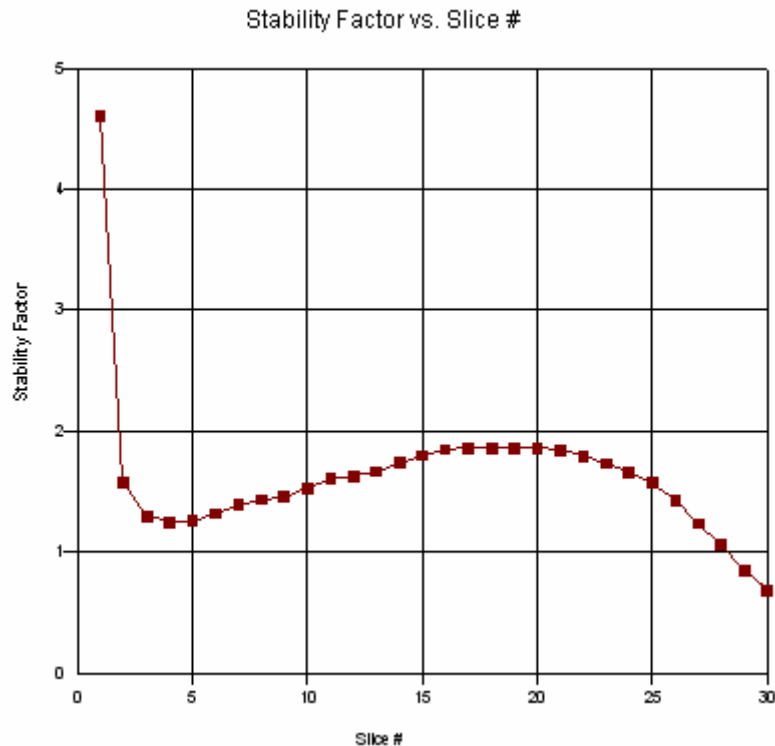


Figure 11-55 Stability factor as it varies across the slip surface

For more information on the differences between limit equilibrium and the finite element method refer to the chapter on Factor of Safety Methods.

11.14 Rapid drawdown analysis

Included files

- Rapid drawdown before.gsz

- Rapid drawdown after.gsz

The purpose of this illustrative example is primarily to show how to conduct a rapid drawdown analysis without conducting a finite element analysis with SEEP/W. Other special features include:

- Analysis method: Morgenstern-Price (half-sine function)
- Multiple soil layers
- Piezometric line
- SI Units

To evaluate the scenario of rapid drawdown, it is usually beneficial to conduct a stability analysis of the slope before rapid drawdown as well as the post drawdown scenario.

Before drawdown

Before rapid drawdown occurs, the cross-section resembles the profile shown in Figure 11-56.

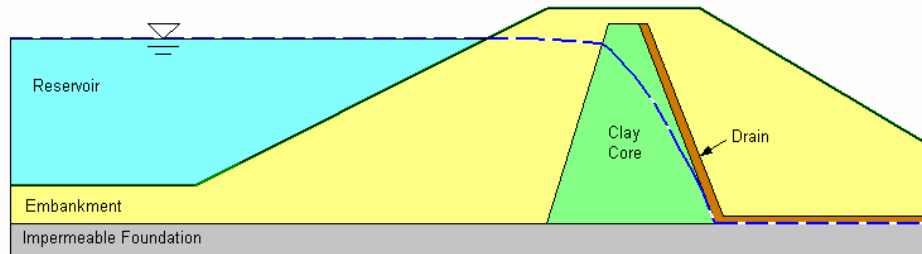


Figure 11-56 Profile used for rapid drawdown example before drawdown

Water is ponded up against the slope and the assumption is that the pore-water pressure conditions in the ground have reached some steady-state conditions. The ponded water layer is modeled as a no strength soil layer which ensures that the weight of the water is included in the analysis. The ponded water layer results in a hydrostatic force which acts on the left side of the first slice. A piezometric line is drawn across the surface of the water layer and through the rest of the profile. The

piezometric line is used during the analysis to compute the pore-water pressures that exist at the base of each slice.

The vertical effective stress at the base of every slice is based on the height of the water and the height of the soil. For discussion purposes, the water height is H_w and soil height is H_s . The unit weight of the water is γ_w and the total unit weight of the soil is γ_s . The vertical effective stress then is:

$$\sigma'_v = \sigma - u$$

$$\sigma'_v = (H_s \gamma_s + H_w \gamma_w) - (H_s + H_w) \gamma_w$$

$$\sigma'_v = H_s (\gamma_s - \gamma_w)$$

A limit equilibrium stability analysis using the Morgenstern-Price method of analysis results in a factor of safety of 1.976 and the critical slip surface as shown in Figure 11-57. A grid of centers was defined and the slip surface was forced to exit at the toe of the upstream embankment by collapsing the search radii into a single point.

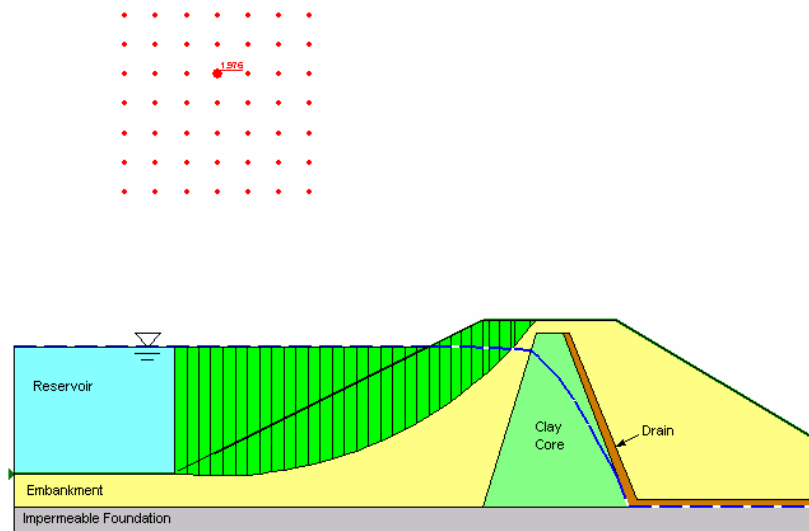


Figure 11-57 Critical slip surface and factor of safety before drawdown

Within SLOPE/W CONTOUR you can generate a graph of the pore-water pressures versus distance across the critical slip surface as shown in Figure 11-58. The pore-water pressures are high at the toe of the embankment and decrease as they should with elevation until they are set equal to zero for those slices that exist above the piezometric line.

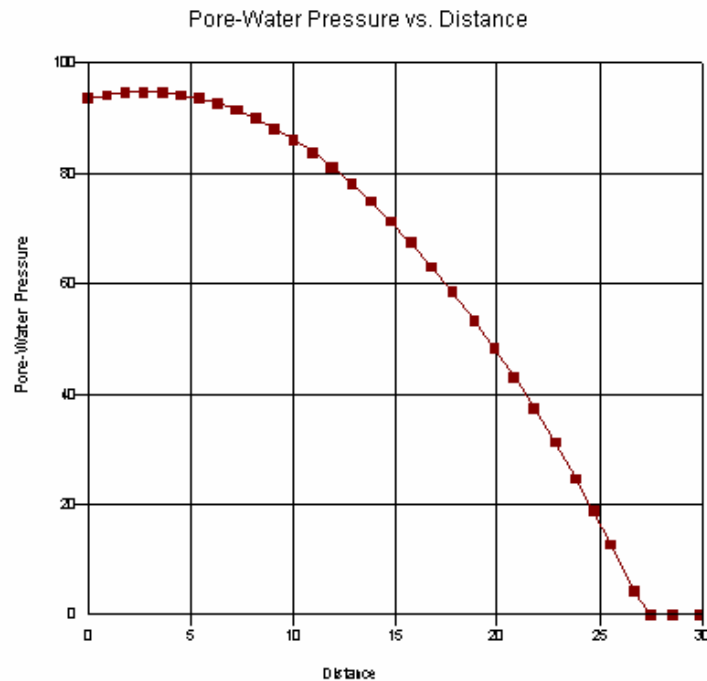


Figure 11-58 Pore-water pressures across the slip surface before rapid drawdown

After drawdown

To model the rapid drawdown conditions in SLOPE/W, we need to remove the ponded soil layer and place the piezometric line along the ground surface of the upstream embankment as shown in Figure 11-59.

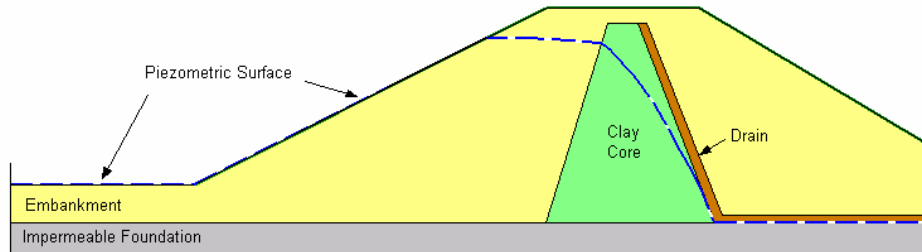


Figure 11-59 Profile used for rapid drawdown example after drawdown

By removing the ponded water and adjusting the piezometric line, the hydrostatic force offered by the ponded water is gone, but the effective stress remains the same at the base of each slice, as indicated by the following equation:

$$\sigma'_v = \sigma - u$$

$$\sigma'_v = H_s \gamma_s - H_w \gamma_w$$

$$H_w = H_s$$

$$\therefore \sigma'_v = H_s (\gamma_s - \gamma_w)$$

Note that the height of the soil and water are the same since the piezometric line is on the ground surface. When effective stress does not change, the shear resistance to sliding does not change as a result of the rapid drawdown.

Recall that the factor of safety before drawdown was 1.976. Following rapid drawdown, the factor of safety has been reduced down to 0.972. The resulting critical slip surface is shown in Figure 11-60.

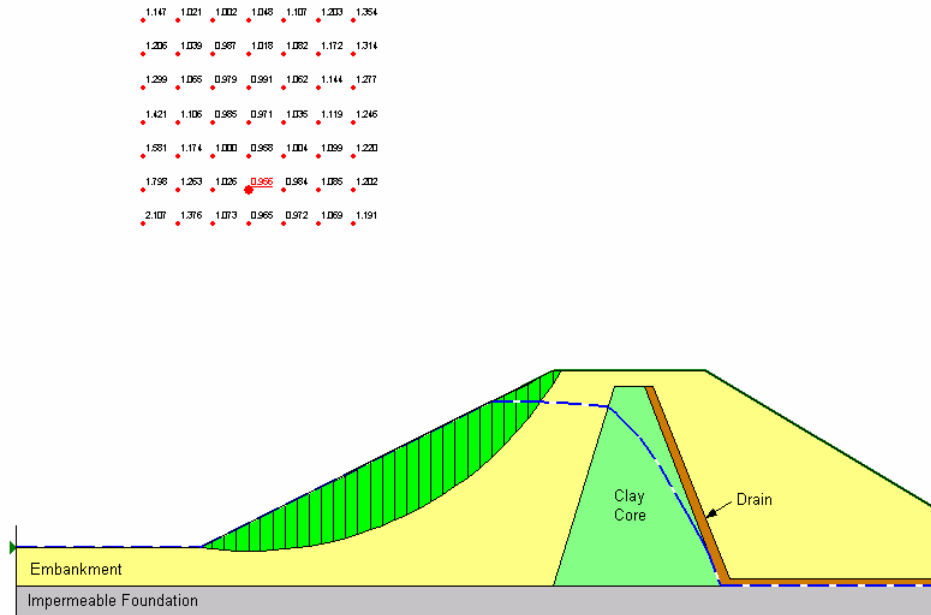


Figure 11-60 Critical slip surface and factor of safety after drawdown

While the slip surface has still been forced to exit at the toe of the embankment, a different center was determined more critical within the search grid, resulting in a slightly different critical slip surface. Viewing the factors of safety displayed on the search grid reveals that the same center that was used to determine the critical slip surface in the “before” analysis gave an “after” factor of safety of 0.991.

The pore-water pressures distribution across the slip surface following rapid drawdown is shown in Figure 11-61.

The approach used to model rapid drawdown in this example is based on the assumption that the soil has some finite hydraulic conductivity such that the change in pore-water pressure at the base of the slice is instantaneously equal to the change in ponded water pressure head above the slice. Considering that water is incompressible and that soils near the slope face likely have at least some finite conductivity, this is not an unrealistic assumption. In most situations, this approach is likely a worst case situation. Practically, it is not possible to drawdown the water instantaneously and to totally prevent at least some of the water from flowing out of the embankment during the drawdown. In this context, the approach presented here should be considered conservative and on the safe side.

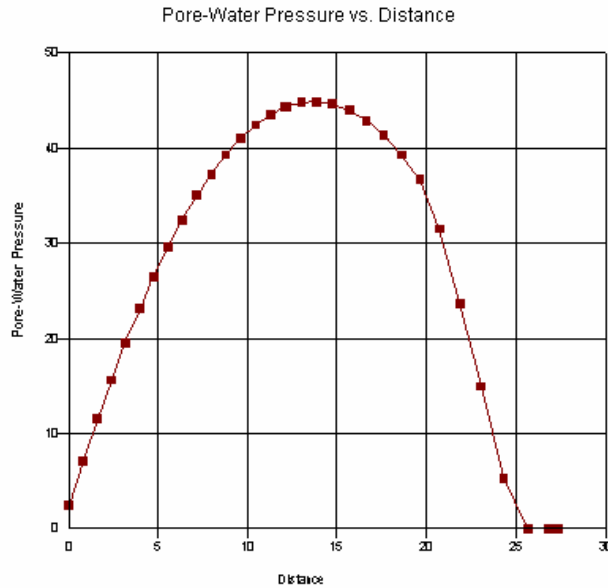


Figure 11-61 Pore-water pressures across the slip surface after rapid drawdown

A more accurate way of analyzing drawdown is to use the seepage results from a SEEP/W analysis. This more advanced approach uses the exact pore-water pressures that were in the soil before the drawdown, as opposed to simply getting the pore-water pressure from the vertical distance between the piezometric line and the base of the slice. You must have the SEEP/W module to use this approach.

11.15 Slope reinforcement with anchor

Included file

- Anchor.gsz

The purpose of this illustrative example is to show how anchors can be used to improve the stability of a slope. Features of this simulation include:

- Analysis method: Morgenstern-Price with Half-sine function
- Multiple soil layers with Mohr Coulomb soil model
- No pore-water pressure

- Two sloping anchors
- Surcharge load modeled as pressure boundary
- Single slip surface with Grid and Radius
- SI units

Figure 11-62 shows the geometry, the material properties and the two anchors. Note that the single circular slip surface is modeled by collapsing the 3 search grid points to a single point (Point 11) and collapsing the 4 radius points to a single point (Point 1). The surcharge load on the crest of the slope is modeled with a pressure line (Points 7 and 8).

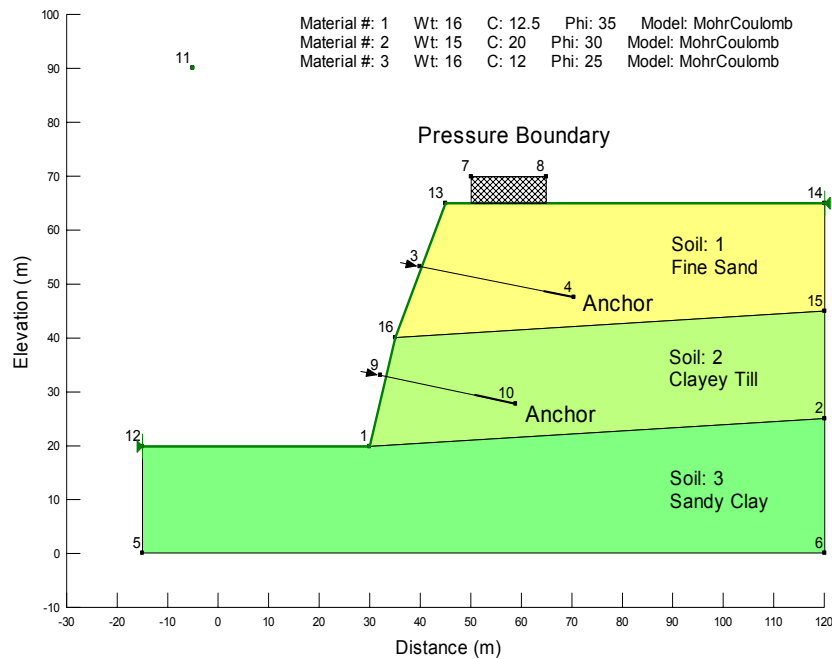


Figure 11-62 Geometry and material properties

The factor of safety of this step slope without the reinforcement is 0.750. By adding two anchors with working load of 2000 kN, the factor of safety is improved to 1.228 (Figure 11-63). To begin, the anchors are specified with a constant load option, when the critical slip surface is obtained, the anchors are also specified with a variable load option. Both options give the same factor of safety. The

position of the red box on each anchor indicates that both anchors are deep enough and the bond length is also sufficient to deliver the working load.

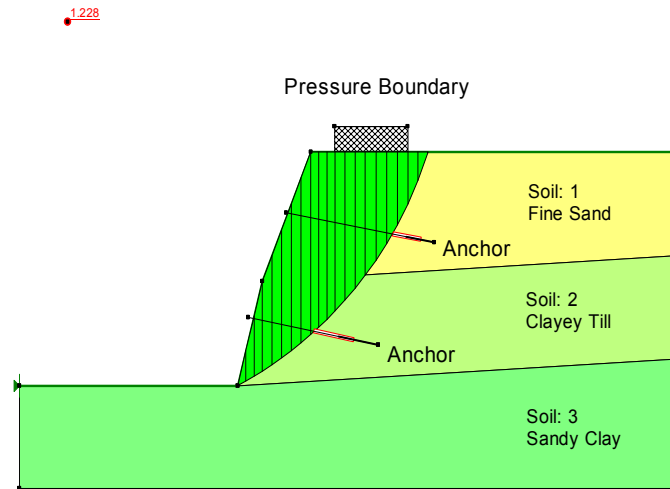


Figure 11-63 Factor of safety of the example ANCHOR

It is important to check the anchor load used in the factor of safety calculation with the View Slice Information feature. The free body diagram and force polygon for Slice 17 is shown in Figure 11-64. The anchor is specified with a constant working load of 2000 kN, which is shown correctly on the free body diagram of Slice 17.

The applied surcharge is simulated with a pressure line boundary of 5 kN per m height per m width of slice. Since the pressure line is 5 m above the top of the slice and the width of slice is 2.1942 m, the applied surcharge load on Slice 17 can be calculated as:

$$\text{Applied surcharge load} = 5 \text{ kN/m/m} * 5 \text{ m} * 2.1942 \text{ m} = 54.855 \text{ kN}$$

This is identical to the computed force used by SLOPE/W as shown on the free body diagram. The force polygon closes (Figure 11-64), showing that force equilibrium is satisfied.

Figure 11-65 shows a graph of the shear resistance along the slip surface. Since the anchors intercept the slip surface at the base of slice 9 and 17, the shear resistance on slice 9 and 17 are much higher due to the anchor loads.

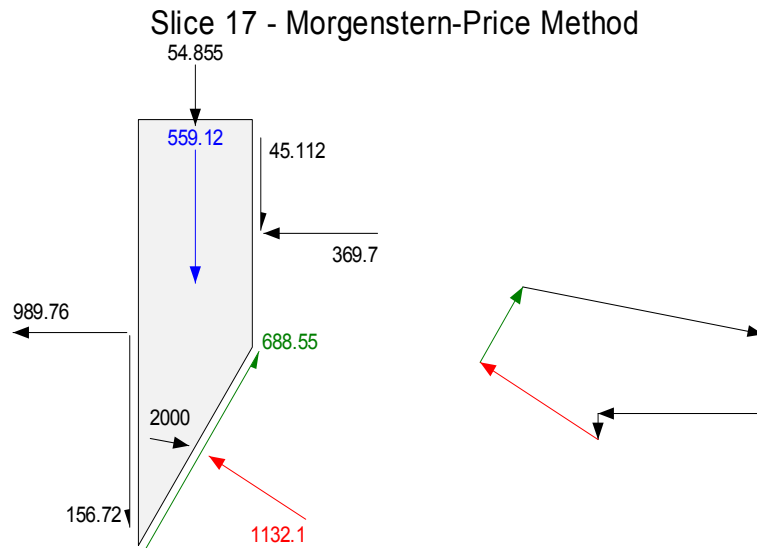


Figure 11-64 Free body diagram and force polygon

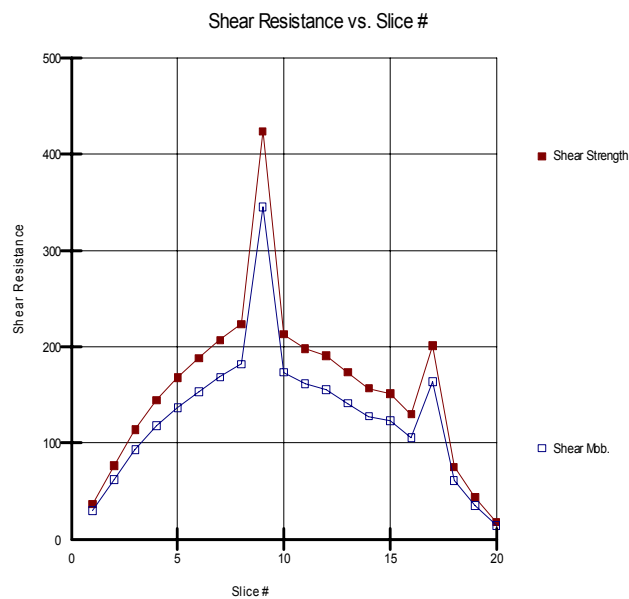


Figure 11-65 Shear resistance along slip surface

You can also examine the detail result of the anchor design with the View Reinforcement Information feature in SLOPE/W CONTOUR (Figure 11-66). In this example, the anchors are assumed to be pre-stressed or tensioned, therefore, the “F of S Dependent” option is set to No. Because of the constant loading condition, the anchor load of 2000 kN is used in the factor of safety calculation. The bond safety factor is 1.0 and the required bond length is 5.9913, if the bond safety factor is 2.0, the computed required bond length will be doubled.

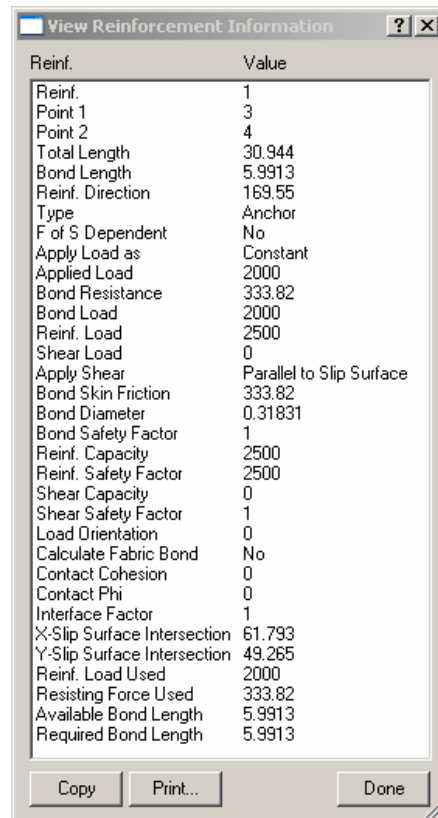


Figure 11-66 Examine details result of a reinforcement with View Reinforcement Information

Please also note that the spacing of the reinforcement is assumed to be 1.0 in this example. This means that the specified anchor loading is per unit width of the slope. If the spacing is 2.0, the applied load will be half (i.e., 1000 kN) and the factor of safety will be lower than 1.228.

11.16 Slope reinforcement with geo-fabric

Included file

- Fabric.gsz

It is quite common to stabilize a man-made embankment with geo-fabrics. The purpose of this illustrative example is to show how geo-fabrics can be used to improve the stability of a slope. Features of this simulation include:

- Analysis method: GLE with half-sine function
- Multiple soil layers with Mohr Coulomb soil model
- No pore-water pressure
- Two horizontal geo-fabrics
- A line load applied on the crest
- Single slip surface with Grid and Radius
- SI units

Figure 11-67 shows the geometry, the material properties and the two geo-fabrics. Note that the single circular slip surface is modeled by collapsing the 3 search grid points to a single point (Point 6) and collapsing the 4 radius points to a 2 points radius (Points 8 and 9). Point 15 is the position of the applied line load on the crest of the slope.

In this example, the bond resistance of the geo-fabric is assumed to be calculated based on the contact cohesion of 2 kPa and a frictional angle of 15° between the soil and fabric. The interface factor is set to 2.0 meaning that both faces of the fabrics are considered in the bond resistance calculation. The geo-fabric capacity (tear strength) is set at 200 kN

Without the geo-fabric, the slope is unstable with a factor of safety is 0.977. With the presence of the geo-fabric reinforcement, the factor of safety is 1.478, as shown in Figure 11-68.

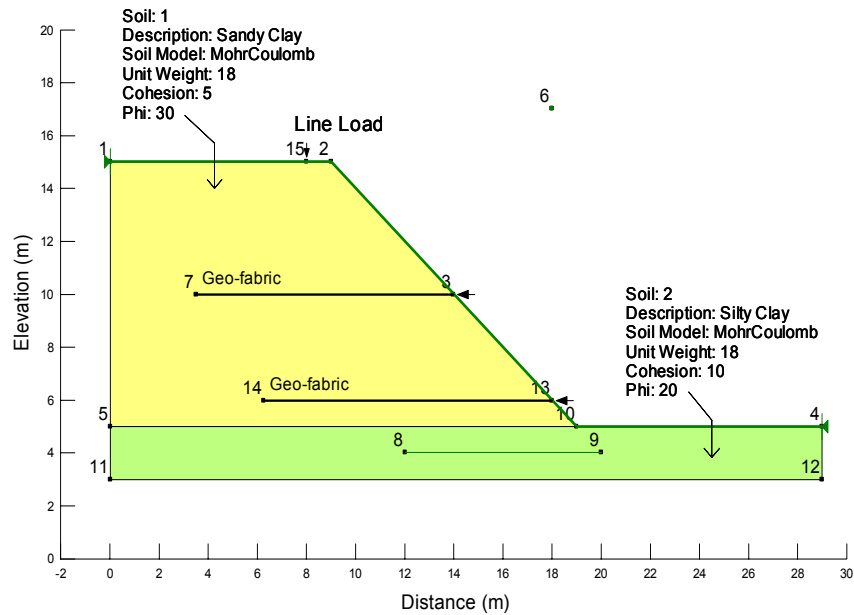


Figure 11-67 Geometry and material properties

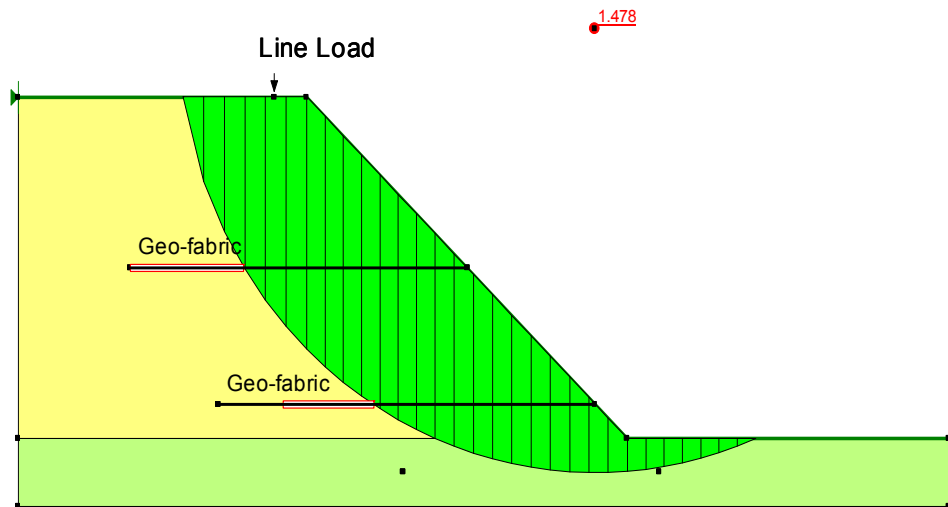


Figure 11-68 Factor of safety of the example FABRIC when the "F of S Dependent" option is "No"

It is important to examine the actual reinforcement load used in the factor of safety calculations. Figure 11-69 show the free body diagram and the force polygon of the slice containing the upper geo-fabric. The applied load of the geo-fabric is 169.14 kN.

The average effective overburden stress at the base of the slice is 81.475 kPa which is calculated by dividing the total weight (52.215 kN) with the slice width (0.64087 m). The unit bond skin friction will be 2 sides \times (2 kPa + 81.475 kPa \times $\tan 15^\circ$) which is equal to 47.662 kPa. Since the available bond length is 3.5487 m, the applied reinforcement load is 169.14 kN, as shown in Figure 11-69. The applied reinforcement load is smaller than the specified geo-fabric capacity (200 kN), therefore, the bond resistance governs, and the required bond length (3.5487 m) is the same as the available bond length. This is correctly represented by the red box of the upper geo-fabric in Figure 11-68.

Slice 3 - GLE Method

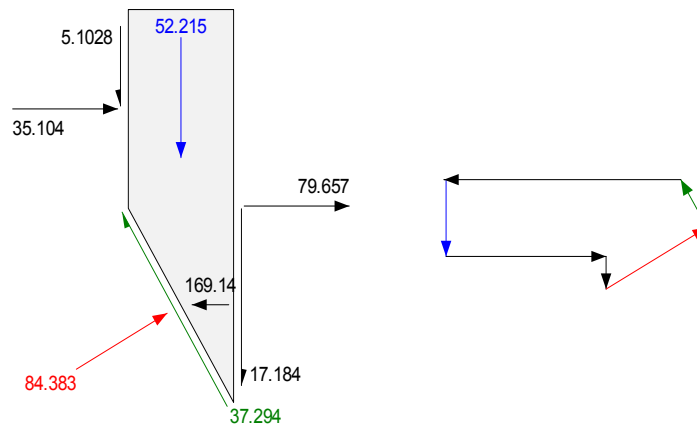


Figure 11-69 Free body diagram and force polygon

For the lower geo-fabric, since the overburden stress is higher, the unit bond skin friction can be computed to be 71.084 kPa, with an available bond length of 4.8295 m, the applied load from the bond can be 343.30 kN which is much higher than the specified geo-fabric capacity. As a result, the geo-fabric capacity governs and only 200 kN is used as the applied reinforcement load in the factor of safety

calculation Figure 11-70. The required bond length is 2.8136 m which is shorter than the available bond length as indicated by the red box in Figure 11-68.

Slice 10 - GLE Method

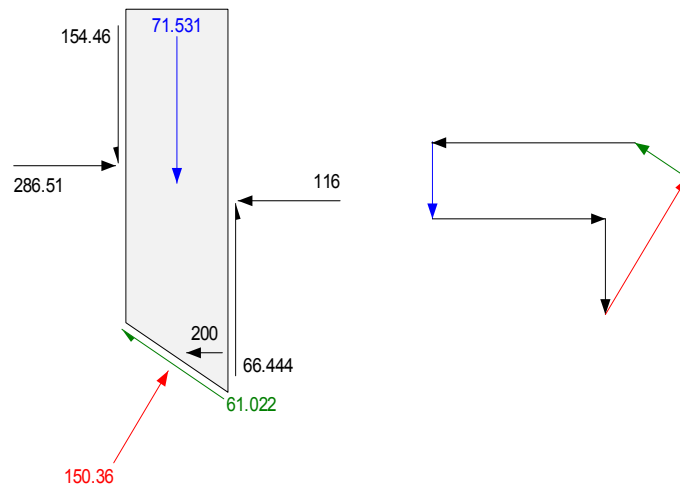


Figure 11-70 Free body diagram and force polygon

In modeling geo-fabric, SLOPE/W has an option of allowing you to specify a unit bond friction instead of the contact cohesion or friction angle. In this example, if you specify the upper geo-fabric with the same computed unit bond skin friction, 47.664 kPa and the lower geo-fabric with 71.084 kPa. You will get the same solution.

Since a geo-fabric is seldom pre-stressed or tensioned as in the case of an anchor, the applied load may not be there and must be developed with the strain of the slope. As a result, the geo-fabric loading can be considered as an addition to the resisting force and it is mobilized in the same manner as the soil strength. In SLOPE/W this is the “F of S Dependent” option, if you select “Yes” to the option, the applied reinforcement load is actually the mobilized reinforcement load and is depending on the computed factor of safety in the same manner as the mobilized shear resistant. Figure 11-71 shows the new result when “F of S Dependent” option is “Yes”. The factor of safety is now 1.323.

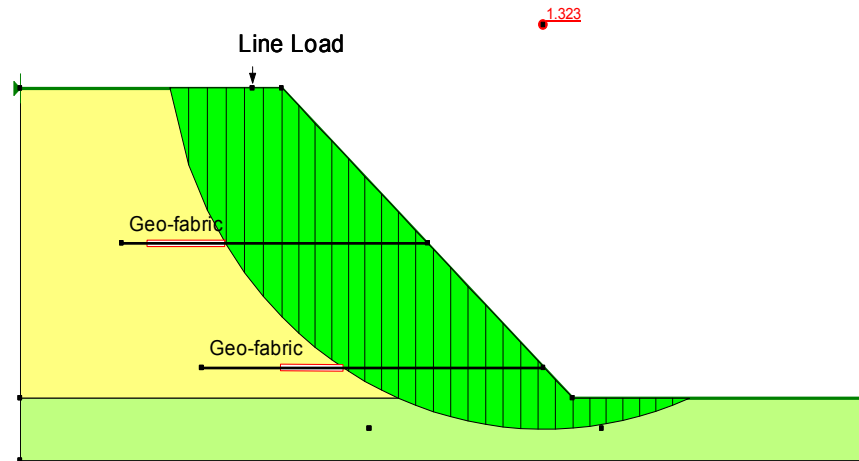


Figure 11-71 Factor of safety of the example FABRIC when the “F of S Dependent” option is “Yes”

Figure 11-72 and Figure 11-73 show the free body diagram and the force polygons for the two slices containing the geo-fabrics. The mobilized reinforcement load for the upper geo-fabric is 127.93 kN which can be computed as 169.14 kN (Figure 11-69) divided by the factor of safety. Similarly, the mobilized reinforcement load for the lower geo-fabric is 151.26 kN which can be computed as 200 kN (Figure 11-70) divided by the factor of safety.

Slice 3 - GLE Method

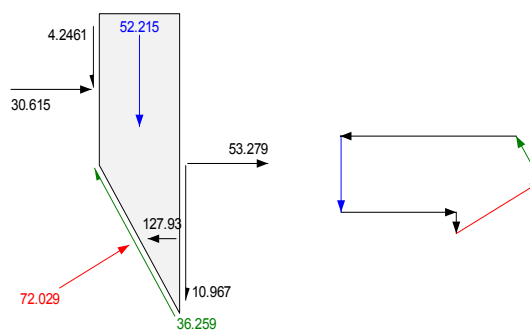


Figure 11-72 Free body diagram and force polygon

Slice 10 - GLE Method

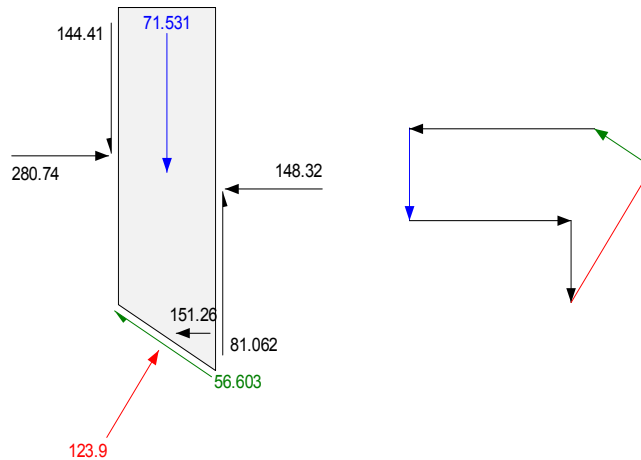


Figure 11-73 Free body diagram and force polygon

Note that with a smaller mobilized reinforcement load and the same bond skin friction, the required bond length will be smaller than the case when “F of S Dependent” option is “No” (Figure 11-68). When you use “View Reinforcement Information” in CONTOUR to examine the detail results of the geo-fabric, you will see that the required bond lengths for the upper and lower geo-fabrics are 2.684 m and 2.128 m respectively.

11.17 Probabilistic analysis example

Included file

- Probabilistic.gsz

The purpose of this illustrative example is to show how you can do a probabilistic analysis of the stability of a slope. Features of this simulation include:

- Analysis method: Morgenstern-Price with Half-sine function
- Statistical variability in some parameters
- Multiple soil layers with different soil models

- Pore water pressure with piezometric line
- Entry and Exit slip surface with projection angle
- Auto search for tension crack zone
- SI units

Figure 11-74 shows the geometry, the soil models used, the piezometric line and the entry and exit search zones. The red arrows on the entry zone indicate the projection angle of the slip surfaces.

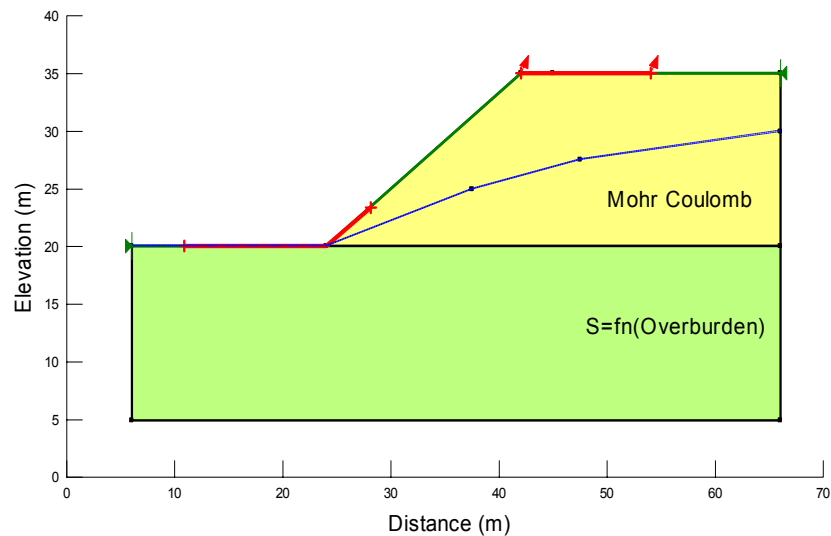


**Figure 11-74 Geometry and material models of the example
PROBABILISTIC**

Figure 11-75 shows the most critical slip surface and the computed factor of safety when there is no tension crack. The factor of safety is 1.204. Figure 11-77 shows the free body diagram and the force polygon of slice 31 near the crest of the slope. Note that the base normal force is negative, indicating that the base normal force is in tension. Negative base normal force is quite common for slices near the crest of the slope when the entry angle is steep and when the underlying soil is weak. The negative normal force is troublesome, since soil cannot be in tension theoretically.

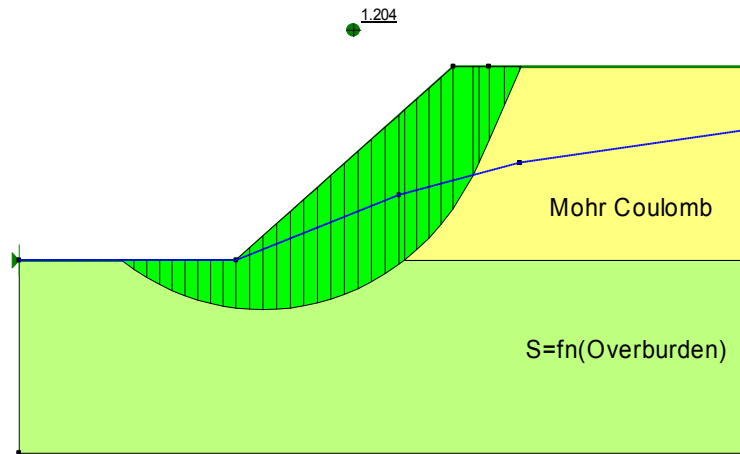


Figure 11-75 Factor of safety of the example PROBABILISTIC without any tension crack

Slice 31 - Morgenstern-Price Method

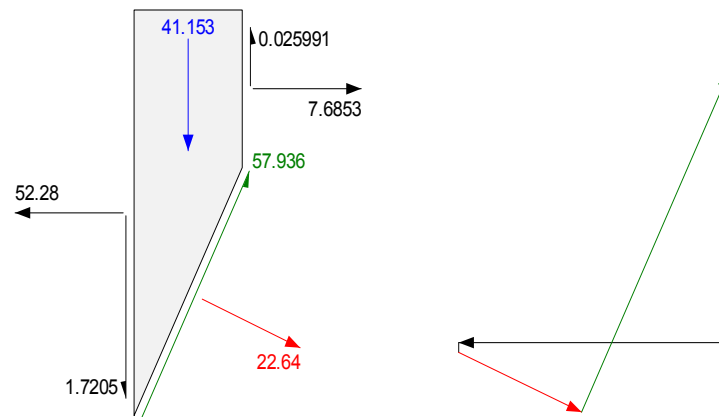


Figure 11-76 Free body diagram and force polygon showing negative base normal force

SLOPE/W has the option of automatically searching for tension crack zone. This is helpful in cases where the tension crack zone is not known. Figure 11-77 shows

the most critical slip surface and the computed factor of safety when the option of auto search for tension crack is selected. The factor of safety is 1.187, and a tension crack is located about 3 m below the crest. Figure 11-78 shows free body diagram and the force polygon of the last slice near the crest of the slope. Note that the normal force is positive.

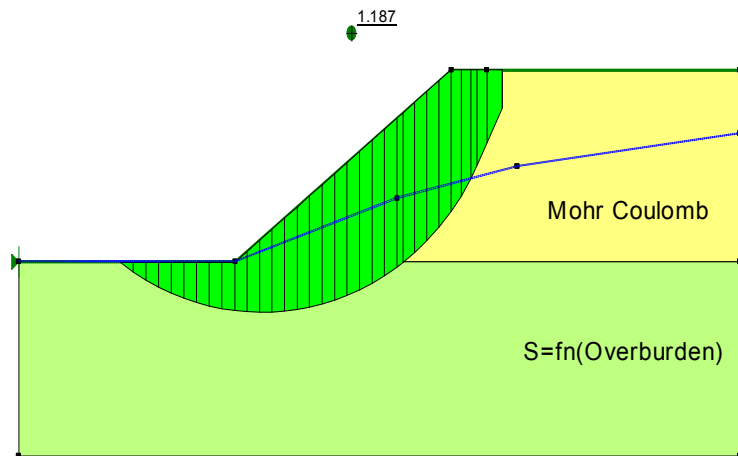


Figure 11-77 Factor of safety of the example PROBABILISTIC with auto search for tension crack

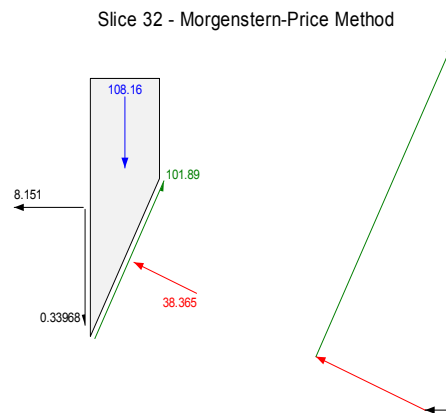


Figure 11-78 Free body diagram and force polygon showing positive base normal force

A probabilistic analysis can be performed quite easily with SLOPE/W when the variability of the soil properties or other input parameters is known. For example, let us assume that the variability of the soil properties and the piezometric line is normally distributed, as shown in Figure 11-79 and Figure 11-80.

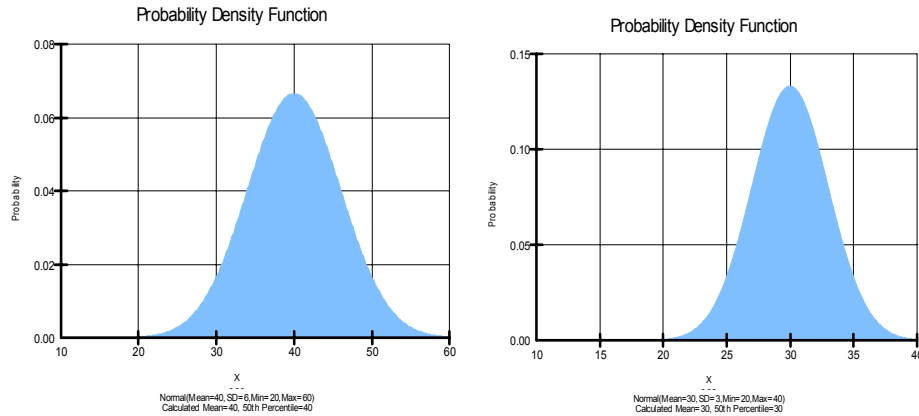


Figure 11-79 Normal distribution of ϕ (Left) and cohesion (Right) for the upper soil layer

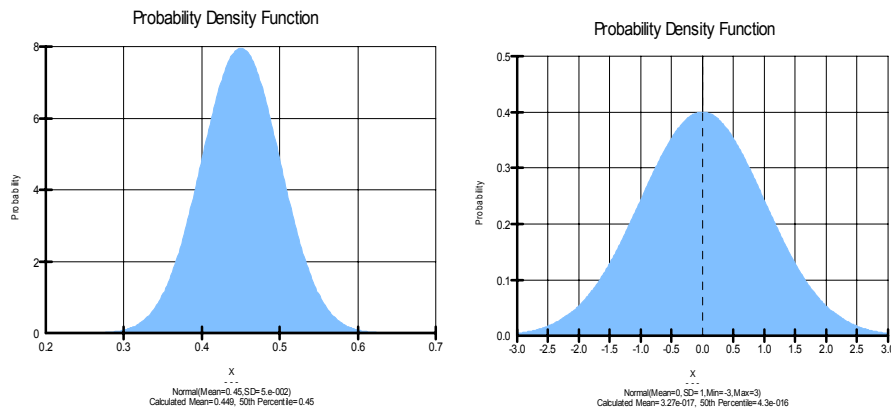


Figure 11-80 Normal distribution of Tau/Sigma Ratio of the lower soil layer (Left) and the piezometric line (Right)

After 5000 Monte Carlo trials, the following results are obtained:

Mean F of S = 1.2004

Reliability Index = 1.42

Probability of Failure = 6.66 %

Standard deviation of F of S = 0.141

Min F of S = 0.76145

Max F of S = 1.7178

Using the “Draw Probability” feature in CONTOUR, you can get a probability density function of the 5000 computed factor of safety. Since the variability of the soil properties is normally distributed, the probability density function of the factor of safety (Figure 11-81) is also normally distributed as expected.

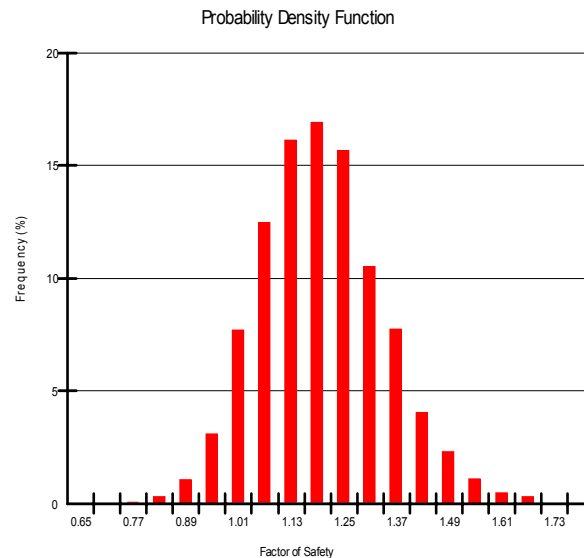


Figure 11-81 Probability density function of the 5000 Monte Carlo factors of safety

Figure 11-82 shows the probability distribution function of the 5000 Monte Carlo factors of safety. The red line represents the probability of failure. In this case, for each Monte Carlo trial, the soil properties of the entire soil layer is only sampled once, the sampling value is applied to all slices within the same soil layer, the

probability of failure is 6.66%. The other extreme is to sample new soil properties for every slice in each Monte Carlo trial. The probability of failure is now reduced to 1.12%. These two options are useful to compute the range of the probability of failure. The more realistic probability of failure is likely in between of 1.12% and 6.66%. When more field investigation and soil testing are available, and when more statistical data become available to justify the use of a certain sampling distance, the probability of failure can be more accurately estimated. For example, if you assume a sampling distance of 10 m, you will get a probability of failure of 3.62%.

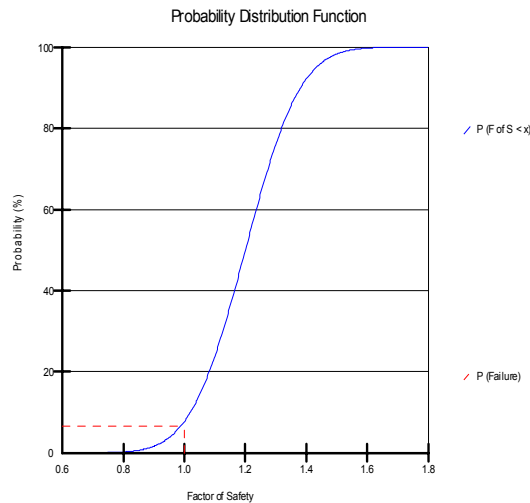


Figure 11-82 probability distribution function of the 5000 Monte Carlo factors of safety showing probability of failure

11.18 Auto locate slip surface example

Included file

- Auto locate.gsz

The purpose of this illustrative example is to show how a sensitivity study of some material properties to the factors of safety can be conducted. Features of this simulation include:

- Analysis method: Spencer

- Homogenous material with a weak layer
- One piezometric line
- Auto locate slip surface
- Auto search for tension crack zone
- Sensitivity study of material density, cohesion and friction angle to the computed factor of safety
- Safety map
- SI units

Figure 11-83 shows the geometry of the slope, the soil properties and the location of the weak layer. The auto locate slip surface search is used to find the critical slip surface.

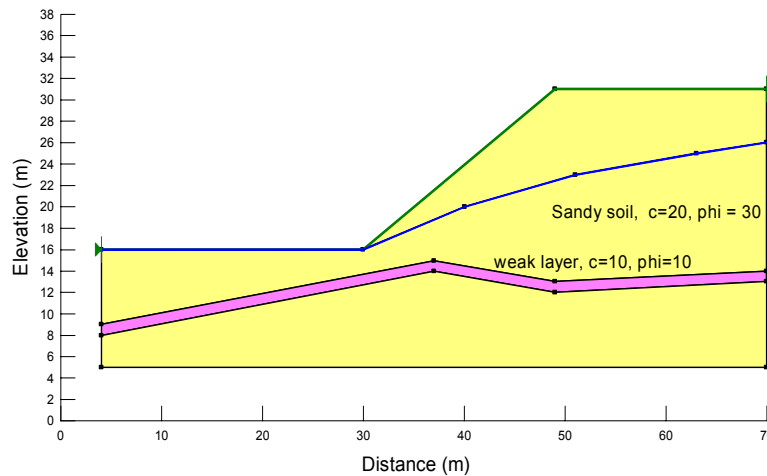


Figure 11-83 Geometry and material properties

Figure 11-84 shows the factor of safety and the critical slip surface found by the auto locate procedure. Note that the critical slip surface is not circular and the lower portion of the slip surface is inside the shallow weak layer. The factor of safety is 1.111 and a tension crack depth of about 2.5 m is located by the auto tension crack search.

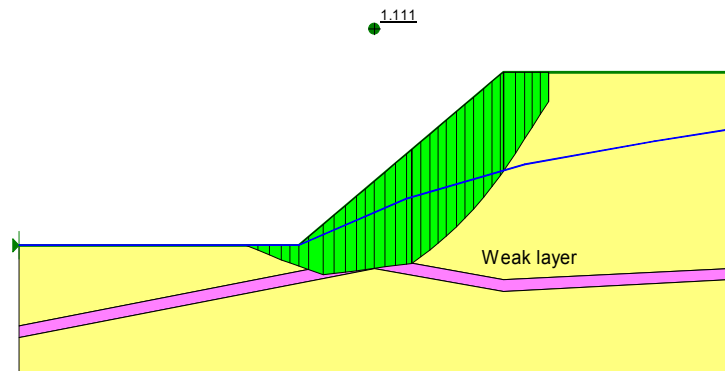


Figure 11-84 Auto locate critical slip surface and factor of safety with a shallow weak layer

Figure 11-85 shows the factor of safety and the critical slip surface found by the auto locate procedure when the weak layer is a little deeper. The critical slip surface moved with the deeper weak layer and the factor of safety is 1.207, which is a little higher than the case with shallow weak layer (Figure 11-84).

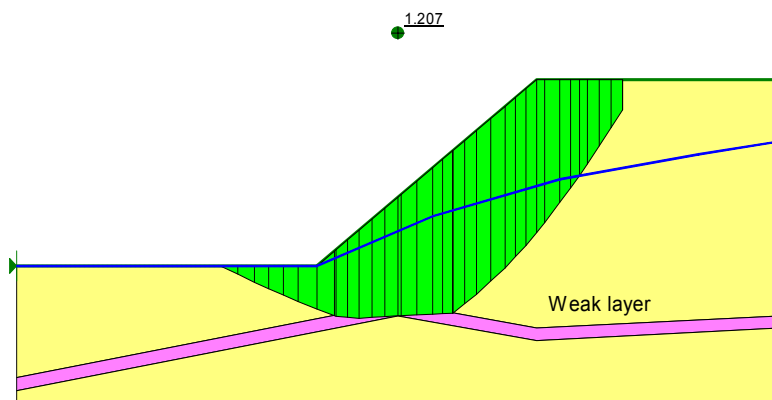


Figure 11-85 Auto locate critical slip surface and factor of safety with a deeper weak layer

Figure 11-86 shows the factor of safety and the critical slip surface found by the auto locate procedure when the same weak layer is at a deep position. Note that the

critical slip surface does not go through the deep weak layer and the factor of safety is 1.381. This will be the same critical slip surface and factor of safety obtained by the auto locate procedure if the weak layer is not present. This does not mean that the auto locate procedure fails to find the weak layer, it simply means that when the weak layer is deep, the slip surface going through the weak layer is no longer critical, and auto locate finds a more critical slip surface above the weak layer. This is intuitively correct.

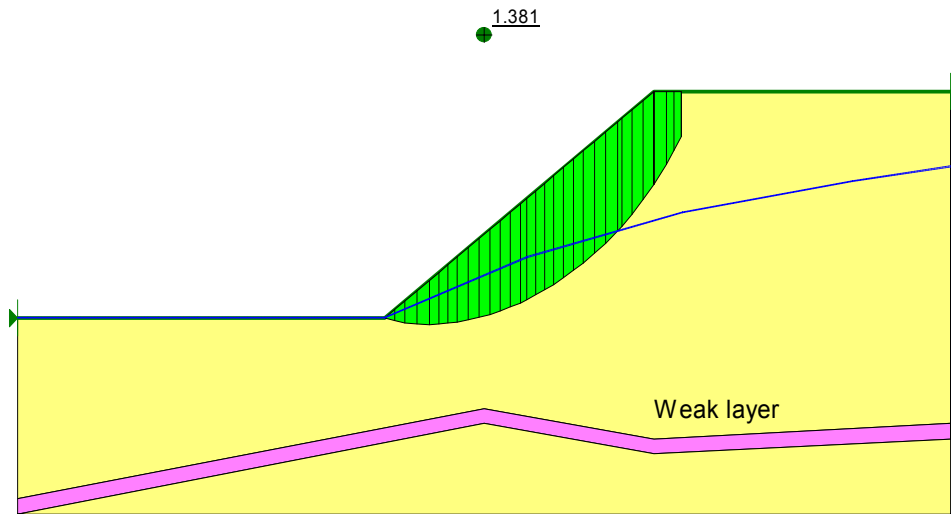


Figure 11-86 Auto locate critical slip surface and factor of safety with a deep weak layer

SLOPE/W allows you to look at the sensitivity of the soil properties to the factor of safety easily. Let's assume that you are interested in the following soil properties ranges:

- Unit weight - mean value at 20, study from 15 to 25 with 10 increments
- Cohesion – mean value at 20, study from 15 to 25 with 10 increments
- Friction angle – mean value at 30, study from 15 to 45 with 10 increments

Using the Draw Sensitivity feature, SLOPE/W generates a plot of factor of safety versus the sensitivity range (Figure 11-87).

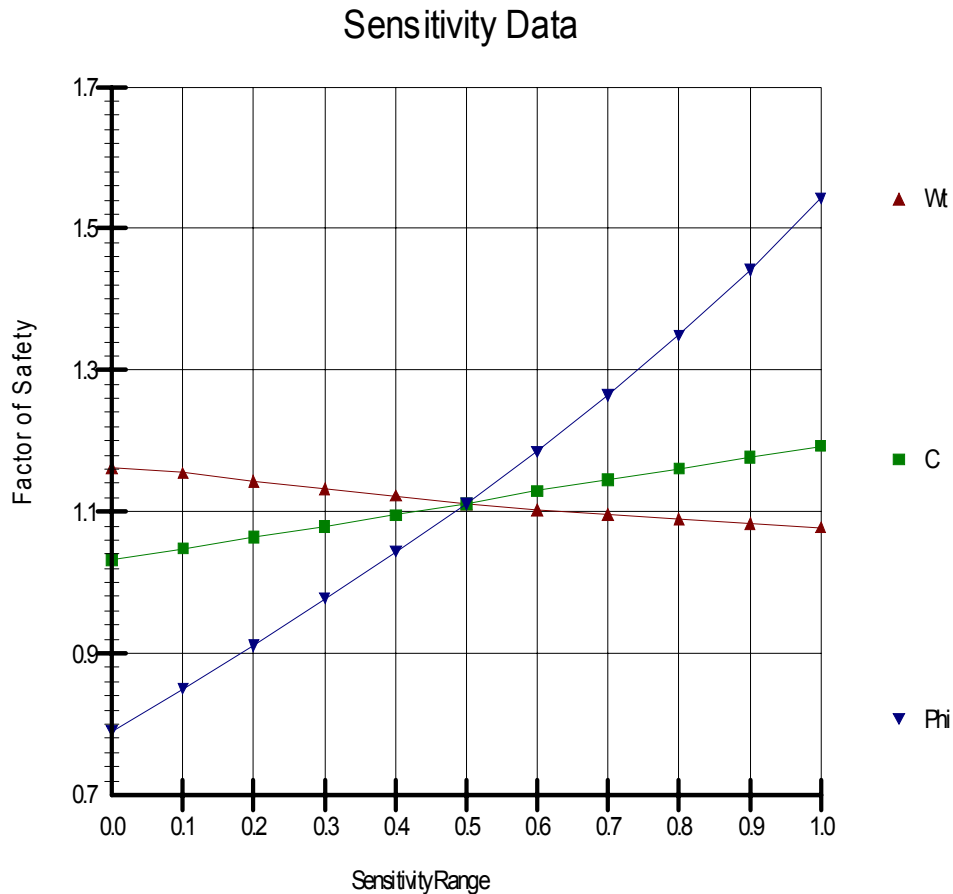


Figure 11-87 Sensitivity plot

In this example, it is clear that the factor of safety is more sensitive to frictional angle than the cohesion of the material. The unit weight of the material has a negative effect to the factor of safety. That is, the higher the unit weight, the lower the factor of safety.

The crossing point in the middle of the plot is the result when the mean values of all three parameters are used. The factor of safety at the crossing point is 1.111, which is identical to the result shown in Figure 11-84.

It is of interest to plot the safety map of all the trial slip surfaces. Figure 11-88 is the safety map of the analysis with the shallow weak layer (Figure 11-84). Using the auto locate slip surface method, circular trial slip surfaces are generated automatically for the entire slope. The critical slip surface is then optimized to find the most critical slip surface. The white line is the optimized slip surface.

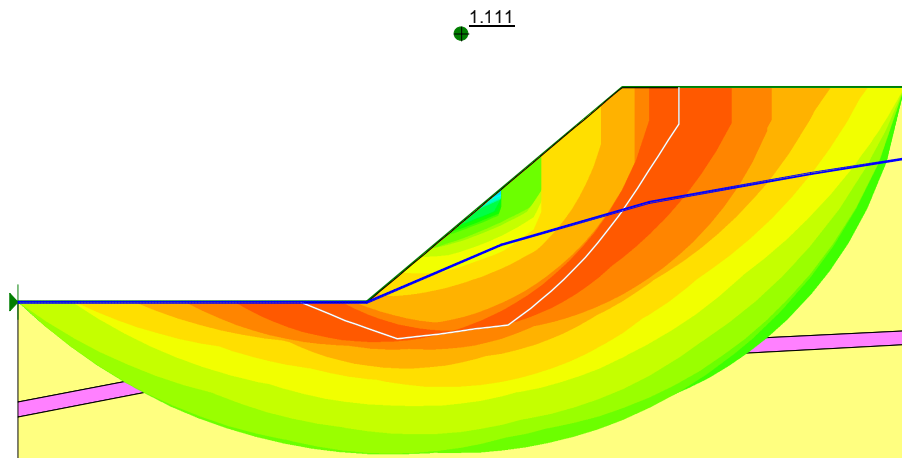


Figure 11-88 Safety map showing the extent of the trial slip surfaces and the auto located slip surface

11.19 Partially and fully submerged slope

Included files

- Partially submerged.gsz
- Fully submerged.gsz

The purpose of this illustrative example is to show how the stability of a partially submerged slope or a fully submerged slope can be modeled with SLOPE/W.

Features of this simulation include:

- Analysis method: GLE with half-sine function
- Entry and Exit slip surface
- Partial submerged slope
- Fully submerged slope

- SI units

Partial submergence can be modeled in one of two ways. One is to model the water layer as a no-strength soil region. The second way is to model the water layer with a pressure line.

Figure 11-89 shows the geometry of the partial submerged slope modeled with a no-strength soil region (blue color region). Even though it is defined as a no-strength soil region, it is important that the piezometric line must be defined on the top of the no-strength soil region as shown. SLOPE/W uses a vertical slip surface through the no-strength (water) region and applies a hydrostatic horizontal force on the vertical portion of the slip surface.

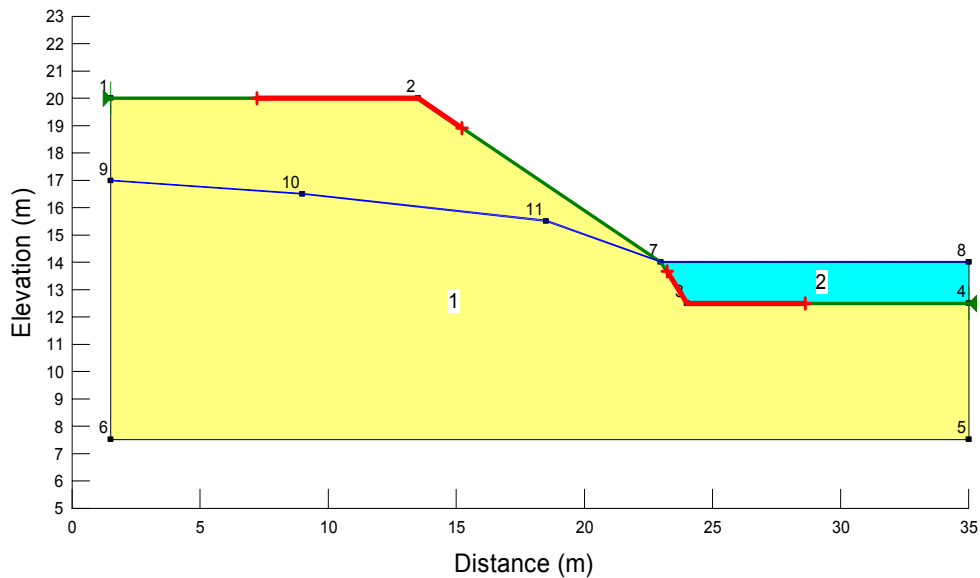


Figure 11-89 Geometry of the partial submerged slope when modeled with a no-strength (water) soil region

Figure 11-90 shows the critical slip surface and the factor of safety of the partially submerged slope. The factor of safety is 1.109.

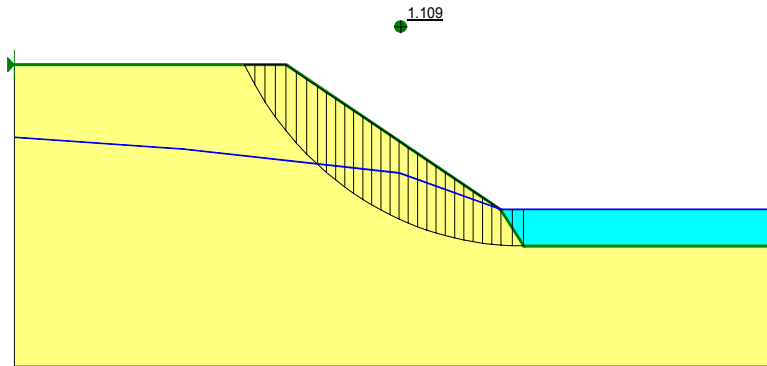


Figure 11-90 Critical slip surface and factor of safety of the partial submerged slope when modeled with a no-strength (water) soil region

Figure 11-91 show the free body diagram and the force polygon of the last slice on the downstream slope. The horizontal force of about 11 kN is shown on the right vertical side of the slice. This is the stabilizing force, due to the no-strength water layer. Since the water layer is 1.5 m thick, you can calculate by hand that the horizontal stabilizing force due to this water layer is about 11 kN (i.e., $9.807 \times 1.5 \times 1.5 / 2.0$).

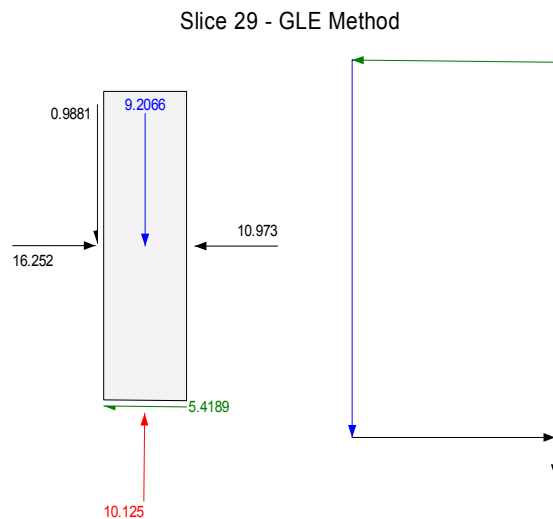


Figure 11-91 Free body diagram and force polygon of the last slice in the water layer

Figure 11-92 shows the geometry when the partial submerged slope is modeled with a pressure line. The pressure line has the same value as the unit weight of water. Note that the pressure line represents the weight of the water layer only; the piezometric must also be specified on the pressure line to model the pore water pressure properly.

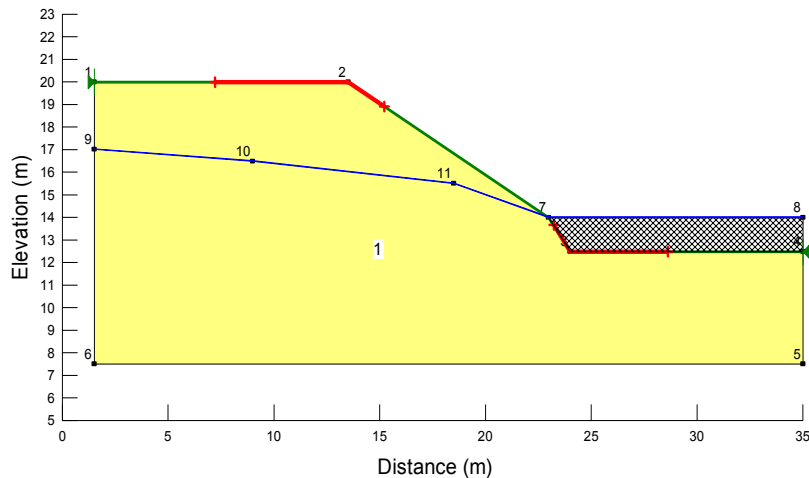


Figure 11-92 Geometry of the partial submerged slope when modeled with a pressure line

Figure 11-93 shows the critical slip surface and the factor of safety of the partial submerged slope when modeled with a pressure boundary. The factor of safety is 1.109, which is very close to the case when modeled with a no-strength soil region (Figure 11-90).

The free body diagram and the force polygon of the last slice is shown in Figure 11-94. There is no horizontal force acting on the vertical side of the slice, but there is an extra load acting on the top of the slice at an angle normal to the ground surface. This extra force is due to the pressure line, that is, the weight of the water layer.

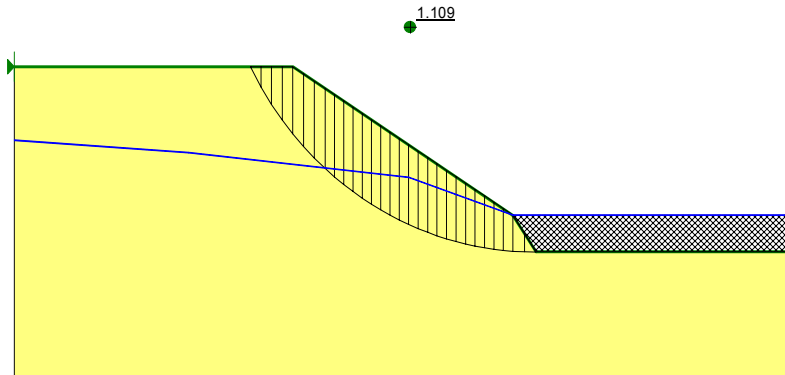


Figure 11-93 Critical slip surface and factor of safety of the partial submerged slope when modeled with a pressure line

Slice 29 - GLE Method

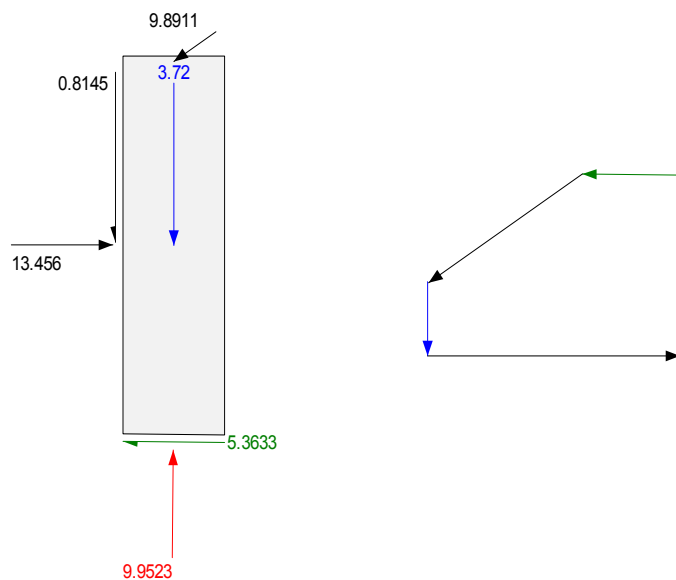


Figure 11-94 Free body diagram and force polygon of the last slice in the pressure line

When a slope is fully submerged, you may model the water as no-strength soil region or pressure line in the same manner as the partial submerged slope, or

alternatively, you can modeled the fully submerged slope using the submerged weight approach.

Figure 11-95 shows the factor of safety of the fully submerged slope when model with a no-strength (water) soil region. The factor of safety is 1.727.

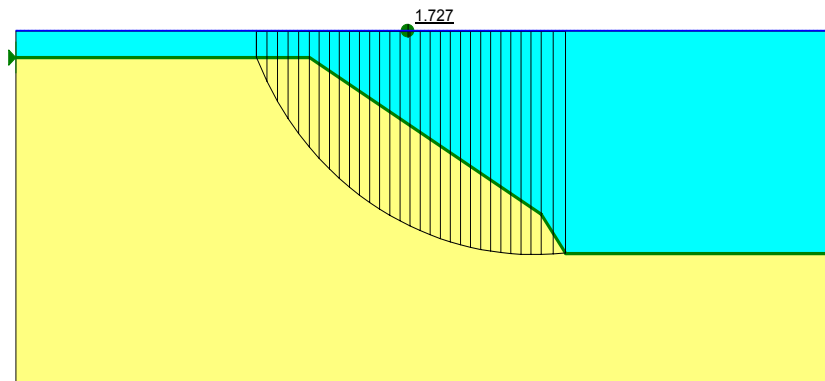


Figure 11-95 Critical slip surface and factor of safety of fully submerged slope when modeled with a no-strength (water) soil region

Figure 11-96 shows the factor of safety of the fully submerged slope when modeled with a pressure boundary. The factor of safety is 1.736.

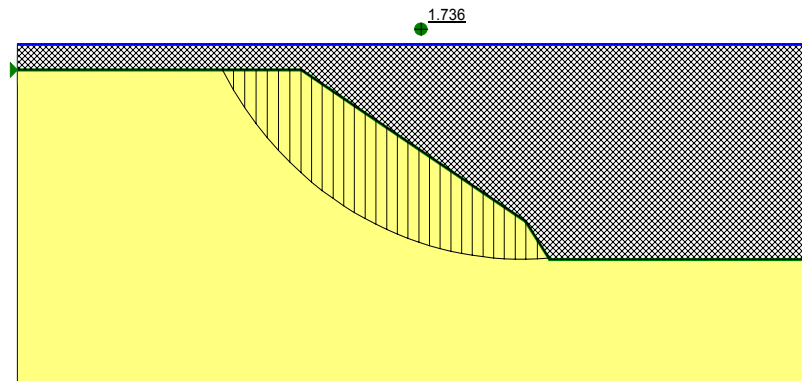


Figure 11-96 Critical slip surface and factor of safety of fully submerged slope when modeled with a pressure line

Perhaps, the simplest way to model a fully submerged slope is to model the material with a submerged unit weight instead of the total unit weight. The submerged unit weight without the water is:

$$\gamma_{\text{submerged}} = \gamma_{\text{total}} - \gamma_{\text{water}}$$

For example, the total weight of the material is 20 kN/m^3 , and the unit weight of water is 9.807 kN/m^3 , the submerged unit weight will be 10.193 kN/m^3 . Using this submerged unit weight approach, there is no need to model the piezometric line. Figure 11-97 illustrates the case when the slope is fully submerged. The computed factor of safety of the fully submerged slope is 1.738 which is essentially the same as the other two cases (Figure 11-95 and Figure 11-96).

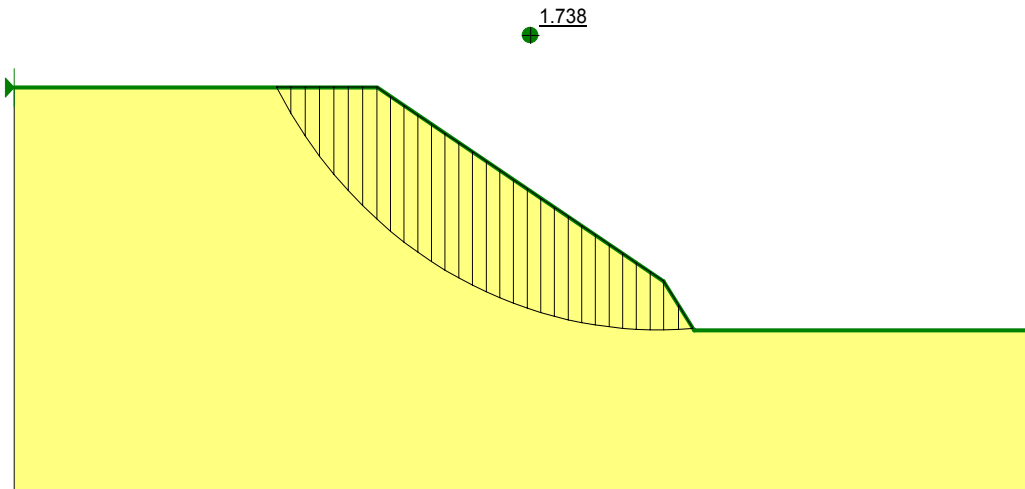


Figure 11-97 Critical slip surface and factor of safety of fully submerged slope when modeled with submerged weight

Ideally, there should be no shear between the slices within the water. However, depending on the selected method of analysis and the selected interslice force function, there may be a small shear force. The presence of such small shear between the slices does not significantly affect the factor of safety.

The interslice shear forces are not an issue for the Bishop, Janbu and Ordinary analysis methods, since these methods ignore interslice shear forces. They are only an issue when you use a method such as Spencer, Morgenstern-Price or GLE, since these methods include interslice shear forces. When using these more rigorous

methods, it is best to also use an interslice side force function to reduce the shear component in the crest and toe areas. A half-sine function, for example, is better than a constant function. The analysis could be further refined with a fully specified interslice side force function.

Refining the analysis with a particular side force function may not be warranted when the depth of submergence is shallow relative to the slope height. Special consideration of the interslice force function may become more important as the depth of submergence approaches the slope height.

11.20 Permanent deformation analysis

Included file

- Deformation.gsz

SLOPE/W can use the results from a QUAKE/W dynamic analysis to examine the stability and permanent deformation of earth structures subjected to earthquake shaking using a procedure similar to the Newmark method. QUAKE/W is a finite element program for analyzing the effects of earthquakes on embankments and natural slopes. QUAKE/W computes the static plus dynamic ground stresses at specified intervals during an earthquake. SLOPE/W can use these stresses to analyze the stability variations during the earthquake and estimate the resulting permanent deformation.

The purpose of this illustrative example is to show how to do a QUAKE/W Dynamic analysis to examine the stability and permanent deformation of a slope subjected to earthquake shaking. Features of this simulation include:

- Analysis method: QUAKE/W Dynamic
- Homogeneous soil with Mohr Coulomb model
- No pore-water pressure
- Multiple slip surface with Grid and Radius
- SI units

To do a QUAKE/W Dynamic analysis, you must start your analysis with QUAKE/W. First, you need to establish the initial static stress of the slope, you then do the dynamic stress analysis of the slope using the initial static stress as initial condition. Please refer to the QUAKE/W engineering book for details of

doing a QUAKE/W analysis. It is important that you are satisfied with the computed results in QUAKE/W before you proceed to the Dynamic analysis in SLOPE/W.

Assume that you have done the QUAKE/W analysis and you are happy with the results, you can then shift to SLOPE/W by clicking the SLOPE/W icon in GeoStudio. You are now ready to define the shear strength properties of the material and the trial slip surface method. Figure 11-98 shows the geometry, the finite element mesh, the soil model of the material and the position of the search grid.

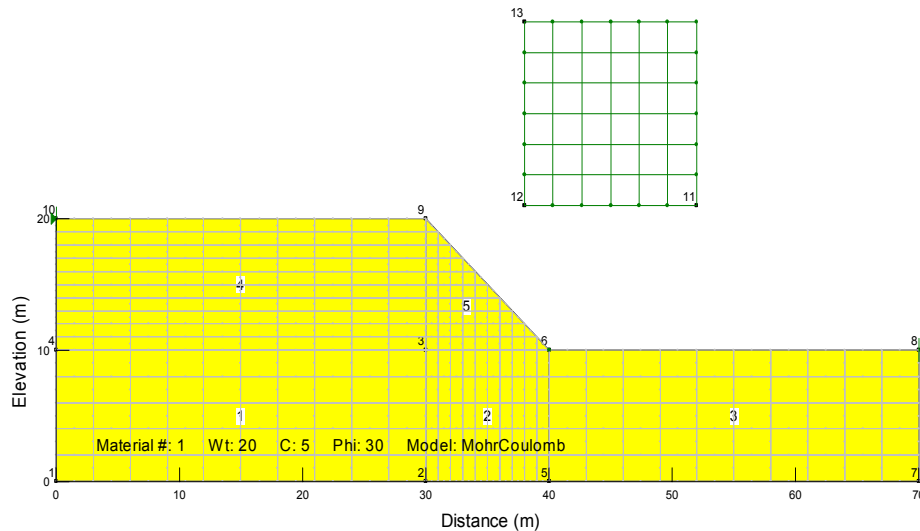


Figure 11-98 The geometry, finite element mesh of the DEFORMATION example

For each trial slip surface, SLOPE/W uses the initial stress condition to establish the static strength of the slope and the dynamic stress at all time steps to compute the dynamic shear stress of the slope and the factor of safety at all time during the shaking process. SLOPE/W determines the total mobilized shear arising from the dynamic inertial forces. This dynamically driven mobilized shear is divided by the total slide mass to obtain an average acceleration. This average acceleration for the entire potential sliding mass represents one acceleration value that affects the stability at an instance in time.

In this example, the shaking of the slope is 10 seconds long and is modeled with 500 time steps. Figure 11-99 shows the critical slip surface at the end of the shaking (i.e., at time step 500). The critical factor of safety is 1.095 at time step 500, the smallest factor of safety during the entire shaking may occur at other time steps.

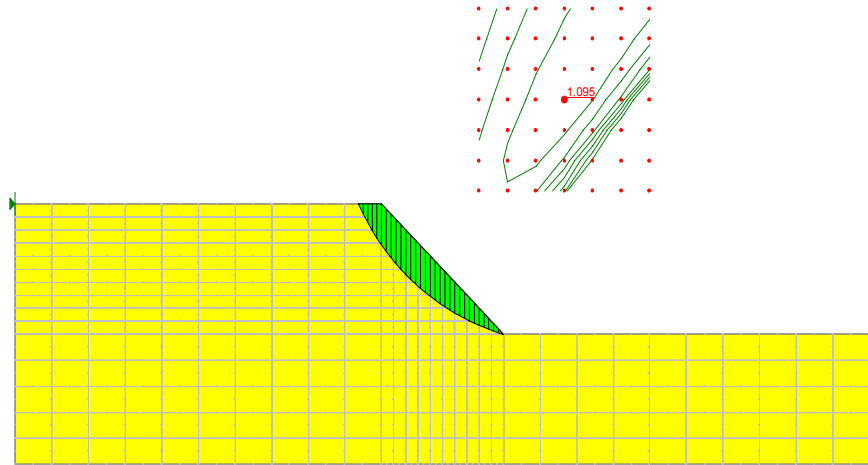


Figure 11-99 Critical slip surface and factor of safety at time step 500

Figure 11-100 shows the factor of safety of the same slip surface (Figure 11-99) during the shaking process. You can see that the smallest factor of safety of this slip surface is about 0.9 at about 2.5 seconds into the shaking, and the highest factor of safety of this slip surface is about 1.46 at about 6 seconds into the shaking.

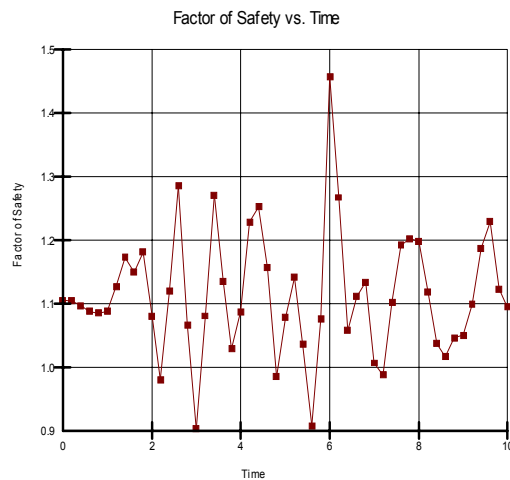


Figure 11-100 Factor of safety of a slip surface during the 10 seconds shaking

Figure 11-101 shows the computed factor of safety versus the average acceleration of the slip surface. As expected, the factor of safety is inversely proportional to the average acceleration. From this plot, SLOPE/W computes the acceleration corresponding to a factor of safety of 1.0. This is called the yield acceleration. The yield acceleration of this slip surface is 0.05691.

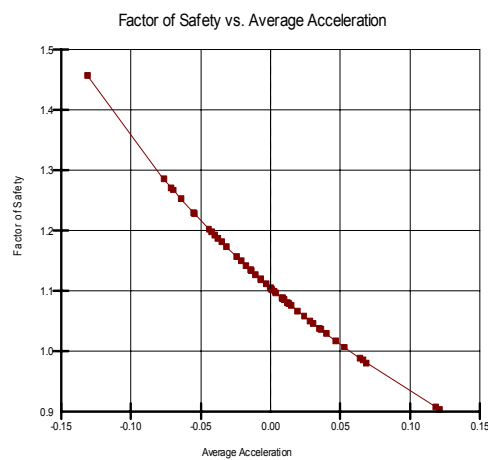


Figure 11-101 Factor of safety versus average acceleration

Figure 11-102 shows the average acceleration of the slip surface during the 10 seconds of shaking. By integrating the area of the graph when the average acceleration is at yield acceleration, we can get a velocity versus time plot during the shaking period (Figure 11-103).

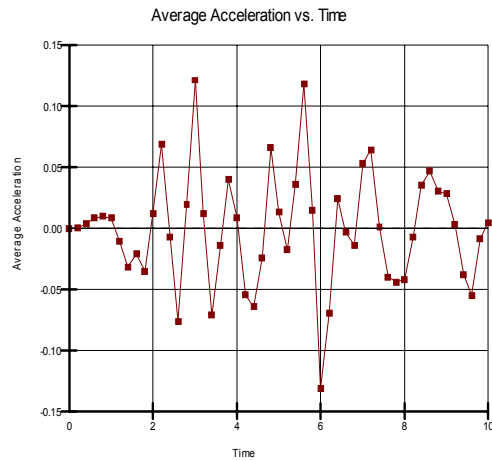


Figure 11-102 Average acceleration versus time

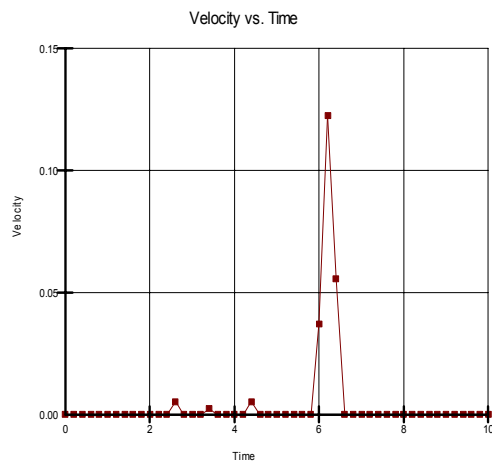


Figure 11-103 Velocity versus time plot

Figure 11-104 shows the permanent deformation versus time of the slip surface. It is obtained by integrating the area under the velocity graph (Figure 11-103) when there is a positive velocity. The maximum permanent deformation of this slip surface is 0.0457 m. You may examine and plot results of any slip surfaces at any time steps using the Draw Slip Surface feature in CONTOUR.

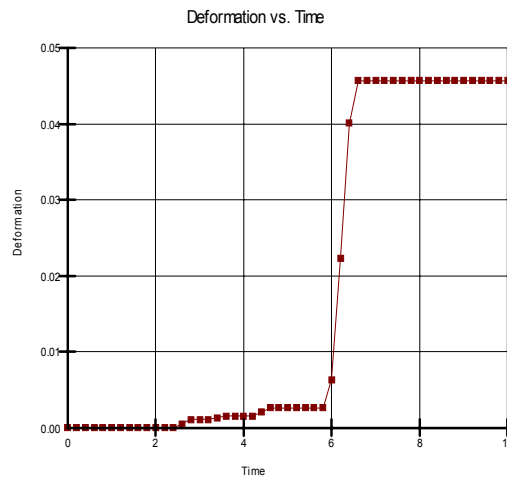


Figure 11-104 Permanent deformation versus time

Please note that this type of analysis is sometimes referred to as an undrained dynamic deformation analysis. The soil is deemed to behave in an undrained manner during the earthquake shaking; that is, the total soil strength does not change much during the shaking. According to S.L. Kramer in his book "Geotechnical Earthquake Engineering" (page 462), this type of analysis is only appropriate if there is less than about 15% degradation in strength due to the shaking. This type of analysis is not considered appropriate for cases where there is a large build-up of pore pressures, which in turn may lead to large strength losses causing the soil to liquefy. Examining the possibility of a liquefaction flow failure requires a different type of analysis.

12 Theory

12.1 Introduction

This chapter explains the theory used in the development of SLOPE/W. The variables used are first defined, followed by a brief description of the General Limit Equilibrium method (GLE). The relevant equations are derived, including the base normal force equation and the factor of safety equations. This is followed by a section describing the iterative procedure adopted in solving the nonlinear factor of safety equations. Attention is then given to aspects of the theory related to soils with negative pore-water pressures.

SLOPE/W solves two factor of safety equations; one equation satisfies force equilibrium and the other satisfies moment equilibrium. All the commonly used methods of slices can be visualized as special cases of the General Limit Equilibrium (GLE) solution.

The theory of the Finite Element Stress method is presented as an alternative to the limit equilibrium stability analysis. This method computes the stability factor of a slope based on the stress state in the soil obtained from a finite element stress analysis. Finally, the theory of probabilistic slope stability using the Monte Carlo method is also presented.

12.2 Definition of variables

SLOPE/W uses the theory of limit equilibrium of forces and moments to compute the factor of safety against failure. The General Limit Equilibrium (GLE) theory is presented and used as the context for relating the factors of safety for all commonly used methods of slices.

A factor of safety is defined as that factor by which the shear strength of the soil must be reduced in order to bring the mass of soil into a state of limiting equilibrium along a selected slip surface.

For an effective stress analysis, the shear strength is defined as:

$$s = c' + (\sigma_n - u) \tan \phi'$$

where:

s	=	shear strength,
c'	=	effective cohesion,
ϕ'	=	effective angle of internal friction,
σ_n	=	total normal stress, and
u	=	pore-water pressure.

For a total stress analysis, the strength parameters are defined in terms of total stresses and pore-water pressures are not required.

The stability analysis involves passing a slip surface through the earth mass and dividing the inscribed portion into vertical slices. The slip surface may be circular, composite (i.e., combination of circular and linear portions) or consist of any shape defined by a series of straight lines (i.e., fully specified slip surface).

The limit equilibrium formulation assumes that:

The factor of safety of the cohesive component of strength and the frictional component of strength are equal for all soils involved.

The factor of safety is the same for all slices.

Figure 12-1 and Figure 12-2 show all the forces acting on a circular and a composite slip surface. The variables are defined as follows:

W	=	the total weight of a slice of width b and height h
N	=	the total normal force on the base of the slice
S_m	=	the shear force mobilized on the base of each slice.
E	=	the horizontal interslice normal forces. Subscripts L and R designate the left and right sides of the slice, respectively.
X	=	the vertical interslice shear forces. Subscripts L and R define the left and right sides of the slice, respectively.
D	=	an external line load.
kW	=	the horizontal seismic load applied through the centroid of each slice.
R	=	the radius for a circular slip surface or the moment arm associated with the mobilized shear force, S_m for any shape of slip surface.

f	=	the perpendicular offset of the normal force from the center of rotation or from the center of moments. It is assumed that f distances on the right side of the center of rotation of a negative slope (i.e., a right-facing slope) are negative and those on the left side of the center of rotation are positive. For positive slopes, the sign convention is reversed.
x	=	the horizontal distance from the centerline of each slice to the center of rotation or to the center of moments.
e	=	the vertical distance from the centroid of each slice to the center of rotation or to the center of moments.
d	=	the perpendicular distance from a line load to the center of rotation or to the center of moments.
h	=	the vertical distance from the center of the base of each slice to the uppermost line in the geometry (i.e., generally ground surface).
a	=	the perpendicular distance from the resultant external water force to the center of rotation or to the center of moments. The L and R subscripts designate the left and right sides of the slope, respectively.
A	=	the resultant external water forces. The L and R subscripts designate the left and right sides of the slope, respectively.
ω	=	the angle of the line load from the horizontal. This angle is measured counter-clockwise from the positive x-axis.
α	=	the angle between the tangent to the center of the base of each slice and the horizontal. The sign convention is as follows. When the angle slopes in the same direction as the overall slope of the geometry, α is positive, and vice versa.

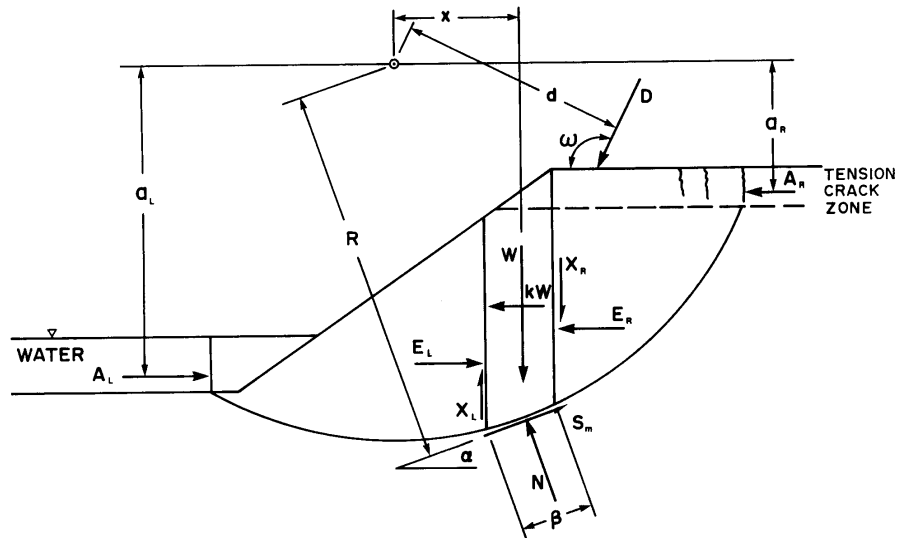


Figure 12-1 Forces acting on a slice through a sliding mass with a circular slip surface

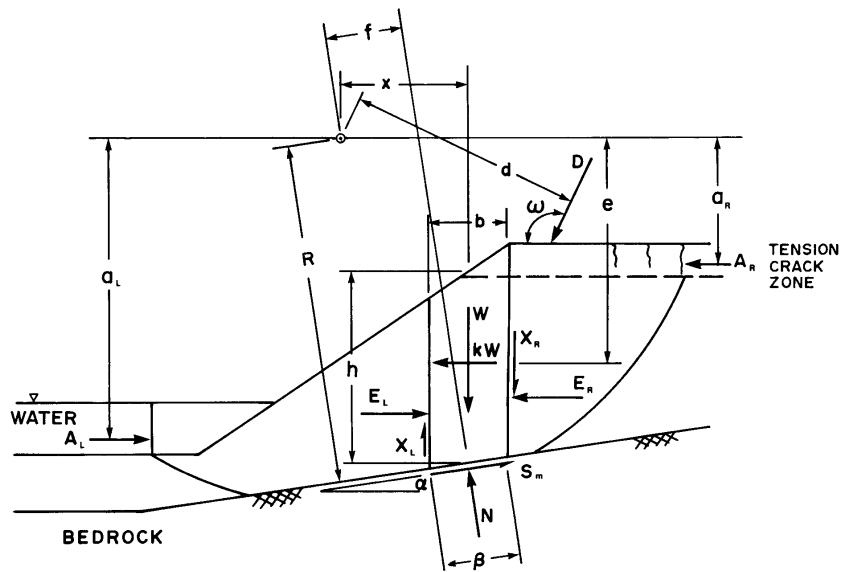


Figure 12-2 Forces acting on a slice through a sliding mass with a composite slip surface

$$S_m = \frac{s \beta}{F} = \frac{\beta \left(c' + \left(\sigma_n - u \right) \tan \phi' \right)}{F}$$

Page 361

$$\sigma_n = \frac{N}{\beta} \quad = \quad \text{average normal stress at the base of each slice,}$$

$$F \quad = \quad \text{the factor of safety, and}$$

$$\beta \quad = \quad \text{the base length of each slice.}$$

The elements of statics that can be used to derive the factor of safety are the summations of forces in two directions and the summation of moments. These, along with failure criteria, are insufficient to make the problem determinate. More information must be known about either the normal force distribution at the base of the slices or the interslice force distribution. Table 12-1 and Table 12-2 summarize the known and unknown quantities associated with a slope stability analysis.

Table 12-1 Summary of known quantities in solving for a safety factor

Number of Known Quantities	Description
n	Summation of forces in the horizontal direction
n	Summation of forces in the vertical direction
n	Summation of moments
n	Material Shear Failure Criterion
4n	Total number of equations

Table 12-2 Summary of unknown quantities in solving for a safety factor

Number of Unknown Quantities	Description
n	Magnitude of the normal force at the base of a slice, N
n	Point of application of the normal force at the base of each slice
n - 1	Magnitude of the interslice normal forces, E
n - 1	Magnitude of the interslice shear force, X
n - 1	Point of application of the interslice forces
n	Shear force on the base of each slice, S _m
1	Factor of safety, F
1	Value of Lambda, λ
6n - 1	Total number of unknowns

Since the number of unknown quantities exceeds the number of known quantities, the problem is indeterminate. Assumptions regarding the directions, magnitude, and/or point of application of some of the forces must be made to render the analysis determinate. Most methods first assume that the point of application of the normal force at the base of a slice acts through the centerline of the slice. Then an assumption is most commonly made concerning the magnitude, direction, or point of application of the interslice forces.

In general, the various methods of slices can be classified in terms of:

- the statics used in deriving the factor of safety equation, and
- the interslice force assumption used to render the problem determinate.

12.3 General limit equilibrium method

The General Limit Equilibrium method (GLE) uses the following equations of statics in solving for the factor of safety:

- The summation of forces in a vertical direction for each slice is used to compute the normal force at the base of the slice, N .
- The summation of forces in a horizontal direction for each slice is used to compute the interslice normal force, E . This equation is applied in an integration manner across the sliding mass (i.e., from left to right).
- The summation of moments about a common point for all slices. The equation can be rearranged and solved for the moment equilibrium factor of safety, F_m .
- The summation of forces in a horizontal direction for all slices, giving rise to a force equilibrium factor of safety, F_f .

The analysis is still indeterminate, and a further assumption is made regarding the direction of the resultant interslice forces. The direction is assumed to be described by a interslice force function. The direction together with the interslice normal force is used to compute the interslice shear force. The factors of safety can now be computed based on moment equilibrium (F_m) and force equilibrium (F_f). These factors of safety may vary depending on the percentage (λ) of the force function used in the computation. The factor of safety satisfying both moment and force equilibrium is considered to be the converged factor of safety of the GLE method.

Using the same GLE approach, it is also possible to specify a variety of interslice force conditions and satisfy only the moment or force equilibrium conditions. The assumptions made to the interslice forces and the selection of overall force or moment equilibrium in the factor of safety equations, give rise to the various methods of analysis.

12.4 Moment equilibrium factor of safety

Reference can be made to Figure 12-1, Figure 12-2 and Figure 12-3 for deriving the moment equilibrium factor of safety equation. In each case, the summation of moments for all slices about an axis point can be written as follows:

$$\sum Wx - \sum S_m R - \sum Nf + \sum kWe \pm \sum Dd \pm \sum Aa = 0$$

After substituting for S_m and rearranging the terms, the factor of safety with respect to moment equilibrium is:

$$F_m = \frac{\sum (c'\beta R + (N - u\beta) R \tan \phi')}{\sum Wx - \sum Nf + \sum kWe \pm \sum Dd \pm \sum Aa}$$

This equation is a nonlinear equation since the normal force, N , is also a function of the factor of safety. The procedure for solving the equation is described below in this chapter.

12.5 Force equilibrium factor of safety

Again, reference can be made to Figure 12-1, Figure 12-2 and Figure 12-3 for deriving the force equilibrium factor of safety equation. The summation of forces in the horizontal direction for all slices is:

$$\begin{aligned} &\sum (E_L - E_R) - \sum (N \sin \alpha) + \sum (S_m \cos \alpha) \\ &- \sum (kW) + \sum D \cos \omega \pm \sum A = 0 \end{aligned}$$

The term $\sum (E_L - E_R)$ presents the interslice normal forces and must be zero when summed over the entire sliding mass. After substituting for S_m and rearranging the terms, the factor of safety with respect to horizontal force equilibrium is:

$$F_f = \frac{\sum (c'\beta \cos \alpha + (N - u\beta) \tan \phi' \cos \alpha)}{\sum N \sin \alpha + \sum kW - \sum D \cos \omega \pm \sum A}$$

12.6 Slice normal force at the base

The normal force at the base of a slice is derived from the summation of forces in a vertical direction on each slice.

$$(X_L - X_R) - W + N \cos \alpha + S_m \sin \alpha - D \sin \omega = 0$$

Once again, after substituting for S_m the equation for the normal at the base of each slice is:

$$N = \frac{W + (X_R - X_L) - \frac{c'\beta \sin \alpha + u\beta \sin \alpha \tan \phi'}{F} + D \sin \omega}{\cos \alpha + \frac{\sin \alpha \tan \phi'}{F}}$$

The normal equation is nonlinear, with the value dependent on the factor of safety, F . The factor of safety is equal to the moment equilibrium factor of safety, F_m , when solving for moment equilibrium, and equal to the force factor of safety, F_f , when solving for force equilibrium.

The base normal equation cannot be solved directly, since the factor of safety (F) and the interslice shear forces, (i.e., X_L and X_R) are unknown. Consequently, N needs to be determined using an interactive scheme.

To commence the solution for the factor of safety, the interslice shear and normal forces are neglected and the normal force on each slice can be computed directly by summing forces in the same direction as the normal force.

$$N = W \cos \alpha - kW \sin \alpha + [D \cos(\omega + \alpha - 90)]$$

We can use this simplified normal equation to obtain starting values for the factor of safety computations. The factors of safety obtained using this simplified equation is the Fellenius or Ordinary method factor of safety.

If we ignore the interslice shear forces, but retain the interslice normal forces, then the slice base normal force equation is:

$$N = \frac{W - \frac{c'\beta \sin \alpha + u\beta \sin \alpha \tan \phi'}{F} + [D \sin \omega]}{\cos \alpha + \frac{\sin \alpha \tan \phi'}{F}}$$

When we use this equation for the base normal, the factor of safety with respect to moment equilibrium is the Bishop Simplified factor of safety, and the factor of safety with respect to force equilibrium is the Janbu Simplified factor of safety.

12.7 *M-alpha values*

The denominator in the base normal equation is commonly given the variable name, m_α . This term can become problematic when the slice base inclination is too steep. As we can see from the above base normal equation and the diagram in Figure 12-4, the variable m_α is a function of inclination of the base of a slice, α , and $\tan \phi'/F$. Computational difficulties occur when m_α approaches zero. This situation can occur when α is negative and $\tan \phi'/F$ is large or when α is large and $\tan \phi'/F$ is small. Specifically, the m_α value will become zero when the base inclination of any slice, α , bears the following relationship to the mobilized friction angle, $\tan \phi'/F$:

$$\frac{\cos \alpha}{\sin \alpha} = \frac{1}{\tan \alpha} = -\frac{\tan \phi'}{F}$$

When the m_α value approaches zero, the computed normal force, N , on the slice becomes excessively large. As a result, the mobilized shearing resistance, S_m , becomes very large and exerts a disproportionately large influence on the computation of the factor of safety.

The factor of safety calculation can take on another extreme when m_α is negative. The m_α term can be negative when the base angle of the slice, α , is more negative than the limiting angle, α_1 . In this case, the computed normal force is negative. Consequently, the computed factor of safety may be under-estimated, since the total mobilized shearing resistance is reduced. When a slice has a small, but negative m_α value, its normal force becomes large and negative when compared with other slices. The large, negative value then dominates the stability calculations, and the computed factor of safety can go less than zero, which of course is meaningless.

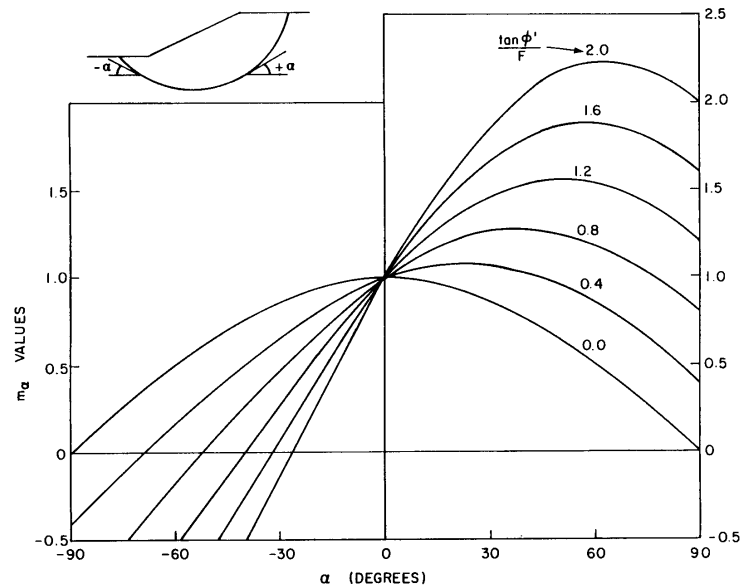


Figure 12-4 Magnitude of m_α for various α , ϕ , and F values

Problems associated with the magnitude of m_α are mainly the result of an inappropriately assumed shape for the slip surface. Ideally, the classic earth pressure theory should be used to establish the limiting conditions for the shape of the slip surface. In applying the earth pressure theory, the soil is divided into two regions, namely an active earth pressure zone and a passive earth pressure zone. The inclination of the slip surface in the passive (toe) zone of the sliding mass should be limited to the maximum obliquity for the passive state. That is:

$$\alpha_1 < 45^\circ - \frac{\phi'}{2}$$

Likewise, the inclination of the slip surface in the active (crest) zone should not exceed the value obtained from the following equation:

$$\alpha_1 < 45^\circ + \frac{\phi'}{2}$$

These solutions will generally resolve the m_α problems. The active zone also may be combined with a vertical tension crack zone to alleviate m_α problems.

It is the responsibility of the user to ensure that the limiting angles with respect to the active and passive zones are not violated. However, if the conditions are violated, there is a check in SLOPE/W to prevent the absolute value of m_α from going below 1.0×10^{-5} .

12.8 Interslice forces

The interslice forces are the normal and shear forces acting in the vertical faces between slices. The interslice normal forces are solved using an integration procedure commencing at the left end of each slip surface.

The summation of forces in a horizontal direction can be written for each slice as:

$$(E_L - E_R) - N \sin \alpha + S_m \cos \alpha - kW + D \cos \omega = 0$$

Substituting S_m in this and then solving for the interslice normal on the right side of each slice gives:

$$E_R = E_L + \frac{(c'\beta - u\beta \tan \phi') \cos \alpha}{F} + N \left(\frac{\tan \phi' \cos \alpha}{F} - \sin \alpha \right) - kW + D \cos \omega$$

Since the left interslice normal force of the first slice is zero (i.e., $E_L=0$), integrating from the left end of all slices, the interslice normal force of all slices can be computed. Note that the equation for computing the interslice normal force is depending on the factor of safety and it is updated during the iteration process.

Once the interslice normal force is known, the interslice shear force is computed as a percentage of the interslice normal force according to the following empirical equation proposed by Morgenstern and Price (1965):

$$X = E \lambda f(x)$$

where:

- λ = the percentage (in decimal form) of the function used, and
- $f(x)$ = interslice force function representing the relative direction of the resultant interslice force.

Figure 12-5 shows some typical function shapes. The type of force function used in calculating the factor of safety is the prerogative of the user.

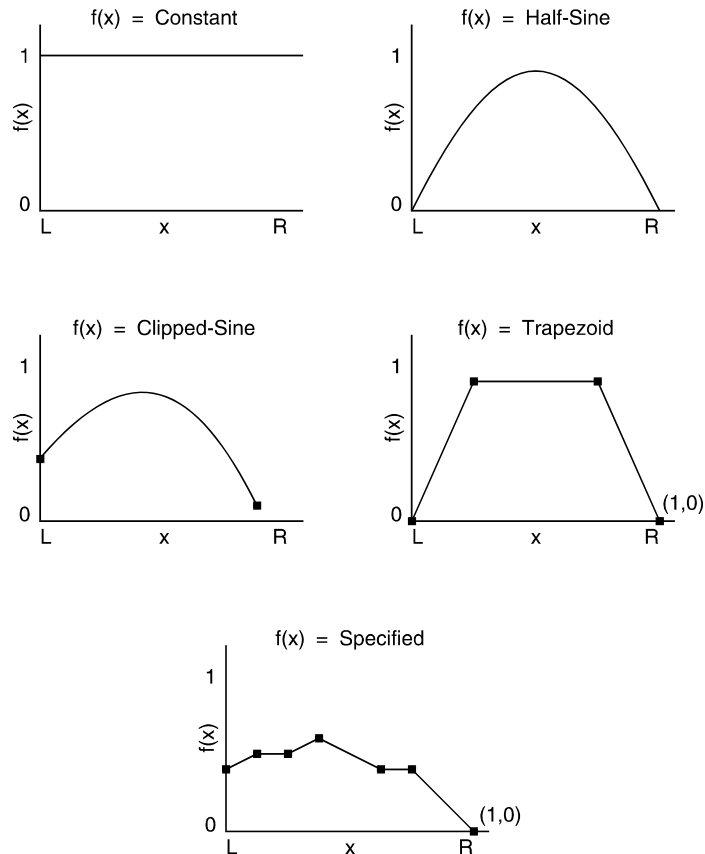


Figure 12-5 Example interslice force functions

The slices' interslice shear forces are required to calculate the normal force at the base of each slice. Figure 12-6 illustrates how the interslice force function $f(x)$ is used to compute the interslice shear force. Assume the use of a half-sine force function. Assume that the normal force E between Slice 1 and 2 is 100 kN, the applied Lambda value λ is 0.5 and a half-sine interslice force function is used. The $f(x)$ value at the location between Slice 1 and 2 is 0.45. The shear force X then is:

$$f(x) = 0.45$$

$$\lambda = 0.5$$

$$E = 100 \text{ kN}$$

$$X = 100 \times 0.5 \times 0.45 = 22.5 \text{ kN}$$

For this example, the ratio of shear to normal varies from 0.0 at the crest and at the toe, to a maximum of 0.5 at the midpoint along the slip surface.

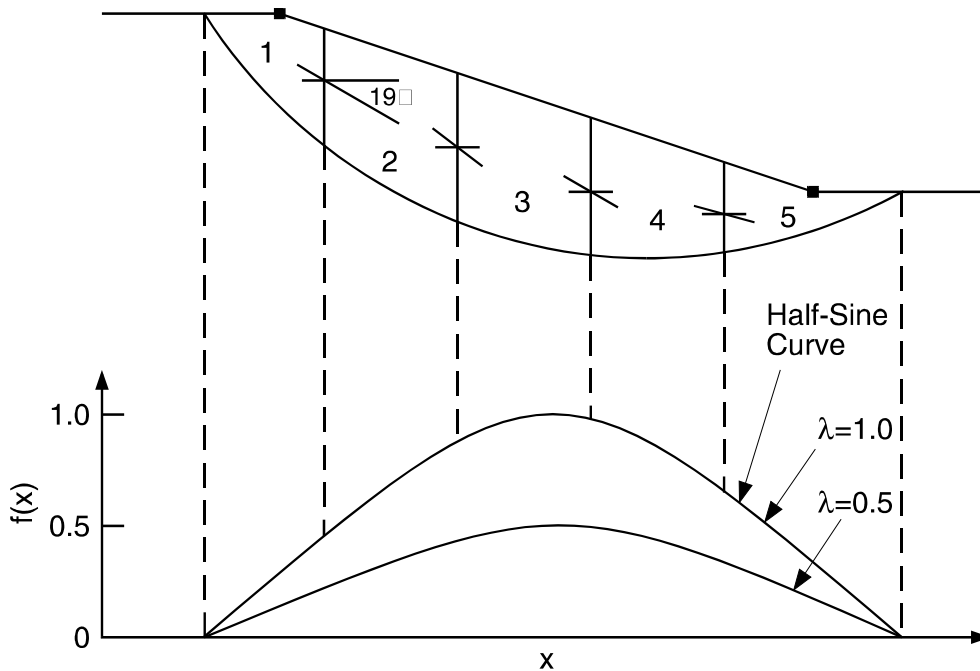


Figure 12-6 Example use of half-sine interslice force function

12.9 Effect of negative pore-water pressures

In locations above the groundwater table, the pore-water pressure in a soil is negative relative to the pore-air pressure. This negative pore-water pressure is commonly referred to as the matric suction of the soil. Under negative pore-water pressure conditions the shear strength may not change at the same rate as for total and positive pore-water pressure changes. Therefore, a modified form of the Mohr-Coulomb equation must be used to describe the shear strength of an unsaturated soil (i.e., a soil with negative pore-water pressures). The shear strength equation is:

$$s = c' + (\sigma_n - u_a) \tan \phi' + (u_a - u_w) \tan \phi^b$$

where:

- u_a = pore-air pressure,
 u_w = pore-water pressure, and
 ϕ^b = an angle defining the increase in shear strength for an increase in suction.

This equation indicates that the shear strength of a soil can be considered as having three components: the cohesive strength due to c' , the frictional strength due to ϕ and the suction strength due to ϕ^b .

12.10 Factor of safety for unsaturated soil

The mobilized shear can also be written for unsaturated soil conditions. In equation form:

$$S_m = \frac{\beta}{F} \left(c' + (\sigma_n - u_a) \tan \phi' + (u_a - u_w) \tan \phi^b \right)$$

The normal at the slice base is:

$$N = \frac{W + (X_R - X_L) - \frac{c'\beta \sin \alpha + u_a \beta \sin \alpha (\tan \phi' - \tan \phi^b) + u_w \beta \sin \alpha \tan \phi^b}{F} + D \sin \omega}{\cos \alpha + \frac{\sin \alpha \tan \phi'}{F}}$$

The above equation can be used for both saturated and unsaturated soils. For most analyzes the pore-air pressure can be set to zero. SLOPE/W uses ϕ^b whenever the pore-water pressure is negative and ϕ' whenever the pore-water pressure is positive.

SLOPE/W uses two independent factor of safety equations; one with respect to moment equilibrium and the other with respect to horizontal force equilibrium. When only moment equilibrium is satisfied, the factor of safety equation is:

$$F_m = \frac{\sum \left(c'\beta R + \left[N - u_w \beta \frac{\tan \phi^b}{\tan \phi'} - u_a \beta \left(1 - \frac{\tan \phi^b}{\tan \phi'} \right) \right] R \tan \phi' \right)}{\sum W_x - \sum N_f + \sum kW_e \pm \sum Dd \pm \sum Aa}$$

The factor of safety equation with respect to horizontal force equilibrium is:

$$F_f = \frac{\sum \left(c'\beta \cos \alpha + \left[N - u_w \beta \frac{\tan \phi^b}{\tan \phi'} - u_a \beta \left(1 - \frac{\tan \phi^b}{\tan \phi'} \right) \right] \tan \phi' \cos \alpha \right)}{\sum N \sin \alpha + \sum kW - \sum D \cos \omega \pm \sum A}$$

12.11 Use of unsaturated shear strength parameters

SLOPE/W only considers unsaturated soil shear strength conditions when the pore-water pressures are negative. Under these conditions the angle, ϕ^b , is used to compute the mobilized shear strength force at the base of a slice.

The following types of input data help in understanding how SLOPE/W accommodates unsaturated soil conditions:

When ϕ^b is left blank or set to 0.0, any negative pore water pressure will be set to zero. There will be no increase in the shear strength due to the negative pore-water pressures (suction). Often the engineer does not want to rely upon any shear strength due to the negative pore-water pressures. In this case, the ϕ^b angles should be set to 0.0.

The upper limit of ϕ^b is ϕ' . The input of a value of this magnitude states that negative pore-water pressures will be as effective in increasing the shear strength of a soil as positive pore-water pressures are in reducing the shear strength. This may be reasonable for the saturated capillary zone immediately above the groundwater table. However, the engineer must make the decision whether these negative pore-water pressures are likely to remain near the same magnitudes over the time span of interest.

Usually ϕ^b is greater than zero, but less than ϕ' . All published research literature has shown this to be the case in laboratory testing programs. Most common values range from 15 to 20 degrees. However, the engineer must again decide whether the

negative pore-water pressures are likely to remain near the same magnitudes during the time span under consideration.

12.12 Solving for the factors of safety

Four different stages are involved in computing the various factors of safety. The following section describes these stages.

Stage 1 solution

For the first iteration, both the interslice normal and shear forces are set to zero. The resulting moment equilibrium factor of safety is the Ordinary or Fellenius factor of safety. The force equilibrium factor of safety has received little mention in the literature and is of little significance. The first iteration factors of safety are used as approximations for starting the second stage.

Stage 2 solution

Stage 2 starts the solution of the nonlinear factor of safety equations. Lambda (λ) is set to zero and therefore, the interslice shear forces are set to zero. Usually 4 to 6 iterations are required to ensure convergence of the moment and force equilibrium factor of safety equations. The answer from the moment equation corresponds to Bishop's Simplified method. The answer from the force equilibrium equation corresponds to Janbu's Simplified method without any empirical correction.

Stage 3 solution

Except for the GLE method, Stage 3 solution is required for all methods that consider interslice forces. Stage 3 computes the moment and force equilibrium factors of safety for any general interslice force function.

In Stage 3, SLOPE/W computes a λ value that provides an equal value for the force and moment equilibrium factors of safety (i.e., $F_m = 1$). The technique used is called the "Rapid Solver" and is similar in concept to a Newton-Raphson technique.

The Rapid Solver technique works as follows. SLOPE/W computes the initial value for λ as being equal to 2/3 of the slope between crest and toe. The moment and force equilibrium factors of safety are computed using this estimate of lambda. These factors of safety along with the factors of safety corresponding to a lambda equal to 0.0 are used to predict a lambda value where the force and moment

equilibrium factors of safety will be equal. This procedure of estimating new lambda values is repeated until the force and moment equilibrium factors of safety are within the selected tolerance.

Any one of the interslice force functions, $f(x)$, can be used when solving for the factor of safety.

Stage 4 solution

Stage 4 is used when a series of lambda values are selected and the moment and/or force equilibrium factors of safety are solved. Stage 4 is always used for the GLE method of analysis. The factors of safety for various lambda values can be plotted as shown in Figure 12-7. The factor of safety satisfying both moment and force equilibrium is selected from the plot.

Stage 4 provides a complete understanding of the relationship between the moment and force equilibrium factors of safety for a specific interslice force function. It can be used to simulate essentially all slope stability methods that consider the interslice force function.

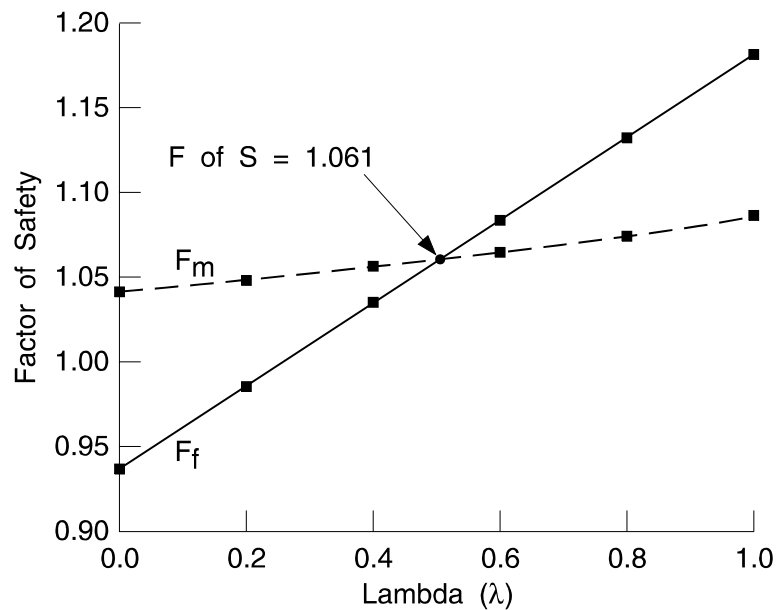


Figure 12-7 Example factor of safety versus lambda plot

12.13 Simulation of the various methods

The General Limit Equilibrium (GLE) formulation and solution can be used to simulate most of the commonly used methods of slices. From a theoretical standpoint, the various methods of slices can be categorized in terms of the conditions of static equilibrium satisfied and the assumption regarding the interslice forces. Table 12-3 summarizes the conditions of static equilibrium satisfied by many of the commonly used methods of slices. Table 12-4 summarizes the assumption used in each of the methods of slices to render the analysis determinate.

Table 12-3 Conditions of static equilibrium satisfied by various limit equilibrium methods

Method	Force Equilibrium		Moment Equilibrium
	1st Direction (e.g., Vertical)	2nd Direction (e.g., Horizontal)	
Ordinary or Fellenius	Yes	No	Yes
Bishop's Simplified	Yes	No	Yes
Janbu's Simplified	Yes	Yes	No
Spencer	Yes	Yes	Yes
Morgenstern-Price	Yes	Yes	Yes**
GLE	Yes	Yes	Yes
Corps of Engineers	Yes	Yes	No
Lowe-Karafiath	Yes	Yes	No
Janbu Generalized	Yes	Yes	No
Sarma	Yes	Yes	Yes
** Moment equilibrium on individual slice is used to calculate interslice shear forces			

Table 12-4 Assumptions used in various limit equilibrium methods

Method	Assumption
Ordinary or Fellenius	Interslice forces are neglected.
Bishop's Simplified	Resultant interslice forces are horizontal (i.e., there are no interslice shear forces).
Janbu's Simplified	Resultant interslice forces are horizontal. An empirical correction factor, f_o , can be used to account for interslice shear forces.
Spencer	Resultant interslice forces are of constant slope throughout the sliding mass.
Morgenstern-Price	Direction of the resultant interslice forces is determined using an arbitrary function. The percentage of the function, λ , required to satisfy moment and force equilibrium is computed with a rapid solver.
GLE	Direction of the resultant interslice forces is defined using an arbitrary function. The percentage of the function, λ , required to satisfy moment and force equilibrium is computed by finding the intersecting point on a factor of safety versus Lambda plot.
Corps of Engineers	Direction of the resultant interslice force is: i) equal to the average slope from the beginning to the end of the slip surface or ii) parallel to the ground surface.
Lowe-Karafiath	Direction of the resultant interslice force is equal to the average of the ground surface and the slope at the base of each slice.
Janbu Generalized	Location of the interslice normal force is defined by an assumed line of thrust.
Sarma	Direction of the resultant interslice force is calculated based on the interslice normal force and the user-specified cohesion and frictional angle between the interslice surface.

12.14 Spline interpolation

A spline interpolation technique is used to determine the pore-water pressure at the base of a slice when the pore-water pressures are defined at discrete points.

The technique involves the fitting of a spline function to a series of spatially distributed points. The fitting of the function to the points results in the calculation of weighting coefficients. The weighting coefficients can then be used to compute values for any other point in the region. Although the solving of a large problem

using this technique requires considerable computer storage, it has been found that a small number of designated points can provide reasonably accurate results.

To illustrate the spline interpolation technique, consider the following two-dimensional problem. Suppose we know a set of values, u_i , at N given points (x_i, y_i) with $i=1, N$, and we want to estimate the value of u at some other points, $M(x, y)$.

Let:

$$u(x, y) = P(x, y) + \sum_{i=1}^N \lambda_i K(h_m - h_i)$$

where:

$P(x, y)$ = the chosen trend,

$K(h)$ = the chosen interpolation function,

h = the distance between two points, (e.g., $h = h_m - h_i$), where:

$$(h_m - h_i) = (x_m - x_i)^2 + (y_m - y_i)^2$$

λ_i = the computed weighting coefficients referred to as Kriging coefficients.

In the SLOPE/W formulation:

$$P(x, y) = a + bx + cy$$

and:

$$K(h) = \delta(0) + h^2 \log h$$

where $\delta(0)$ is the nugget effect. This will be explained later; for the present it is assumed to be zero.

The weighting coefficients $(a, b, c, \lambda_1, \lambda_2, \dots, \lambda_N)$ are the solution of the following set of linear equations:

$$\begin{bmatrix} K(0) & \dots & K(h_1-h_n) & 1 & x_1 & y_1 \\ & & \cdot & \cdot & \cdot & \cdot \\ & & & 1 & x_N & y_N \\ & & & 0 & 0 & 0 \\ & & & & 0 & 0 \\ & & & & & 0 \end{bmatrix} \begin{bmatrix} \lambda_1 \\ \cdot \\ \cdot \\ a \\ b \\ c \end{bmatrix} = \begin{bmatrix} u_1 \\ \cdot \\ u_N \\ 0 \\ 0 \\ 0 \end{bmatrix}$$

This system of linear equations is solved for the weighting coefficients. The value of $u(x,y)$ can now be computed at any point, x,y using the equation:

$$u(x,y) = a + bx + cy + \sum_{i=1}^N \left(\lambda_i (h_m - h_i)^2 \log(h_m - h_i) \right)$$

The following properties can be derived from this equation: At a point x_l, y_l , if $a(0) = 0$ and $K(0) = 0$, then $u(x_l, y_l) = u_l$. If for the point $x_l, y_l, K(0) = a_l$ and $u(x_l, y_l) \neq u_l$, then, $\delta(0) = \delta(l) \neq 0$.

Therefore, by selecting different nugget values for the initial points, it is possible to help the estimated values coincide with the initial values. At its limit, if $\delta(0)$ is the same for all points and its value becomes large:

$$u(x,y) = P(x,y) = a + bx + cy$$

This is equivalent to the least square solution of fitting.

With a function, $K(h) = h^2 \log h$, the solution of this spline problem can be visualized as a thin plate deforming in such a way as to pass through the deflection, u_i , at all points, x_i, y_i .

12.15 Moment axis

When the grid and radius method is used by default the moment factor of safety is computed by summing moments about each grid point. However, it is possible to use one single point at which to sum moments for all slip surfaces. This point is known as the axis. The grid point is used to define the shape of the slip surface, and the axis point is used for summing moments.

The position of the moment center has a negligible effect on factors of safety computed by methods that satisfy both force and moment equilibrium (e.g., the GLE, the Morgenstern-Price and the Spencer methods). The factor of safety can be slightly affected by the position of the moment axis when the slip surface is non-circular and the method satisfies only force or only moment equilibrium.

As a general rule, the axis point should be located approximately at the center of rotation of the slip surfaces.

12.16 Finite element stress method

In addition to the limit equilibrium methods of analysis, SLOPE/W also provides an alternative method of analysis using the stress state obtained from SIGMA/W, a GEO-SLOPE/W program for stress and deformation analysis. The following sections outline the theoretical basis and the solution procedures used by the SLOPE/W Finite Element Stress method.

Stability factor

As mentioned earlier in the Chapter, the factor of safety obtained using a limit equilibrium method is defined as that factor by which the shear strength of the soil must be reduced in order to bring the mass of soil into a state of limiting equilibrium along a selected slip surface. Furthermore, due to the nature of the method, the following two assumptions are made with respect to the factor of safety:

The factor of safety of the cohesive component of strength and the frictional component of strength are equal for all soils involved.

The factor of safety is the same for all slices.

The above assumptions are no longer necessary in the finite element stress method. In other words, the computed “factor of safety” using the finite element stress approach is not the same factor of safety as in the limit equilibrium approach. To preserve the original meaning of the factor of safety, the “factor of safety” computed using the Finite Element Stress method is referred to as the *stability factor* in SLOPE/W.

The stability factor (S.F.) of a slope by the finite element stress method is defined as the ratio of the summation of the available resisting shear force S_r along a slip

surface to the summation of the mobilized shear force S_m along a slip surface. In equation form, the stability factor (S.F.) is expressed as:

$$S.F. = \frac{\sum S_r}{\sum S_m}$$

The available resisting force of each slice is calculated by multiplying the shear strength of the soil at the base center of the slice with the base length. Therefore, from the modified form of the Mohr-Coulomb equation for an unsaturated soil the available resisting force is:

$$S_r = s\beta = \left(c' + (\sigma_n - u_a) \tan \phi' + (u_a - u_w) \tan \sigma^b \right) \beta$$

where:

- s = effective shear strength of the soil at the base center of a slice
- β = base length of a slice
- σ_n = normal stress at base center of a slice

Similarly, the mobilized shear force of each slice is calculated by multiplying the mobilized shear stress (τ_m) at the base center of the slice with the base length.

$$S_m = \tau_m \beta$$

A local stability factor of a slice can also be obtained when the available resisting shear force of a slice is compared to the mobilized shear force of a slice.

$$Local \ S.F. = \frac{S_r}{S_m} = \frac{s\beta}{\tau\beta}$$

Of significance is the fact that both the normal stress (σ_n) and the mobilized shear stress (τ_m) are computable values from a SIGMA/W analysis. Therefore, the equations for computing the stability factors are linear; that is, no iteration is required to establish the stability factors as in the limit equilibrium method. Iterations may be required in the SIGMA/W analysis, but not in the SLOPE/W analysis.

Normal stress and mobilized shear stress

To use the Finite Element Stress method, you need to start by performing a SIGMA/W analysis.

The information required from the SIGMA/W analysis is the stress state as describe by σ_x , σ_y and τ_{xy} at each Gauss point within each element. These stress values are used to compute the normal stress and the mobilized shear stress at the base center of each slice. The procedure is as follows:

Step 1: Element Nodal Stresses

SIGMA/W calculates and stores the computed stresses at element Gauss points. To compute the stress state at the slice base center, it is first necessary to establish the stress state at the element nodes. This is done by projecting the Gauss values to the nodes and then averaging the nodal values obtained from each adjoining element.

The projection is done with the use of the interpolating functions. In equation form:

$$f = \langle N \rangle \{ F \}$$

where:

f	=	stress at the element nodes
$\langle N \rangle$	=	matrix of the interpolating functions
$\{ F \}$	=	stress values at the Gauss points

The interpolating functions are the same as the standard functions used to describe a variable within an element in terms of nodal values, except that the local coordinates are the reciprocal of the standard Gauss point integration points.

Consider, for example, if the local coordinates of a Gauss integration point inside an element are (0.577, 0.577). When the Gauss points are projected outward from the Gauss point to the corner node, the local coordinates for the closest corner node are (1.73, 1.73). Figure 12-8 illustrates this projection scheme for a quadrilateral element.

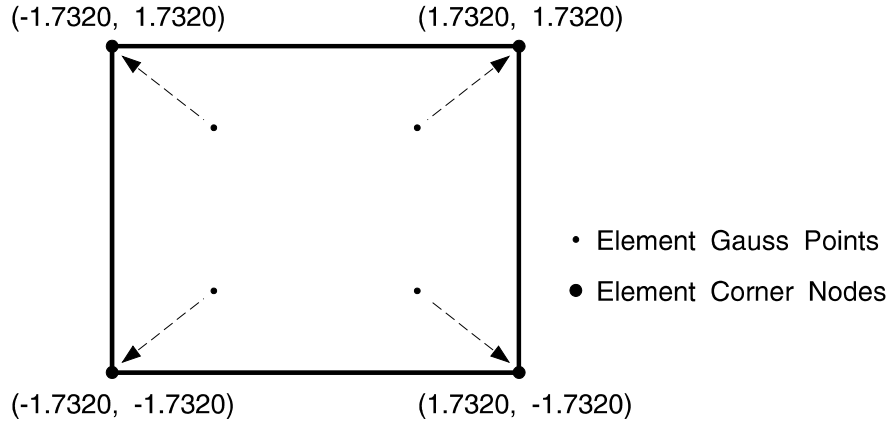


Figure 12-8 Projection from Gauss points to corners

The above projection is carried out for each element in a problem, and the values from each adjoining element are then averaged. Upon completing this procedure, σ_x , σ_y and τ_{xy} are known at each node in the entire mesh.

Step 3: Base Normal and Shear Stresses

The normal stress $\{\sigma_n\}$ and the mobilized shear stress (τ_m) at the base center are computed using the following Mohr circle-based equations:

$$\sigma_n = \frac{\sigma_x + \sigma_y}{2} + \frac{\sigma_x - \sigma_y}{2} \cos 2\theta + \tau_{xy} \sin 2\theta$$

$$\tau_m = \tau_{xy} \cos 2\theta - \frac{\sigma_x - \sigma_y}{2} \sin 2\theta$$

where:

- σ_x = total stress in x-direction at the base center,
- σ_y = total stress in y-direction at the base center,
- τ_{xy} = shear stress in x- and y-directions at the base center, and
- θ = angle measured from positive x-axis to the line of application of the normal stress.

The line of application of the normal stress is perpendicular to the base plane of the slice, whereas the line of application of the mobilized shear stress is parallel to the base plane.

12.17 Probabilistic slope stability analysis

Deterministic slope stability analyses compute the factor of safety based on a fixed set of conditions and material parameters. If the factor of safety is greater than unity, the slope is considered to be stable. On the contrary, if the factor of safety is less than unity, the slope is considered to be unstable or susceptible to failure. Deterministic analyses suffer from limitations; such as that the variability of the input parameters is not considered, and questions like “How stable is the slope?” cannot be answered.

Probabilistic slope stability analysis allows for the consideration of variability in the input parameters and it quantifies the probability of failure of a slope. SLOPE/W can perform probabilistic slope stability analyses using the Monte Carlo method.

SLOPE/W allows the following parameter variability distribution functions: Normal, Lognormal, Uniform, Triangular and Generalized Spline function. Details of these functions are discussed in the Probabilistic and Sensitivity Analyses Chapter.

Monte Carlo method

The Monte Carlo method is a simple, but versatile computational procedure that is suitable for a high speed computer. In general, the implementation of the method involves the following steps:

- The selection of a deterministic solution procedure, such as the Spencer’s method or the finite element stress method.
- The decisions regarding which input parameters are to be modeled probabilistically and the representation of their variability in terms of a selected distribution model.
- The conversion of any distribution function into a sampling function, the random sampling of new input parameters and the determination of new factors of safety many times.

- The computation of the probability of failure based on the number of factors of safety less than 1.0 with respect to the total number of converged slip surfaces. For example, in an analysis with 1000 Monte Carlo trials, 980 trials produce a converged factor of safety and 98 trials produce a factor of safety of less than 1.0. The probability of failure is 10.0 %.

In SLOPE/W, one or more most critical slip surfaces are first determined based on the mean value of the input parameters using any of the limit equilibrium and finite element stress methods. Probabilistic analysis is then performed on these critical slip surfaces, taking into consideration the variability of the input parameters.

The number of Monte Carlo trials in an analysis is dependent on the number of variable input parameters and the expected probability of failure. In general, the number of required trials increases as the number of variable input increases or the expected probability of failure becomes smaller. It is not unusual to do thousands of trials in order to achieve an acceptable level of confidence in a Monte Carlo probabilistic slope stability analysis.

Parameter variability

Soils are naturally formed materials; consequently their physical properties vary from point to point. This variation occurs even in an apparently homogeneous layer. The variability in the value of soil properties is a major contributor to the uncertainty in the stability of a slope. Laboratory results on natural soils indicate that most soil properties can be considered as random variables conforming to the normal distribution function.

In SLOPE/W, the variability of the input parameters is assumed to be normally distributed. The variability of the following input parameters can be considered:

- Material parameters for the various material strength models, including unit weight, cohesion and frictional angles,
- Pore-water pressure conditions,
- The magnitude of the applied line loads, and
- The horizontal and vertical seismic coefficients.

Random number generation

Fundamental to the Monte Carlo method are the randomly generated input parameters that are fed into a deterministic model. In SLOPE/W, this is done using a random number generation function. The random numbers generated from the function are uniformly distributed with values between 0 and 1.0

Correlation coefficient

A correlation coefficient expresses the relative strength of the association between two parameters. Laboratory tests on a wide variety of soils (; and W) show that the shear strength parameters c and ϕ are often negatively correlated with correlation coefficient ranges from -0.72 to 0.35. Correlation between strength parameters may affect the probability distribution of a slope. SLOPE/W allows the specification of c and ϕ correlation coefficients for all soil models using c and ϕ parameters. Furthermore, in the case of a bilinear soil model, SLOPE/W allows the specification of correlation coefficient for ϕ and ϕ_2 .

Correlation coefficients will always fall between -1 and 1. When the correlation coefficient is positive, c and ϕ are positively correlated implying that larger values of c are more likely to occur with larger values of ϕ . Similarly, when the correlation coefficient is negative, c and ϕ are negatively correlated and reflects the tendency of a larger value of c to occur with a smaller value of ϕ . A zero correlation coefficient implies that c and ϕ are independent parameters.

In SLOPE/W, when estimating a new trial value for ϕ and ϕ_2 , the normalized random number is adjusted to consider the effect of correlation. The following equation is used in the adjustment:

$$N_a = N_1 k + (1 - |k|) N_2$$

where:

- k = correlation coefficient between the first and second parameters,
- N_1 = normalized random number for the first parameter,
- N_2 = normalized random number for the second parameter, and
- N_a = adjusted normalized random number for the second parameter.

Number of Monte Carlo trials

Probabilistic slope stability analysis using the Monte Carlo method involves many trial runs. Theoretically, the more trial runs used in an analysis the more accurate the solution will be. How many trials are required in a probabilistic slope stability analysis? It has been suggested that the number of required Monte Carlo trials is dependent on the desired level of confidence in the solution, as well as the number of variables being considered. Statistically, the following equation can be developed:

$$N_{mc} = \left[\frac{(d^2)}{(4(1-\varepsilon)^2)} \right]^m$$

where:

N_{mc}	=	number of Monte Carlo trials,
ε	=	the desired level of confidence (0 to 100%) expressed in decimal form,
d	=	the normal standard deviate corresponding to the level of confidence, and
m	=	number of variables.

The number of Monte Carlo trials increases geometrically with the level of confidence and the number of variables. For example, if the desired level of confidence is 80%, the normal standard deviate will be 1.28; the number of Monte Carlo trials will be 10 for 1 variable, 100 for 2 variables and 1,000 for 3 variables. For a 90% level of confidence, the normal standard deviate will be 1.64; the number of Monte Carlo trials will be 67 for 1 variable, 4,489 for 2 variables and 300,763 for 3 variables. In fact, for a 100% level of confidence, an infinite number of trials will be required.

For practical purposes, the number of Monte Carlo trials to be conducted is usually in the order of thousands. This may not be sufficient for a high level of confidence with multiple variables; fortunately, in most cases, the solution is not very sensitive to the number of trials after a few thousands trials have been run. Furthermore, for most engineering projects, the degree of uncertainty in the input parameters may not warrant a high level of confidence in a probabilistic analysis.

References

- Abramson, L.W., Lee, T.S., Sharma, S., and Boyce, G.M., 2002. Slope Stability and Stabilization Methods. John Wiley & Sons Inc. pp.712.
- Bishop, A.W. and Morgenstern, N., 1960. Stability coefficients for earth slopes. *Geotechnique*, Vol. 10, No. 4, pp. 164 169.
- Christian, J.T., Ladd, C.C. and Baecher, G.B., 1994. Reliability Applied to Slope Stability Analysis. *Journal of Geotechnical Engineering*, Vol. 120, No. 12. pp. 2180-2207.
- El-Ramly, H., Morgenstern, N.R., Cruden, D.M. 2002. Probabilistic Slope Stability Analysis for Practice. *Canadian Geotechnical Journal*. Vol. 39. pp. 665-683.
- Fellenius, W., 1936. Calculation of the Stability of Earth Dams. *Proceedings of the Second Congress of Large Dams*, Vol. 4, pp. 445-463.
- Fredlund, D.G., 1974. Slope Stability Analysis. User's Manual CD-4, Department of Civil Engineering, University of Saskatchewan, Saskatoon, Canada.
- Fredlund, D.G., and Krahn, J., 1977. Comparison of slope stability methods of analysis. *Canadian Geotechnical Journal*, Vol. 14, No. 3, pp. 429 439.
- Fredlund, D.G., Zhang, Z.M. and Lam, L., 1992. Effect of the Axis of Moment Equilibrium in Slope Stability Analysis. *Canadian Geotechnical Journal*, Vol. 29, No. 3.
- Greco, V.R. 1996. Efficient Monte Carlo Technique for Locating Critical Slip Surface. *Journal of Geotechnical Engineering*. Vol 122, No. 7. ASCE, pp.517-525.
- Grivas, D.A., 1981. How Reliable are the Present Slope Failure Prediction Methods? *Proceedings of the Tenth International Conference of Soil Mechanics and Foundation Engineering*, Stockholm, Sweden, Vol. 3, pp.427-430.

- Harr, M.E., 1987. Reliability-Based Design in Civil Engineering. McGraw-Hill Book Company. pp. 290.
- Higdon A., Ohlsen, E.H., Stiles, W.B., Weese, J.A. and Riley, W.F., 1978. Mechanics of Materials. John Wiley & Sons. pp.752.
- Hoek, E. 2000. Course Notes entitled Practical Rock Engineering (2000 ed., Chapter 11).
- Hoek, E., Carranza-Torres, C. and Corkum, B., 2002. Hoek-Brown Failure Criterion – 2002 Edition. Proc. North American Rock Mechanics Society meeting in Toronto in July 2002.
- Janbu, N., Bjerrum, J. and Kjaernsli, B., 1956. Stabilitetsberegning for Fyllinger Skjaeringer og Naturlige Skraninger. Norwegian Geotechnical Publications, No. 16, Oslo.
- Janbu, N. 1954. Applications of Composite Slip Surfaces for Stability Analysis. In Proceedings of the European Conference on the Stability of Earth Slopes, Stockholm, Vol. 3, p. 39-43.
- Krahn, J., 2003. The 2001 R.M. Hardy Lecture: The Limits of Limit Equilibrium Analyses. Canadian Geotechnical Journal, Vol. 40. pp.643-660.
- Krahn, J., Price, V.E., and Morgenstern, N.R., 1971. Slope Stability Computer Program for Morgenstern-Price Method of Analysis. User's Manual No. 14, University of Alberta, Edmonton, Canada.
- Kramer, S.L. 1996. Geotechnical Earthquake Engineering. Prentice Hall, pp. 437.
- Ladd, C.C., 1991. Stability evaluation during staged construction: 22nd Terzaghi Lecture. Journal of Geotechnical Engineering, ASCE, 117(4), pp. 537-615
- Ladd, C.C. and Foott, R. 1974. New Design Procedure for Stability of Soft Clays. Journal of the Geotechnical Engineering Division, ASCE, Vol. 100, (GT7), pp. 763-786.
- Lam, L., and Fredlund D.G., 1993. A general Limit Equilibrium Model for Three-Dimensional Slope Stability Analysis. Canadian Geotechnical Journal. Vol. 30. pp. 905-919.

- Lambe, T.W. and Whitman, R.V., 1969. Soil Mechanics. John Wiley and Sons, pp. 359-365.
- Lapin, L.L., 1983. Probability and Statistics for Modern Engineering. PWS Publishers. pp. 624.
- Li, K.S. and Lumb, P., 1987. Probabilistic Design of Slopes. Canadian Geotechnical Journal, Vol. 24, No. 4, pp. 520-535.
- Lumb, P., 1966. The Variability of Natural Soils. Canadian Geotechnical Journal, Vol. 3, No. 2, pp. 74-97.
- Lumb, P., 1970. Safety Factors and the Probability Distribution of Soil Strength. Canadian Geotechnical Journal, Vol. 7, No. 3, pp. 225-242.
- Malkawi, A.I.H, Hassan, W.F. and Sarma, S.K. 2001. Global Search Method for Locating General Slip Surface Using Monte Carlo Technique. Journal of Geotechnical and Geoenvironmental Engineering. Vol 127, No. 8, pp. 688-698.
- Morgenstern, N.R., and Price, V.E., 1965. The Analysis of the Stability of General Slip Surfaces. Geotechnique, Vol. 15, pp. 79-93.
- Mostyn, G.R. and Li, K.S., 1993. Probabilistic Slope Stability Analysis - State-of-Play, Proceedings of the Conference on Probabilistic Methods in Geotechnical Engineering, Canberra, Australia. pp. 281-290.
- Petterson, K.E. 1955. The Early History of Circular Sliding Surfaces, Geotechnique, Vol. 5, p. 275-296.
- Sarma, S.K., 1973. Stability Analysis of Embankments and Slopes. Geotechnique, Vol. 23 (3), pp. 423-433.
- Sarma, S.K., 1979. Stability Analysis of Embankments and Slopes. Journal of the Geotechnical Engineering Division. ASCE. Vol. 105, No. GT12. pp. 1511-1524.
- Spencer, E. 1967. A Method of Analysis of Embankments assuming Parallel Interslice Forces. Geotechnique, Vol 17 (1), pp. 11-26.

- Vanmarcke, E.H., 1983. Random Fields: Analysis and Synthesis. MIT Press, Cambridge, Mass.
- Whitman, R.V. and Bailey, W.A., 1967. Use of Computer for Slope Stability Analysis. Journal of the Soil Mechanics and Foundation Division of ASCE, Vol. 93, No. SM4.
- Wolff, T.F., 1985. Analysis and Design of Embankment Dams: A Probabilistic Approach. Ph.D. Thesis, Purdue University, West Lafayette, IN.

Index

Anchors.....	184	Force equilibrium	364
Anisotropic strength.....	144	Fully specified slip surfaces.....	92
Auto-search.....	104	General limit equilibrium method 11, 363	
B-bar coefficients.....	166	General Limit Equilibrium Method	37
Bedrock.....	141	Geo-fabric.....	193
Bilinear	141	Geometry	125
Bishop's simplified.....	47	Grid and radius for circular slips ...	82
Block slip surface	19	Ground surface line	131
Block specified slip surface	94	Hoek & Brown.....	149
Circular slip surface.....	16	Illustrative Examples	386
Composite slip surface.....	18	Interslice assumption	58
Composite slip surfaces	89	Interslice force functions	15
Corps of Engineers method	58	Interslice forces.....	368
Deep-seated instability.....	200	Janbu generalized method.....	28
Definition of variables	357	Janbu's simplified method.....	50
Dynamic Stability	217	Limit Equilibrium Fundamentals.....	7
Entry and exit specification	99	line loads.....	136
Finite element computed pressures	168	Liquefaction stability	230
Finite element stress method	379	Lowe-Karafiath method.....	63
Finite element stress-based method	69	M-alpha.....	366

Material Strength	139	Seismic	217
Method basics	8	Sensitivity Analyses	233
Minimum depth	111	SHANSEP	148
Missing physics	29	Sheet pile walls	198
Mohr-Coulomb	139	Shoring wall.....	20
Moment equilibrium	364	Slice discretization.....	128
Monte Carlo	383	Slip surface shapes.....	16, 31
Morgenstern-Price method	54	Slip Surface Shapes	81
Nails.....	190	soil strength.....	106
Optimization	101	Soil-structure interaction	210
Ordinary or Fellenius.....	42	Spatial variability.....	247
Parameter variability.....	384	Spencer method	51
Piezometric surfaces	161	Stress distributions.....	21
Piles and dowels	197	Structural Components	173
Planar slip surface.....	17	surcharge pressures.....	132
Pore-water.....	161	Tension crack.....	135
Probabilistic	233	Tension cracks	112
Regions	125	Undrained strength	108, 141
Reinforcement	173	unit weight	157
R_u Coefficients.....	164	unsaturated shear strength.....	372
Sarma method	65	Unsaturated shear strength.....	156
Seepage forces	32	Wall facing	196

A consistent set of units

		Example of	Example of
Property	Units	Metric Units	Imperial Units
Geometry	L	meters	feet
Unit Weight of Water	F/L^3	kN/m^3	p.c.f.
Soil Unit Weight	F/L^3	kN/m^3	p.c.f.
Cohesion	F/L^2	kN/m^2	p.s.f.
Water Pressure	F/L^2	kN/m^2	p.s.f.
Pressure Head	L	m	ft.
Line Load	F/L	kN/m	lbs/ft.
acceleration	F/T^2	m/s^2	ft/s^2
velocity	F/L	m/s	ft/s
deformation	L	m	ft.

A consistent set of units

		Example of	Example of
Property	Units	Metric Units	Imperial Units
Geometry	L	meters	feet
Unit Weight of Water	F/L^3	kN/m^3	p.c.f.
Soil Unit Weight	F/L^3	kN/m^3	p.c.f.
Cohesion	F/L^2	kN/m^2	p.s.f.
Water Pressure	F/L^2	kN/m^2	p.s.f.
Pressure Head	L	m	ft.
Line Load	F/L	kN/m	lbs/ft.
acceleration	F/T^2	m/s^2	ft/s^2
velocity	F/L	m/s	ft/s
deformation	L	m	ft.